

IMPERIAL COLLEGE OF SCIENCE, TECHNOLOGY  
AND MEDICINE

University of London

**Dynamic Response Analysis of Structures  
with Nonlinear Components**

by

**Janito Vaqueiro Ferreira**

A thesis submitted to the University of London  
for the Degree of Doctor of Philosophy and  
for the Diploma of Imperial College

Department of Mechanical Engineering  
Imperial College of Science, Technology and Medicine  
London SW7

May, 1998

*Dedicated to my beloved wife and children,  
**Maria Antonia, Janito and Danilo,**  
for their love and patience  
during my PhD course*

# Abstract

Engineering structures are often very complex and difficult to analyse for their dynamic, or vibrational, behaviour. It is common practice to divide a complex structure into a number of components, or substructures, so that each of these can be analysed individually using whichever method is the most convenient. In this way, by applying structural assembly analysis methods, it is possible to predict the dynamic behaviour of the whole assembled structure. Coupled structure analysis is a standard tool in structural dynamics when dealing with linear structures. Many different methods for assembling linear structures have been developed and are usually referred to as "coupling techniques". However, many practical mechanical structures exhibit a degree of nonlinearity due to the complex nature of the joints, microclearances in slides or bearings, nonlinear damping and material properties. So existing methods cannot be applied. The aim of this work is to advance developments in analytical coupling methods for prediction of the response of complex nonlinear structures.

The work initially reviews existing techniques of analysing linear and nonlinear structures. First, a time-domain analysis formulation and the computational aspects of the technique are described. Then, a frequency-domain method of analysis is introduced. Different coupling techniques for the solution of linear problems are investigated and presented in a unified notation. The frequency response function coupling method often used in linear applications is identified as a possible method applicable to nonlinear structures through the introduction of a describing function method that can deal with the representation of the nonlinearities involved in such systems.

The basic FRF coupling algorithm is modified by using the describing function. Then, the combined formulation, namely harmonic nonlinear receptance coupling approach (*HANORCA*) is used as a basis to derive a multi-harmonic nonlinear receptance coupling approach (*MUHANORCA*). In parallel with these new coupling methods, models of a number of nonlinear elements are also developed. The *MUHANORCA* analysis method is then used to predict the behaviour of simulated multidegree-of-freedom coupled systems with strongly nonlinear components. Finally, the *MUHANORCA* method is used to analyse two experimental systems, one a stationary structure with a cubic stiffness nonlinearity and the other a rotating structure with polynomial stiffness nonlinearity. The limitations and difficulties of some of the problems encountered during these experiments are discussed in details and the control technique used to obtain the experimental data is also discussed.

The FRFs generated by *MUHANORCA* are in good agreement with those measured on the test rigs. From these case studies it is concluded that the methods developed are capable of accurately predicting the dynamic behaviour of stationary and rotating structures with pronounced nonlinearities.

# Acknowledgements

I am very grateful to my supervisor, Professor D.J. Ewins, for his encouragement, interest, stimulus and guidance throughout this project. It was due to his initiatives and valuable instructions that helped to develop this work. Special thanks go to other members of staff, both past and present, that helped so much during these years, mainly, Dr. Imregun, Mr. D. Rob, Ms. Val Davenport, Miss. Liz Hearn, Ms. Lisa Whitelaw, Mr. Paul Woodward and Mr. John Miller.

I would also like to thank my colleagues at Dynamics Section who provided friendly cooperation and useful discussion throughout the period of this research. I would particularly like to mention Saeed, Michael, Gotz and Henning.

I wish to express my gratitude to my good friends and colleagues, Yon, Sangjun, Reza, Jeonhoon, Sherman, Mohamed and John Huges who directly or indirectly helped during this period.

Special thanks are due to my father who passed away, my mother and brothers for all their love, constant support and encouragement.

The author is indebted to the CNPq (Conselho Nacional de Desenvolvimento Científico e Tecnológico) and to the UNICAMP (Universidade de Campinas) for providing the financial support for this research.

Finally, I wish to express my deepest gratitude to my wife and two children, Maria Antonia, Janito and Danilo, for their love and sacrifice. They shared my successes and disappointments over these years. Without their full support and encouragement, this thesis would not have been completed.

# Nomenclature

## *Roman letters*

$t$  time

$i$  unity imaginary number

## *Roman letters (vectors and matrices)*

$[C]$  viscous damping matrix

$[D]$  structural damping matrix

$[I]$  identity matrix

$[K]$  stiffness matrix

$[M]$  mass matrice

## *Time Domain*

$\{\mathbf{f}\}$  internal nonlinear forces vector

$\{f\}$  external excitation force vector

$\{x\}$  displacement vector

$\{x\}^m$   $m_{th}$  displacement response order

$h$  impulse response function

$y_{kl}$  inter-coordinate relative displacement response  $y$  between coordinates  $j$  and  $k$

$\{\ddot{x}\}$  acceleration vector

$\{\dot{x}\}$  velocity vector

## *Frequency Domain*

$\mathcal{G}$  multi-harmonic describing function

$\nu$  describing function

$\{\bar{X}\}$  magnitude of harmonic displacement

$\{\mathcal{F}\}$  complex harmonic nonlinear function

$\{\tilde{A}\}^{(q_r)}$  approximate variable  $A$  considering harmonics up to  $q_r$

$\{F\}$  complex harmonic force  
 $\{X\}$  complex harmonic displacement  
 $\{Y\}$  inter-coordinate complex harmonic displacement  
 $C, \bar{C}, \tilde{C}$  connection DOFs of assembled system  
 $c, \bar{c}, \tilde{c}$  connection DOFs of collected substructure  
 $H^m$   $m_{th}$  order frequency response function  
 $H^{nm}, H^n$  experimental higher-order frequency response function  
 $H_n$  ideal higher-order frequency response function  
 $I$  internal DOFs of assembled system  
 $i$  internal DOFs of collected substructure  
 $Q$  set of harmonics considered in the approximated response  
 $R$  DOFs of assembled system  
 $r$  DOFs of collected substructure  
 $r$  number of harmonics considered in the approximated response  
 $s$  number of harmonics considered in the approximated nonlinear force  
 $xl$  slip limit deformation  
 $[\Sigma]$  singular values matrix  
 $[U], [V]$  orthonormal matrices  
 $[Z]$  impedance of the assembled system  
 $[z]$  impedance of the substructures  
 $\bar{c}_d, \tilde{c}_d$  connection DOFs of collected substructure where the response is required  
 $\bar{c}_d, \tilde{c}_d$  connection DOFs of collected substructure where the response is required  
 $\bar{c}_f, \tilde{c}_f$  connection DOFs of collected substructure where the force is excited  
 $\bar{c}_u, \tilde{c}_u$  connection DOFs of collected substructure where the response is not required  
 $\bar{c}_u, \tilde{c}_u$  connection DOFs of collected substructure where the response is not required  
 $I_d$  internal DOFs of assembled system where the response is required  
 $I_d$  internal DOFs of assembled system where the response is required  
 $i_d$  internal DOFs of collected substructure where the response is required  
 $i_d$  internal DOFs of collected substructure where the response is required  
 $i_f$  internal DOFs of collected substructure where the force is excited  
 $i_u$  internal DOFs of collected substructure where the response is not required

$i_u$  internal DOFs of collected substructure where the response is not required

*Greek letters*

$\omega$  frequency

$\phi$  phase of harmonic displacement response

$\psi$  phase of inter-coordinate-relative harmonic displacement response

$\tau$   $\omega t$

$\tau$  time

$\delta t$  time step interval

*Other symbols*

– magnitude of a complex variable

$\sim$  approximate variable

*Subscripts*

$j$  general coordinate

$kl$  inter-coordinate

$m$  harmonic order

*Abbreviations*

**BBA** building block approach

**FEM** finite element method

**FRF** frequency response function

**HAIM** harmonic nonlinear impedance coupling approach

**HANORCA** harmonic nonlinear receptance coupling approach

**HODEF** higher-order describing function

**MDOF** multiple degree-of-freedom

**MUHADEF** multi-harmonic describing function

**MUHAIM** multi-harmonic harmonic nonlinear impedance coupling approach

**MUHANORCA** multi-harmonic harmonic nonlinear receptance coupling approach

**NLBBA** nonlinear building block approach

**SDOF** single degree of freedom

**SVD** singular value decomposition

# Contents

<b>1</b>	<b>Introduction</b>	<b>20</b>
1.1	Introduction to the Problem . . . . .	20
1.2	Review of Current State-of-the-Art . . . . .	24
1.3	Proposed Developments . . . . .	27
1.4	Summary of the thesis . . . . .	28
<b>2</b>	<b>Types of Dynamic Analysis of Nonlinear Structures</b>	<b>30</b>
2.0.1	Introduction . . . . .	30
2.1	Nonlinear Structures . . . . .	31
2.2	Modelling of Nonlinear Structures . . . . .	32
2.3	Time-Domain Analysis . . . . .	34
2.3.1	Introduction . . . . .	34
2.3.2	Runge-Kutta Method . . . . .	35
2.4	Frequency-Domain Analysis . . . . .	37
2.4.1	Introduction . . . . .	37
2.4.2	Analysis . . . . .	38
2.5	Frequency-Domain Harmonic Analysis . . . . .	41
2.5.1	Fundamental Harmonic Analysis . . . . .	41
2.5.2	First-Order Frequency Response Functions . . . . .	43
2.5.3	Harmonic Balance Method . . . . .	43
2.5.4	Describing Functions . . . . .	45
2.6	Frequency-Domain Multi-Harmonic Analysis . . . . .	49
2.6.1	Multi-Harmonic Analysis . . . . .	49
2.6.2	Higher-Order Frequency Response Functions . . . . .	51

---

2.6.3	Higher-Order Harmonic Balance Method . . . . .	57
2.6.4	Higher-Order Describing Functions ( <i>HODEF</i> ) . . . . .	59
2.6.5	Multi-Harmonic Describing Functions ( <i>MUHADEF</i> ) . . . . .	61
2.7	Newton-Raphson Method . . . . .	65
<b>3</b>	<b>Construction of Models for Nonlinear Joint Components</b>	<b>67</b>
3.1	Introduction . . . . .	67
3.2	Linear Joints . . . . .	69
3.2.1	Spring . . . . .	69
3.2.2	Rigid connection . . . . .	70
3.2.3	Ground . . . . .	70
3.2.4	Viscous Damping . . . . .	71
3.3	Nonlinear Joints . . . . .	72
3.3.1	Cubic Stiffness . . . . .	73
3.3.2	Coulomb Friction . . . . .	73
3.3.3	Slip Friction . . . . .	76
3.3.3.1	Bilinear Macroslip element . . . . .	76
3.3.3.2	Burdekin's Microslip Model . . . . .	77
3.3.3.3	Shoukry's Microslip Model . . . . .	78
3.3.3.4	Ren's Microslip Model . . . . .	79
3.4	Concluding Remarks . . . . .	81
<b>4</b>	<b>Impedance Coupling Methods</b>	<b>82</b>
4.1	Introduction . . . . .	82
4.2	Coupling Analysis Notation . . . . .	83
4.3	Linear Impedance Coupling Methods . . . . .	84
4.3.1	Introduction . . . . .	84
4.3.2	Spatial Coupling Method . . . . .	85
4.3.3	FRF Coupling Method . . . . .	87
4.4	Harmonic Nonlinear Coupling Approaches . . . . .	88
4.4.1	Introduction . . . . .	88
4.4.2	Harmonic Nonlinear Building Block . . . . .	89

---

4.4.3	Harmonic Nonlinear Impedance Coupling using Harmonic Balance Method . . . . .	92
4.4.4	Harmonic Nonlinear Impedance Coupling using Describing Functions ( <i>HAIM</i> ) . . . . .	94
4.4.5	Harmonic Nonlinear Receptance Coupling Approach ( <i>HANORCA</i> )	95
4.4.6	Refinements in <i>HANORCA</i> . . . . .	101
4.4.6.1	Pseudo inverse using Singular Value Decomposition (SVD) . . . . .	101
4.4.6.2	Inverse of a partitioned matrix $[B]$ . . . . .	102
4.4.6.3	Local iterations . . . . .	105
4.5	Multi-Harmonic Nonlinear Coupling Approaches . . . . .	108
4.5.1	Introduction . . . . .	108
4.5.2	Multi-Harmonic Nonlinear Impedance Coupling using Multi-Harmonic Balance Method . . . . .	109
4.5.3	Multi-Harmonic Nonlinear Impedance Coupling using High-Order Describing Function ( <i>MUHAIM</i> ) . . . . .	110
4.5.4	Multi-Harmonic Nonlinear Impedance Coupling using Multi-Harmonic Describing Function ( <i>MUHANORCA</i> ) . . . . .	112
4.5.5	Multi-Harmonic Nonlinear Receptance Coupling using Multi-Harmonic Describing Function . . . . .	114
4.6	Concluding Remarks . . . . .	117
<b>5</b>	<b>Intelligent Nonlinear Coupling Analysis <i>INCA</i><sup>++</sup></b>	<b>118</b>
5.1	Introduction . . . . .	118
5.2	Object-Oriented Language . . . . .	120
5.2.1	Introduction . . . . .	120
5.2.2	Object Model . . . . .	120
5.2.3	Basic Elements of Object Model . . . . .	121
5.2.3.1	Abstraction . . . . .	121
5.2.3.2	Object . . . . .	121
5.2.3.3	Encapsulation . . . . .	122
5.2.3.4	Modularity . . . . .	123

---

5.2.3.5	Hierarchy . . . . .	123
5.2.3.6	Polymorphism . . . . .	124
5.2.4	Advanced Concept . . . . .	126
5.2.5	Achieving Object Model . . . . .	126
5.3	Specifications of <i>INCA<sup>++</sup></i> . . . . .	127
5.4	First Design of <i>INCA<sup>++</sup></i> Object Model . . . . .	129
<b>6</b>	<b>Numerical Case Studies of Coupled Structures using <i>INCA<sup>++</sup></i></b>	<b>134</b>
6.1	Introduction . . . . .	134
6.2	Linear Numerical Simulation . . . . .	134
6.3	Simulation using <i>HANORCA</i> . . . . .	136
6.4	Simulation using <i>MUHAIM</i> . . . . .	141
6.5	Simulation using <i>MUHANORCA</i> . . . . .	145
6.6	Concluding Remarks . . . . .	149
<b>7</b>	<b>Experimental Case Studies</b>	<b>150</b>
7.1	Introduction . . . . .	150
7.2	FRF Measurements on Nonlinear Structures . . . . .	150
7.2.1	Sine Excitation . . . . .	151
7.2.2	Random Excitation . . . . .	153
7.2.3	Impact Excitation . . . . .	154
7.2.4	Discussion of Different Excitation Techniques . . . . .	155
7.2.5	Practical Considerations of Measuring FRF properties of Non-linear Structures . . . . .	155
7.2.6	Nonlinear Force Control Algorithm . . . . .	157
7.2.7	Acceleration Control Algorithm . . . . .	160
7.3	Experimental Setup . . . . .	161
7.4	Experimental Test Rig I . . . . .	168
7.4.1	Test Rig Model . . . . .	168
7.4.2	Linear Test Rig I Assembly . . . . .	168
7.4.3	Measured and Updated FRF of Linear Test Rig I Assembly . . . . .	169
7.4.4	Nonlinear Test Rig Assembly . . . . .	172

---

7.4.5	Experimental properties of the joints . . . . .	173
7.4.6	First Assembly Model Test Rig I . . . . .	174
7.4.7	Measured FRFs of Test Rig I . . . . .	174
7.4.8	Measured and Predicted Coupling FRFs using First Assembly Model Test Rig I . . . . .	178
7.4.9	Discussion of Results . . . . .	182
7.4.10	Second Assembly Model Test Rig I . . . . .	183
7.4.11	Measured and Predicted Coupling FRFs using Second Assem- bly Model Test Rig I . . . . .	186
7.4.12	Discussion of Results . . . . .	190
7.5	Experimental Test Rig II . . . . .	191
7.5.1	Test Rig II . . . . .	191
7.5.2	Modified Test Rig II . . . . .	191
7.5.3	Linear Test Rig Assembly . . . . .	193
7.5.4	Measured and Updated FRF of Linear Test Rig II Assembly .	193
7.5.5	Nonlinear Test Rig Assembly . . . . .	202
7.5.6	Analytical properties of the joints . . . . .	203
7.5.7	Assembly Model Test Rig II . . . . .	205
7.5.8	Measured FRFs of Test Rig II . . . . .	205
7.5.9	Measured and Predicted Coupling FRFs using Assembly Model Test Rig II . . . . .	207
7.5.10	Discussion of Results . . . . .	211
7.5.11	Conclusions . . . . .	211
<b>8</b>	<b>Conclusion and Future work</b>	<b>213</b>
8.1	Introduction . . . . .	213
8.2	Conclusions on the Nonlinear Receptance Coupling Technique . . . .	213
8.3	Contributions . . . . .	216
8.4	Prospects . . . . .	217
<b>A</b>	<b>Refined Formulation of FRF Coupling</b>	<b>234</b>
<b>B</b>	<b>Local iterations</b>	<b>239</b>

---

<b>C</b>	<b>Floating-Point Operations in <i>HANORCA</i></b>	<b>245</b>
C.1	Basic Concepts . . . . .	245
C.2	Matrix Algebra . . . . .	245
C.2.1	Matrix Addition and Subtraction . . . . .	245
C.2.2	Matrix Multiplication . . . . .	245
C.2.3	Matrix Inverse . . . . .	246
C.2.4	Matrix Inverse using Singular Value Decomposition . . . . .	246
C.2.5	Partitioned Matrix Inverse . . . . .	248
C.2.6	Partitioned Matrix Inverse using Singular Value Decomposition	249
C.2.7	Partitioned Matrix Inverse using Singular Value Decomposition for <i>HANORCA</i> . . . . .	250
C.3	KFLOPS in Traditional Impedance Method . . . . .	251
C.4	KFLOPS in <i>HANORCA</i> in General Equation . . . . .	252
C.5	KFLOPS in <i>HANORCA</i> considering local iterations refinements in response desired coordinate . . . . .	253
C.6	KFLOPS in <i>HANORCA</i> considering local iterations refinements in response desired and excitation force coordinates . . . . .	254
C.7	KFLOPS in refined <i>HANORCA</i> equation . . . . .	256
<b>D</b>	<b>Multi-Harmonic Nonlinear Receptance Coupling using Multi-Harmonic     Describing Function</b>	<b>258</b>
<b>E</b>	<b>Illustration of the <i>HANORCA</i></b>	<b>265</b>
E.1	Basic Impedance Coupling Process . . . . .	265
E.2	<i>HANORCA</i> of two linear structures with a local nonlinear element .	273
E.3	<i>HANORCA</i> of three linear structures with a local nonlinear element and rigid connections . . . . .	275
<b>F</b>	<b>Booch Notation</b>	<b>280</b>

# List of Figures

2.1	Nonlinear function $\mathcal{F}(x)$ and describing function $\nu^1(x)$ . . . . .	49
2.2	Nonlinear function $\mathbf{f}(\tilde{y}^{(3)})$ and approximate functions $\tilde{\mathbf{f}}^{(1)}(\tilde{y}^{(1)})$ , $\tilde{\mathbf{f}}^{(3)}(\tilde{y}^{(3)})$ . . . . .	64
3.1	Characteristic of linear spring . . . . .	70
3.2	Characteristic of linear viscous damper . . . . .	71
3.3	Characteristic of nonlinear cubic spring . . . . .	73
3.4	Characteristic of Coulomb friction . . . . .	75
3.5	Characteristic of a bilinear element . . . . .	76
3.6	Characteristic of Burdekin's element . . . . .	77
3.7	Characteristic of Shoukry's element . . . . .	78
3.8	Characteristic of Ren's element . . . . .	80
4.1	Collected Substructures . . . . .	83
4.2	Assembled System . . . . .	84
4.3	Illustration of Nonlinear Building Block Approach . . . . .	90
5.1	Example of structure A composition . . . . .	128
5.2	Class <b>Structure</b> . . . . .	130
5.3	Enhanced <b>Structure</b> class . . . . .	131
5.4	Modules of <i>INCA++</i> . . . . .	132
5.5	Hierarchy tree . . . . .	133
6.1	Collected Substructure . . . . .	135
6.2	Assembled Structure . . . . .	135
6.3	Displacement in coordinate $X4$ . . . . .	137
6.4	Displacement in coordinate $X5$ . . . . .	137

6.5	Displacement in coordinate $X_{10}$ . . . . .	138
6.6	Collected Substructure . . . . .	138
6.7	Assembled Structure . . . . .	139
6.8	Receptance $\alpha_{41}$ . . . . .	141
6.9	Receptance $\alpha_{101}$ . . . . .	142
6.10	Assembled Structure . . . . .	142
6.11	Influence of the number of harmonic terms on the frequency response for $\mu.N=5$ and $\mu.N=7.5$ . . . . .	143
6.12	Frequency Response $\{H_{11}^{11}\}^1$ . . . . .	144
6.13	Frequency Response $\{H_{11}^{11}\}^3$ . . . . .	144
6.14	Frequency Response $\{H_{11}^{11}\}^5$ . . . . .	145
6.15	Collected Substructure . . . . .	146
6.16	Assembled Structure . . . . .	146
6.17	Influence of the number of harmonic terms on the FRF . . . . .	148
6.18	Comparison of $\{H_{31}^{31}\}^3$ , $\{H_{31}^{31}\}^5$ and $H_{31}^t$ . . . . .	148
6.19	Frequency Response $\{H_{31}^{51}\}^5$ . . . . .	149
7.1	Overall setup Test Rig I . . . . .	162
7.2	Overall setup Test Rig II . . . . .	163
7.3	Block diagram of the linear experimental setup Test Rig I . . . . .	164
7.4	Block diagram of the nonlinear experimental setup Test Rig I . . . . .	164
7.5	Block diagram of the linear experimental setup Test Rig II . . . . .	165
7.6	Block diagram of the nonlinear experimental setup Test Rig II . . . . .	165
7.7	Calibration Setup . . . . .	167
7.8	System configuration . . . . .	168
7.9	Linear Test Rig I assembly . . . . .	169
7.10	Analytical linear model test rig I . . . . .	169
7.11	Frequency Response Function $H_{11}$ . . . . .	170
7.12	Frequency Response Function $H_{21}$ . . . . .	171
7.13	Frequency Response Function $H_{31}$ . . . . .	171
7.14	Test Rig I assembly . . . . .	172
7.15	Relationship between loading and deformation . . . . .	173

---

7.16	Analytical model Test Rig I . . . . .	174
7.17	Measured Frequency Response $H_{11}^{11}$ . . . . .	175
7.18	Measured Frequency Response $H_{11}^{31}$ . . . . .	175
7.19	Measured Frequency Response $H_{21}^{11}$ . . . . .	176
7.20	Measured Frequency Response $H_{21}^{31}$ . . . . .	176
7.21	Measured Frequency Response $H_{31}^{11}$ . . . . .	177
7.22	Measured Frequency Response $H_{31}^{31}$ . . . . .	177
7.23	Frequency Response $\{H_{11}^{11}\}^3$ . . . . .	179
7.24	Frequency Response $\{H_{11}^{31}\}^3$ . . . . .	179
7.25	Frequency Response $\{H_{21}^{11}\}^3$ . . . . .	180
7.26	Frequency Response $\{H_{21}^{31}\}^3$ . . . . .	180
7.27	Frequency Response $\{H_{31}^{11}\}^3$ . . . . .	181
7.28	Frequency Response $\{H_{31}^{31}\}^3$ . . . . .	181
7.29	Frequency Response $\{H_{11}^{11}\}^3$ . . . . .	182
7.30	Second analytical model Test Rig I . . . . .	184
7.31	Frequency Response $\{H_{11}\}$ . . . . .	185
7.32	Frequency Response $\{H_{21}\}$ . . . . .	185
7.33	Frequency Response $\{H_{31}\}$ . . . . .	186
7.34	Frequency Response $\{H_{11}^{11}\}^3$ . . . . .	187
7.35	Frequency Response $\{H_{11}^{31}\}^3$ . . . . .	187
7.36	Frequency Response $\{H_{21}^{11}\}^3$ . . . . .	188
7.37	Frequency Response $\{H_{21}^{31}\}^3$ . . . . .	188
7.38	Frequency Response $\{H_{31}^{11}\}^3$ . . . . .	189
7.39	Frequency Response $\{H_{31}^{31}\}^3$ . . . . .	189
7.40	RK4 Rotor Kit . . . . .	191
7.41	System configuration . . . . .	192
7.42	Rigid bearing housing design . . . . .	194
7.43	Rigid bearing housing photograph . . . . .	195
7.44	Nonlinear bearing housing design . . . . .	196
7.45	Nonlinear bearing housing photograph . . . . .	197
7.46	Linear Test Rig II assembly . . . . .	198

---

7.47	Analytical linear model Test Rig II . . . . .	199
7.48	Frequency Response Function $H_{11}$ . . . . .	200
7.49	Frequency Response Function $H_{21}$ . . . . .	200
7.50	Frequency Response Function $H_{33}$ . . . . .	201
7.51	Frequency Response Function $H_{43}$ . . . . .	201
7.52	Test Rig II assembly . . . . .	202
7.53	Relationship between loading and deformation . . . . .	203
7.54	Static test setup . . . . .	204
7.55	Analytical assembly model Test Rig II . . . . .	205
7.56	Measured Frequency Response $H_{11}^{11}$ . . . . .	206
7.57	Measured Frequency Response $H_{11}^{31}$ . . . . .	206
7.58	Frequency Response $\{H_{11}^{11}\}^3$ for $0.5N$ . . . . .	208
7.59	Frequency Response $\{H_{11}^{31}\}^3$ for $0.5N$ . . . . .	208
7.60	Frequency Response $\{H_{11}^{11}\}^3$ for $1.0N$ . . . . .	209
7.61	Frequency Response $\{H_{11}^{31}\}^3$ for $1.0N$ . . . . .	209
7.62	Frequency Response $\{H_{11}^{11}\}^3$ for $1.5N$ . . . . .	210
7.63	Frequency Response $\{H_{11}^{31}\}^3$ for $1.5N$ . . . . .	210
C.1	Fitted curve in INV . . . . .	246
C.2	Fitted curve in SVD . . . . .	247
C.3	SVD and INV . . . . .	248
C.4	INV partitioned . . . . .	249
C.5	SVD and INV partitioned . . . . .	250
E.1	Two structures connected with one local nonlinear element . . . . .	265
E.2	Force applied in $x_1$ . . . . .	266
E.3	Force applied in $x_2$ . . . . .	267
E.4	Force applied in $x_3$ . . . . .	269
E.5	Force applied in $x_4$ . . . . .	271
E.6	Two linear structures with local nonlinear element . . . . .	273
E.7	Three linear structures with local nonlinear element and rigid connections	275

# Chapter 1

## Introduction

### 1.1 Introduction to the Problem

The ongoing demand for lighter structures and higher-speed machinery has introduced many vibration problems that can compromise the performance and reliability of the structures involved. The acceptable behaviour of a structure can be maximised by anticipating any performance-related problem during the design process. Design considerations in vibration involve adjusting the physical parameters of a structure to meet a required level of performance and reliability. Thus, in the design process, it is often desirable to be able to predict the dynamic response of a structure accurately under certain excitation conditions or to understand the effects of structural modifications in order to be able to make changes to solve possible vibration problems. In recent years, a range of techniques has been developed to help dynamic design and vibration analysis of complex structures, and these techniques represent the structure through models so that the dynamic properties of the structure can be studied. These models can be broadly categorised into Spatial Models, Modal Models and Response Models.

The spatial model is a theoretical model in which the differential equations of motion are obtained by a variety of methods. The two most prevalent methods are the transfer matrix approach used in some works [75, 76, 77] and the stiffness approach used in many others works [20, 44, 90]. One of the stiffness approaches is the finite element method (FEM) which has become the most popular modelling approach to

obtaining a spatial model. Although a complex structure can be modelled by FEM, the model derived has to be based on certain idealised assumptions and element representations and this results in an approximated model of the real structure and also generally requires the assembly and solution of large-order sets of ordinary differential equations for complex structures.

The modal model is also a theoretical model which is obtained by extracting dynamic properties from analytical or experimental frequency response function (FRF) measurements such as natural frequencies, mode shapes and damping ratios. Although the model obtained is much closer to the real assembly, called the physical model, it also shows discrepancies when comparing the vibration results between analytical and physical models, due to the fact that the mathematical model is derived from incomplete measurements and measurements with noise.

The response model is an analytical or experimental model characterised by the ratio of a response of the structure to the sinusoidal force. This model is often considered more promising for the representation of the physical model since it does not have any approximations due to idealisation or incompleteness of the measurements. However it still presents the problem of noise and systematic errors in the measurements.

Although the response model can be applied to a very complex structure, it is incompatible with the design process where design changes have to be made in prototypes and then evaluated until acceptable performance is obtained. Furthermore, most complex structures are obtained by assembling components or substructures designed by different engineering groups, at different times and in different locations. It is desirable, therefore, to be able to use an approach where such designs and modifications may proceed as independently as possible and accurate predictions of the total system behaviour obtained. The basic approach which has to be applied with this aim in mind is related to substructure analysis. In substructure analysis it is common to break down the whole structure into a number of components, or substructures, each of which is analysed individually using whichever method is the most convenient. The total system response is then obtained by appropriately coupling the dynamic characteristics for each component. This technique is very interesting

for industry since it spreads out the analysis and parallels the design process across different engineering groups leaving to each group the decision of which model best represents their components. Thus, engineers responsible for evaluating the total system dynamic performance can vary single components in the design and determine the effect of each change on the performance of the complete system with a high degree of confidence before the system is fully assembled.

Good results have been obtained with substructure analysis when the assembled structures are basically linear as shown by Urgueira [131]. On the other hand, improvements are required for other cases that are basically composed of linear substructures and a few nonlinear components mainly concentrated at the joints.

Substructure analysis of linear mechanical systems has been well known since the 1960s with the analytical work on the development of the Receptance Coupling concept published by Bishop and Johnson [10], and later on in the work on Component Mode Synthesis published by Hurty [61] whose formulation was simplified by Craig and Brampton [24].

Many different substructure methods for assembling linear structures have been developed and are usually referred to as "coupling techniques". Examples are impedance coupling, receptance coupling and coupling using measured data [32, 67, 100, 131].

Most of the analytical methods available to extract the spatial, modal and response models of structures are based on the assumption that the structure to be analysed is linear. The resultant models are frequently used for examining the dynamic response of linear structures [6, 31]. The accuracy of the dynamic response when using the spatial model depends heavily on the system idealisation and element representation whereas the modal model depends on the completeness of the original modal database of the structure. In spite of the fact that mathematical models can never completely describe real structures, due to model simplifications during discretisation process and parameter inaccuracies, they can be improved to give better representation of a structure under relevant conditions by applying a correlation of the analytical data with the experimental data, followed by a process known as model updating [98]. However, sometimes these mathematical models can not be improved if structural oddities, including nonlinearities, often present in most engineering struc-

tures are not incorporated into the model. For these structures the model can only be improved by including the structural oddities, therefore introducing nonlinear models. Although there are many sources of nonlinearity, most practical mechanical structures exhibit a certain degree of nonlinearity that can be found locally or globally. Global nonlinearity can be found in the stiffness of structures with large amplitude of vibration and/or nonlinear material properties. On the other hand, due to the nature of many structures which have been made up through the assembly of many components, local nonlinearities can be found in the complex stiffness in joints, microclearances in slides or bearings and nonlinear damping. If the nonlinearity can be localised and identified, a better definition of a model for the structure will be possible by defining a separate appropriate model for the nonlinearity and for the linear structure and then by combining both models to obtain the model of the complete structure.

In contrast with the well-known methods for linear structures, the methods available for analysis of nonlinear systems are generally very complicated, restricted to specific kinds of nonlinearity, applicable to systems with only a few degrees of freedom and incompatible with experimental modal analysis techniques [57], [65].

With the increasing interest in nonlinear structures, current efforts are being directed towards developing approaches to obtain nonlinear models. Although it is possible to obtain a nonlinear spatial model by using FEM for complex structures, the resultant analysis generally requires the assembly and solution of large order sets of ordinary differential equations. Yao [141], applied the FEM to obtain a reduced nonlinear spatial model. The large system of equations usually obtained with FEM is reduced to a very small set by applying a special transformation matrix. However, the method is not suitable for all dynamic problems especially when the excitation is random or transient. Nelson [90] applied the component mode synthesis method to reduce the order of the spatial model and then to obtain the response of nonlinear multi-shaft rotor-bearing systems. Although the analytical procedures of the standard methods available for obtaining the modal model can be applied in nonlinear modal analysis, they are based on the theory of linear systems and sometimes fail to give correct results when the system presents evidence of significant nonlinear behaviour. Various modal synthesis approaches have been applied to nonlinear dy-

dynamic analysis [87, 92], but these approaches still seem very costly for large nonlinear systems. Improvements in non-linear modal analysis have been achieved by Jezequel [64] extending the linear modal synthesis method by utilising the nonlinear modes initially introduced by Rosenberg [105] and later discussed and generalised by Szemplinska [119, 120]. This improvement however, cannot be applied to structures with close natural frequencies. On the other hand, Watanabe and Sato [136] succeeded in obtaining a first-order nonlinear response model by extending a linear coupling analysis method called the Building Block Approach (BBA) to a nonlinear coupling analysis method called the Nonlinear Building Block which uses a frequency-domain describing function to model the localised nonlinearity.

In general, there are many conditions that can influence the choice of the best model to represent a structure and therefore the dynamic properties of its components. However, one must realise that the method to be applied usually requires a specific model as an input. Therefore, it is necessary to be able to convert from one model to another. Conversion is possible, but sometimes results in approximations. The only conversion that does not necessarily involve any approximation is from the spatial and modal models to a response Model, as presented by Ewins [31]. Accordingly, there is considerable interest in methods that can predict the dynamics of an assembled structure using FRFs obtained from different models.

## 1.2 Review of Current State-of-the-Art

Engineering structures are often assembled from their components by using clamping devices or mechanisms. The dynamic behaviour of the assembled structures depends not only on the behaviour of the clamping mechanisms, but also on the properties of the connecting parts such as the roughness of the surfaces. Clamping mechanisms and connecting parts together are known as "joints". Although in coupling analysis, joints are usually represented analytically by linear models, they are generally the main source of nonlinearities and sometimes a nonlinear model is required. A typical example is the dynamic analysis of a rotor system with multiple bearings. The nonlinearity is concentrated in the bearing support and it is usually considered

as a linear model for small vibration amplitudes. Although the majority of rotating structures behave almost linearly for low amplitudes of motion when using journal bearings, there are many other situations where even with low vibration amplitudes a linearised model can be unsatisfactory in predicting the dynamic behaviour of the rotor-bearing structure. This can be found in rotating structures containing dry friction sliding surfaces, impacts due to contact between components and components that have material nonlinearities. In such cases, the frequency response functions are distorted and conventional methods do not lead to accurate models.

Usually, friction forces from dry friction dampers cause nonlinear behaviour and are the primary source of hysteresis, rather than material damping. Friction dampers are widely used in order to reduce resonant vibration amplitudes. The simplest interface representation is the well-known Coulomb friction model where the contact points do not move with respect to each other unless the friction force exceeds a certain limit. Den Hartog [25] was one of the first researchers to study the dynamic behaviour of structures with Coulomb friction, as shown in section 3.3.2. One of the most important properties of frictional joints is the relationship between loading and deformation, particularly in the tangential direction [140]. Goodman [52], Masuko [78] and Burdekin [16] have shown that slip can initiate at some parts of the interface before the gross slip occurs. This kind of slip, known as micro-slip, starts because the contact interface is neither flat nor completely smooth, but composed of a large number of tiny asperities. Burdekin [17] represented the asperities by equal stiffness prismatic rods, where each asperity behaves like a macro slip element but the combined effect is that of micro slip behaviour. Rogers [104] suggested an exponential curve to represent the observed load-displacement behaviour of the friction interfaces. Shoukry [112] derived an analytical expression to relate the parameters of the exponential curve to the design parameters. Later on Ren [140] pointed out that the contact interface consists of numerous tiny asperities that are different in size and stiffness.

Various models have been proposed to simulate the tangential force-deformation relationship of joints [17, 83, 112, 140]. Most of these models are assemblies of either the bilinear element [62] or the spherical contact element [86]. Ren [140] proposed a

new model based on the concept of stiffness area which assumes that a tiny area of the interface can be modelled by a bilinear friction element and this is presented in section 3.3.3. Sanliturk and Ewins [107] proposed a new approach to the modelling of two-dimensional behaviour of a point friction contact.

These models require certain parameters which need to be identified. Identification and response analysis of nonlinear structures are the two main fields in the study of nonlinear structures. There has been much research devoted to detecting and to identifying nonlinear characteristics in structures utilising frequency response functions obtained experimentally [5, 18, 30, 35, 58, 59, 66, 114, 125, 126, 127, 128, 134].

The most common approach to the analysis of nonlinear multiple degree-of-freedom (MDOF) systems is numerical integration and the dynamic response of structures is usually determined by time-integration of the system differential equations [1, 29, 53, 106]. The integration methods used to obtain steady-state analysis are computationally very expensive and aiming to overcome this problem, approximate frequency domain methods are being developed [19, 23, 33, 69, 70, 73, 88, 121, 122, 136, 139, 140]. In all these methods, the starting point of the analysis is the nonlinear ordinary differential equations of motion. These equations can be obtained by using discretisation techniques such as the Ritz-Galerkin Method, the Finite Element Method or the Modal Decomposition Method. In this differential equations, the localised nonlinearities can also be represented by either internal or external forces, although, for frequency-domain analysis the nonlinearities are found to be more appropriately represented by internal forces since the number of iterations at each frequency point is reduced significantly [108, 107]. Then the nonlinear differential equations are converted to a set of nonlinear algebraic equations. The approximate approaches utilise such techniques as the Perturbation Method [55], the Average Method [51], the Ritz-Galerkin Method [55], the Harmonic Balance Method [142], and the Describing Function Method [46]. The response of the system is obtained by solving the resulting simultaneous equations iteratively and this is achieved by applying a root-finding method such as Newton-Raphson [97], described in section 2.7. These approximate methods using the fundamental frequency component have been used by many researchers, estimating that the error due to neglecting the higher harmonic

components is generally small [73, 88, 121, 122, 136, 137, 139, 143]. Others have improved the results by including higher harmonics [23, 69, 70, 101, 135, 140].

Using structural assembly analysis methods, it is possible to predict the behaviour of the whole structure. The approaches dealing with this type of problem are known as "substructure synthesis", "substructuring", "building block" and "coupling" methods. These techniques can work with spatial models, modal models or response models. The response model can be analytically calculated or measured experimentally using techniques of modal analysis, or a mixture of both, and are usually referred as to "Frequency Response Function Methods".

Recent researchers have developed techniques to assemble two structures with nonlinear local elements. Basically, these are programs using the building block approach [67] extended for nonlinear analysis. A nonlinear building block using a frequency-domain describing function approach was proposed by Watanabe and Sato to evaluate the first-order frequency response characteristics of nonlinear structures systems [136], and this is summarised in section 4.4.2.

Some researchers have successfully applied substructure synthesis for analysis of nonlinear phenomena in rotor-bearing systems [50, 91].

### 1.3 Proposed Developments

This thesis is concerned with the development of an FRF substructure approach that can deal with vibration analysis of complex nonlinear engineering structures. Recent research has suggested methods which can generate nonlinear FRFs for linear systems with localised nonlinearities. These theoretical formulations are reviewed here in this thesis, and then implemented and improved by including higher harmonics and joint models for combined nonlinear effects. The nonlinearities are represented by internal forces using describing functions in order to reduce the number of iterations at each frequency point. The insights gained are applied to predict the response of complex nonlinear MDOF systems. The effectiveness of the method developed is illustrated through simulation and experimental analysis.

## 1.4 Summary of the thesis

Although the various phenomena of nonlinear oscillations have long been recognised by many scientists, the practical solution of nonlinear problems has only been stimulated by the growing development in computers. A large volume of investigation was carried out using the classical time domain techniques. However, as a means of obtaining the steady-state response solution, these methods are very time consuming. Current efforts are directed towards the development of new techniques to seek approximate solutions for the nonlinear vibration problem. The research presented in this thesis is intended to improve current coupling analysis methods for structural dynamic analysis and to develop a new generation of methods with special reference to nonlinear multi-degree-of-freedom systems. In Chapter 2 the basic theoretical vibration analysis of nonlinear structures is given which includes the linearisation concept, the modelling of nonlinear structures, the time-domain analysis, the frequency-domain harmonic analysis, the frequency-domain multi-harmonic analysis and the solution of a set of nonlinear algebraic equation by the Newton-Raphson Method. Chapter 3 reviews the most common joint models already available and develops the describing function concept. In Chapter 4, the standard linear impedance coupling methods with recent improvements are presented, and a coupling analysis notation is proposed. The methods currently available for analysing the vibration behaviour of coupled nonlinear structures are reviewed and the developed methods for coupling nonlinear structures are presented. Also presented are some refinements in the proposed methods in order to speed up the computational process. Moreover, special attention is given to the necessity of developing the multi-harmonic describing function over the high-order describing function. In Chapter 5 an intelligent nonlinear coupling analysis algorithm using object oriented language is presented. Various methods have been implemented and the performance of the proposed approach is demonstrated via various simulations reported in Chapter 6. In Chapter 7, the proposed coupling method is applied to two experimental test cases and special attention is paid to the measured frequency response functions of the nonlinear structures. The problems arising from the response of a shaker attached to a nonlinear structure are discussed and a solution is presented. The algorithm developed to control the force

is also discussed. Finally, in Chapter 8, all the new developments proposed in the thesis are brought together and recommendations for further work in this area are suggested.

## Chapter 2

# Types of Dynamic Analysis of Nonlinear Structures

### 2.0.1 Introduction

Over the years, numerical techniques have been developed continuously to reduce the time required to solve mathematical models which allow us to predict FRFs of nonlinear structures without compromising the accuracy of the analysis. This chapter first provides a classification of structures concerned with linear or nonlinear vibration behaviour. Then the generally established time- and frequency-domain dynamic analysis techniques to solve nonlinear problems are presented, with emphasis placed on approximate frequency-domain techniques for the harmonic and higher-harmonics analysis. Next, the definition of the ideal and measured first- and higher-order frequency response functions, which are the dynamic characteristic of a nonlinear structure, are introduced. Particular interest is placed here on the Describing Function and Harmonic Balance methods because these provide the mathematical basis for a new multi-harmonic describing function technique used in the development of the Multi-Harmonic Nonlinear Receptance Coupling approach described in Chapter 4. Finally, the Newton-Raphson method for solving the nonlinear equations of motion of the above techniques is presented in detail.

## 2.1 Nonlinear Structures

Most of the problems in mechanics exhibit a certain degree of nonlinearity but good linearisation solutions are quite satisfactory for most purposes. However, when the degree of nonlinearity is too high, linear treatments fail to give satisfactory results. Therefore it is necessary to classify the dynamic behaviour of the system in linear or nonlinear terms. The way to detect whether a system is to be categorised as linear or nonlinear can be based on the presence or the absence of the superposition characteristic. A system shows the superposition characteristic when doubling the input force results in doubling the vibration response and when the summation of the responses due to two independent inputs gives the same response as the summation of these two inputs individually. Simplified forms of the principle of superposition for categorisation of a system are based on the presence of homogeneity characteristics and correlation characteristics. A system displays the homogeneity characteristic when doubling the input force implies doubling the vibration response. A system shows the correlation characteristic when all the input energy in the structure is completely correlated with the output. Although these simplified forms give some indication of nonlinearity, they are a necessary but not sufficient condition for checking linearity. Linearity can only be fully determined by using the full principle of superposition. On the other hand, the simplified forms are very easily applied and usually used as a first check for nonlinearities. If the superposition characteristic is not present, the system is considered nonlinear. Therefore when the system is classified as nonlinear, nonlinear techniques must be available which permit the inclusion of nonlinear phenomena in the dynamic model description and the solution of the nonlinear equations of motion. The first technique used at the beginning of this century was the analytical solution of differential equations [57]. Although this can give an exact solution for simple cases, most nonlinear systems are complex, making it impossible to obtain an analytical closed-form solution. Thus, for a certain class of differential equations, where the nonlinear terms are associated with a small parameter, an approximate analytical solution can be obtained by developing the desired solution in a power series with respect to the small parameter. The important methods available to find approximate analytical solutions are (i) the perturbation method, (ii) the iteration method, (iii)

the averaging method and (iv) the harmonic balance method [57]. The application of these methods became possible with the invention of high-speed computers and was a breakthrough in the history of nonlinear dynamics. The computers encouraged the development of approximate numerical solutions to hitherto intractable analytical problems and also allowed the experimentation of the analytical solution in a way that was impossible before [144]. One of the first approximate numerical methods applied to solving nonlinear problems was the step-by-step numerical integration of the differential equation in the time domain [26, 27, 118]. Although this method generally gives accurate results, the procedure is usually extremely time-consuming. To overcome this problem, approximate frequency-domain methods have been developed instead [64, 136].

## **2.2 Modelling of Nonlinear Structures**

For many engineering applications, accurate mathematical models are required in order to predict effects due to structural modifications or to correct undesired high response levels. The precise derivation of a mathematical model can only be achieved firstly by choosing the right model assumptions and then selecting the right technique to solve the problem. Therefore, the first step is to check for the presence of nonlinear behaviour, so that a linear or nonlinear classification can be determined. Then a choice must be made either for an analytical model or discretised model. The last step is the application of the corresponding linear or nonlinear analysis based on the previous choice.

A better derivation of a nonlinear model can be obtained by studying all the information available about the particular nonlinearity. Usually, the source of a nonlinearity and its classification give a basic understanding of the nonlinearities involved. The source of the nonlinearity can be due to many different mechanisms. For example, measured damping is almost always nonlinear, although usually it is approximated as linear. This can be seen in a plot of force versus velocity [35]. Stiffness nonlinearity can be found in springs [136]. Boundary conditions can introduce nonlinearities into otherwise linear systems. An example is a beam which is clamped at one end and

has a clearance at the other end [88]. Some elements such as rubber and composites have nonlinear material elastic properties [84]. Systems with self-excitation such as dry friction have nonlinear behaviour [140]. Another nonlinear phenomenon often undetected is the internal resonance [13, 145]. Even rigid body systems like a crank mechanism are kinematically nonlinear. These and other nonlinearities can even be found together in the same structure [144]. The presence of nonlinearities can be regarded either as a useful characteristic or sometimes as an undesirable one. There are situations where nonlinearities are useful and even so designed. An example is the desired friction between the blades in the turbines of an aircraft engine [108]. On the other hand, there are situations where the same kind of nonlinearity can be awkward, for example, the undesired instability in steam turbines due to internal friction [68, 135].

Although there are large numbers of nonlinearities from different mechanisms, it is possible to classify the nonlinearities into a global nonlinear behaviour, such as material properties [103], and a local nonlinear behaviour, such as localised nonlinear springs [136]. Many of the localised nonlinear phenomena are due to a nonlinear interaction taking place between two connecting parts. The region between the two connected parts is usually known as a joint. A real mechanical structure usually consists of many components which are connected together through different joints such as bolted joints [45], riveted joints, welded joints, adhesive joints or any other clamping mechanism [108, 102]. Although the joints are very easily identified on the structure, a mathematical model of the joint is usually difficult to obtain [12, 45]. One way of obtaining a mathematical model of a joint is by finding the relationship between an external excitation force applied to the joint and the response [17]. For a linear joint, the force-response relation can be expressed by equation (2.1).

$$f(\ddot{x}, \dot{x}, x) = m\ddot{x} + c\dot{x} + kx \quad (2.1)$$

However, for a nonlinear joint the relation becomes much more complicated and is difficult to generalise. An example of a force-response relationship of a nonlinear joint where the mass varies with time, the damping varies with velocity and the stiffness varies with displacement can be expressed by equation (2.2).

$$\mathbf{f}(t, \ddot{x}, \dot{x}, x) = m(t)\ddot{x} + c(\dot{x})\dot{x} + k(x)x \quad (2.2)$$

The model validation of a joint is done by correlating the analytical model with measured dynamic test data, since most structural nonlinearities cannot be predicted from geometrical information alone and therefore can only be measured. Furthermore, as stated before, the more information known about the nonlinearities is known, the better the analytical model derived will be [56].

Once the structure is classified as nonlinear, it becomes necessary to choose which kind of model is to be used to represent its dynamic behaviour. The dynamic behaviour of the structure can be represented by an analytical model or by a discretised model. Although analytical models can give accurate solutions, for complicated practical structures it is extremely difficult to find such solutions. Therefore discrete approximate models are usually used instead. Three different models can be used for discretisation of structures, spatial models, modal models and response models. Although any of the models can be used to represent a structure, there is usually one model that is more appropriate than the others for the representation [64, 110, 136].

## 2.3 Time-Domain Analysis

### 2.3.1 Introduction

Although the main concern in this thesis is to develop an approximate method that can be used to examine the dynamic behaviour of nonlinear structures, a time-domain vibration analysis is required to assess the advantages and shortcomings of the approximate frequency-domain methods which have been developed [9]. Here, time-domain methods serve as a reference and are often referred as "exact" methods owing to their high degree of accuracy in nonlinear analysis.

Since a global mathematical model is derived, different methods can be used to predict the system's vibration response under certain external excitation conditions. If the derived mathematical model is in a spatial form, the differential equation of motion is known and therefore a solution can be obtained. In structural vibration, most of the mathematical models are described in terms of second-order differential

equations. The analytical solution of these differential equations can sometimes be so complicated that a numerical solution is used instead. The time-domain integration method is among the many procedures used to solve second-order differential equations which describe a structure subject to a well-defined excitation [26, 27]. Although the exact methods can be used to predict the response of linear structures, they are applied only when required due to its very low computational efficiency. Therefore, they are much more used for problems that involve nonlinearities. As stated before, they are a very useful tool to evaluate other approximate methods.

A practical numerical method for solving ordinary differential equations is the Runge-Kutta method [97]. This is a very well-known method because no knowledge is required about the nonlinear structure and it virtually always succeeds with reasonable precision.

### 2.3.2 Runge-Kutta Method

The basic idea of the Runge-Kutta integration method is to find a solution for the equilibrium equation at a discrete time point. In the case of a dynamic engineering structure, the equilibrium equation can be described by a set of second-order differential equations (2.3).

$$[M]\{\ddot{x}\} + [C]\{\dot{x}\} + i[D]\{x\} + [K]\{x\} + \{\mathbf{f}\} = \{f\} \quad (2.3)$$

Integration of equation (2.3) by the Runge-Kutta method involves first reducing the second-order differential equation into a first-order differential equation by rewriting it as two first-order equations (2.4).

$$\begin{aligned} \{\dot{x}\} &= \{u\} \\ [M]\{\dot{u}\} + [C]\{u\} + i[D]\{x\} + [K]\{x\} + \{\mathbf{f}\} &= \{f\} \end{aligned} \quad (2.4)$$

The equation (2.4) can be rewritten in matrix form as shown in equation (2.5).

$$\begin{bmatrix} [M] & 0 \\ 0 & [I] \end{bmatrix} \begin{Bmatrix} \dot{u} \\ \dot{x} \end{Bmatrix} + \begin{bmatrix} [C] & [K] + i[D] \\ [I] & 0 \end{bmatrix} \begin{Bmatrix} u \\ x \end{Bmatrix} = \begin{Bmatrix} f - \mathbf{f} \\ 0 \end{Bmatrix} \quad (2.5)$$

Thus, the ordinary differential equation (2.3) is reduced to a coupled first-order differential equation (2.5) which has the explicit form shown by equation (2.6),

$$\left\{ \dot{z} \right\} = \left\{ f(t, z) \right\} \quad (2.6)$$

where  $\{f(t, z)\}$  is known and given by equation (2.7),

$$\left\{ f(t, z) \right\} = \left[ \begin{array}{cc} [M] & 0 \\ 0 & [I] \end{array} \right]^{-1} \left( \left\{ f - \mathbf{f} \right\} - \left[ \begin{array}{cc} [C] & [K] + i[D] \\ [I] & 0 \end{array} \right] \left\{ z \right\} \right) \quad (2.7)$$

and the displacement  $\{z\}$  is given by equation (2.8).

$$\left\{ z \right\} = \left\{ \begin{array}{c} \dot{x} \\ x \end{array} \right\} = \left\{ \begin{array}{c} u \\ x \end{array} \right\} \quad (2.8)$$

The procedure of the integration methods is that given the initial value  $\{z\}_n$  for a starting time value  $t_n$ , the approximate solution  $\{z\}_{n+1}$  at some final point  $t_{n+1}$  or at some discrete list of points stepped by stepsize intervals  $\delta t$  can be found. In the Runge-Kutta method, the solution is propagated over the interval  $\delta t$  from  $\{z\}_n$  to  $\{z\}_{n+1}$  by combining the information from several smaller steps, each one involving the evaluation of the right-hand side of equation (2.7), and then using the information obtained to match a Taylor series expansion up to some higher order. Then the solution for the next step interval is treated in an identical manner. The fact that no prior behaviour of the solution is used in its propagation, allows any point along the trajectory of an ordinary differential equation to be used as an initial point. The classical fourth-order Runge-Kutta formula is by far the most often used. In each step the derivative is evaluated four times, once at the initial point, twice at trial point and once at a trial endpoint. From these derivatives the final function value is calculated as shown in equation (2.9),

$$\{z\}_{n+1} = \{z\}_n + \frac{h}{6}\{k_1\} + \frac{h}{3}\{k_2\} + \frac{h}{3}\{k_3\} + \frac{h}{6}\{k_4\} \quad (2.9)$$

where:

$$\begin{aligned}
 \{k_1\} &= \{f(t_n, \{z_n\})\} \\
 \{k_2\} &= \{f(t_n + \frac{h}{2}, \{z_n + \frac{k_1}{2}\})\} \\
 \{k_3\} &= \{f(t_n + \frac{h}{2}, \{z_n + \frac{k_2}{2}\})\} \\
 \{k_4\} &= \{f(t_n + h, \{z_n + k_3\})\} \\
 z &= \text{step increment}
 \end{aligned}
 \tag{2.10}$$

## 2.4 Frequency-Domain Analysis

### 2.4.1 Introduction

The steady-state dynamic response of a multi-degree of freedom nonlinear structure is usually determined by numerical integration of the equations of motion [26, 27]. Although very high accuracy can be obtained from time-marching analysis, the computational efficiency can be of concern. Generally, the time required depends on the level of precision aimed at and also on the characteristics of the structure such as damping, highest natural frequency of interest and the size of the theoretical model. The level of precision is related to the time step used in the integration. For high level accuracy, a small fraction of the period that corresponds to the highest natural frequency of interest must be used. The damping has influence in the transient response of the structure. The low damping levels in some dynamic structures imply very long transients. The size of the model has a direct influence on the time spent for integration. Consequently, long transients combined with small time steps and large numbers of degrees-of-freedom result in a very costly computational procedure for steady-state response analysis. Therefore, special attention has been focused on alternative, frequency-domain approximate methods for determining the steady-state response of structures, particularly to periodic external excitation, in which there is no need for analysis of transient motion. These approximate linearised methods use techniques that convert the nonlinear differential equations of motion, derived from the application of a selected model procedure, into nonlinear algebraic equations. These techniques are known as "harmonic balance" in mechanical engineering [57] and "describing function" in electrical and control engineering [47, 113]. The concept of linearisation in these techniques differs from the so-called "true" linearisation in

its basic assumptions. The true linearised methods are applied only for small oscillations, imposing restrictions on the amplitude of vibration. By contrast, with the approximate linearised methods there is no restriction on the amplitude of vibration, thus allowing for vibration analysis of systems that have high levels of response. Furthermore, a true-linearisation model follows the linear theory of superposition and the approximate linearised methods exhibit the response dependency of the input that is the basic characteristic of nonlinear behaviour. Besides these advantages, the approximate linearised methods have some limitations. One important limitation is related to the hypotheses assumed for the excitation. Thus once the excitation has sinusoidal form, the method can only be applied for obtaining a periodic solution of a nonlinear differential equation.

### 2.4.2 Analysis

Considering a nonlinear structure subject to an external excitation, the matrix differential equation of motion derived by the spatial model procedure can be written as:

$$[M]\{\ddot{x}\} + [C]\{\dot{x}\} + i[D]\{x\} + [K]\{x\} + \{\mathbf{f}\} = \{f\} \quad (2.11)$$

Assuming the external excitation to be a sinusoidal force, then  $\{f(t)\}$  can be written as:

$$\{f(t)\} = \{F\}e^{i\omega t} = \{F\}e^{i\tau} \quad (2.12)$$

When a nonlinear system is subjected to a sinusoidal excitation, the response is generally not exactly sinusoidal. Often, the response is periodic, having a period the same as that of the excitation and can be represented by Fourier series written as:

$$\{x(t)\} = \sum_{m=0}^{\infty} \{x^m(t)\} = \sum_{m=0}^{\infty} \{X^m\}e^{im\omega t} = \sum_{m=0}^{\infty} \{X^m\}e^{im\tau} \quad (2.13)$$

where subscript  $m$  indicates the  $m_{th}$  harmonic order and  $\{x^m\}$  is the  $m_{th}$  displacement response order. Then the complex displacement response amplitude  $X$  at coordinate  $j_{th}$  in the  $m_{th}$  harmonic,  $X_j^m$ , can be written as

$$X_j^m = \bar{X}_j^m e^{i\phi_j^m} \quad (2.14)$$

where  $\bar{X}_j^m$  is the magnitude and  $\phi_j^m$  is the phase of the complex displacement  $X_j$  at harmonic  $m$ .

Assuming that the response  $\{x(t)\}$  in equation (2.13) can be well approximated by a set,  $Q$ , of  $p$  harmonic terms written as:

$$Q = \{q_1, q_2, \dots, q_p\} \quad (2.15)$$

or by  $Q_r$ , a subset of  $Q$ , composed of its first  $r$ -elements defined as:

$$Q_r = \{q_1, q_2, \dots, q_r\} \text{ for } 1 \leq r \leq n \quad (2.16)$$

then the approximate time response  $\{\tilde{x}^{(q_r)}(t)\}$  can be written as:

$$\{x(t)\} \approx \{\tilde{x}^{(q_r)}(t)\} = \sum_{m=q_1}^{q_r} \{x^m(t)\} \quad (2.17)$$

Similarly, the inter-coordinate relative displacement response  $y$  between coordinates  $k$  and  $l$ ,  $y_{kl}$ , can be represented as:

$$y_{kl} = x_k - x_l = \sum_{m=0}^{\infty} y_{kl}^m = \sum_{m=0}^{\infty} Y_{kl}^m e^{im\tau} \quad (2.18)$$

and the approximate response  $\{\tilde{y}_{kl}^{(q_r)}\}$  can be written as:

$$\{y_{kl}\} \approx \{\tilde{y}_{kl}^{(q_r)}\} = \sum_{m=q_1}^{q_r} \{y_{kl}^m\} = \sum_{m=q_0}^{q_r} Y_{kl}^m e^{im\tau} \quad (2.19)$$

where:

$$\begin{aligned} Y_{kl}^m &= X_k^m - X_l^m, \quad (k \neq l) \\ Y_{kl}^m &= \bar{Y}_{kl}^m e^{i\psi_{kl}^m} \end{aligned} \quad (2.20)$$

If the variable  $y_{kl}$  in the nonlinear function  $\mathbf{f}_{kl}(y_{kl})$  has the form assumed in (2.19), the nonlinear function  $\mathbf{f}_{kl}(\tilde{y}_{kl}^{(q_r)})$  is complex and is also a periodic function of time. Then the nonlinear function  $\mathbf{f}_{kl}(\tilde{y}_{kl}^{(q_r)})$  can be expressed by a Fourier series as:

$$\mathbf{f}_{kl}(\tilde{y}_{kl}^{(q_r)}) = \sum_{m=0}^{\infty} \mathbf{f}_{kl}^m = \sum_{m=0}^{\infty} \mathcal{F}_{kl}^m e^{im\tau} \quad (2.21)$$

where:

$$\begin{aligned}
\mathcal{F}_{kl}^m &= \bar{\mathcal{F}}_{kl}^m e^{i\varphi_{kl}^m} \\
\mathcal{F}_{kl}^0 &= \frac{1}{2\pi} \int_0^{2\pi} \mathbf{f}(\tilde{y}_{kl}^{(q_r)}) d\tau \\
\mathcal{F}_{kl}^m &= \frac{1}{\pi X} \int_0^{2\pi} \mathbf{f}(\tilde{y}_{kl}^{(q_r)}) e^{-im\tau} d\tau, \quad (m \geq 1)
\end{aligned} \tag{2.22}$$

The Fourier series written in complex form (2.21) can be expressed as a function of *sin* and *cos*:

$$\sum_{m=0}^{\infty} \mathcal{F}_{kl}^m e^{im\tau} = A_{kl}^0 + \sum_{m=0}^{\infty} (A_{kl}^m \cos(n\tau) + B_{kl}^m \sin(n\tau)) \tag{2.23}$$

where:

$$\begin{aligned}
A_{kl}^0 &= \frac{1}{2\pi} \int_0^{2\pi} f(\tilde{y}_{kl}^{(q_r)}) d\tau \\
A_{kl}^1 &= \frac{1}{\pi} \int_0^{2\pi} f(\tilde{y}_{kl}^{(q_r)}) \sin\tau d\tau \\
B_{kl}^1 &= \frac{1}{\pi} \int_0^{2\pi} f(\tilde{y}_{kl}^{(q_r)}) \cos\tau d\tau \\
A_{kl}^2 &= \frac{1}{\pi} \int_0^{2\pi} f(\tilde{y}_{kl}^{(q_r)}) \sin 2\tau d\tau \\
B_{kl}^2 &= \frac{1}{\pi} \int_0^{2\pi} f(\tilde{y}_{kl}^{(q_r)}) \cos 2\tau d\tau \\
&\vdots
\end{aligned}$$

Assuming that the function  $\mathbf{f}_{kl}(\tilde{y}_{kl}^{(q_r)})$  can also be well approximated by *s* harmonic terms given by a subset  $Q_s$ , of the set defined in equation (2.15), written as:

$$Q_s = \{q_1, q_2, \dots, q_s\} \text{ for } 1 \leq s \leq n \tag{2.24}$$

then the approximate nonlinear function  $\tilde{\mathbf{f}}_{kl}^{(q_s)}(\tilde{y}_{kl}^{(q_r)})$  can be written as:

$$\tilde{\mathbf{f}}_{kl}^{(q_s)}(\tilde{y}_{kl}^{(q_r)}) = \sum_{m=q_1}^{q_s} \mathbf{f}_{kl}^m = \sum_{m=q_1}^{q_s} \mathcal{F}_{kl}^m e^{im\tau} \tag{2.25}$$

## 2.5 Frequency-Domain Harmonic Analysis

### 2.5.1 Fundamental Harmonic Analysis

For a nonlinear structure subject to an external excitation, the matrix differential equation of motion derived by the spatial model procedure can be written as:

$$[M]\{\ddot{x}\} + [C]\{\dot{x}\} + i[D]\{x\} + [K]\{x\} + \{f\} = \{f\} \quad (2.26)$$

Assuming the external excitation as a sinusoidal excitation, then  $\{f(t)\}$  can be written as:

$$\{f(t)\} = \{F\}e^{i\omega t} = \{F\}e^{i\tau} \quad (2.27)$$

then the steady-state solution can be represented by a Fourier series as:

$$\{x(t)\} = \sum_{m=0}^{\infty} \{x^m\} = \sum_{m=0}^{\infty} \{X^m\}e^{im\omega t} = \sum_{m=0}^{\infty} \{X^m\}e^{im\tau} \quad (2.28)$$

When the higher harmonic terms of the response have small amplitudes relative to the fundamental component, the response is dominated by the fundamental component of the Fourier series for  $x(t)$ . Thus, the response  $\{x(t)\}$  can be written as:

$$\{x\} \approx \{\tilde{x}^{(1)}\} = \{x^1\} = \{X^1\}e^{i\tau} \quad (2.29)$$

and the response  $x$  at a general coordinate  $j$  can be written as:

$$x_j \approx \tilde{x}_j^{(1)} = x_j^1 = X_j^1 e^{i\tau} \quad (2.30)$$

where the complex displacement response  $X_j^1$  can be written as:

$$X_j^1 = \bar{X}_j^1 e^{i\phi_j^1} \quad (2.31)$$

Similarly, the inter-coordinate relative displacement response  $y$  between coordinates  $k$  and  $l$  can be represented as:

$$y_{kl} = x_k - x_l \approx \tilde{y}_{kl}^{(1)} = y_{kl}^1 = Y_{kl}^1 e^{i\tau} \quad (2.32)$$

where:

$$\begin{aligned} Y_{kl}^1 &= X_k^1 - X_l^1, \quad (k \neq l) \\ Y_{kl}^1 &= \bar{Y}_{kl}^1 e^{i\psi_{kl}^1} \end{aligned} \quad (2.33)$$

The assumed solution  $y_{kl}$  in equation (2.32) is then inserted in the nonlinear function  $\mathbf{f}_{kl}(y_{kl})$ , resulting in a nonlinear force  $\mathbf{f}_{kl}(\tilde{y}_{kl}^1)$  that can also be expanded by a Fourier series and expressed in complex form as:

$$\mathbf{f}_{kl}(\tilde{y}_{kl}^1) = \sum_{m=0}^{\infty} (\mathbf{f}_{kl})^m = \sum_{m=0}^{\infty} \mathcal{F}_{kl}^m e^{im\tau} \quad (2.34)$$

where:

$$\begin{aligned} (\mathcal{F}_{kl})^m &= \bar{\mathcal{F}}_{kl}^m e^{i\varphi^m} \\ (\mathcal{F}_{kl})^0 &= \frac{1}{2\pi} \int_0^{2\pi} \mathbf{f}(\tilde{y}_{kl}^1) d\tau \\ (\mathcal{F}_{kl})^m &= \frac{1}{\pi} \int_0^{2\pi} \mathbf{f}(\tilde{y}_{kl}^1) e^{-im\tau} d\tau, \quad (m \geq 1) \end{aligned} \quad (2.35)$$

Assuming now that the nonlinear force  $\mathbf{f}_{kl}(\tilde{y}_{kl}^1)$  is also dominated by its fundamental term, then the approximate nonlinear force  $\tilde{\mathbf{f}}_{kl}^{(1)}(\tilde{y}_{kl}^1)$  can be written as:

$$\mathbf{f}_{kl}(y_{kl}) \approx \tilde{\mathbf{f}}_{kl}^{(1)}(\tilde{y}_{kl}^1) = \mathcal{F}_{kl}^1 e^{i\tau} = A_{kl}^1 \cos(n\tau) + B_{kl}^1 \sin(n\tau) \quad (2.36)$$

where:

$$\begin{aligned} A_{kl}^1 &= \frac{1}{\pi} \int_0^{2\pi} \mathbf{f}_{kl}(\tilde{y}_{kl}^1) \sin\tau d\tau \\ B_{kl}^1 &= \frac{1}{\pi} \int_0^{2\pi} \mathbf{f}_{kl}(\tilde{y}_{kl}^1) \cos\tau d\tau \end{aligned}$$

### 2.5.2 First-Order Frequency Response Functions

In concept, the first-order frequency response functions are an extension of the frequency response functions of linear structures to nonlinear structures. In the case of a pure sinusoidal excitation, the first-order frequency response function of a nonlinear structure is defined as the spectral ratio of the response  $x_i$  and the force  $f_j$  at the frequency of excitation,  $\omega$ , written as:

$$(H_{ij}^{11}(\omega))^{(q_r)} = \frac{X_i^1}{F_j^1} \quad (2.37)$$

In this case, only the fundamental frequency component of the response  $x$  composed of  $r$  harmonics is retained and all the subharmonics, superharmonics and combinations of both are ignored.

### 2.5.3 Harmonic Balance Method

The Harmonic Balance Method (HBM) is frequently used for the analysis of periodic oscillations of nonlinear systems [39, 81, 82, 108, 109] as an alternative to its expensive time-marching counterpart. The basis of the method is described below.

Assuming a nonlinear system subjected to harmonic excitation,  $\{F^1\}$ , the system differential equation can be written, as before, as:

$$[M]\{\ddot{x}\} + [C]\{\dot{x}\} + i[D]\{x\} + [K]\{x\} + \{\mathbf{f}(\{x\}, \{\dot{x}\})\} = \{F^1\}e^{i\omega t} \quad (2.38)$$

The steady-state solution for  $x(t)$  can be represented by a Fourier series as:

$$\{x(t)\} = \sum_{m=0}^{\infty} \{x^m\} = \sum_{m=0}^{\infty} \{X^m\}e^{im\tau} \quad (2.39)$$

Considering the response to be dominated by the fundamental component of the Fourier series, then it is assumed that the response  $\{x(t)\}$  can be approximate by the fundamental component,  $\{x^1(t)\}$  written as:

$$\{x(t)\} \approx \{\tilde{x}^{(1)}(t)\} = \{x^1(t)\} = \{X^1\}e^{im\tau} \quad (2.40)$$

and the response  $x$  at a general coordinate  $j$  can be written as:

$$x_j \approx \tilde{x}_j^{(1)} = x_j^1 = \bar{X}_j^1 e^{i\phi_j^1} = C_j^1 + iD_j^1 \quad (2.41)$$

where:

$$\begin{aligned} C_j^1 &= \bar{X}_j^1 \sin(\phi_j^1) \\ D_j^1 &= \bar{X}_j^1 \cos(\phi_j^1) \end{aligned} \quad (2.42)$$

The nonlinear force can be approximate by the fundamental component in its Fourier series written as:

$$\mathbf{f}_{kl}(y_{kl}) \approx \tilde{\mathbf{f}}_{kl}^{(1)}(\tilde{y}_{kl}^1) = \mathbf{f}_{kl}^1 = \mathcal{F}_{kl}^1 e^{i\tau} = A_{kl}^1 \cos(n\tau) + B_{kl}^1 \sin(n\tau) \quad (2.43)$$

where:

$$\begin{aligned} A_{kl}^1 &= \frac{1}{\pi} \int_0^{2\pi} \mathbf{f}_{kl}(\tilde{y}_{kl}^{(1)}) \sin n\tau d\tau \\ B_{kl}^1 &= \frac{1}{\pi} \int_0^{2\pi} \mathbf{f}_{kl}(\tilde{y}_{kl}^{(1)}) \cos n\tau d\tau \end{aligned}$$

Substituting the fundamental component of response given by equation (2.40) and the fundamental component of nonlinear force given by equation (2.43) into the nonlinear differential equation (2.38), yields:

$$[[K] - [M]\omega^2 + i\omega[C] + i[D]]\{X^1\} = \{F^1\} - \{\mathcal{F}^1\} \quad (2.44)$$

The solution of the response is based on finding the fundamental linear coefficients  $C_j^1$  and  $D_j^1$  for the response and  $A_{kl}^1$  and  $B_{kl}^1$  for the nonlinear force in which all the fundamental harmonic forces in equation (2.44) are balanced by each other. Different iterative methods are available to solve this kind of mathematical problem.

### 2.5.4 Describing Functions

In nonlinear system analysis, the describing function method is frequently used where the system response may exhibit periodic oscillations close to a pure sinusoid. The theoretical basis of this describing function is related to the Van der Pol method of slowly-varying coefficients [132] and to the method of equivalent linearisation proposed by Bogoliubov and Mitroposky [11], both developed to solve nonlinear problems. Recently, Watanabe and Sato investigated the effects of nonlinear stiffness by developing a modal analysis approach [137] where the nonlinearity is substituted by the equivalent first-order describing function. Later, they applied the describing function method to extend the Building Block Approach (BBA) developed for coupling linear structures to obtain the Nonlinear Building Block Approach (NLBBA) developed for coupling nonlinear structures having local nonlinearities [136]. Murakami and Sato experimentally applied the NLBBA method to evaluate the frequency response characteristics of a beam with support-accompanying clearance [88]. Tanrikulu et al. proposed a new spatial frequency domain method for fundamental harmonic response analysis of structures with general symmetrical nonlinearities using the describing function method [122]. Kuran and Ozguven developed a modal superposition method for nonlinear structures based on internal nonlinear forces expressed in matrix form by using describing functions [70].

The describing function method linearises the nonlinearity by defining the transfer function as the relation of the fundamental components of the input and the output to the nonlinearity. In order to present the concept of the describing function method, consider an SDOF system with a nonlinear restoring force driven by a sinusoidal excitation written as:

$$M\ddot{x} + C\dot{x} + Kx + \mathcal{F}(x, \dot{x}) = A \sin\omega t \quad (2.45)$$

To solve the proposed problem by the describing function method it is required to assume that the variable  $x$  appearing in the nonlinear function  $\mathcal{F}(x, \dot{x})$  is sufficiently close to a sinusoidal oscillation expressed as:

$$x \approx X^1 \sin(\omega t + \phi) = X^1 \sin\tau \quad (2.46)$$

where  $X^1$  is a complex response amplitude,  $\omega$  is the excitation frequency and  $\phi$  is phase angle.

If the variable  $x$  in the nonlinear function  $\mathcal{F}(x, \dot{x})$  has the sinusoidal form assumed in (2.46), the nonlinear function  $\mathcal{F}(x, \dot{x})$  is complex and is also a periodic function of time. Defining now the describing function  $\nu$  as the optimum equivalent linear complex stiffness representation of the nonlinear force  $\mathcal{F}(x, \dot{x})$  for the harmonic response  $X^1$ , the coefficients of the describing function  $\nu(x, \dot{x})$  can be obtained from an expansion of the nonlinear function  $\mathcal{F}(x, \dot{x})$  by a Fourier series as:

$$\mathcal{F}(x, \dot{x}) \approx \tilde{\mathcal{F}}(x, \dot{x}) = (\nu(x, \dot{x}))x = N^1x + jN_2x + \dots \quad (2.47)$$

where the corresponding coefficients of the describing function are:

$$\begin{aligned} N_1 &= \frac{1}{\pi X} \int_0^{2\pi} \mathcal{F}(X^1 \sin\tau, \omega X^1 \cos\tau) \sin\tau d\tau \\ N_2 &= \frac{1}{\pi X} \int_0^{2\pi} \mathcal{F}(X^1 \sin\tau, \omega X^1 \cos\tau) \cos\tau d\tau \\ N_3 &= \frac{1}{\pi X} \int_0^{2\pi} \mathcal{F}(X^1 \sin\tau, \omega X^1 \cos\tau) \sin 2\tau d\tau \\ N_4 &= \frac{1}{\pi X} \int_0^{2\pi} \mathcal{F}(X^1 \sin\tau, \omega X^1 \cos\tau) \cos 2\tau d\tau \\ &\vdots \end{aligned} \quad (2.48)$$

Assuming now that the nonlinear force  $\mathcal{F}(x, \dot{x})$  is also dominated by its fundamental term, then it can be simplified by its first harmonic component,  $\mathcal{F}^1(x, \dot{x})$ , as:

$$\mathcal{F}(x, \dot{x}) \approx \mathcal{F}^1(x, \dot{x}) = N_1x + jN_2x \quad (2.49)$$

and the first-order describing function can be written as:

$$\nu^1(x, \dot{x}) = N_1 + jN_2 \quad (2.50)$$

If the kind of nonlinearity in  $\mathcal{F}(x, \dot{x})$  is known, a describing function  $\nu$  can be calculated from equations (2.48) and (2.50). An important nonlinearity to be analysed is the cubic stiffness, because many nonlinear physical systems exhibit a behaviour

of forces proportional to cube of displacement. Therefore the case chosen to demonstrate the describing function is composed of a spring whose stiffness has a cubic nonlinearity. Here, the nonlinear force can be written as:

$$\mathcal{F}(x) = K_0x + \beta x^3 \quad (2.51)$$

Substituting the nonlinear function (2.51) into the equation (2.48), the coefficients of the describing function (2.48) can be written as:

$$\begin{aligned} N_1 &= \frac{1}{\pi X^1} \int_0^{2\pi} (K_0x + \beta x^3) \sin\tau d\tau \\ N_2 &= 0 \end{aligned} \quad (2.52)$$

Substituting equation (2.46) into (2.52),

$$N_1 = \frac{1}{\pi X^1} \int_0^{2\pi} (K_0X^1 \sin\tau + \beta X^{1^3} \sin^3\tau) \sin\tau d\tau \quad (2.53)$$

and splitting equation (2.53) into two integrals,

$$N_1 = \frac{1}{\pi X^1} \int_0^{2\pi} K_0X^1 \sin^2\tau d\tau + \frac{1}{\pi X^1} \int_0^{2\pi} \beta X^{1^3} \sin^4\tau d\tau \quad (2.54)$$

then equation (2.54) can be written as:

$$N_1 = \frac{K_0}{\pi} A + \frac{\beta X^{1^2}}{\pi} B \quad (2.55)$$

where:

$$\begin{aligned} A &= \int_0^{2\pi} \sin^2\tau d\tau \\ B &= \int_0^{2\pi} \sin^4\tau d\tau \end{aligned} \quad (2.56)$$

The solution of both integrals,  $A$  and  $B$ , are easily calculated, resulting in:

$$A = \int_0^{2\pi} \sin^2\tau d\tau = \pi$$

$$B = \int_0^{2\pi} \sin^4 \tau d\tau = \frac{3}{4}\pi \quad (2.57)$$

Substituting equation (2.57) in (2.55), yields:

$$N^1 = K_0 + \frac{3}{4}\beta X^{1^2} \quad (2.58)$$

Therefore, the nonlinear force and the approximate nonlinear force represented by the describing function can be written as:

$$\mathcal{F}(x) = K_0 x + \beta x^3 \approx \tilde{\mathcal{F}}^{(1)}(x) = \nu^1(x)x = (K_0 + \frac{3}{4}\beta X^{1^2})x \quad (2.59)$$

Substituting equation (2.46) into equation (2.59), yields:

$$K_0 X^1 \sin \tau + \beta X^{1^3} \sin^3 \tau \approx (K_0 + \frac{3}{4}\beta X^{1^2})X^1 \sin \tau \quad (2.60)$$

From equation (2.60) it is possible to see that the nonlinear function  $\mathcal{F}(x)$  has a linear term  $\sin \tau$  and a nonlinear term  $\sin^3 \tau$ , whereas the describing function has only the linear approximate term  $\sin \tau$ . Figure 2.1 shows the overlay of nonlinear function  $\mathcal{F}(x)$  and the approximate nonlinear force represented by the describing function,  $\nu^1(x)$ .

Substituting now the assumed response solution given by equation (2.46) and the approximate nonlinear force given by equation (2.59) into the nonlinear differential equation (2.45), yields:

$$(K - \omega^2 M + i\omega C + iD + \nu^1(x))X^1 = F \quad (2.61)$$

The describing function coefficients of some of the most common nonlinearities can be found tabulated in [74].

After establishing the describing function, the system of nonlinear differential equations involved in the coupling analysis is converted in a system of nonlinear algebraic equations, where a solution can be obtained by any of several different iterative methods available to solve this kind of mathematical problem.

The describing function method may be regarded as an application of the har-

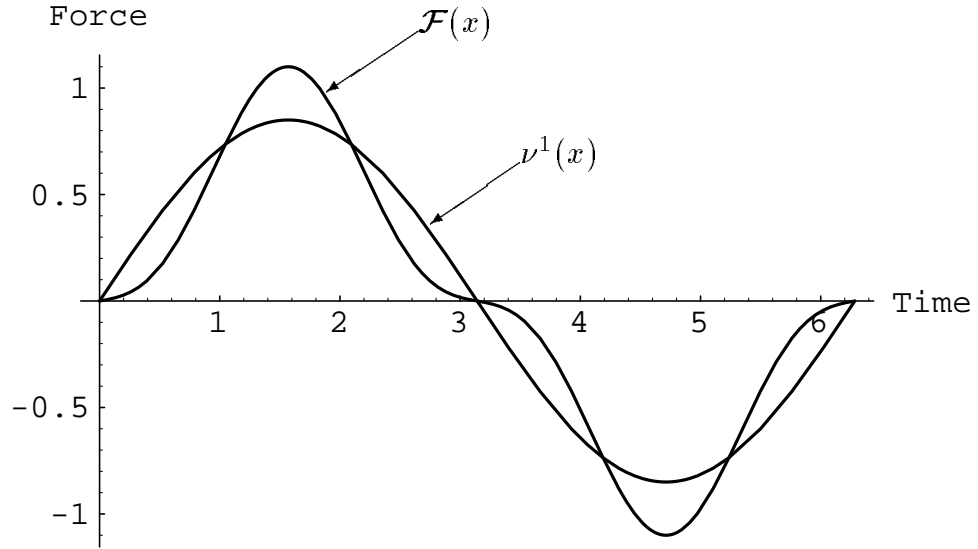


Figure 2.1: Nonlinear function  $\mathcal{F}(x)$  and describing function  $\nu^1(x)$

monic balance method. A small difference in application can be noticed in the final system of nonlinear algebraic equations obtained. In the harmonic balance method the nonlinear force is modelled as an external force, equation (2.44), and in the describing function method the nonlinear force is modelled as an internal force, equation (2.61). However, the describing function can also be applied as an external force [139].

## 2.6 Frequency-Domain Multi-Harmonic Analysis

### 2.6.1 Multi-Harmonic Analysis

Harmonics are frequency components which are multiples of the fundamental input frequency. When a structure is highly nonlinear then it is important not to neglect the effects of these higher-order terms. In multi-harmonic analysis, the response of a structure subject to simple harmonic excitation can be written as:

$$\{x\} \approx \{\tilde{x}^{(q_r)}\} = \sum_{m=q_1}^{q_r} \{x^m\} = \sum_{m=q_1}^{q_r} \{X^m\} e^{im\omega t} = \sum_{m=q_1}^{q_r} \{X^m\} e^{im\tau} \quad (2.62)$$

where  $q_1, \dots, q_r$  are the elements of the set of harmonics  $Q_r$  defined in equation (2.16).

The response  $X$  at a general coordinate  $j$  in the  $m_{th}$  harmonic can be written as:

$$X_j^m = \bar{X}_j^m e^{i\phi_j^m} \quad (2.63)$$

Similarly, the response in the inter-coordinate relative displacement can be represented as:

$$y_{kl} \approx \tilde{y}_{kl}^{(q_r)} = \sum_{m=q_1}^{q_r} y_{kl}^m = \sum_{m=q_1}^{q_r} Y_{kl}^m e^{im\tau} \quad (2.64)$$

where:

$$\begin{aligned} Y_{kl}^m &= X_k^m - X_l^m, \quad (k \neq l) \\ Y_{kl}^m &= \bar{Y}_{kl}^m e^{i\psi^m} \end{aligned} \quad (2.65)$$

If the variable  $y_{kl}$  in the nonlinear function  $\mathbf{f}_{kl}(y_{kl})$  has the form assumed in (2.64), the nonlinear function  $\mathbf{f}_{kl}(y_{kl}^{(q_r)})$  is complex and is also a periodic function of time. Then the nonlinear function  $\mathbf{f}_{kl}(y_{kl})$  can be expressed by a Fourier series of the form:

$$\mathbf{f}_{kl}(y_{kl}) \approx \tilde{\mathbf{f}}_{kl}^{(q_s)}(\tilde{y}_{kl}^{(q_r)}) = \sum_{m=q_1}^{q_s} \mathbf{f}_{kl}^m = \sum_{m=q_1}^{q_s} \mathcal{F}_{kl}^m e^{im\tau} \quad (2.66)$$

and:

$$\begin{aligned} \mathcal{F}_{kl}^m &= \bar{\mathcal{F}}_{kl}^m e^{i\varphi^m} \\ \mathcal{F}_{kl}^0 &= \frac{1}{2\pi} \int_0^{2\pi} \mathbf{f}(\tilde{y}_{kl}^{(q_r)}) d\tau \\ \mathcal{F}_{kl}^m &= \frac{1}{\pi} \int_0^{2\pi} \mathbf{f}(\tilde{y}_{kl}^{(q_r)}) e^{-im\tau} d\tau, \quad (m \geq 1) \end{aligned} \quad (2.67)$$

where  $s$  is the number of harmonics in the approximated nonlinear function  $\tilde{\mathbf{f}}_{kl}^{(q_s)}(\tilde{y}_{kl}^{(q_r)})$ .

The Fourier series expressed in complex form in equation (2.66) can also be expressed as a function of *sin* and *cos* terms as:

$$\sum_{m=q_1}^{q_s} \mathcal{F}_{kl}^m e^{im\tau} = A_{kl}^0 + \sum_{m=q_1}^{q_s} (A_{kl}^m \cos(m\tau) + B_{kl}^m \sin(m\tau)) \quad (2.68)$$

where:

$$\begin{aligned}
A_{kl}^0 &= \frac{1}{2\pi} \int_0^{2\pi} f(\tilde{y}_{kl}^{(q_r)}) d\tau \\
A_{kl}^1 &= \frac{1}{\pi} \int_0^{2\pi} f(\tilde{y}_{kl}^{(q_r)}) \sin\tau d\tau \\
B_{kl}^1 &= \frac{1}{\pi} \int_0^{2\pi} f(\tilde{y}_{kl}^{(q_r)}) \cos\tau d\tau \\
A_{kl}^2 &= \frac{1}{\pi} \int_0^{2\pi} f(\tilde{y}_{kl}^{(q_r)}) \sin 2\tau d\tau \\
B_{kl}^2 &= \frac{1}{\pi} \int_0^{2\pi} f(\tilde{y}_{kl}^{(q_r)}) \cos 2\tau d\tau \\
&\vdots
\end{aligned} \tag{2.69}$$

## 2.6.2 Higher-Order Frequency Response Functions

The higher-order frequency response functions have their basis in the Volterra series [48]. The Volterra series is a general mathematical model used to express the relationship between the response and excitation of dynamic systems. If the nonlinear system is time-invariant and stable, the Volterra series can be applied to express the nonlinearity in polynomial form. The behaviour of a wide range of nonlinear systems in engineering can be represented as Volterra series. Exceptions are related mainly to systems with discontinuities. However, even these systems can either be approximate by a continuous polynomial where this polynomial system will have a Volterra series representation, or can be represented by a different definition of higher-order FRFs.

Although, in theory, it is possible to calculate the higher-order FRFs obtained from the Volterra series, the measurement of these quantities has proved difficult in practice. Several techniques have been developed for obtaining the ideal higher-order FRFs [7, 48], but when applied to physical structures, the procedures do not obtain FRFs of good quality [43, 48]. The most promising one is the NARMAX procedure [7, 8]. Apart from this mathematical definition of higher-order FRF obtained from the Volterra series, there are other definitions based on experimental measurements that are approximations of the ideal one [72]. In the current work, another experimental definition of higher-order FRFs will be introduced in order to be compatible with the analytical methods that are based on experimental FRFs. These non-unique

definitions will still contain useful information about the behaviour of a system and can be used to represent the system to a good degree of approximation.

In order to define the ideal higher-order FRFs it is necessary to describe briefly the characteristics of the Volterra series. Considering a nonlinear structure which can be represented by a Volterra model, the total response at one DOF,  $x(t)$ , can be written as

$$x(t) = \int_{-\infty}^{\infty} h_1(\tau_1) f(t - \tau_1) d\tau_1 + \int_{-\infty}^{\infty} \int_{-\infty}^{\infty} h_2(\tau_1, \tau_2) f(t - \tau_1) f(t - \tau_2) d\tau_1 d\tau_2 + \dots \\ \int_{-\infty}^{\infty} \dots \int_{-\infty}^{\infty} h_n(\tau_1, \tau_2, \dots, \tau_n) f(t - \tau_1) f(t - \tau_2) \dots f(t - \tau_n) d\tau_1 d\tau_2 \dots d\tau_n \quad (2.70)$$

Equation (2.70) is the Volterra series and the terms  $h_1(\tau_1), h_2(\tau_1, \tau_2), \dots, h_n(\tau_1, \tau_2, \dots, \tau_n)$  are known as the first, second, ...,  $n$ th order Volterra kernels of the system. Equation (2.70) can be expressed as

$$x(t) = \sum_{n=1}^{\infty} x_n(t) \quad (2.71)$$

where

$$x_n(t) = \int_{-\infty}^{\infty} \dots \int_{-\infty}^{\infty} h_n(\tau_1, \tau_2, \dots, \tau_n) \prod_{i=1}^n f(t - \tau_i) d\tau_i \quad (2.72)$$

Taking the multiple Fourier transform of the  $n$ th order kernel  $h_n(\tau_1, \tau_2, \dots, \tau_n)$  [7], the generalised  $n$ th order frequency response function,  $H_n(\omega_1, \omega_2, \dots, \omega_n)$ , can be written as:

$$H_n(\omega_1, \omega_2, \dots, \omega_n) = \int_{-\infty}^{\infty} \dots \int_{-\infty}^{\infty} h_n(\tau_1, \tau_2, \dots, \tau_n) e^{-i(\omega_1 \tau_1 + \dots + \omega_n \tau_n)} d\tau_1 \dots d\tau_n \quad (2.73)$$

Thus the  $n$ th order kernel transform,  $H_n(\omega_1, \dots, \omega_n)$ , is the  $n$ th order frequency response function, where the expression  $H_n(\omega_1, \dots, \omega_n)$  gives the magnitude and phase

of the  $n$ th power output component at a frequency equal to  $\omega = \sum_{i=1}^n \omega_i$  due to input sinusoids at frequencies  $\omega_1, \omega_2, \dots, \omega_n$ . It is interesting to notice that the generalised higher-order frequency response function defined in equation (2.73) are mathematically unique and independent of the excitation level. Therefore, different kinds of excitation can be used to measure the ideal higher-order FRFs defined in equation (2.73). A very useful excitation to measure FRFs in practice is the sinusoidal excitation. The experimental FRFs of nonlinear systems measured in practice using the sinusoidal excitation are usually input- and output-dependent. For sinusoidal excitation, the experimental higher-order FRFs are related to the ideal higher-order FRFs.

In order to define the measured higher-order FRFs and to describe the relationship with the ideal higher-order FRFs obtained from the Volterra series using harmonic excitation, the input force to be considered is the idealised simple harmonic function written as

$$f(t) = F e^{i\omega t} \quad (2.74)$$

Substituting equation (2.74) into the Volterra series equation (2.70), the input/output relationship can be written as

$$\begin{aligned} x(t) = & \int_{-\infty}^{\infty} h_1(\tau_1) F e^{i\omega(t-\tau_1)} d\tau_1 + \int \int_{-\infty}^{\infty} h_2(\tau_2, \tau_2) F e^{i\omega(t-\tau_2)} F e^{i\omega(t-\tau_2)} d\tau_2 d\tau_2 + \dots \\ & \int \dots \int_{-\infty}^{\infty} h_n(\tau_n, \dots, \tau_n) F e^{i\omega(t-\tau_n)} \dots F e^{i\omega(t-\tau_n)} d\tau_n \dots d\tau_n \end{aligned} \quad (2.75)$$

Putting the constants outside of the integrals in equation (2.75) yields

$$x(t) = F e^{i\omega t} \int_{-\infty}^{\infty} h_1(\tau_1) e^{-i\omega\tau_1} d\tau_1 + F^2 e^{i2\omega t} \int \int_{-\infty}^{\infty} h_2(\tau_2, \tau_2) e^{-i2\omega\tau_2} d\tau_2 d\tau_2 + \dots$$

$$F^n e^{in\omega t} \int \cdots \int_{-\infty}^{\infty} h_n(\tau_1, \dots, \tau_n) e^{-in\omega\tau_n} d\tau_1 \cdots d\tau_n \quad (2.76)$$

From equation (2.76) it is possible to see that the terms of the integral are the multi-dimensional Fourier transforms. Substituting equation (2.73) into equation (2.76) yields

$$x(t) = H_1(\omega) F e^{i\omega t} + H_2(\omega, \omega) F^2 e^{i2\omega t} + \cdots + H_n(\omega, \dots, \omega) F^n e^{in\omega t} \quad (2.77)$$

The response  $x(t)$  can also be expressed by a Fourier series as

$$x(t) = X^1(\omega) e^{i\omega t} + X_2(2\omega) e^{i2\omega t} + \cdots + X_n(n\omega) e^{in\omega t} \quad (2.78)$$

Assuming that the input used to derive equation (2.77) is no longer the ideal harmonic excitation but the physical harmonic excitation expressed as

$$f(t) = F \cos(\omega t) = \frac{F}{2} (e^{i\omega t} + e^{-i\omega t}) \quad (2.79)$$

Substituting the ideal harmonic excitation  $F e^{i\omega t}$  in equation (2.77) by the physical

harmonic excitation  $\frac{F}{2}(e^{i\omega t} + e^{-i\omega t})$  yields

$$\begin{aligned}
x(t) = & H_1(\omega)\left(\frac{F}{2}\right)e^{i\omega t} + H_1(-\omega)\left(\frac{F}{2}\right)e^{-i\omega t} \\
& + H_2(\omega, \omega)\left(\frac{F}{2}\right)^2 e^{i2\omega t} + H_2(-\omega, -\omega)\left(\frac{F}{2}\right)^2 e^{-i2\omega t} \\
& + H_2(\omega, -\omega)\left(\frac{F}{2}\right)^2 + H_2(-\omega, \omega)\left(\frac{F}{2}\right)^2 \\
& + H_3(\omega, \omega, \omega)\left(\frac{F}{2}\right)^3 e^{i3\omega t} + H_3(-\omega, -\omega, -\omega)\left(\frac{F}{2}\right)^3 e^{-i3\omega t} \\
& + H_3(\omega, -\omega, \omega)\left(\frac{F}{2}\right)^3 e^{i\omega t} + H_3(-\omega, \omega, -\omega)\left(\frac{F}{2}\right)^3 e^{-i\omega t} \\
& + H_3(-\omega, \omega, \omega)\left(\frac{F}{2}\right)^3 e^{i\omega t} + H_3(\omega, -\omega, -\omega)\left(\frac{F}{2}\right)^3 e^{-i\omega t} \\
& + H_3(\omega, \omega, -\omega)\left(\frac{F}{2}\right)^3 e^{i\omega t} + H_3(-\omega, -\omega, \omega)\left(\frac{F}{2}\right)^3 e^{-i\omega t} \\
& + H_4(\omega, \omega, \omega, \omega)\left(\frac{F}{2}\right)^4 e^{i4\omega t} + H_4(-\omega, -\omega, -\omega, -\omega)\left(\frac{F}{2}\right)^4 e^{-i4\omega t} \\
& + H_4(\omega, \omega, \omega, -\omega)\left(\frac{F}{2}\right)^4 e^{i2\omega t} + H_4(-\omega, -\omega, -\omega, \omega)\left(\frac{F}{2}\right)^4 e^{-i2\omega t} \\
& + H_4(\omega, \omega, -\omega, \omega)\left(\frac{F}{2}\right)^4 e^{i2\omega t} + H_4(-\omega, -\omega, \omega, -\omega)\left(\frac{F}{2}\right)^4 e^{-i2\omega t} \\
& + H_4(\omega, -\omega, \omega, \omega)\left(\frac{F}{2}\right)^4 e^{i2\omega t} + H_4(-\omega, \omega, -\omega, -\omega)\left(\frac{F}{2}\right)^4 e^{-i2\omega t} \\
& + H_4(-\omega, \omega, \omega, \omega)\left(\frac{F}{2}\right)^4 e^{i2\omega t} + H_4(\omega, -\omega, -\omega, -\omega)\left(\frac{F}{2}\right)^4 e^{-i2\omega t} \\
& + H_4(\omega, \omega, -\omega, -\omega)\left(\frac{F}{2}\right)^4 + H_4(-\omega, -\omega, \omega, \omega)\left(\frac{F}{2}\right)^4 \\
& + H_4(\omega, -\omega, \omega, -\omega)\left(\frac{F}{2}\right)^4 + H_4(-\omega, \omega, -\omega, \omega)\left(\frac{F}{2}\right)^4 \\
& + H_4(-\omega, \omega, \omega, -\omega)\left(\frac{F}{2}\right)^4 + H_4(\omega, -\omega, -\omega, \omega)\left(\frac{F}{2}\right)^4 \\
& + \dots
\end{aligned} \tag{2.80}$$

Considering the symmetry property of the ideal higher-order FRFs, expressed as

$$\begin{aligned}
H_2(\omega, -\omega) &= H_2(-\omega, \omega) \\
H_3(\omega, \omega, -\omega) &= H_3(-\omega, \omega, \omega) = H_3(\omega, -\omega, \omega) \\
H_4(\omega, \omega, \omega, -\omega) &= H_4(-\omega, \omega, \omega, \omega) = H_4(\omega, -\omega, \omega, \omega) = H_4(\omega, \omega, -\omega, \omega) \\
H_4(\omega, \omega, -\omega, -\omega) &= H_4(-\omega, -\omega, \omega, \omega) = H_4(\omega, -\omega, \omega, -\omega) = H_4(-\omega, \omega, \omega, -\omega) \\
&\vdots
\end{aligned} \tag{2.81}$$

and using the symmetry property described in equation (2.81), the expression (2.80)

can be simplified to

$$\begin{aligned}
x(t) = & H_1(\omega)\left(\frac{F}{2}\right)e^{i\omega t} + H_1(-\omega)\left(\frac{F}{2}\right)e^{-i\omega t} \\
& + H_2(\omega, \omega)\left(\frac{F}{2}\right)^2 e^{i2\omega t} + H_2(-\omega, -\omega)\left(\frac{F}{2}\right)^2 e^{-i2\omega t} + 2H_2(\omega, -\omega)\left(\frac{F}{2}\right)^2 \\
& + H_3(\omega, \omega, \omega)\left(\frac{F}{2}\right)^3 e^{i3\omega t} + H_3(-\omega, -\omega, -\omega)\left(\frac{F}{2}\right)^3 e^{-i3\omega t} \\
& + 3H_3(\omega, -\omega, \omega)\left(\frac{F}{2}\right)^3 e^{i\omega t} + 3H_3(-\omega, \omega, -\omega)\left(\frac{F}{2}\right)^3 e^{-i\omega t} \\
& + H_4(\omega, \omega, \omega, \omega)\left(\frac{F}{2}\right)^4 e^{i4\omega t} + H_4(-\omega, -\omega, -\omega, -\omega)\left(\frac{F}{2}\right)^4 e^{-i4\omega t} \\
& + 3H_4(\omega, \omega, -\omega, -\omega)\left(\frac{F}{2}\right)^4 + 3H_4(-\omega, -\omega, \omega, \omega)\left(\frac{F}{2}\right)^4 \\
& + 4H_4(\omega, \omega, \omega, -\omega)\left(\frac{F}{2}\right)^4 e^{i2\omega t} + 4H_4(-\omega, -\omega, -\omega, \omega)\left(\frac{F}{2}\right)^4 e^{-i2\omega t} \\
& + \dots
\end{aligned} \tag{2.82}$$

After obtaining the response of the system excited by a physical harmonic excitation as a function of the idealised higher-order FRFs, equation (2.82), the same response must be obtained under the same conditions as a function of higher-order FRFs that can be experimentally measured. The experimental higher-order frequency response function is defined as the spectral ratio of the  $n$ th harmonic response and the  $m$ th harmonic force

$$H^{nm}(\omega) = \frac{X(n\omega)}{F(m\omega)} \tag{2.83}$$

In the case where the input is composed of one sinusoid, the higher-order frequency response function  $H^{n1}(\omega)$  simplified as  $H^n(\omega)$  is defined as the spectral ratio of the  $n$ th harmonic response and the harmonic force

$$H^n(\omega) = \frac{X(n\omega)}{F(\omega)} \tag{2.84}$$

In the case of a sinusoidal excitation, the FRFs measured using the definition of equation (2.84) are related with the FRFs obtained using the definition of equation (2.73). Using the definition of equation (2.84), the total response  $x(t)$  can be expressed as

$$\begin{aligned}
x(t) = & H^1(\omega)\frac{F}{2}e^{i\omega t} + H^1(-\omega)\frac{F}{2}e^{-i\omega t} + H^2(2\omega)\frac{F}{2}e^{i2\omega t} + H^2(2\omega)\frac{F}{2}e^{-i2\omega t} + \dots \\
& \dots + H^n(n\omega)\frac{F}{2}e^{in\omega t} + H^n(-n\omega)\frac{F}{2}e^{-in\omega t}
\end{aligned} \tag{2.85}$$

Comparing equation (2.85) and equation (2.82) yields

$$\begin{aligned}
H^1(\omega) &= H_1(\omega) + \frac{3}{4}H_3(\omega, \omega, -\omega)F(\omega)^2 + \frac{5}{8}H_5(\omega, \omega, \omega, -\omega, -\omega)F(\omega)^4 + \dots \\
H^2(\omega) &= \frac{1}{2}H_2(\omega, \omega)F(\omega) + \frac{1}{2}H_4(\omega, \omega, \omega, -\omega)F(\omega)^3 \\
&\quad + \frac{15}{32}H_6(\omega, \omega, \omega, \omega, -\omega, -\omega)F(\omega)^5 + \dots \\
&\vdots \\
H^n(\omega) &= \sum_{i=0}^{\infty} \frac{(n+2i)!}{(n+i)!i!2^{n+2i-1}} H_{n+2i}(n(\omega), i(-\omega))F(\omega)^{n+2i-1}
\end{aligned} \tag{2.86}$$

In equation (2.86) it is possible to see that the experimental higher-order FRFs are input dependent and that the first-order measured FRF is equal to the first-order ideal FRF only when the system is linear.

### 2.6.3 Higher-Order Harmonic Balance Method

The Higher-Order Harmonic Balance Method proposed by Cameron and Griffin [19] is an extension of the Harmonic Balance Method.

Assuming a nonlinear system subject to harmonic excitation  $\{F\}$ , the system differential equation can be written as:

$$[M]\{\ddot{x}\} + [C]\{\dot{x}\} + i[D]\{x\} + [K]\{x\} + \{\mathbf{f}(\{x\}, \{\dot{x}\})\} = \{F\}e^{i\omega t} \tag{2.87}$$

The steady-state solution can be represented by a Fourier series as:

$$\{x\} = \sum_{m=0}^{\infty} \{x^m\} = \sum_{m=0}^{\infty} \{X^m\}e^{im\tau} \tag{2.88}$$

The response  $x$  at a general coordinate  $j$  can be written as:

$$x_j = \sum_{m=0}^{\infty} x_j^m = \sum_{m=0}^{\infty} \bar{X}_j^m e^{im\phi_j^m} = C_j^m + iD_j^m \tag{2.89}$$

where:

$$\begin{aligned} C_j^m &= \bar{X}_j^m \sin(m\phi_j^m) \\ D_j^m &= \bar{X}_j^m \cos(m\phi_j^m) \end{aligned} \quad (2.90)$$

and the inter-coordinate relative displacement response  $y$  between coordinates  $j$  and  $k$  can be written as:

$$y_{kl} = \sum_{m=0}^{\infty} y_{kl}^m = \sum_{m=0}^{\infty} \bar{Y}_{kl}^m e^{im\psi^m} \quad (2.91)$$

The assumed solution  $y_{kl}$  is then inserted in the nonlinear function  $\mathbf{f}_{kl}(y_{kl})$  and expanded by a Fourier series expressed in complex form as:

$$\mathbf{f}_{kl}(y_{kl}) = \sum_{m=0}^{\infty} \mathbf{f}_{kl}^m = \sum_{m=0}^{\infty} \mathcal{F}_{kl}^m e^{im\tau} \quad (2.92)$$

where:

$$\begin{aligned} \mathcal{F}_{kl}^m &= \bar{\mathcal{F}}_{kl}^m e^{i(\varphi)^m} \\ \mathcal{F}_{kl}^0 &= \frac{1}{2\pi} \int_0^{2\pi} \mathbf{f}(y_{kl}) d\tau \\ \mathcal{F}_{kl}^m &= \frac{1}{\pi} \int_0^{2\pi} \mathbf{f}(y_{kl}) e^{-im\tau} d\tau, \quad (m \geq 1) \end{aligned} \quad (2.93)$$

or expressed as a function of *sin* and *cos* terms as:

$$\sum_{m=0}^{\infty} (\mathcal{F}_{kl}^m)^m e^{im\tau} = A^0 + \sum_{m=0}^{\infty} (A^m \cos(n\tau) + B^m \sin(n\tau)) \quad (2.94)$$

where:

$$\begin{aligned} A_{kl}^0 &= \frac{1}{2\pi} \int_0^{2\pi} f(y_{kl}) d\tau \\ A_{kl}^1 &= \frac{1}{\pi} \int_0^{2\pi} f(y_{kl}) \sin\tau d\tau \\ B_{kl}^1 &= \frac{1}{\pi} \int_0^{2\pi} f(y_{kl}) \cos\tau d\tau \\ A_{kl}^2 &= \frac{1}{\pi} \int_0^{2\pi} f(y_{kl}) \sin 2\tau d\tau \end{aligned} \quad (2.95)$$



To solve the proposed problem by the describing function method it is required to make the same hypothesis as used in the multi-harmonic analysis presented in section (2.6.1); namely, that  $x = x(t)$  appearing in the nonlinear function  $\mathbf{f}(x, \dot{x})$  is sufficiently close to a periodic function represented by the following equation:

$$\{x\} \approx \{\tilde{x}^{(q_r)}\} = \sum_{m=q_1}^{q_r} \{x^m\} = \sum_{m=q_1}^{q_r} \{X^m\} e^{im\tau} \quad (2.98)$$

Then the components  $\mathcal{F}_{kl}^m$  of the nonlinear force  $\mathbf{f}_{kl}(\tilde{y}_{kl}^{(q_r)})$  can be written as:

$$\mathcal{F}_{kl}^m = \nu_{kl}^m Y_{kl}^m \quad (2.99)$$

The known describing function  $\nu_{kl}^m$ , can be expressed as

$$\nu_{kl}^m = \frac{\mathcal{F}_{kl}^m}{Y_{kl}^m} \quad (2.100)$$

Considering  $m$  harmonics in the Equation (2.99), this can be written in matrix form as:

$$\begin{Bmatrix} \mathcal{F}_{kl}^1 \\ \mathcal{F}_{kl}^2 \\ \vdots \\ \mathcal{F}_{kl}^m \end{Bmatrix} = \begin{bmatrix} \nu_{kl}^1 & 0 & 0 & \dots & 0 \\ 0 & \nu_{kl}^2 & 0 & \dots & 0 \\ \vdots & & \ddots & & \vdots \\ 0 & 0 & 0 & \dots & \nu_{kl}^m \end{bmatrix} \begin{Bmatrix} Y_{kl}^1 \\ Y_{kl}^2 \\ \vdots \\ Y_{kl}^m \end{Bmatrix} \quad (2.101)$$

Equation (2.101) can be expressed in terms of the general coordinates,  $\{X\}$ , as:

$$\begin{Bmatrix} \mathcal{F}_k^1 \\ \mathcal{F}_l^1 \\ \mathcal{F}_k^2 \\ \mathcal{F}_l^2 \\ \vdots \\ \mathcal{F}_k^m \\ \mathcal{F}_l^m \end{Bmatrix} = \begin{bmatrix} \nu_{kl}^1 & -\nu_{kl}^1 & 0 & 0 & \dots & 0 & 0 \\ -\nu_{kl}^1 & \nu_{kl}^1 & 0 & 0 & \dots & 0 & 0 \\ 0 & 0 & \nu_{kl}^2 & -\nu_{kl}^2 & \dots & 0 & 0 \\ 0 & 0 & -\nu_{kl}^2 & \nu_{kl}^2 & \dots & 0 & 0 \\ \vdots & & \ddots & & \vdots & & \\ 0 & 0 & 0 & 0 & \dots & \nu_{kl}^m & -\nu_{kl}^m \\ 0 & 0 & 0 & 0 & \dots & -\nu_{kl}^m & \nu_{kl}^m \end{bmatrix} \begin{Bmatrix} X_k^1 \\ X_l^1 \\ X_k^2 \\ X_l^2 \\ \vdots \\ X_k^m \\ X_l^m \end{Bmatrix} \quad (2.102)$$

Equation (2.102) can be written in a more concise form as:

$$\begin{Bmatrix} \mathcal{F}_k^m \\ \mathcal{F}_l^m \end{Bmatrix} = [\Theta]_{kl}^m \begin{Bmatrix} X_k^i \\ X_l^i \end{Bmatrix} \quad (2.103)$$

## 2.6.5 Multi-Harmonic Describing Functions (MUHADEF)

Accepting all the hypotheses already defined in section (2.6.1), the components  $\mathcal{F}_{kl}^m$  of the approximate nonlinear force  $\tilde{\mathbf{f}}_{kl}^{(q_s)}(\tilde{\mathbf{y}}_{kl}^{(q_r)})$  can be written as:

$$\mathcal{F}_{kl}^m = \sum_{n=q_1}^{q_r} \mathcal{G}_{kl}^{mn} Y_{kl}^n \quad \text{for } (m = q_1, q_2, \dots, q_s) \quad (2.104)$$

Equation (2.104) can be rewritten in a matrix form as:

$$\begin{Bmatrix} \mathcal{F}_{kl}^{q_1} \\ \mathcal{F}_{kl}^{q_2} \\ \vdots \\ \mathcal{F}_{kl}^{q_s} \end{Bmatrix} = \begin{bmatrix} \mathcal{G}_{kl}^{q_1 q_1} & \mathcal{G}_{kl}^{q_1 q_2} & \mathcal{G}_{kl}^{q_1 q_3} & \dots & \mathcal{G}_{kl}^{q_1 q_r} \\ \mathcal{G}_{kl}^{q_2 q_1} & \mathcal{G}_{kl}^{q_2 q_2} & \mathcal{G}_{kl}^{q_2 q_3} & \dots & \mathcal{G}_{kl}^{q_2 q_r} \\ \vdots & & \ddots & & \\ \mathcal{G}_{kl}^{q_s q_1} & \mathcal{G}_{kl}^{q_s q_2} & \mathcal{G}_{kl}^{q_s q_3} & \dots & \mathcal{G}_{kl}^{q_s q_r} \end{bmatrix} \begin{Bmatrix} Y_{kl}^{q_1} \\ Y_{kl}^{q_2} \\ \vdots \\ Y_{kl}^{q_r} \end{Bmatrix} \quad (2.105)$$

Then the new describing function called  $\mathcal{G}_{kl}^{mn}$  for  $m = q_s$  and  $n = q_r$  can be obtained from the following expression:

$$\mathcal{G}_{kl}^{q_s q_r} = \frac{\mathbf{f}_{kl}^{q_s}(\tilde{\mathbf{y}}_{kl}^{(q_r)}) - \mathbf{f}_{kl}^{q_s}(\tilde{\mathbf{y}}_{kl}^{(q_r-1)})}{Y_{kl}^{q_r}} \quad (2.106)$$

Equation (2.105) can be written as a function of the general coordinate,  $\{X\}$ , as:

$$\begin{Bmatrix} \mathcal{F}_k^{q_1} \\ \mathcal{F}_l^{q_1} \\ \mathcal{F}_k^{q_2} \\ \mathcal{F}_l^{q_2} \\ \vdots \\ \mathcal{F}_k^{q_s} \\ \mathcal{F}_l^{q_s} \end{Bmatrix} = \begin{bmatrix} \mathcal{G}_{kl}^{q_1 q_1} & -\mathcal{G}_{kl}^{q_1 q_1} & \mathcal{G}_{kl}^{q_1 q_2} & -\mathcal{G}_{kl}^{q_1 q_2} & \dots & \mathcal{G}_{kl}^{q_1 q_r} & -\mathcal{G}_{kl}^{q_1 q_r} \\ -\mathcal{G}_{kl}^{q_1 q_1} & \mathcal{G}_{kl}^{q_1 q_1} & -\mathcal{G}_{kl}^{q_1 q_2} & \mathcal{G}_{kl}^{q_1 q_2} & \dots & -\mathcal{G}_{kl}^{q_1 q_r} & \mathcal{G}_{kl}^{q_1 q_r} \\ \mathcal{G}_{kl}^{q_2 q_1} & -\mathcal{G}_{kl}^{q_2 q_1} & \mathcal{G}_{kl}^{q_2 q_2} & -\mathcal{G}_{kl}^{q_2 q_2} & \dots & \mathcal{G}_{kl}^{q_2 q_r} & -\mathcal{G}_{kl}^{q_2 q_r} \\ -\mathcal{G}_{kl}^{q_2 q_1} & \mathcal{G}_{kl}^{q_2 q_1} & -\mathcal{G}_{kl}^{q_2 q_2} & \mathcal{G}_{kl}^{q_2 q_2} & \dots & -\mathcal{G}_{kl}^{q_2 q_r} & \mathcal{G}_{kl}^{q_2 q_r} \\ \vdots & & \ddots & & \vdots & & \\ \mathcal{G}_{kl}^{q_s q_1} & -\mathcal{G}_{kl}^{q_s q_1} & \mathcal{G}_{kl}^{q_s q_2} & -\mathcal{G}_{kl}^{q_s q_2} & \dots & \mathcal{G}_{kl}^{q_s q_r} & -\mathcal{G}_{kl}^{q_s q_r} \\ -\mathcal{G}_{kl}^{q_s q_1} & \mathcal{G}_{kl}^{q_s q_1} & -\mathcal{G}_{kl}^{q_s q_2} & \mathcal{G}_{kl}^{q_s q_2} & \dots & -\mathcal{G}_{kl}^{q_s q_r} & \mathcal{G}_{kl}^{q_s q_r} \end{bmatrix} \begin{Bmatrix} X_k^{q_1} \\ X_l^{q_1} \\ X_k^{q_2} \\ X_l^{q_2} \\ \vdots \\ X_k^{q_r} \\ X_l^{q_r} \end{Bmatrix} \quad (2.107)$$

Equation (2.107) can be written in a more concise form as:

$$\begin{Bmatrix} \mathcal{F}_k^m \\ \mathcal{F}_l^m \end{Bmatrix} = \sum_{n=q_1}^{q_r} [\Delta]_{kl}^{mn} \begin{Bmatrix} X_k^n \\ X_l^n \end{Bmatrix} \quad \text{for } (m = q_1, q_2, \dots, q_s) \quad (2.108)$$

where:

$$[\Delta]_{kl}^{mn} = \begin{bmatrix} \mathcal{G}_{kl}^{mn} & -\mathcal{G}_{kl}^{mn} \\ -\mathcal{G}_{kl}^{mn} & \mathcal{G}_{kl}^{mn} \end{bmatrix} \quad (2.109)$$

If the form of nonlinearity  $\mathbf{f}(x, \dot{x})$  is known, all describing functions,  $\mathcal{G}_{kl}^{mn}$  for  $m = q_s$  and  $n = q_r$ , can be calculated by using equation (2.106). The case used to demonstrate here the multi-harmonic describing function is again the cubic stiffness, composed of a spring whose stiffness has a cubic non linearity. For this, the nonlinear force can be written as:

$$\mathbf{f}(y) = K_0 y + \beta y^3 \quad (2.110)$$

Using the notation of equation (2.62), for the first and the third harmonics ( $r = 2$ ), the set of harmonics  $Q_r$  can be written as:

$$Q_r = \{1, 3\} \quad (2.111)$$

Assuming that the response  $y$  is composed essentially of the first harmonic, then the displacement  $\tilde{y}_{h(1)}$  can be written as:

$$y \approx \tilde{y}^{(1)} = \bar{Y}^1 \sin(\tau) + \bar{Y}^1 \cos(\tau) \quad (2.112)$$

Assuming that the response  $y$  is composed by the first and third harmonics, then the displacement  $\tilde{y}^{(3)}$  can be written as:

$$y \approx \tilde{y}^{(3)} = \bar{Y}^1 \sin(\tau) + \bar{Y}^1 \cos(\tau) + \bar{Y}^3 \sin(3\tau) + \bar{Y}^3 \cos(3\tau) \quad (2.113)$$

Using equation (2.105) the components  $\mathcal{F}_{kl}^1$  and  $\mathcal{F}_{kl}^3$  of the nonlinear function  $\mathbf{f}$  can be written as:

$$\begin{Bmatrix} \mathcal{F}_{kl}^1 \\ \mathcal{F}_{kl}^3 \end{Bmatrix} = \begin{bmatrix} \mathcal{G}_{kl}^{11} & \mathcal{G}_{kl}^{13} \\ \mathcal{G}_{kl}^{31} & \mathcal{G}_{kl}^{33} \end{bmatrix} \begin{Bmatrix} Y_{kl}^1 \\ Y_{kl}^3 \end{Bmatrix} \quad (2.114)$$

Using equation (2.106) it is possible to have the expression of all describing functions  $\mathcal{G}_{kl}^{sr}$  necessary in equation (2.114) as:

$$\begin{aligned} \mathcal{G}_{kl}^{11} &= \frac{\mathcal{F}^1(\tilde{y}^{(1)})}{Y^1} \\ \mathcal{G}_{kl}^{13} &= \frac{\mathcal{F}^1(\tilde{y}^{(3)}) - \mathcal{F}^1(\tilde{y}^{(1)})}{Y^3} \\ \mathcal{G}_{kl}^{31} &= \frac{\mathcal{F}^3(\tilde{y}^{(1)})}{Y^1} \\ \mathcal{G}_{kl}^{33} &= \frac{\mathcal{F}^3(\tilde{y}^{(3)}) - \mathcal{F}^3(\tilde{y}^{(1)})}{Y^3} \end{aligned} \quad (2.115)$$

Functions  $\mathcal{F}^1(\tilde{y}^{(1)})$  and  $\mathcal{F}^3(\tilde{y}^{(1)})$  can be calculated using equations (2.68) and (2.112) as follows:

$$\mathcal{F}^1(\tilde{y}^{(1)}) = (K_0\bar{Y}^1 + \frac{3}{2}\beta\bar{Y}^{1^3}) + i(K_0\bar{Y}^1 + \frac{3}{2}\beta\bar{Y}^{1^3}) \quad (2.116)$$

$$\mathcal{F}^3(\tilde{y}^{(1)}) = (\frac{1}{2}\beta\bar{Y}^{1^3}) + i(-\frac{1}{2}\beta\bar{Y}^{1^3}) \quad (2.117)$$

and  $\mathcal{F}^1(\tilde{y}^{(3)})$  and  $\mathcal{F}^3(\tilde{y}^{(3)})$  can be calculated using equations (2.68) and (2.113) as:

$$\begin{aligned} \mathcal{F}^1(\tilde{y}^{(3)}) &= (K_0\bar{Y}^1 + \frac{3}{2}\beta\bar{Y}^{1^3} + 3\beta\bar{Y}^1\bar{Y}^{3^2} - \frac{3}{2}\beta\bar{Y}^{1^2}\bar{Y}^3) + \\ &+ i(K_0\bar{Y}^1 + \frac{3}{2}\beta\bar{Y}^{1^3} + 3\beta\bar{Y}^1\bar{Y}^{3^2} + \frac{3}{2}\beta\bar{Y}^{1^2}\bar{Y}^3) \end{aligned} \quad (2.118)$$

$$\begin{aligned} \mathcal{F}^3(\tilde{y}^{(3)}) &= (\frac{1}{2}\beta\bar{Y}^{1^3} + K_0\bar{Y}^3 + 3\beta\bar{Y}^{1^2}\bar{Y}^3 + \frac{3}{2}\beta\bar{Y}^{3^3}) + \\ &+ i(-\frac{1}{2}\beta\bar{Y}^{1^3} + K_0\bar{Y}^3 + 3\beta\bar{Y}^{1^2}\bar{Y}^3 + \frac{3}{2}\beta\bar{Y}^{3^3}) \end{aligned} \quad (2.119)$$

Substituting equations (2.116),(2.117),(2.118),(2.119) in equation (2.115), the describing functions can be written as:

$$\begin{aligned} \mathcal{G}_{kl}^{11} &= (K_0 + \frac{3}{2}\beta\bar{Y}^{1^2}) + i(K_0 + \frac{3}{2}\beta\bar{Y}^{1^2}) \\ \mathcal{G}_{kl}^{13} &= (3\beta\bar{Y}^1\bar{Y}^3) - \frac{3}{2}\beta\bar{Y}^{1^2} + i(3\beta\bar{Y}^1\bar{Y}^3 + \frac{3}{2}\beta\bar{Y}^{1^2}) \end{aligned}$$

$$\begin{aligned}\mathcal{G}_{kl}^{31} &= \left(\frac{1}{2}\beta\bar{Y}^{12}\right) + i\left(-\frac{1}{2}\beta\bar{Y}^{12}\right) \\ \mathcal{G}_{kl}^{33} &= \left(K_0 + 3\beta\bar{Y}^{12} + \frac{3}{2}\beta\bar{Y}^{32}\right) + i\left(K_0 + 3\beta\bar{Y}^{12} + \frac{3}{2}\beta\bar{Y}^{32}\right)\end{aligned}\quad (2.120)$$

Substituting the variable  $y$  by the equation (2.113) in the nonlinear function  $\mathbf{f}(y)$  given by equation (2.110) and in the approximate function  $\tilde{\mathbf{f}}(y)$  given by equation (2.66), yields:

$$\begin{aligned}K_0(\bar{Y}^1 \sin(f) + \bar{Y}^1 \cos(f) + \bar{Y}^3 \sin(3f) + \bar{Y}^3 \cos(3f)) + \beta(\bar{Y}^1 \sin(f) + \bar{Y}^1 \cos(f) + \bar{Y}^3 \sin(3f) + \bar{Y}^3 \cos(3f))^3 \\ \approx (K_0 + \frac{3}{2}\beta\bar{Y}^{12})\bar{Y}^1 \sin\tau + (\frac{1}{2}\beta\bar{Y}^{12})\bar{Y}^1 \sin 3\tau + (3\beta\bar{Y}^1\bar{Y}^3 - \frac{3}{2}\beta\bar{Y}^{12})\bar{Y}^3 \sin\tau + \\ + (K_0 + \frac{3}{2}\beta\bar{Y}^{12})\bar{Y}^1 \cos\tau + (-\frac{1}{2}\beta\bar{Y}^{12})\bar{Y}^1 \cos 3\tau + (3\beta\bar{Y}^1\bar{Y}^3 + \frac{3}{2}\beta\bar{Y}^{12})\bar{Y}^3 \cos\tau + \\ + (K_0 + 3\beta\bar{Y}^{12} + \frac{3}{2}\beta\bar{Y}^{32})\bar{Y}^3 \sin 3\tau + (K_0 + 3\beta\bar{Y}^{12} + \frac{3}{2}\beta\bar{Y}^{32})\bar{Y}^3 \cos 3\tau\end{aligned}\quad (2.121)$$

The nonlinear function  $\mathbf{f}(y^{(3)})$  shown on the left-hand side of equation (2.121) has linear and nonlinear terms whereas the nonlinear approximate function  $\tilde{\mathbf{f}}^{(3)}(y^{(3)})$  shown on the right-hand side of equation (2.121) has only linear terms as  $\sin\tau$ ,  $\cos\tau$ ,  $\sin 3\tau$ ,  $\cos 3\tau$ . Figure 2.2 shows the nonlinear function  $\mathbf{f}(\tilde{y}^{(3)})$  and the approximate nonlinear functions  $\tilde{\mathbf{f}}^{(1)}(\tilde{y}^{(1)})$  and  $\tilde{\mathbf{f}}^{(3)}(\tilde{y}^{(3)})$ .

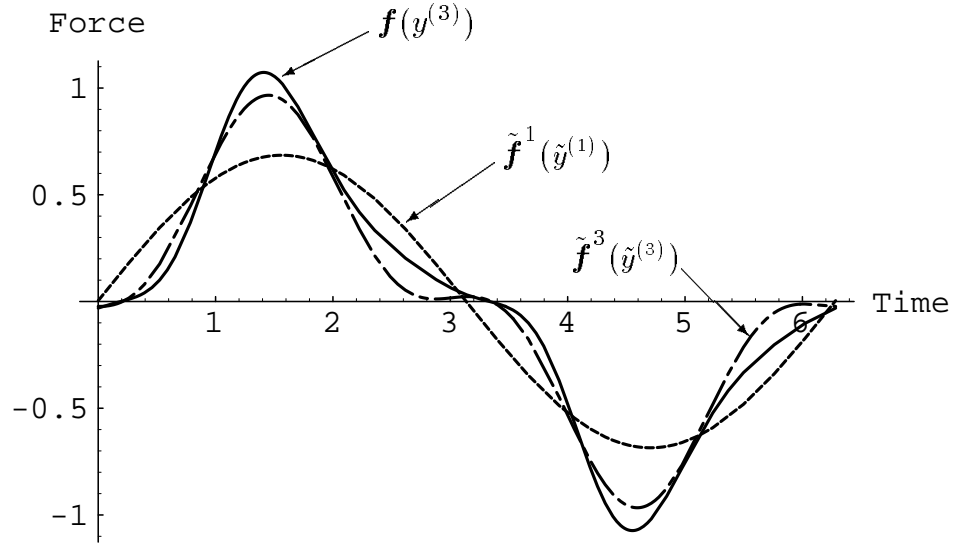


Figure 2.2: Nonlinear function  $\mathbf{f}(\tilde{y}^{(3)})$  and approximate functions  $\tilde{\mathbf{f}}^{(1)}(\tilde{y}^{(1)})$ ,  $\tilde{\mathbf{f}}^{(3)}(\tilde{y}^{(3)})$

## 2.7 Newton-Raphson Method

The advantage of applying the approximate linearised methods to find the solution of the nonlinear equations of motion, is to convert from finding a solution of a nonlinear differential equation to finding a solution of a nonlinear system of equations. Most of these equations have both a right-hand side and a left-hand side. If all the terms from the right-hand side are moved to the left-hand side, the solutions are also called roots of the equations. The most well-known root-finding method is the Newton-Raphson method. This method gives a very efficient mechanism of converging to a root, given a sufficiently good initial guess. If the initial estimation is too far from the real solution, the iteration process may not converge. Different implementations of the Newton-Raphson method can be found for improving special characteristics. One of the sophisticated implementations which improves the global convergence, combines the rapid local convergence of the Newton-Raphson method with a globally-convergent strategy which will guarantee some progress towards the solution of each iteration.

Considering a typical problem of a vector of function  $g(y)$  written as:

$$\{g(\{y\})\} = \{0\} \quad (2.122)$$

where  $\{y\}$  is a vector involving the unknown variables, the iterative solution by applying the modified Newton-Raphson can be written as:

$$\{y^{i+1}\} = \{y^i\} - \lambda [J]^{-1} g(y^i) \quad 0 < \lambda < 1 \quad (2.123)$$

where:

$$[J] = \frac{\partial \{g(y^i)\}}{\partial \{y^i\}} = \begin{bmatrix} \frac{\partial g^i(1)}{\partial y^i(1)} & \frac{\partial g^i(1)}{\partial y^i(2)} & \cdots & \frac{\partial g^i(1)}{\partial y^i(n)} \\ \frac{\partial g^i(2)}{\partial y^i(1)} & \frac{\partial g^i(2)}{\partial y^i(2)} & \cdots & \frac{\partial g^i(2)}{\partial y^i(n)} \\ \vdots & \vdots & \ddots & \vdots \\ \frac{\partial g^i(n)}{\partial y^i(1)} & \frac{\partial g^i(n)}{\partial y^i(2)} & \cdots & \frac{\partial g^i(n)}{\partial y^i(n)} \end{bmatrix} \quad (2.124)$$

On each iteration, the aim now is to find a value of  $\lambda$  such that the new step  $\{y^{i+1}\}$

always reduces  $G$ , given by:

$$G = \frac{1}{2} g \cdot g \quad (2.125)$$

The full step is always the first guess. If  $G(\{y^{i+1}\})$  does not meet the acceptance criteria, a smaller value of  $\lambda$  is tried, until a suitable step is found. After finding suitable step, the procedure will repeat until the unknown vector  $\{y\}$  is obtained for a prescribed tolerance  $\epsilon$ .

# Chapter 3

## Construction of Models for Nonlinear Joint Components

### 3.1 Introduction

Accurate modelling for predicting the dynamic behaviour of mechanical systems is an essential tool in both design and operational stages. During these stages, a physical structure for practical tests is generally not available. and an analytical model that represents the structure is used instead. Many modelling approaches can be used to obtain a model. In the field of structural vibration analysis, the finite element method has become the most popular modelling approach used to study the vibration of structures. Although in principle any structure can be modelled by the finite element method, in practice it is not so straightforward. Many complex mechanical structures are composed of several substructures connected by different kinds of clamping mechanisms, and sometimes the dynamic behaviour predicted is unrepresentative due to difficulties in modelling the connection parts of the substructure, [34]. The clamping mechanism, usually referred to as a joint, is defined as any connection between two distinct parts of a structure and the contact surfaces of a joint are defined as the interface. These joints have a considerable effect in the dynamic behaviour of the assembled structures, and so it is important to establish an accurate mathematical model for them. Although the modelling of the substructures can be obtained by their mass, stiffness and damping matrices derived from the design

data, the modelling of the properties of joints is usually a major problem in vibration analysis, resulting in significant discrepancies between the numerical predictions and the measurements. To overcome this problem, hybrid techniques that utilise both analytical and experimental data have been developed to produce more reliable and accurate models. Although these techniques can be applied directly to obtain a global model that represents the physical structure over a frequency range [4, 130], more accurate and general models can be derived if the joints are first modelled and then incorporated with the substructure models to produce a model of the final assembly structure [140].

Understanding the nature and configuration of a joint can lead to a suitable model for it. The most effective way of modelling a joint is first by studying its dynamic characteristics. This can be done by finding the force-response relationship obtained, for example, from a response at the joint caused by an external force. The second step is the development of an accurate general mathematical model of the joint behaviour. This is the greatest challenge since sometimes a general explicit equation is difficult to obtain and the resulting model developed can be dependent on the type of excitation, frequency range and on amplitudes of the response. The analysis of the force-response relationship can lead to an explicit equation for the practical force-vibration situation. The last step is to have the parameters of the proposed model identified. For simple cases this can be obtained by curve-fitting the experimental force-response relationship.

The force-response relationship used to characterise the joint can be linear or nonlinear. When it is nonlinear, the first problem of evaluating the vibration behaviour is to choose an appropriate excitation force that allows the nonlinear joint to be easily characterised and then identified. Amongst the excitation methods currently used in vibration study, the sinusoidal excitation method is strongly favoured for nonlinearity investigation because of its uniqueness and precision [116].

Many frequently-encountered types of joint have already been studied and identified [2, 45, 72, 73, 126]. They are a useful reference for later investigations of practical applications. For example, the results from such studies can provide input data for the joint characteristic dependent method, such as coupling methods. Usu-

ally, different mechanisms of connections can be related with a particular joint model, each of which can be represented by a describing function. This assumption of representing each of the connections by a describing function can overcome some problems related with the representation of some basic joints such as springs and dampers in the coupling procedure. Some of these connections, which are used in the numerical simulations, are discussed in the following sections.

## 3.2 Linear Joints

Theoretical linear joints are joints that obey the superposition principle described previously. On the other hand, it is known that all physical joints exhibit a certain degree of nonlinearity. For practical purposes, they are regarded as linear joints when the degree of nonlinearity is small enough to be insignificant in the response range of interest. For this group, a linearised equivalent model usually represents the consequent dynamic behaviour. A characteristic of a typical linear joint is that when a joint is excited at one frequency, it responds only at that frequency. Then, there is no transfer of energy in frequency domain. These linear joints can be represented by describing functions in the coupling techniques. The characteristics of the describing function for this group of linear joints can be summarised as follows:

- The Matrix  $[\mathcal{G}_{kl}^{mn}]$  in equation (2.105) is not amplitude-dependent
- The off-diagonal elements of matrix  $[\mathcal{G}_{kl}^{mn}]$  are zero. Therefore the force harmonic equations become uncoupled.

### 3.2.1 Spring

A massless spring, where a force applied to the spring is proportional to the stretch of the spring, is considered. The equation that describes the relation between the force and the response can be written as:

$$f = Kx \tag{3.1}$$

The describing function  $\mathcal{G}_{kl}^{mn}$  for the linear spring with a constant stiffness  $K$  given by equation (3.1) and shown in Figure 3.1 can be written as follows:

$$\mathcal{G}_{kl}^{mn} = \begin{cases} K & \text{if } m = n \\ 0 & \text{otherwise} \end{cases}$$

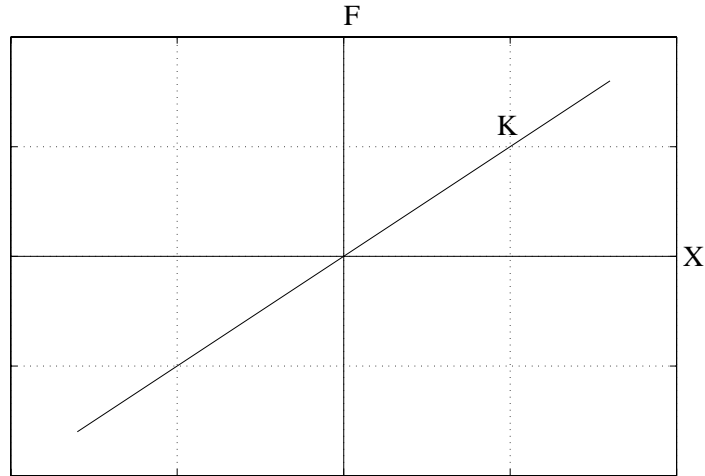


Figure 3.1: Characteristic of linear spring

### 3.2.2 Rigid connection

A rigid connection between two coordinates of a structure can be interpreted physically as coupling these coordinates using a spring joint, which has a very high stiffness,  $K$ . When using the describing function method in coupling analysis, the term related to the describing function in the coupling equation is the inverse of the describing function, i.e. the matrix  $[\mathcal{G}_{kl}^{mn}]^{-1}$ , [136]. Therefore, the inverse of a matrix  $[\mathcal{G}_{kl}^{mn}]$  for a linear spring with a very high stiffness is close to zero. For an infinitely rigid connection, matrix  $[\mathcal{G}_{kl}^{mn}]^{-1}$  is actually zero.

### 3.2.3 Ground

Grounding some DOFs of a structure can be physically interpreted as coupling these DOFs to DOFs of a structure with infinite mass using rigid connections. As the

receptance of a structure with infinite mass is zero, all the receptances in the coupling procedure that involve these DOFs will be zero and all the inverses of the describing functions corresponding to the rigid connection will be also zero.

### 3.2.4 Viscous Damping

This is a massless damper where the force applied across the damper is proportional to the relative velocity of the damper. The equation that describes the relationship between the force and the response can be written as:

$$f = C\dot{x} \quad (3.2)$$

The describing function  $\mathcal{G}_{kl}^{mn}$  for a linear viscous damper with constant damping  $C$  given by equation (3.2) and shown in Figure 3.2 can be written as follows:

$$\mathcal{G}_{kl}^{mn} = \begin{cases} i\Omega Ch_i & \text{if } m = n \\ 0 & \text{otherwise} \end{cases}$$

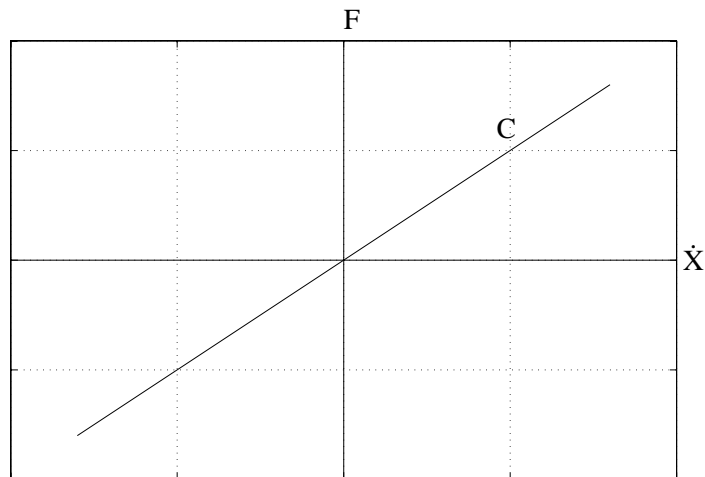


Figure 3.2: Characteristic of linear viscous damper

### 3.3 Nonlinear Joints

Nonlinear joints are joints where the effect of nonlinearity in the response range of interest is so significant that it has to be taken into account in the mathematical model. These nonlinear joints are usually found in joints designed for ease of assembly and disassembly of substructures. Their dynamic behaviour is often difficult to predict and is sensitive to many parameters. The most pronounced characteristic of a typical nonlinear joint is its energy transfer in the frequency domain. When the joint is excited at one frequency, it responds in many frequencies, resulting in an harmonic distortion of the response. The nonlinear joint can be represented by a describing function whose characteristics can be summarised as follows:

- The Matrix  $[\mathcal{G}_{kl}^{mn}]$  in equation (2.105) is amplitude-dependent.
- As the describing function is dependent on the number of harmonics considered in the set, it is difficult to find the corresponding analytical describing function for each case. Instead of obtaining the describing function analytically, it is much easier to obtain it numerically.

### 3.3.1 Cubic Stiffness

Consider a massless nonlinear spring where a force applied across the spring is proportional to the cube of the stretch of the spring,  $x$ . The equation that describes the relation between the force and the response can be written as:

$$f = Kx^3 \quad (3.3)$$

The describing functions  $\mathcal{G}_{kl}^{mn}$  for a nonlinear cubic stiffness with stiffness  $K$  given by equation (3.3), shown in Figure 3.3, and with just two harmonics, first and third, in the set  $Q$ , can be written as follows:

$$\begin{aligned} \mathcal{G}_{kl}^{11} &= 3/4 KY_1^3 \\ \mathcal{G}_{kl}^{13} &= 3/2 KY_1 Y_3 - 3/4 KY_1^2 \\ \mathcal{G}_{kl}^{31} &= -1/4 KY_1^2 \\ \mathcal{G}_{kl}^{33} &= -3/2 KY_1^2 + 3/4 KY_3^2 \end{aligned} \quad (3.4)$$

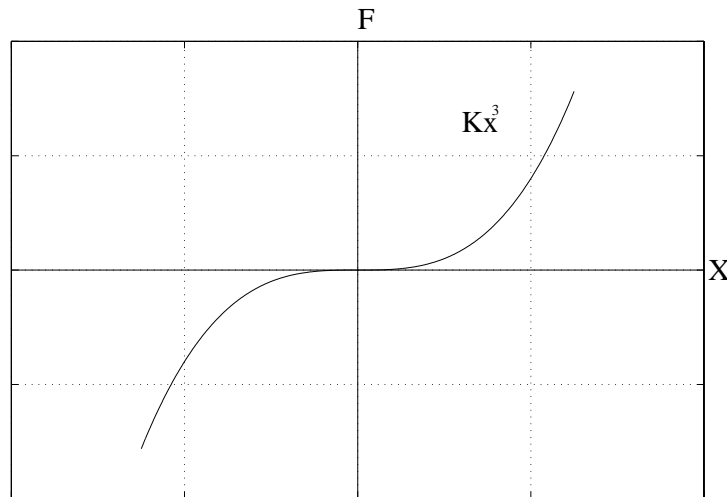


Figure 3.3: Characteristic of nonlinear cubic spring

### 3.3.2 Coulomb Friction

Consider a joint where a constant resisting force, known as a friction force, is affected by the sign of the relative velocity at the interface of the joint and the value of the

external force,  $F$ . The equation that describes the relationship between the force,  $f$ , and the response,  $x$ , can be written as:

$$\begin{aligned} f &= Fl = \mu N & \dot{x} > 0 \\ f &= F & \dot{x} = 0 \\ f &= -Fl & \dot{x} < 0 \end{aligned} \tag{3.5}$$

where:

- $Fl$  = limit friction force
- $F$  = external force
- $\mu$  = friction coefficient
- $N$  = normal clamping force
- $\dot{x}$  = relative velocity

From equation (3.5) it is possible to conclude that if the external force is smaller than the friction limit,  $Fl$ , the two interfaces of the joint will remain locked and the friction force at the interface has the same magnitude as the external force acting in the opposite direction. Once sliding starts, the resistance force is equal to the friction force limit, and the direction of the friction force is always opposite to the direction of motion and no force greater than the friction force can be transmitted through the interface.

The describing function  $\mathcal{G}_{kl}^{mn}$  for a Coulomb friction damper with friction force limit  $F_l$ , given by equation (3.3) and shown in Figure 3.4, can be written as follows:

$$\mathcal{G}_{kl}^{mn} = \begin{cases} \frac{4F_l}{h_i Y_1 \Pi} & \text{if } m = n \text{ and } m = \text{odd} \\ 0 & \text{otherwise} \end{cases}$$

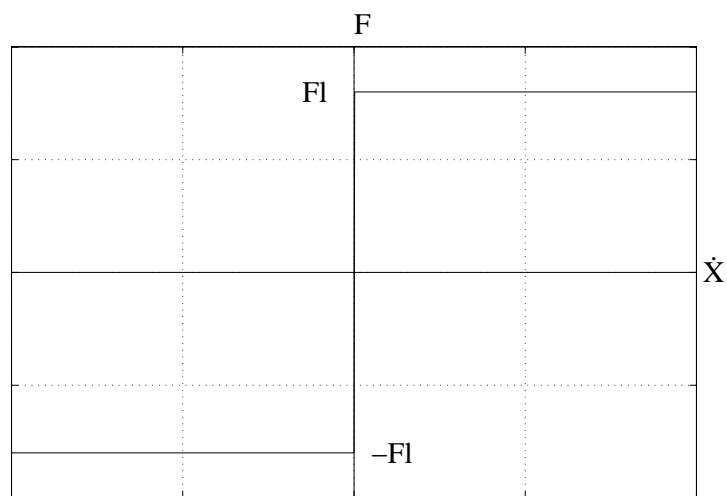


Figure 3.4: Characteristic of Coulomb friction

### 3.3.3 Slip Friction

#### 3.3.3.1 Bilinear Macroslip element

The bilinear friction element consists of a linear spring with a constant stiffness,  $K$ , and a dry friction element. When the deformation,  $x$ , is less than the limiting deformation,  $xl$ , the force/deformation relation of the element is linear. When the deformation,  $x$ , exceeds the limit,  $xl$ , the force/deformation relation of the element is constant. The equation that describes the relation between the force and the response can be written as:

$$\begin{aligned} f &= Kx & x < xl \\ f &= Kxl & x > xl \end{aligned} \quad (3.6)$$

When the element is subjected to a cyclic load, a hysteresis loop is formed, as shown in Figure 3.5:

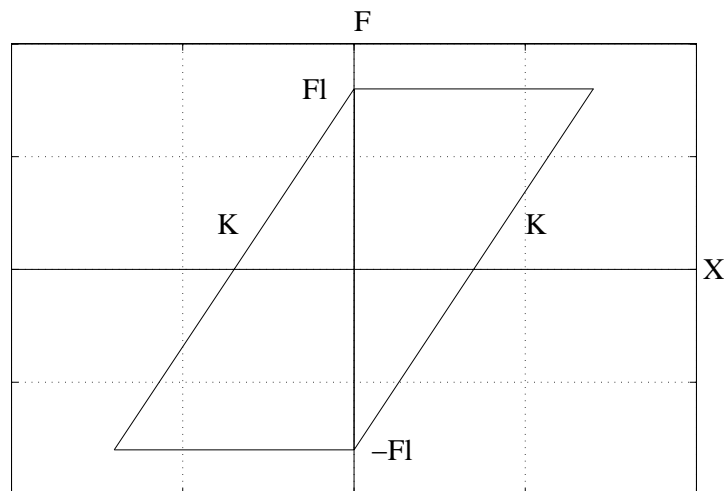


Figure 3.5: Characteristic of a bilinear element

where:

- $Fl$  = Limit friction force
- $K$  = tangential or shear stiffness

### 3.3.3.2 Burdekin's Microslip Model

The Burdekin microslip model [17] is an analytical model that considers the effects of asperities on the mounting surfaces. Each asperity is represented as a prismatic rod with the same stiffness but different amplitude where each rod is modelled as a bilinear element. The height distribution for the rods is such that the number of these contacting rods increases linearly with the approach of the two surfaces. The force deformation relation can be written as:

$$F = \begin{cases} ax - bx^2 & \text{if } 0 < x < \frac{a}{2b} \\ \frac{a^2}{4b} & \text{if } x \geq \frac{a}{2b} \end{cases}$$

where  $a$  and  $b$  are parameters determined by the apparent contact area, normal and shear stiffness of the asperities, normal displacement, friction coefficient and a constant relating the number of contacts to the normal displacement of the surfaces.

When the element is subject to a cyclic load, a hysteresis loop is formed as shown in Figure 3.6:

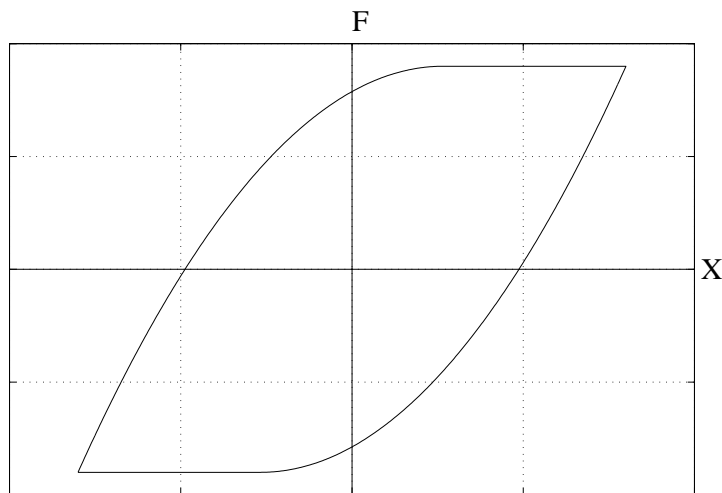


Figure 3.6: Characteristic of Burdekin's element

### 3.3.3.3 Shoukry's Microslip Model

The Shoukry Microslip model [112] is a model that uses a spherical contact element as the basic element. The height distribution of the contact of the peak height of the elements is assumed to be exponential. The force/deformation relation can be written as:

$$F = \mu N (1 - e^{-\frac{\gamma x}{\sigma}})$$

where:

- $\mu$  = friction coefficient
- $N$  = normal force
- $\gamma$  = standard deviation of peak height distribution
- $\sigma = \frac{2(1-\nu)}{\mu(2-\nu)}$
- $\nu$  = Poisson ratio

When the element is subject to a cyclic load, a hysteresis loop is formed as shown in Figure 3.7:

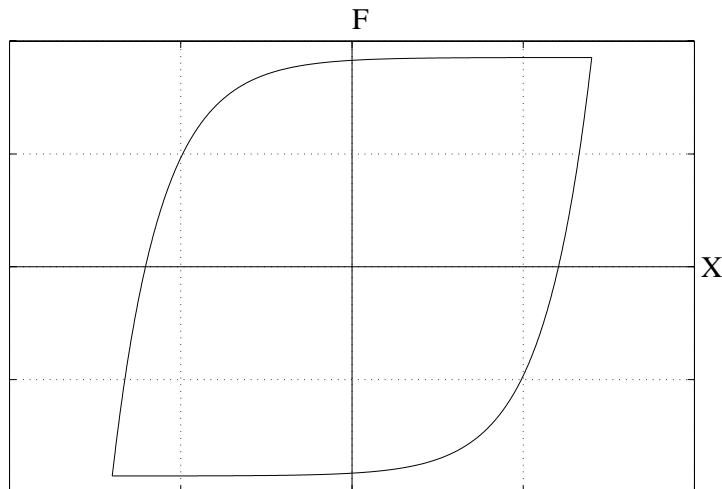


Figure 3.7: Characteristic of Shoukry's element

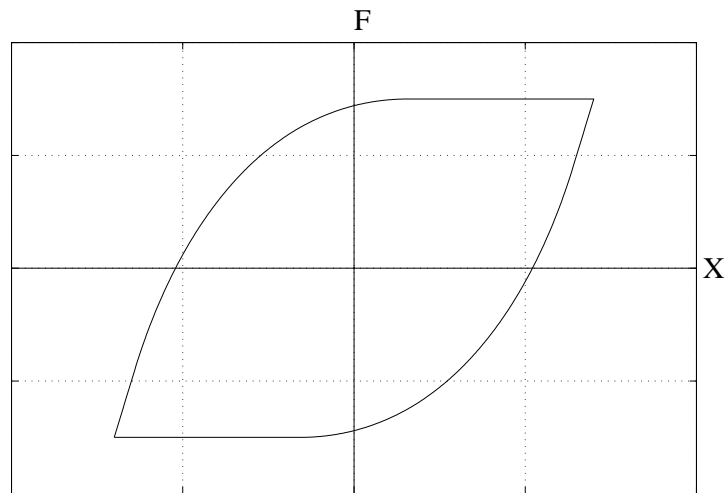
### 3.3.3.4 Ren's Microslip Model

The Ren Microslip model [140] is a model that uses a small area of the interface as the basic element instead of using an element for each single asperity as assumed in Burdekin's and Shoukry's models. Each area is modelled by a bilinear element. A stiffness area  $h$  was defined as a proportion of the total initial stiffness contributed from the area. The total stiffness area  $h$  is unity. Defining this stiffness area, the problem was transformed from modelling the joint in the displacement domain  $x [0, \infty]$  to  $h$  domain  $[0, 1]$ , where  $x_i = x(h_i)$ . Now all the bilinear elements have the same stiffness  $k_i$  but not the same maximum elastic deformation  $x_i$ . The force deformation relation can be written as:

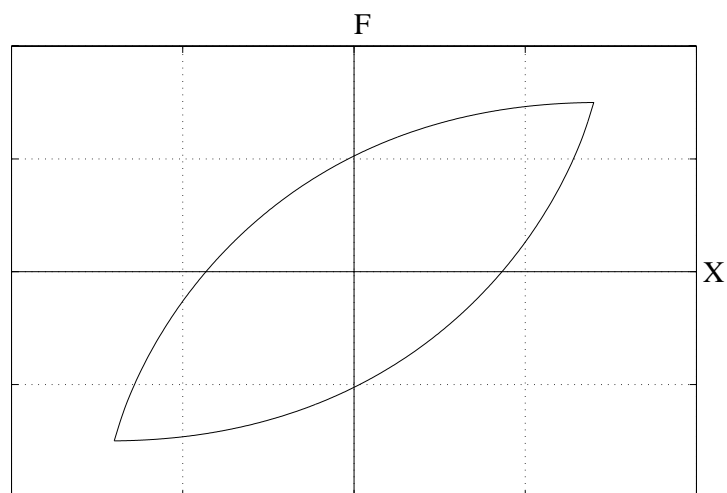
$$F = \begin{cases} kx & x < a \\ -\frac{k(x-a+x(b-\ln x+\ln a))}{b} & a \leq x < a\epsilon^b \\ \frac{Ka(\epsilon^b-1)}{b} & \text{if } x \geq a\epsilon^b \end{cases}$$

where  $a$  represents the maximum elastic deformation, and  $b$  represents the difference between microslip and bilinear elements.

When the element is subject to a cyclic load, depending on the values chosen for  $a$  and  $b$ , different hysteresis loops can be formed. When  $b$  is close to zero, the hysteresis loop formed is the same as the bilinear element as shown in Figure 3.5. When  $b$  starts to increase, the hysteresis loop has a mixture of macro and microslip as shown Figure 3.8(a). As the difference increases, the hysteresis loop will mainly contain microslip as shown in Figure 3.8(b).



(a) Microslip and Macroslip



(b) Microslip

Figure 3.8: Characteristic of Ren's element

### 3.4 Concluding Remarks

In this Chapter, the relationship between force and deflection for different kinds of joints are presented. It was shown that the describing function can be applied for different linear and nonlinear joints. A review of the available friction models is presented.

The major drawback of the describing function is the difficulty encountered in seeking to obtain the analytical describing function coefficients. On the other hand, once the relationship between the force and the deflection has been obtained, the coefficients of the describing functions can be easily numerically calculated.

# Chapter 4

## Impedance Coupling Methods

### 4.1 Introduction

The problem of modelling a complex structure can be greatly simplified by first dividing the structure into substructures where each substructure can be better represented by a smaller, more accurate and refined mathematical model. Then, using a coupling analysis, the dynamic response of the assembled system can be calculated from the properties of the substructures. The great popularity of this analysis is related to the information about the system often being known only at the substructure level, thus allowing each substructure model to be obtained by the ideal model approach. When analysing a complex structure, there are situations where the dynamic properties of some components are best described by an experimental model and others by an analytical model. As a result, attention has been focused on coupling methods that allow a mixture of theoretical and experimental models. The impedance coupling methods were proposed to provide these advantages. This chapter outlines the coupling notation used in this thesis, reviews the existing impedance coupling methods available for the analysis of linear and nonlinear structures and also deals with the development of new nonlinear coupling methods using the multi-harmonic describing function presented in Chapter 2.

## 4.2 Coupling Analysis Notation

Although several methods of predicting the dynamic behaviour of the assembled structure from the properties of the substructures are available, there is no consistent basic notation available [4, 63, 94, 115, 131, 140]. The objective of this section is to propose a standard reference notation in FRF coupling analysis to support later developments. The coupling analysis process involves structures, DOFs, FRFs, and also forces and responses. There are two distinct stages, before-coupling and after-coupling. All the representation of variables in the before-coupling stage will be represented by small letters and after-coupling by capital letters. All the structures in the before-coupling stage will be collected into a unique set and will be called Collected Substructures. The resulting structure in the after-coupling stage will be called Assembled System. All the DOFs of a structure belong to a set denoted by the subscript  $r$ . This set will be divided into two groups. DOFs related with the connections are called "connection DOFs" and are denoted by the subscript  $c$ , and DOFs not related with the connections are called "internal DOFs" and are denoted by the subscript  $i$ . A connection, usually represented by a joint, is composed of two DOFs. In order to give a separate identity for each degree of freedom of the joint involved in the connection, the connection DOFs set  $c$  will be subdivided in two groups,  $\bar{c}$  and  $\tilde{c}$ , where both DOFs that belong to each joint are split, one in each group.

All the substructures to be connected as a Collected Substructure can be represented graphically as shown in Figure 4.1:

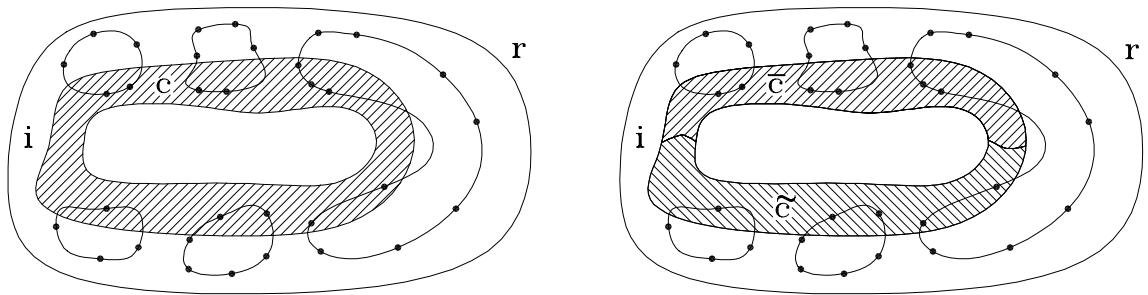


Figure 4.1: Collected Substructures

where:

$r$  = all DOFs

$i$  = internal DOFs

$c, \bar{c}, \tilde{c}$  = connection DOFs

A diagram of the Assembled System having DOFs with local linear elements, local nonlinear elements, rigid and ground connections is shown in Figure 4.2:

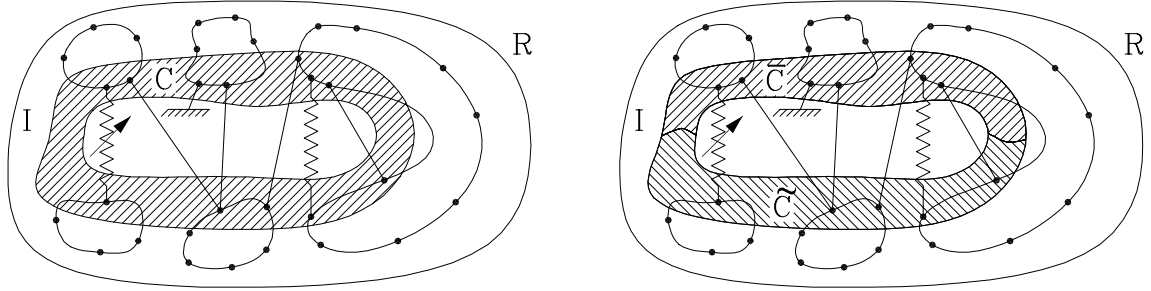


Figure 4.2: Assembled System

where:

$R$  = all DOFs

$I$  = internal DOFs

$C, \bar{C}, \tilde{C}$  = connection DOFs

## 4.3 Linear Impedance Coupling Methods

### 4.3.1 Introduction

Impedance Coupling Methods can be classified into two groups, Spatial Coupling Methods and FRF Coupling Methods. The first group is extensively applied in theoretical analysis where substructure models are derived from spatial models and are based on the application of analytical impedance of the substructures. The second group is utilised in experimental analysis where substructure models are derived from response models and are based on the application of measured FRFs of the substructures. Since all the models can be interrelated with each other [131], both methods allow the use of a combination of analytical and experimental data. However, the disadvantage of the spatial coupling methods when using experimental data is that the accuracy of the assembled system obtained is related to the frequency truncation of the substructure models. This accuracy is always difficult to achieve because the

substructure models derived from experimental data have the shortcoming of including data for only a limited number of measured nodes and a limited frequency range of interest, which implies a propagation of errors in each phase of the conversion process from the response model to the spatial model[28]. The FRF coupling methods do not suffer from frequency truncation since the effects of the higher modes are inherent in the measured data.

### 4.3.2 Spatial Coupling Method

This is the method used in theoretical analysis where the impedance matrix of the assembled system,  $[Z]$ , is obtained from the impedance matrix of the substructures,  $[z]$ , by applying the basic conditions of compatibility of displacements and equilibrium of forces between the substructures.

Consider two substructures  $a$  and  $b$  described by their impedance properties, where the internal DOFs are represented by  $i_a$  and  $i_b$ , respectively, and the connection DOFs are represented by  $c_a$  and  $c_b$ , respectively. The corresponding equilibrium equation of each substructure can be written as:

$$\begin{Bmatrix} f_{i_a} \\ f_{c_a} \end{Bmatrix} = \begin{bmatrix} z_{i_a i_a} & z_{i_a c_a} \\ z_{c_a i_a} & z_{c_a c_a} \end{bmatrix} \begin{Bmatrix} x_{i_a} \\ x_{c_a} \end{Bmatrix} \quad (4.1)$$

$$\begin{Bmatrix} f_{i_b} \\ f_{c_b} \end{Bmatrix} = \begin{bmatrix} z_{i_b i_b} & z_{i_b c_b} \\ z_{c_b i_b} & z_{c_b c_b} \end{bmatrix} \begin{Bmatrix} x_{i_b} \\ x_{c_b} \end{Bmatrix} \quad (4.2)$$

The coupling coordinate sets can be written as:

$$\begin{aligned} i &= \{i_a i_b\} \\ c &= \{c_a c_b\} \\ \bar{c} &= \{c_a\} \\ \tilde{c} &= \{c_b\} \end{aligned} \quad (4.3)$$

The equilibrium equation of the collected substructures can be written in terms of

the coordinate sets (4.3) as:

$$[z] = \begin{bmatrix} z_{ii} & z_{i\bar{c}} & z_{i\check{c}} \\ z_{\bar{c}i} & z_{\bar{c}\bar{c}} & z_{\bar{c}\check{c}} \\ z_{\check{c}i} & z_{\check{c}\bar{c}} & z_{\check{c}\check{c}} \end{bmatrix} = \begin{bmatrix} z_{i_a i_a} & z_{i_a i_b} & z_{i_a c_a} & z_{i_a c_b} \\ z_{i_b i_a} & z_{i_b i_b} & z_{i_b c_a} & z_{i_b c_b} \\ z_{c_a i_a} & z_{c_a i_b} & z_{c_a c_a} & z_{c_a c_b} \\ z_{c_b i_a} & z_{c_b i_b} & z_{c_b c_a} & z_{c_b c_b} \end{bmatrix} = \begin{bmatrix} z_{i_a i_a} & 0 & z_{i_a c_a} & 0 \\ 0 & z_{i_b i_b} & 0 & z_{i_b c_b} \\ z_{c_a i_a} & 0 & z_{c_a c_a} & 0 \\ 0 & z_{c_b i_b} & 0 & z_{c_b c_b} \end{bmatrix} \quad (4.4)$$

The equilibrium of the forces between the substructures can be written as:

$$\begin{aligned} \{F_{\bar{C}}\} &= \{F_{\check{C}}\} = \{f_{\bar{c}}\} + \{f_{\check{c}}\} \\ \{f_i\} &= \{F_I\} \end{aligned} \quad (4.5)$$

The compatibility of displacements of the substructures can be written as:

$$\begin{aligned} \{x_i\} &= \{X_I\} \\ \{x_{\bar{c}}\} &= \{X_{\bar{C}}\} \\ \{x_{\check{c}}\} &= \{X_{\check{C}}\} \\ \{x_{\bar{c}}\} - \{x_{\check{c}}\} &= \{0\} \end{aligned} \quad (4.6)$$

Substituting the compatibility and equilibrium equations (4.5) and (4.6) into (4.1) and (4.2), the overall impedance of the assembled system can be written in terms of the collected substructure properties as:

$$[Z] = \begin{bmatrix} z_{ii} & z_{i\bar{c}} + z_{i\check{c}} \\ z_{\bar{c}i} + z_{\check{c}i} & z_{\bar{c}\bar{c}} + z_{\bar{c}\check{c}} + z_{\check{c}\bar{c}} + z_{\check{c}\check{c}} \end{bmatrix} = \begin{bmatrix} z_{i_a i_a} & 0 & z_{i_a c_a} \\ 0 & z_{i_b i_b} & z_{i_b c_b} \\ z_{c_a i_a} & z_{c_b i_b} & z_{c_a c_a} + z_{c_b c_b} \end{bmatrix} \quad (4.7)$$

The overall impedance of the assembled system given by equation (4.7) can be derived by the FE assembling technique written in a standard form as:

$$[Z] = [{}_a z] \uplus [{}_b z] \quad (4.8)$$

where the operation sign  $\uplus$  means the following impedance assembly:

$$[Z] = \begin{bmatrix} z_{i_a i_a} & z_{i_a c_a} & 0 \\ z_{c_a i_a} & z_{c_a c_a} + z_{c_b c_b} & z_{c_b i_b} \\ 0 & z_{i_b c_b} & z_{i_b i_b} \end{bmatrix} \quad (4.9)$$

This analysis is suitable when the substructure model is theoretically-derived, but it is not generally used for experimentally-derived models.

### 4.3.3 FRF Coupling Method

The FRF coupling method is based on using FRFs derived from two sources, usually from measured data and sometimes from theoretical models. This method represents each substructure by a set of suitably chosen physical DOFs of the system, which provides an exact coupled system. Care must be taken to include the maximum amount of relevant data, especially if the interactions between systems involve not only forces but also moments. In these cases, the inclusion of translational quantities only will introduce errors. Thus, it is necessary to have a sufficient number of connection DOFs that can really represent the physical behaviour involved in the connection.

There are different formulations for the FRF coupling method [131]. The basic formulation is based on converting the FRFs measured from the substructures to the corresponding impedance functions using the following expression:

$$[Z] = [H]^{-1} \quad (4.10)$$

After converting all the measured FRFs to the impedance functions, the spatial coupling method developed in section 4.3.2 is applied. Then, the calculated impedance functions of the assembled structure are converted back to FRFs. The simplest coupling procedure where it is possible to describe the procedure method by mathematical expression, is the coupling of two substructures. For two substructures,  $a$  and  $b$ , the FRF of the assembled structure can be written as:

$$[H(\omega)] = \left[ [H_a(\omega)]^{-1} \uplus [H_b(\omega)]^{-1} \right]^{-1} \quad (4.11)$$

From equation (4.11), it is possible to see that the whole assembled system FRF is obtained after three matrix inversions, two of them carried out in the substructures FRFs matrices  $[H_a(\omega)], [H_b(\omega)]$  and another inversion on the assembled impedance matrix. The advantage of this method is that it involves only the basic matrix operations and requires no data processing such as in the modal coupling or spatial coupling where a modal analysis is first required. The disadvantage is related to the number of matrix inverses necessary in the procedure which not only make it slow but also increase the problems related with numerical errors. However, the development of an alternative impedance coupling method proposed by Jetmundsen, Bielawa and Flannelly [63], reduced the number of matrix inversions at each frequency point from three to one, and the size of the matrix for inversion is restricted to that of the number of connection DOFs, regardless of the number of internal DOFs used in the formulation. The algorithm is derived in full in Appendix A, leading to the following expression:

$$\begin{Bmatrix} X_{i_a} \\ X_{c_a} \\ X_{c_b} \\ X_{i_b} \end{Bmatrix} = \left( \begin{bmatrix} H_{i_a i_a} & H_{i_a c_a} & 0 & 0 \\ H_{c_a i_a} & H_{c_a c_a} & 0 & 0 \\ 0 & 0 & H_{c_b c_b} & H_{c_b i_b} \\ 0 & 0 & H_{i_b c_b} & H_{i_b i_b} \end{bmatrix} - \begin{Bmatrix} H_{i_a c_a} \\ H_{c_a c_a} \\ H_{c_b c_b} \\ H_{i_b c_a} \end{Bmatrix} [H_{c_a c_a} + H_{c_b c_b}]^{-1} \begin{Bmatrix} H_{i_a c_a} \\ H_{c_a c_a} \\ H_{c_b c_b} \\ H_{i_b c_a} \end{Bmatrix}^T \right) \begin{Bmatrix} F_{i_a} \\ F_{c_a} \\ F_{c_b} \\ F_{i_b} \end{Bmatrix} \quad (4.12)$$

where:

**subscript a** = substructure a

**subscript b** = substructure b

**subscript i** = internal connections

**subscript c** = coupling connections

## 4.4 Harmonic Nonlinear Coupling Approaches

### 4.4.1 Introduction

The substructuring methods discussed so far are based on the assumption that the resultant system to be coupled is linear. This assumption is often inadequate for the accurate description of some systems due to the inevitable existence of nonlinearity at many structural joints. One of the outcomes of this problem where the

methods of solving the nonlinear equation of motion by approximate procedures. These approximate procedures assume that the steady-state response is essentially harmonic, keep only the first term of the Fourier series expansion of the nonlinear force and finally convert the nonlinear differential equation of motion to a nonlinear algebraic equation. Two of the most popular procedures are known as Harmonic Balance Method [57] and Describing Function Method [47, 113], as described in Chapter 2. In the following section we discuss the coupling methods available based on these procedures such as Harmonic Nonlinear Building Block Approach and Harmonic Nonlinear Impedance Coupling using the Harmonic Balance Method, and the ones developed during this work such as Harmonic Nonlinear Impedance Coupling using Describing Functions (*HANIM*), Harmonic Nonlinear Receptance Coupling Approach (*HANORCA*), Multi-Harmonic Nonlinear Impedance Coupling using Multi-Harmonic Balance Method, Multi-Harmonic Nonlinear Impedance Coupling using High-Order Describing Function, Multi-Harmonic Nonlinear Impedance Coupling using Multi-Harmonic Describing Function (*MUHANIM*), and Multi-Harmonic Nonlinear Receptance Coupling using Multi-Harmonic Describing Function (*MUHANORCA*).

#### 4.4.2 Harmonic Nonlinear Building Block

This was one of the first coupling techniques proposed to evaluate analytically the frequency response characteristics of a nonlinear system containing nonlinear elements. This is an extension of the Building Block Approach [67] for structures containing nonlinearities. This method linearises the nonlinearity by using the describing function method.

In order to describe the method, the assembled system to be analysed is divided into two substructures as shown in Figure 4.3.

Equations for each substructure are described by the FRF matrices as follows:

$$\begin{Bmatrix} x_1 \\ x_2 \\ x_3 \end{Bmatrix} = \begin{bmatrix} H_{11} & H_{12} & H_{13} \\ H_{21} & H_{22} & H_{23} \\ H_{31} & H_{32} & H_{33} \end{bmatrix} \begin{Bmatrix} F_1 \\ F_2 \\ F_3 \end{Bmatrix} \quad (4.13)$$

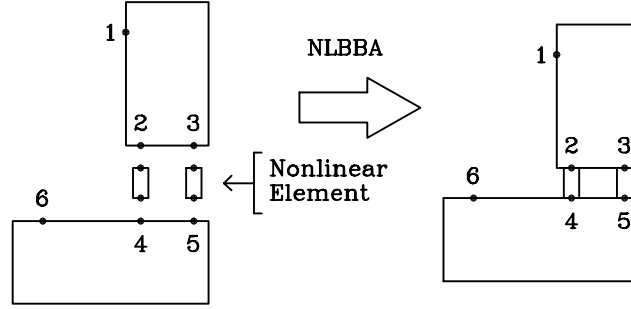


Figure 4.3: Illustration of Nonlinear Building Block Approach

$$\begin{Bmatrix} x_4 \\ x_5 \\ x_6 \end{Bmatrix} = \begin{bmatrix} H_{44} & H_{45} & H_{46} \\ H_{54} & H_{55} & H_{56} \\ H_{64} & H_{65} & H_{66} \end{bmatrix} \begin{Bmatrix} F_4 \\ F_5 \\ F_6 \end{Bmatrix} \quad (4.14)$$

The conditions of equilibrium are:

$$\begin{aligned} F_2 + F_4 = 0 &\implies F_2 = -F_4 = f_1 \\ F_3 + F_5 = 0 &\implies F_3 = -F_5 = f_2 \end{aligned} \quad (4.15)$$

If the joints are assumed to have infinite stiffness, then the compatibility conditions can be written as:

$$\begin{aligned} x_2 &= x_4 \\ x_3 &= x_5 \end{aligned} \quad (4.16)$$

If the joints are not of infinite stiffness, the compatibility conditions can be written as:

$$x_2 - x_4 = -f_1/\mathcal{G}_{24}^{11} \quad (4.17)$$

$$x_3 - x_5 = -f_2/\mathcal{G}_{35}^{11} \quad (4.18)$$

where:

$\mathcal{G}_{24}^{11}$  : describing function of element 1

$\mathcal{G}_{35}^{11}$  : describing function of element 2

From equations (4.13) and (4.17), we have:

$$H_{21}F_1 + H_{22}F_2 + H_{23}F_3 - H_{44}F_4 - H_{45}F_5 - H_{46}F_6 = -f_1/\mathcal{G}_{24}^{11} \quad (4.19)$$

Substituting equation (4.15) into equation (4.19), yields:

$$H_{21}F_1 + H_{22}f_1 + H_{23}f_2 + H_{44}f_1 + H_{45}f_2 - H_{46}F_6 = -f_1/\mathcal{G}_{24}^{11} \quad (4.20)$$

$$H_{21}F_1 - H_{46}F_6 + (H_{22} + H_{44} + 1/\mathcal{G}_{24}^{11})f_1 + (H_{23} + H_{45})f_2 = 0 \quad (4.21)$$

From equations (4.14) and (4.18), we have:

$$H_{31}F_1 + H_{32}F_2 + H_{33}F_3 - H_{54}F_4 - H_{55}F_5 - H_{56}F_6 = -f_2/\mathcal{G}_{35}^{11} \quad (4.22)$$

Substituting equation (4.15) into equation (4.22), yields:

$$H_{31}F_1 + H_{32}f_1 + H_{33}f_2 + H_{54}f_1 + H_{55}f_2 - H_{56}F_6 = -f_2/\mathcal{G}_{35}^{11} \quad (4.23)$$

$$H_{31}F_1 - H_{56}F_6 + (H_{32} + H_{54})f_1 + (H_{33} + H_{55} + 1/\mathcal{G}_{35}^{11})f_2 = 0 \quad (4.24)$$

Using equations (4.13,4.14,4.15,4.21,4.24), the full equation of the assembled structure can be written as:

$$\begin{pmatrix} x_1 \\ x_2 \\ x_3 \\ x_4 \\ x_5 \\ x_6 \\ 0 \\ 0 \end{pmatrix} = \begin{bmatrix} H_{11} & 0 & H_{12} & H_{13} \\ H_{21} & 0 & H_{22} & H_{23} \\ H_{31} & 0 & H_{32} & H_{33} \\ 0 & H_{46} & -H_{44} & -H_{45} \\ 0 & H_{56} & -H_{54} & -H_{55} \\ 0 & H_{66} & -H_{64} & -H_{65} \\ H_{21} & -H_{46} & H_{22} + H_{44} + 1/\mathcal{G}_{24}^{11} & H_{23} + H_{45} \\ H_{31} & -H_{56} & H_{32} + H_{54} & H_{33} + H_{55} + 1/\mathcal{G}_{35}^{11} \end{bmatrix} \begin{pmatrix} F_1 \\ F_6 \\ f_1 \\ f_2 \end{pmatrix} \quad (4.25)$$

Equation (4.25) can be written in a simplified form as:

$$\begin{pmatrix} \{X_r\} \\ \{0\} \end{pmatrix} = \begin{bmatrix} [H_{ri}] & [H_{rc}] \\ [H_{ci}] & [H_{cc}] + [\mathcal{G}_{\bar{c}\bar{c}}^{11}]^{-1} \end{bmatrix} \begin{pmatrix} \{F_i\} \\ \{f_c\} \end{pmatrix} \quad (4.26)$$

From equation (4.26),  $\{f_c\}$  can be written as:

$$\{f_c\} = ([H_{ci}] \{F_i\}) \left[ [H_{cc}] + [\mathcal{G}_{\bar{c}\bar{c}}^{11}]^{-1} \right]^{-1} \quad (4.27)$$

Then  $\{X_r\}$  can be derived by substituting  $\{f_c\}$  given by equation (4.27) into equation (4.26) resulting in:

$$\{X_r\} = \left[ [H_{ri}] - [H_{rc}] \left[ [H_{cc}] + [\mathcal{G}_{\bar{c}\bar{c}}^{11}]^{-1} \right]^{-1} [H_{ci}] \right] \{F_i\} \quad (4.28)$$

The above equation is the standard FRF form i.e.:  $\{X\} = [H]\{F\}$  so that it is possible to conclude that the desired FRF matrix of the assembled system,  $[H]$ , in terms of the FRFs matrix of the substructure, is as follows:

$$[H] = \left[ [H_{ri}] - [H_{rc}] \left[ [H_{cc}] + [\mathcal{G}_{\bar{c}\bar{c}}^{11}]^{-1} \right]^{-1} [H_{ci}] \right] \quad (4.29)$$

This equation is used to obtain the FRFs of the assembled structure using the FRFs of the substructures.

### 4.4.3 Harmonic Nonlinear Impedance Coupling using Harmonic Balance Method

The Harmonic Nonlinear Impedance Coupling using the Harmonic Balance Method is applied when spatial properties of the substructure models are available. In this method the nonlinear force,  $\{\mathbf{f}\}$ , is treated as an external force, and all the substructures are considered as linear. Then the spatial coupling technique is applied first to the substructures. Secondly the impedance of the assembled structure is obtained. In the last step, the Harmonic Balance Method is applied to the impedance equation of the linear structure.

Consider the matrix differential equation of motion of the assembled structure where the internal nonlinear forces,  $\{\mathbf{f}\}$ , are treated as pseudo external forces:

$$[M]\{\ddot{x}\} + [C]\{\dot{x}\} + i[D]\{x\} + [K]x = \{f\} - \{\mathbf{f}\} \quad (4.30)$$

Equation (4.30) can be written in impedance form as:

$$[Z]\{x\} = \{f\} - \{\mathcal{F}\} \quad (4.31)$$

where  $[Z]$  is given by:

$$[Z] = [[K] - \omega^2[M] + i\omega[C] + i[D]] \quad (4.32)$$

In order to consider the fundamental harmonics it is necessary to assume that the hypothesis of the absolute response,  $\{x\}$ , the relative response,  $\{y\}$ , and the nonlinear force,  $\{\mathcal{F}\}$ , can be expressed in a Fourier series shown by equations (2.62,2.64,2.66) and also that the external periodic forcing,  $f_{kl}$ , can be represented in a Fourier series as:

$$f_{kl} = \sum_{m=0}^{\infty} f_{kl}^m = \sum_{m=0}^{\infty} F_{kl}^m e^{im\Psi} \quad (4.33)$$

where:

$$F_{kl}^m = \bar{F}_{kl}^m e^{i(\varphi)^m} \quad (4.34)$$

Considering the first harmonic of the force and the response, equation (4.31) can be written as a set of nonlinear algebraic equations as follows:

$$[Z^1]\{X^1\} = \{F^1\} - \{\mathcal{F}^1\} \quad (4.35)$$

The Harmonic Balance Method theory presented in Chapter 2 converts a set of  $n$  nonlinear equations (4.30) to a set of  $n$  nonlinear algebraic equations (4.35). The response of the structure under harmonic excitation can be obtained by solving equation (4.35) iteratively. Equation (4.35) can be written in a more compact form as:

$$\{g^1(y)\} = \{0\} \quad (4.36)$$

where:

$$\left\{ g^1(y) \right\} = \left\{ [Z^1]\{X^1\} - \{F^1\} + \{\mathcal{F}^1\} \right\} \quad (4.37)$$

Equation (4.37) can be solved by using the Newton-Raphson method previous presented in section 2.7.

#### 4.4.4 Harmonic Nonlinear Impedance Coupling using Describing Functions (*HAIM*)

The Harmonic Nonlinear Impedance Coupling using Describing Functions is also applied when the spatial properties of the substructure models are available. After the nonlinear joint is represented by the describing function method, the joint is also considered as a linear substructure together with the other substructures. Thus, the substructures are coupled by the spatial coupling technique.

Consider the matrix differential equation of motion of the structure with internal nonlinear forces:

$$[M]\{\ddot{x}\} + [C]\{\dot{x}\} + i[D]\{x\} + [K]\{x\} + \{\mathbf{f}\} = \{f\} \quad (4.38)$$

where  $\{\mathbf{f}\}$  is the internal nonlinear force.

Equation (4.38) can be written in impedance form as:

$$[Z]\{x\} + \{\mathbf{f}\} = \{f\} \quad (4.39)$$

where  $[Z]$  is given by the following equation:

$$[Z] = [[K] - \omega^2[M] + i\omega[C] + i[D]] \quad (4.40)$$

In order to substitute the nonlinear force by its describing function, it is necessary to assume the hypothesis shown by equations (2.62,2.64,2.66) and also that the external periodic forcing,  $f_{kl}$ , can be represented in a Fourier series as:

$$f_{kl} = \sum_{m=0}^{\infty} f_{kl}^m = \sum_{m=0}^{\infty} F_{kl}^m e^{im\Psi} \quad (4.41)$$

where:

$$F_{kl}^m = \bar{F}_{kl}^m e^{i\varphi^m} \quad (4.42)$$

Substituting the internal nonlinear force  $\{\mathbf{f}\}$  in equation (4.39) by the corresponding describing function, equation (2.103), yields the harmonic differential equation written

as:

$$[[Z^1] + [\Theta^{11}]]\{X^1\} = \{F^1\} \quad (4.43)$$

where  $[Z^1]$  is given by the following equation:

$$[Z^1] = [[K] - (1\omega)^2[M] + i(1\omega)[C] + i[D]]$$

The describing function theory presented in Chapter 2 converts a set of  $n$  nonlinear differential equations (4.38) into a set of  $n$  nonlinear algebraic equations (4.43). The response of the structure under harmonic excitation can then be obtained by solving equation (4.43) iteratively together with the describing functions which couple the harmonic equation. Equations (4.43) can be written together in a more compact form as:

$$\{g^1(y)\} = \{0\} \quad (4.44)$$

where:

$$\left\{ g^1(y) \right\} = \left\{ \begin{array}{l} ([Z^1] + [\Theta]_{kl}^1)\{X^1\} \\ [V]_{kl}^1 (\{X_k^1\} - \{X_l^1\}) - \{\mathcal{F}_{kl}^1\} \end{array} \right\} \quad (4.45)$$

Equation (4.45) can be solved by using the Newton-Raphson method previous presented in section 2.7.

#### 4.4.5 Harmonic Nonlinear Receptance Coupling Approach (HANORCA)

In this section a new FRF coupling method is proposed for predicting the analytical response characteristics of a nonlinear system containing nonlinear joints. Although the linear method proposed by Jetmundsen, Bielawa and Flannelly [63], can be applied for coupling various substructures at the same time, it is difficult to apply it for real complex structures. The reason is related to the fact that this method was first developed to couple two substructures and then extended to couple various substructures. However, the method had a computational and numerical advantage by reducing the essential number of matrix inversions from three to one, and by having the size of the matrix inversion dictated only by the number of connection DOFs,

regardless of the number of internal DOFs used in the model.

In order to preserve this computational and numerical efficiency and to extend this method of analysis to structures with nonlinearities, a new nonlinear receptance coupling approach is proposed. Since the joint is represented by a describing function, the method is applicable to systems containing almost any kind of nonlinear joint. This method also overcomes some common problems encountered when representing some basic linear joints such as springs and dampers in the coupling procedure by representing any kind of connection involved in the procedure by a describing function. Therefore the method developed below can be applied to linear or nonlinear structures. On the other hand, it is possible to see that an accurate model of the joint is crucial in the analysis.

The general nonlinear coupling method *HANORCA* is derived by considering all the different kinds of connections expected to be present in the procedure and by assuming that there are more than two substructures to be coupled. Using the coupling notation presented in section (4.2), where all the substructures and components to be connected are represented by just one structure called the Collected Substructure, shown in Figure 4.1, and the final coupled system called the Assembled System, shown in figure (4.2), the equation for the Collected Substructure, relating the displacement vector and the force vector can be written in matrix form as:

$$\begin{Bmatrix} x_i \\ x_{\bar{c}} \\ x_{\bar{z}} \end{Bmatrix} = \begin{bmatrix} H_{ii} & H_{i\bar{c}} & H_{i\bar{z}} \\ H_{\bar{c}i} & H_{\bar{c}\bar{c}} & H_{\bar{c}\bar{z}} \\ H_{\bar{z}i} & H_{\bar{z}\bar{c}} & H_{\bar{z}\bar{z}} \end{bmatrix} \begin{Bmatrix} f_i \\ f_{\bar{c}} \\ f_{\bar{z}} \end{Bmatrix} \quad (4.46)$$

or in more compact form as:

$$\{x_r\} = [H_r]\{f_r\} \quad (4.47)$$

Looking at the Assembled System, the displacement in each point can be written as

$$\begin{Bmatrix} X_I \\ X_{\bar{c}} \\ X_{\bar{z}} \end{Bmatrix} = \begin{bmatrix} H_{II} & H_{I\bar{c}} & H_{I\bar{z}} \\ H_{\bar{c}I} & H_{\bar{c}\bar{c}} & H_{\bar{c}\bar{z}} \\ H_{\bar{z}I} & H_{\bar{z}\bar{c}} & H_{\bar{z}\bar{z}} \end{bmatrix} \begin{Bmatrix} F_I \\ F_{\bar{c}} \\ F_{\bar{z}} \end{Bmatrix} \quad (4.48)$$

or in more compact form as:

$$\{X_R\} = [H_R]\{F_R\} \quad (4.49)$$

The equilibrium conditions can be written as:

$$\begin{aligned} \{F_{\bar{C}}\} &= \{F_{\bar{C}}\} = \{f_{\bar{c}}\} + \{f_{\bar{c}}\} \\ \{f_i\} &= \{F_I\} \end{aligned} \quad (4.50)$$

The compatibility conditions can be written in two forms:

$$\begin{aligned} \{x_i\} &= \{X_I\} \\ \{x_{\bar{c}}\} &= \{X_{\bar{C}}\} \\ \{x_{\bar{c}}\} &= \{X_{\bar{C}}\} \\ \{x_{\bar{c}}\} - \{x_{\bar{c}}\} &= -[\mathcal{G}_{\bar{c}\bar{c}}]^{-1}\{f_{\bar{c}}\} \end{aligned} \quad (4.51)$$

or:

$$\begin{aligned} \{x_i\} &= \{X_I\} \\ \{x_{\bar{c}}\} &= \{X_{\bar{C}}\} \\ \{x_{\bar{c}}\} &= \{X_{\bar{C}}\} \\ \{x_{\bar{c}}\} - \{x_{\bar{c}}\} &= -[\mathcal{G}_{\bar{c}\bar{c}}]^{-1}\{f_{\bar{c}}\} \end{aligned} \quad (4.52)$$

Now, using equations (4.46,4.48,4.50,4.51,4.52) it is possible to find the desired relationship between the FRF submatrices of the assembled structure,  $[H_R]$ , in terms of the FRF submatrices of the collected substructures,  $[H_r]$ . This relationship can be derived by first substituting equations (4.46) into (4.51) and (4.52), yielding:

$$[H_{\bar{c}i}]\{f_i\} + [H_{\bar{c}\bar{c}}]\{f_{\bar{c}}\} + [H_{\bar{c}\bar{c}}]\{f_{\bar{c}}\} - [H_{\bar{c}i}]\{f_i\} - [H_{\bar{c}\bar{c}}]\{f_{\bar{c}}\} - [H_{\bar{c}\bar{c}}]\{f_{\bar{c}}\} + [\mathcal{G}_{\bar{c}\bar{c}}]^{-1}\{f_{\bar{c}}\} = \{0\} \quad (4.53)$$

$$[H_{\bar{c}i}]\{f_i\} + [H_{\bar{c}\bar{c}}]\{f_{\bar{c}}\} + [H_{\bar{c}\bar{c}}]\{f_{\bar{c}}\} - [H_{\bar{c}i}]\{f_i\} - [H_{\bar{c}\bar{c}}]\{f_{\bar{c}}\} - [H_{\bar{c}\bar{c}}]\{f_{\bar{c}}\} + [\mathcal{G}_{\bar{c}\bar{c}}]^{-1}\{f_{\bar{c}}\} = \{0\} \quad (4.54)$$

Substituting now the equilibrium equations (4.50) into (4.53) and (4.54), yields:

$$[H_{\bar{c}i}]\{F_I\} + [H_{\bar{c}\bar{c}}]\{f_{\bar{c}}\} + [H_{\bar{c}\bar{c}}](\{F_{\bar{C}}\} - \{f_{\bar{c}}\}) - [H_{\bar{c}i}]\{F_I\} - [H_{\bar{c}\bar{c}}]\{f_{\bar{c}}\} - [H_{\bar{c}\bar{c}}](\{F_{\bar{C}}\} - \{f_{\bar{c}}\}) + [\mathcal{G}_{\bar{c}\bar{c}}]^{-1}\{f_{\bar{c}}\} = \{0\} \quad (4.55)$$

$$[H_{\bar{c}i}]\{F_I\} + [H_{\bar{c}\bar{c}}](\{F_{\bar{C}}\} - \{f_{\bar{c}}\}) + [H_{\bar{c}\bar{c}}]\{f_{\bar{c}}\} - [H_{\bar{c}i}]\{F_I\} - [H_{\bar{c}\bar{c}}](\{F_{\bar{C}}\} - \{f_{\bar{c}}\}) - [H_{\bar{c}\bar{c}}]\{f_{\bar{c}}\} + [\mathcal{G}_{\bar{c}\bar{c}}]^{-1}\{f_{\bar{c}}\} = \{0\} \quad (4.56)$$

Isolating the Collected Substructure forces,  $\{f\}$ , in terms of the Assembled System forces,  $\{F\}$ , in equations (4.53,4.54,4.55,4.56), yields:

$$\{f_{\bar{c}}\} = [B]^{-1} \{([H_{\bar{c}i}] - [H_{\bar{c}i}])\{F_I\} + ([H_{\bar{c}\bar{c}}] - [H_{\bar{c}\bar{c}}])\{F_{\bar{C}}\}\} \quad (4.57)$$

$$\{f_{\bar{c}}\} = [B]^{-1} \{([H_{\bar{c}i}] - [H_{\bar{c}i}])\{F_I\} + ([H_{\bar{c}\bar{c}}] - [H_{\bar{c}\bar{c}}])\{F_{\bar{C}}\}\} \quad (4.58)$$

$$\{f_{\bar{c}}\} = ([I] - [B]^{-1}([H_{\bar{c}\bar{c}}] - [H_{\bar{c}\bar{c}}]))\{F_{\bar{C}}\} - [B]^{-1}([H_{\bar{c}i}] - [H_{\bar{c}i}])\{F_I\} \quad (4.59)$$

$$\{f_{\bar{c}}\} = ([I] - [B]^{-1}([H_{\bar{c}\bar{c}}] - [H_{\bar{c}\bar{c}}]))\{F_{\bar{C}}\} - [B]^{-1}([H_{\bar{c}i}] - [H_{\bar{c}i}])\{F_I\} \quad (4.60)$$

where:

$$[B] = [H_{\bar{c}\bar{c}}] + [H_{\bar{c}\bar{c}}] - [H_{\bar{c}\bar{c}}] - [H_{\bar{c}\bar{c}}] + [\mathcal{G}_{\bar{c}\bar{c}}]^{-1} \quad (4.61)$$

Rewriting equation (4.46) as follows,

$$\{x_i\} = [H_{ii}]\{f_i\} + [H_{i\bar{c}}]\{f_{\bar{c}}\} + [H_{i\bar{c}}]\{f_{\bar{c}}\} \quad (4.62)$$

$$\{x_{\bar{c}}\} = [H_{\bar{c}i}]\{f_i\} + [H_{\bar{c}\bar{c}}]\{f_{\bar{c}}\} + [H_{\bar{c}\bar{c}}]\{f_{\bar{c}}\} \quad (4.63)$$

$$\{x_{\bar{c}}\} = [H_{\bar{c}i}]\{f_i\} + [H_{\bar{c}\bar{c}}]\{f_{\bar{c}}\} + [H_{\bar{c}\bar{c}}]\{f_{\bar{c}}\} \quad (4.64)$$

and substituting equations (4.50), (4.60), (4.57) into (4.62), and substituting equations (4.50), (4.59), (4.58) into (4.62) yields the internal displacement of the assembled structure,  $\{X_I\}$ , in terms of the FRFs of the substructures as follows:

$$\begin{aligned} \{X_I\} &= [H_{ii}]\{F_I\} + [H_{i\bar{c}}]\{F_{\bar{C}}\} + ([H_{i\bar{c}}] - [H_{i\bar{c}}])[B]^{-1}([H_{\bar{c}i}] - [H_{\bar{c}i}])\{F_I\} + \\ & \quad ([H_{i\bar{c}}] - [H_{i\bar{c}}])[B]^{-1}([H_{\bar{c}\bar{c}}] - [H_{\bar{c}\bar{c}}])\{F_{\bar{C}}\} \end{aligned} \quad (4.65)$$

$$\begin{aligned} \{X_I\} &= [H_{ii}]\{F_I\} + [H_{i\bar{c}}]\{F_{\bar{C}}\} + ([H_{i\bar{c}}] - [H_{i\bar{c}}])[B]^{-1}([H_{\bar{c}i}] - [H_{\bar{c}i}])\{F_I\} + \\ & \quad ([H_{i\bar{c}}] - [H_{i\bar{c}}])[B]^{-1}([H_{\bar{c}\bar{c}}] - [H_{\bar{c}\bar{c}}])\{F_{\bar{C}}\} \end{aligned} \quad (4.66)$$

Comparing equation (4.48) with equations (4.65) and (4.66) gives the first row of the matrix in equation (4.48). This row comprises submatrices which are given as:

$$[H_{II}] = [H_{ii}] - ([H_{i\bar{c}}] - [H_{i\bar{c}}])[B]^{-1}([H_{\bar{c}i}] - [H_{\bar{c}i}]) \quad (4.67)$$

$$[H_{I\bar{C}}] = [H_{i\bar{c}}] - ([H_{i\bar{c}}] - [H_{i\bar{c}}])[B]^{-1}([H_{\bar{c}\bar{c}}] - [H_{\bar{c}\bar{c}}]) \quad (4.68)$$

$$[H_{I\bar{C}}] = [H_{i\bar{c}}] - ([H_{i\bar{c}}] - [H_{i\bar{c}}])[B]^{-1}([H_{\bar{c}\bar{c}}] - [H_{\bar{c}\bar{c}}]) \quad (4.69)$$

Substituting now equations (4.50), (4.57), (4.60) into (4.63), and substituting equations (4.50), (4.58), (4.59) into (4.63), yields the connection displacements  $\{X_{\bar{C}}\}$  in function of the FRFs of the substructures as follows:

$$\begin{aligned} \{X_{\bar{C}}\} &= [H_{\bar{c}i}]\{F_I\} + [H_{\bar{c}\bar{c}}]\{F_{\bar{C}}\} + ([H_{\bar{c}\bar{c}}] - [H_{\bar{c}\bar{c}}])[B]^{-1}([H_{\bar{c}i}] - [H_{\bar{c}i}])\{F_I\} + \\ &\quad ([H_{\bar{c}\bar{c}}] - [H_{\bar{c}\bar{c}}])[B]^{-1}([H_{\bar{c}\bar{c}}] - [H_{\bar{c}\bar{c}}])\{F_{\bar{C}}\} \end{aligned} \quad (4.70)$$

$$\begin{aligned} \{X_{\bar{C}}\} &= [H_{\bar{c}i}]\{F_I\} + [H_{\bar{c}\bar{c}}]\{F_{\bar{C}}\} + ([H_{\bar{c}\bar{c}}] - [H_{\bar{c}\bar{c}}])[B]^{-1}([H_{\bar{c}i}] - [H_{\bar{c}i}])\{F_I\} + \\ &\quad ([H_{\bar{c}\bar{c}}] - [H_{\bar{c}\bar{c}}])[B]^{-1}([H_{\bar{c}\bar{c}}] - [H_{\bar{c}\bar{c}}])\{F_{\bar{C}}\} \end{aligned} \quad (4.71)$$

Comparing equation (4.48) with equations (4.70) and (4.71) gives the second row of the matrix in equation (4.48). This row comprises submatrices which are given as:

$$[H_{\bar{C}I}] = [H_{\bar{c}i}] - ([H_{\bar{c}\bar{c}}] - [H_{\bar{c}\bar{c}}])[B]^{-1}([H_{\bar{c}i}] - [H_{\bar{c}i}]) \quad (4.72)$$

$$[H_{\bar{C}\bar{C}}] = [H_{\bar{c}\bar{c}}] - ([H_{\bar{c}\bar{c}}] - [H_{\bar{c}\bar{c}}])[B]^{-1}([H_{\bar{c}\bar{c}}] - [H_{\bar{c}\bar{c}}]) \quad (4.73)$$

$$[H_{\bar{C}\bar{C}}] = [H_{\bar{c}\bar{c}}] - ([H_{\bar{c}\bar{c}}] - [H_{\bar{c}\bar{c}}])[B]^{-1}([H_{\bar{c}\bar{c}}] - [H_{\bar{c}\bar{c}}]) \quad (4.74)$$

Substituting now equations (4.50), (4.57), (4.60) into (4.64), and substituting equations (4.50), (4.58), (4.59) into (4.64), yields the connection displacements  $\{X_{\bar{C}}\}$  in function of the FRFs of the substructures as follows:

$$\begin{aligned} \{X_{\bar{C}}\} &= [H_{\bar{c}i}]\{F_I\} + [H_{\bar{c}\bar{c}}]\{F_{\bar{C}}\} + ([H_{\bar{c}\bar{c}}] - [H_{\bar{c}\bar{c}}])[B]^{-1}([H_{\bar{c}i}] - [H_{\bar{c}i}])\{F_I\} + \\ &\quad ([H_{\bar{c}\bar{c}}] - [H_{\bar{c}\bar{c}}])[B]^{-1}([H_{\bar{c}\bar{c}}] - [H_{\bar{c}\bar{c}}])\{F_{\bar{C}}\} \end{aligned} \quad (4.75)$$

$$\begin{aligned} \{X_{\bar{C}}\} &= [H_{\bar{c}i}]\{F_I\} + [H_{\bar{c}\bar{c}}]\{F_{\bar{C}}\} + ([H_{\bar{c}\bar{c}}] - [H_{\bar{c}\bar{c}}])[B]^{-1}([H_{\bar{c}i}] - [H_{\bar{c}i}])\{F_I\} + \\ &\quad ([H_{\bar{c}\bar{c}}] - [H_{\bar{c}\bar{c}}])[B]^{-1}([H_{\bar{c}\bar{c}}] - [H_{\bar{c}\bar{c}}])\{F_{\bar{C}}\} \end{aligned} \quad (4.76)$$

Comparing equation (4.48) with equations (4.75) and (4.76) gives the third row of

the matrix in equation (4.48). This row comprises submatrices which are given as:

$$[H_{\tilde{C}I}] = [H_{\tilde{c}i}] - ([H_{\tilde{c}\tilde{c}}] - [H_{\tilde{c}\tilde{c}}])[B]^{-1}([H_{\tilde{c}i}] - [H_{\tilde{c}i}]) \quad (4.77)$$

$$[H_{\tilde{C}\tilde{C}}] = [H_{\tilde{c}\tilde{c}}] - ([H_{\tilde{c}\tilde{c}}] - [H_{\tilde{c}\tilde{c}}])[B]^{-1}([H_{\tilde{c}\tilde{c}}] - [H_{\tilde{c}\tilde{c}}]) \quad (4.78)$$

$$[H_{\tilde{C}\tilde{C}}] = [H_{\tilde{c}\tilde{c}}] - ([H_{\tilde{c}\tilde{c}}] - [H_{\tilde{c}\tilde{c}}])[B]^{-1}([H_{\tilde{c}\tilde{c}}] - [H_{\tilde{c}\tilde{c}}]) \quad (4.79)$$

Equations (4.67), (4.68), (4.69), (4.72), (4.73), (4.74), (4.77), (4.78), (4.79), can be arranged together to yield the displacement  $\{X\}$  in function of the FRFs of the substructures as follows:

$$\begin{aligned} \begin{Bmatrix} \{X_I\} \\ \{X_{\tilde{C}}\} \\ \{X_{\tilde{C}}\} \end{Bmatrix} &= \begin{pmatrix} \begin{bmatrix} [H_{ii}] & [H_{i\tilde{c}}] & [H_{i\tilde{c}}] \\ [H_{\tilde{c}i}] & [H_{\tilde{c}\tilde{c}}] & [H_{\tilde{c}\tilde{c}}] \\ [H_{\tilde{c}i}] & [H_{\tilde{c}\tilde{c}}] & [H_{\tilde{c}\tilde{c}}] \end{bmatrix} \\ - \end{pmatrix} \quad (4.80) \\ &\begin{Bmatrix} ([H_{i\tilde{c}}] - [H_{i\tilde{c}}]) \\ ([H_{\tilde{c}\tilde{c}}] - [H_{\tilde{c}\tilde{c}}]) \\ ([H_{\tilde{c}\tilde{c}}] - [H_{\tilde{c}\tilde{c}}]) \end{Bmatrix} \left[ [H_{\tilde{c}\tilde{c}}] + [H_{\tilde{c}\tilde{c}}] - [H_{\tilde{c}\tilde{c}}] - [H_{\tilde{c}\tilde{c}}] + [\mathcal{G}_{\tilde{c}\tilde{c}}]^{-1} \right]^{-1} \begin{Bmatrix} ([H_{i\tilde{c}}] - [H_{i\tilde{c}}]) \\ ([H_{\tilde{c}\tilde{c}}] - [H_{\tilde{c}\tilde{c}}]) \\ ([H_{\tilde{c}\tilde{c}}] - [H_{\tilde{c}\tilde{c}}]) \end{Bmatrix}^T \begin{Bmatrix} \{F_I\} \\ \{F_{\tilde{C}}\} \\ \{F_{\tilde{C}}\} \end{Bmatrix} \end{aligned}$$

Equation (4.80) can be arranged in a more concise form resulting the equation of the *HANORCA* approach written as:

$$\begin{aligned} \begin{Bmatrix} \{X_I\} \\ \{X_C\} \end{Bmatrix} &= \begin{pmatrix} \begin{bmatrix} [H_{ii}] & [H_{ic}] \\ [H_{ci}] & [H_{cc}] \end{bmatrix} \\ - \end{pmatrix} \quad (4.81) \\ &\begin{Bmatrix} ([H_{i\tilde{c}}] - [H_{i\tilde{c}}]) \\ ([H_{\tilde{c}\tilde{c}}] - [H_{\tilde{c}\tilde{c}}]) \end{Bmatrix} \left[ [H_{\tilde{c}\tilde{c}}] + [H_{\tilde{c}\tilde{c}}] - [H_{\tilde{c}\tilde{c}}] - [H_{\tilde{c}\tilde{c}}] + [\mathcal{G}_{\tilde{c}\tilde{c}}]^{-1} \right]^{-1} \begin{Bmatrix} ([H_{i\tilde{c}}] - [H_{i\tilde{c}}]) \\ ([H_{\tilde{c}\tilde{c}}] - [H_{\tilde{c}\tilde{c}}]) \end{Bmatrix}^T \begin{Bmatrix} \{F_I\} \\ \{F_C\} \end{Bmatrix} \end{aligned}$$

The previous equation is the standard FRF form i.e.:  $\{X\} = [H]\{F\}$ . So that it is possible to conclude that the desired FRF matrix of the assembled system,  $[H]$ , in terms of the FRFs matrix of the substructure, is as follows:

$$[H] = \begin{pmatrix} \begin{bmatrix} [H_{ii}] & [H_{ic}] \\ [H_{ci}] & [H_{cc}] \end{bmatrix} \\ - \begin{Bmatrix} ([H_{i\tilde{c}}] - [H_{i\tilde{c}}]) \\ ([H_{\tilde{c}\tilde{c}}] - [H_{\tilde{c}\tilde{c}}]) \end{Bmatrix} \left[ [H_{\tilde{c}\tilde{c}}] + [H_{\tilde{c}\tilde{c}}] - [H_{\tilde{c}\tilde{c}}] - [H_{\tilde{c}\tilde{c}}] + [\mathcal{G}_{\tilde{c}\tilde{c}}]^{-1} \right]^{-1} \begin{Bmatrix} ([H_{i\tilde{c}}] - [H_{i\tilde{c}}]) \\ ([H_{\tilde{c}\tilde{c}}] - [H_{\tilde{c}\tilde{c}}]) \end{Bmatrix}^T \end{pmatrix} \quad (4.82)$$

This equation is used to obtain the FRF of the assembled structure using the FRFs of the collected substructures. Here,  $[\mathcal{G}_{\tilde{c}\tilde{c}}]$ , known as the describing function for representing the nonlinear joints, is a function of the harmonic displacement  $\{X_C\}$ . Therefore the describing function assumes different values at different response am-

plitudes. The response is determined by solving the equation (4.81) interactively by applying the Newton-Raphson method previous presented in section 2.7.

## 4.4.6 Refinements in *HANORCA*

### 4.4.6.1 Pseudo inverse using Singular Value Decomposition (SVD)

Inversion of matrices can occasionally lead to numerical difficulties, particularly if the matrix concerned is ill-conditioned. In FRF coupling analysis, this problem can have a significant effect on the prediction of the response of the assembled structure, [131]. A common technique for inverting an ill-conditioned matrix is to calculate the pseudo-inverse based on the singular value decomposition (SVD) method, [97]. The SVD is a numerical algorithm which can minimise computational errors involving large matrix operations. The SVD decomposes a matrix  $[B]$  into three component matrices, as follows:

$$[B]_{m \times n} = [U]_{m \times m} [\Sigma]_{m \times n} [V]_{n \times n}^t \quad (4.83)$$

The diagonal matrix  $[\Sigma]$  contains the singular values of matrix  $[B]$ . The matrices  $[U]$  and  $[V]$  are orthonormal singular vector matrices such that:

$$\begin{aligned} [U]^t [U] &= [I] \\ [V]^t [V] &= [I] \end{aligned} \quad (4.84)$$

where  $[I]$  is a diagonal identity matrix.

If the matrix  $[B]$  is ill-conditioned, one or more singular values are below the limits of numerical precision,  $\epsilon$ . The singular value matrix thus becomes:

$$[\Sigma]_{m \times n} = \begin{bmatrix} [\Sigma]_{m \times r} \\ 0 \end{bmatrix} \quad (4.85)$$

where  $r$  is the rank of matrix  $[B]$ .

Once the SVD of a matrix  $[B]$  is calculated, the pseudo inverse  $[B]^{-1}$  can be

calculated by using the following form:

$$[B]^{-1} = [V] \begin{bmatrix} [\Sigma]_{m \times r}^{-1} \\ 0 \end{bmatrix} [U]^t \quad (4.86)$$

#### 4.4.6.2 Inverse of a partitioned matrix $[B]$

Equation (4.81) has to be solved using an iterative process. The inverse of matrix  $[B]$  represents the most time-consuming calculation involved in the process. Matrix  $[B]$  has to be evaluated and inverted in all the iterations until the solution is obtained. Although the size of this matrix is just related with the interface data between the substructures, usually not all the connections will be nonlinear connections. This indicates that not all the elements in the matrix  $B$  are varying during the iterations, but only those related to the nonlinear connections. For this reason, there are cases where the iteration process can be speeded up by partitioning matrix  $[B]$  in such a way that the submatrix related with the linear connection is inverted just once, while only the submatrix relating to the nonlinear connection DOFs is inverted in all the iterations. These refinements can be derived by assuming that the connection DOFs  $\{X_C\}$  can be partitioned according to two regions corresponding to:

- the linear DOFs denoted as  $l$
- the nonlinear DOFs denoted as  $n$

$$\left\{ X_C \right\} = \begin{Bmatrix} X_l \\ X_n \end{Bmatrix} \quad (4.87)$$

The matrix  $[B]$  can be partitioned as follows:

$$\begin{bmatrix} B \end{bmatrix} = \begin{bmatrix} B_{ll} & B_{ln} \\ B_{nl} & B_{nn} \end{bmatrix} \quad (4.88)$$

where:

$$\begin{aligned} [B_{ll}] &= [B_{ll}]^T \\ [B_{nn}] &= [B_{nn}]^T \\ [B_{nl}] &= [B_{ln}]^T \end{aligned} \quad (4.89)$$

Using the Moore-Penrose inverse equation [95], matrix  $[B]$  can be expressed as

$$[B] = [B][\mathcal{X}][B] \quad (4.90)$$

If  $[B]$  is non-singular, it is clear that  $[\mathcal{X}] = [B]^{-1}$  and yields:

$$[B][\mathcal{X}] = [I] \quad (4.91)$$

The matrix  $[\mathcal{X}]$  can be partitioned as follows:

$$[\mathcal{X}] = \begin{bmatrix} \mathcal{X}_{ll} & \mathcal{X}_{ln} \\ \mathcal{X}_{nl} & \mathcal{X}_{nn} \end{bmatrix} \quad (4.92)$$

Substituting equations (4.88), (4.92) into (4.91) yields

$$\begin{bmatrix} B_{ll} & B_{ln} \\ B_{nl} & B_{nn} \end{bmatrix} \begin{bmatrix} \mathcal{X}_{ll} & \mathcal{X}_{ln} \\ \mathcal{X}_{nl} & \mathcal{X}_{nn} \end{bmatrix} = \begin{bmatrix} I_{ll} & 0 \\ 0 & I_{nn} \end{bmatrix} \quad (4.93)$$

The matrix equation (4.93) can be expressed as the following system of submatrices equations:

$$[B_{ll}][\mathcal{X}_{ll}] + [B_{ln}][\mathcal{X}_{nl}] = [I_{ll}] \quad (4.94)$$

$$[B_{ll}][\mathcal{X}_{ln}] + [B_{ln}][\mathcal{X}_{nn}] = [0] \quad (4.95)$$

$$[B_{nl}][\mathcal{X}_{ll}] + [B_{nn}][\mathcal{X}_{nl}] = [0] \quad (4.96)$$

$$[B_{nl}][\mathcal{X}_{ln}] + [B_{nn}][\mathcal{X}_{nn}] = [I_{nn}] \quad (4.97)$$

The  $[\mathcal{X}_{ln}]$  and  $[\mathcal{X}_{nl}]$  matrices are calculated from equations (4.95) and (4.96) as:

$$[\mathcal{X}_{ln}] = -[B_{ll}]^{-1}[B_{ln}][\mathcal{X}_{nn}] \quad (4.98)$$

$$[\mathcal{X}_{nl}] = -[B_{nn}]^{-1}[B_{nl}][\mathcal{X}_{ll}] \quad (4.99)$$

The well-known properties of the inverse matrix can be written as:

$$\begin{aligned} ([A]^T)^{-1} &= ([A]^{-1})^T \\ ([A][B])^{-1} &= [B]^{-1}[A]^{-1} \\ ([I] - [A][B])^{-1} &= [I] + [A]([I] - [B][A])^{-1}[B] \end{aligned} \quad (4.100)$$

The  $[\mathcal{X}_{nm}]$  matrix is calculated substituting equation (4.98) into equation (4.97) written as follows:

$$[\mathcal{X}_{nm}] = ([B_{nn}] - [B_{nl}][B_{ul}]^{-1}[B_{ln}])^{-1} \quad (4.101)$$

and the  $[\mathcal{X}_{ul}]$  matrix is calculated substituting equations (4.99), (4.100), (4.101) into equation (4.94), yielding:

$$[\mathcal{X}_{ul}] = [B_{ul}]^{-1} + [B_{ul}]^{-1}[B_{ln}][\mathcal{X}_{nm}][B_{nl}][B_{ul}]^{-1} \quad (4.102)$$

The  $[\mathcal{X}_{ln}]$  matrix can be rearranged by substituting equations (4.100), (4.101) into equation (4.98) leading to:

$$[\mathcal{X}_{ln}] = ([B_{nn}][B_{ln}]^{-1}[B_{ul}] - [B_{nl}])^{-1} \quad (4.103)$$

Using equations (4.89) and (4.100), the transpose of equation (4.103) can be calculated as:

$$[\mathcal{X}_{ln}]^T = ([B_{ul}][B_{nl}]^{-1}[B_{nn}] - [B_{ln}])^{-1} \quad (4.104)$$

The  $[\mathcal{X}_{nl}]$  matrix can be rearranged by substituting equations (4.100), (4.102) into equation (4.99), yielding:

$$[\mathcal{X}_{nl}] = ([B_{ul}][B_{nl}]^{-1}[B_{nn}] - [B_{ln}])^{-1} \quad (4.105)$$

From equation (4.104) and (4.105) it is clear that:

$$[\mathcal{X}_{nl}] = [\mathcal{X}_{ln}]^T \quad (4.106)$$

Substituting equations (4.98), (4.101), (4.102) and (4.106) into (4.92), yields the inverse of matrix  $[B]$  in function of the inverse of its submatrices as follows:

$$\begin{bmatrix} B_{ll} & B_{ln} \\ B_{nl} & B_{nn} \end{bmatrix}^{-1} = \begin{bmatrix} [B_{ll}]^{-1} + [B_{ll}]^{-1}[B_{ln}][\mathcal{X}_{nn}][B_{nl}][B_{ll}]^{-1} & -[B_{ll}]^{-1}[B_{ln}][\mathcal{X}_{nn}] \\ (-[B_{ll}]^{-1}[B_{ln}][\mathcal{X}_{nn})^T & [\mathcal{X}_{nn}] \end{bmatrix} \quad (4.107)$$

As mentioned before, the main advantage of using this formulation is related to the crucial operation of inversion during the convergence process. Herein, instead of calculating the inverse of the whole matrix  $[B]_{C \times C}$ , at each iteration it is only necessary to calculate the inverse of a matrix of size  $n \times n$ , the submatrix  $[\mathcal{X}_{nn}]$ , which depends only on the non-linear connection DOFs. All the submatrices of  $[\mathcal{X}]$  include the term  $[B_{ll}]^{-1}$ , which should be calculated only once since it contains only linear DOFs and does not change during the iteration process. After the responses at these connection DOFs  $\{X_C\}$  are calculated, the interior DOFs  $\{X_I\}$  can be easily determined without affecting significantly the required computational time, as it involves only multiplication.

#### 4.4.6.3 Local iterations

When working with an assembled system having a large number of connections and a large number of degrees of freedom, it is generally the case that not all the DOFs involved in the process of the calculation of the response are required or are going to be excited. Therefore, better efficiency can be achieved if only those which are required are involved in the process. The response and excitation vector is going to be subdivided to derive the refined formulation.

Consider the equation for this Collected Substructure, relating the displacement vectors and the force vector shown in matrix form as follows:

$$\begin{Bmatrix} x_i \\ x_{\bar{c}} \\ x_{\bar{c}} \end{Bmatrix} = \begin{bmatrix} H_{ii} & H_{i\bar{c}} & H_{i\bar{c}} \\ H_{\bar{c}i} & H_{\bar{c}\bar{c}} & H_{\bar{c}\bar{c}} \\ H_{\bar{c}i} & H_{\bar{c}\bar{c}} & H_{\bar{c}\bar{c}} \end{bmatrix} \begin{Bmatrix} f_i \\ f_{\bar{c}} \\ f_{\bar{c}} \end{Bmatrix} \quad (4.108)$$

Looking at the Assembled System, the displacement in each point can be written as:

$$\begin{Bmatrix} X_I \\ X_{\bar{C}} \\ X_{\tilde{C}} \end{Bmatrix} = \begin{bmatrix} H_{II} & H_{I\bar{C}} & H_{I\tilde{C}} \\ H_{\bar{C}I} & H_{\bar{C}\bar{C}} & H_{\bar{C}\tilde{C}} \\ H_{\tilde{C}I} & H_{\tilde{C}\bar{C}} & H_{\tilde{C}\tilde{C}} \end{bmatrix} \begin{Bmatrix} F_I \\ F_{\bar{C}} \\ F_{\tilde{C}} \end{Bmatrix} \quad (4.109)$$

The displacement vectors  $\{x_i\}$ ,  $\{x_{\bar{c}}\}$ ,  $\{x_{\tilde{c}}\}$  can be arranged as shown below: as:

$$\{x_i\} = \begin{Bmatrix} x_{i_d} \\ x_{i_u} \end{Bmatrix} \quad \{x_{\bar{c}}\} = \begin{Bmatrix} x_{\bar{c}_d} \\ x_{\bar{c}_u} \end{Bmatrix} \quad \{x_{\tilde{c}}\} = \begin{Bmatrix} x_{\tilde{c}_d} \\ x_{\tilde{c}_u} \end{Bmatrix} \quad (4.110)$$

where subscript  $d$  and  $u$  represent desired and undesired DOF respectively. Therefore, the equation for the Collected Substructure, relating the required displacement vectors and the force vector can be written in matrix form as follows:

$$\begin{Bmatrix} x_{i_d} \\ x_{\bar{c}_d} \\ x_{\tilde{c}_d} \end{Bmatrix} = \begin{bmatrix} H_{i_d i} & H_{i_d \bar{c}} & H_{i_d \tilde{c}} \\ H_{\bar{c}_d i} & H_{\bar{c}_d \bar{c}} & H_{\bar{c}_d \tilde{c}} \\ H_{\tilde{c}_d i} & H_{\tilde{c}_d \bar{c}} & H_{\tilde{c}_d \tilde{c}} \end{bmatrix} \begin{Bmatrix} f_i \\ f_{\bar{c}} \\ f_{\tilde{c}} \end{Bmatrix} \quad (4.111)$$

Looking now at the Assembled System, the equation relating the required displacement vector and the force vector can be written as:

$$\begin{Bmatrix} X_{I_d} \\ X_{\bar{C}_d} \\ X_{\tilde{C}_d} \end{Bmatrix} = \begin{bmatrix} H_{I_d I} & H_{I_d \bar{C}} & H_{I_d \tilde{C}} \\ H_{\bar{C}_d I} & H_{\bar{C}_d \bar{C}} & H_{\bar{C}_d \tilde{C}} \\ H_{\tilde{C}_d I} & H_{\tilde{C}_d \bar{C}} & H_{\tilde{C}_d \tilde{C}} \end{bmatrix} \begin{Bmatrix} F_I \\ F_{\bar{C}} \\ F_{\tilde{C}} \end{Bmatrix} \quad (4.112)$$

where:

$I_d$  = internal DOFs where the response is desired

$\bar{C}_d, \tilde{C}_d$  = connection DOFs where the response is desired

The equilibrium conditions can be written as:

$$\begin{aligned} \{F_{\bar{C}}\} &= \{F_{\tilde{C}}\} = \{f_{\bar{c}}\} + \{f_{\tilde{c}}\} \\ \{f_i\} &= \{F_I\} \end{aligned} \quad (4.113)$$

The compatibility conditions can be written in two forms:

$$\begin{aligned}
\{x_{i_d}\} &= \{X_{I_d}\} \\
\{x_{\bar{c}_d}\} &= \{X_{\bar{C}_d}\} \\
\{x_{\tilde{c}_d}\} &= \{X_{\tilde{C}_d}\} \\
\{x_{\bar{c}}\} - \{x_{\tilde{c}}\} &= -[\mathcal{G}_{\bar{c}\tilde{c}}]^{-1} \{f_{\bar{c}}\}
\end{aligned} \tag{4.114}$$

or:

$$\begin{aligned}
\{x_{i_d}\} &= \{X_{I_d}\} \\
\{x_{\bar{c}_d}\} &= \{X_{\bar{C}_d}\} \\
\{x_{\tilde{c}_d}\} &= \{X_{\tilde{C}_d}\} \\
\{x_{\tilde{c}}\} - \{x_{\bar{c}}\} &= -[\mathcal{G}_{\tilde{c}\bar{c}}]^{-1} \{f_{\tilde{c}}\}
\end{aligned} \tag{4.115}$$

Now by using equations (4.108,4.109,4.113,4.114,4.115) it is possible to find a relationship between the FRF submatrices of the assembled structure,  $[H_R]$ , in terms of the FRF submatrices of the collected substructures,  $[H_r]$ . The detailed derivation of this relationship can be found in Appendix B, resulting the following equation:

$$\begin{aligned}
\begin{Bmatrix} \{X_{I_d}\} \\ \{X_{\bar{C}_d}\} \\ \{X_{\tilde{C}_d}\} \end{Bmatrix} &= \left( \begin{bmatrix} [H_{i_d i}] & [H_{i_d \bar{c}}] & [H_{i_d \tilde{c}}] \\ [H_{\bar{c}_d i}] & [H_{\bar{c}_d \bar{c}}] & [H_{\bar{c}_d \tilde{c}}] \\ [H_{\tilde{c}_d i}] & [H_{\tilde{c}_d \bar{c}}] & [H_{\tilde{c}_d \tilde{c}}] \end{bmatrix} \right) - \\
&\quad \begin{Bmatrix} ([H_{i_d \bar{c}}] - [H_{i_d \tilde{c}}]) \\ ([H_{\bar{c}_d \bar{c}}] - [H_{\bar{c}_d \tilde{c}}]) \\ ([H_{\tilde{c}_d \bar{c}}] - [H_{\tilde{c}_d \tilde{c}}]) \end{Bmatrix} \left[ [H_{\bar{c}\bar{c}}] + [H_{\tilde{c}\tilde{c}}] - [H_{\bar{c}\tilde{c}}] - [H_{\tilde{c}\bar{c}}] + [\mathcal{G}_{\bar{c}\tilde{c}}]^{-1} \right]^{-1} \begin{Bmatrix} ([H_{i\bar{c}}] - [H_{i\tilde{c}}]) \\ ([H_{\bar{c}\bar{c}}] - [H_{\bar{c}\tilde{c}}]) \\ ([H_{\tilde{c}\bar{c}}] - [H_{\tilde{c}\tilde{c}}]) \end{Bmatrix}^T \begin{Bmatrix} \{F_I\} \\ \{F_{\bar{C}}\} \\ \{F_{\tilde{C}}\} \end{Bmatrix}
\end{aligned} \tag{4.116}$$

Equation (4.116) can be arranged in a more concise form resulting the formulation of *HANORCA* with the refinement of local iterations as follows:

$$\begin{aligned}
\begin{Bmatrix} \{X_{I_d}\} \\ \{X_{C_d}\} \end{Bmatrix} &= \left( \begin{bmatrix} [H_{i_d i}] & [H_{i_d c}] \\ [H_{c_d i}] & [H_{c_d c}] \end{bmatrix} \right) - \\
&\quad \begin{Bmatrix} ([H_{i_d \bar{c}}] - [H_{i_d \tilde{c}}]) \\ ([H_{c_d \bar{c}}] - [H_{c_d \tilde{c}}]) \end{Bmatrix} \left[ [H_{\bar{c}\bar{c}}] + [H_{\tilde{c}\tilde{c}}] - [H_{\bar{c}\tilde{c}}] - [H_{\tilde{c}\bar{c}}] + [\mathcal{G}_{\bar{c}\tilde{c}}]^{-1} \right]^{-1} \begin{Bmatrix} ([H_{i\bar{c}}] - [H_{i\tilde{c}}]) \\ ([H_{c\bar{c}}] - [H_{c\tilde{c}}]) \end{Bmatrix}^T \begin{Bmatrix} \{F_I\} \\ \{F_C\} \end{Bmatrix}
\end{aligned} \tag{4.117}$$

This formulation allows us to calculate only the response where it is required to avoid spending time in unnecessary calculations. But there still remains some calculations which can be avoided. One of these is when connecting one point to another point or more than one point with rigid connections. This coordinate in the Assembled

System will be only one coordinate, but in this approach all DOFs are still going to be calculated. To overcome this problem, the connection DOFs  $C$ ,  $c$  are composed of all non repetitive DOFs. Another calculation that can be avoided is related with the excitation force. The excitation can be applied in all points, but usually many of these points do not have excitation, therefore there still remains some multiplication by zero. To eliminate this excitation points, it is necessary to create a new group of points where the excitation points will be desired.

The final refined algorithm can be derived assuming that the DOFs  $I$ ,  $C$ ,  $i$ ,  $c$  can be partitioned again according to two regions corresponding to the DOFs where the force is desired denoted with subscript,  $f$ , and to the DOFs where the force is undesired denoted with subscript,  $u$ . The final equation of the Collected Substructure, relating displacement vectors where the response and force vector are desired is shown in matrix form as: follows:

$$\begin{Bmatrix} \{X_{I_d}\} \\ \{X_{C_d}\} \end{Bmatrix} = \left( \begin{bmatrix} [H_{i_d i_f}] & [H_{i_d c_f}] \\ [H_{c_d i_f}] & [H_{c_d c_f}] \end{bmatrix} - \begin{Bmatrix} ([H_{i_d \bar{c}}] - [H_{i_d \bar{c}}]) \\ ([H_{c_d \bar{c}}] - [H_{c_d \bar{c}}]) \end{Bmatrix} \left[ [H_{\bar{c}\bar{c}}] + [H_{\bar{c}\bar{c}}] - [H_{\bar{c}\bar{c}}] - [H_{\bar{c}\bar{c}}] + [\mathbf{G}_{\bar{c}\bar{c}}]^{-1} \right]^{-1} \begin{Bmatrix} ([H_{i_f \bar{c}}] - [H_{i_f \bar{c}}]) \\ ([H_{c_f \bar{c}}] - [H_{c_f \bar{c}}]) \end{Bmatrix}^T \right) \begin{Bmatrix} \{F_{I_f}\} \\ \{F_{C_f}\} \end{Bmatrix} \quad (4.118)$$

A detailed studied of these improvements based on the number of floating operations can be seen in Appendix C.

## 4.5 Multi-Harmonic Nonlinear Coupling Approaches

### 4.5.1 Introduction

The harmonic analysis technique has been found to be quite successful in many cases where the higher harmonics components are small [23, 88, 136, 139]. However, there are some special nonlinear structures, such as structures containing quadratic or bi-linear joints, where the harmonic response is not enough to represent the dynamic characteristics [72]. Therefore a more accurate representation of the dynamic characteristics can be achieved by the multi-harmonic analysis. In this section, the harmonic nonlinear methods developed in the previous sections were extended to overcome this problem.

## 4.5.2 Multi-Harmonic Nonlinear Impedance Coupling using Multi-Harmonic Balance Method

Consider the matrix differential equation of motion of the structure where the internal nonlinear forces are treated as pseudo external forces:

$$[M]\{\ddot{x}\} + [C]\{\dot{x}\} + i[D]\{x\} + [K]x = \{f\} - \{\mathbf{f}\} \quad (4.119)$$

Equation (4.119) can be written in impedance form as:

$$[Z]\{x\} = \{f\} - \{\mathbf{f}\} \quad (4.120)$$

where  $[Z]$  is given by:

$$[Z] = [[K] - \omega^2[M] + i\omega[C] + i[D]] \quad (4.121)$$

In order to consider the higher harmonics it is necessary to assume the hypothesis shown by equations (2.62,2.64,2.66) and also that the external periodic forcing can be represented in Fourier series as follows:

$$f_{kl} = \sum_{m=0}^{\infty} f_{kl}^m = \sum_{m=0}^{\infty} F_{kl}^m e^{im\Psi} \quad (4.122)$$

Then considering  $n$  harmonics in the response, equation (4.120) can be written as a set of nonlinear algebraic equations as:

$$\begin{bmatrix} [Z^1] & 0 & 0 & \dots & 0 \\ 0 & [Z^2] & 0 & \dots & 0 \\ \vdots & 0 & \ddots & & \vdots \\ 0 & 0 & 0 & \dots & [Z^n] \end{bmatrix} \begin{Bmatrix} \{X^1\} \\ \{X^2\} \\ \vdots \\ \{X^n\} \end{Bmatrix} = \begin{Bmatrix} \{F^1\} \\ \{F^2\} \\ \vdots \\ \{F^n\} \end{Bmatrix} - \begin{Bmatrix} \{\mathcal{F}^1\} \\ \{\mathcal{F}^2\} \\ \vdots \\ \{\mathcal{F}^n\} \end{Bmatrix} \quad (4.123)$$

The quasi-linear theory presented here converts a set of  $n$  nonlinear equations (4.119) to a set of  $n$  nonlinear algebraic equations (4.123). From equation (4.123) it is possible to see that although the harmonics equations are uncoupled, all the harmonics will

be excited as an external force, then the response of the structure under harmonic excitation can be obtained by solving equation (4.123) iteratively. Equation (4.123) can be written in a more compact form as:

$$\{g^m(y)\} = \{0\} \quad (4.124)$$

where:

$$\begin{Bmatrix} \{g(y)^1\} \\ \{g(y)^2\} \\ \vdots \\ \{g(y)^n\} \end{Bmatrix} = \begin{Bmatrix} \{[Z^1]\{X^1\} - \{F^1\} + \{\mathcal{F}^1\}\} \\ \{[Z^2]\{X^2\} - \{F^2\} + \{\mathcal{F}^2\}\} \\ \vdots \\ \{[Z^n]\{X^n\} - \{F^n\} + \{\mathcal{F}^n\}\} \end{Bmatrix} \quad (4.125)$$

Equation (4.125) can be solved by using the Newton-Raphson method previously shown in section (2.7).

### 4.5.3 Multi-Harmonic Nonlinear Impedance Coupling using High-Order Describing Function (*MUHAIM*)

Consider the matrix differential equation of motion of the structure with internal nonlinear forces can be written as:

$$[M]\{\ddot{x}\} + [C]\{\dot{x}\} + i[D]\{x\} + [K]\{x\} + \{\mathbf{f}\} = \{f\} \quad (4.126)$$

Equation (4.126) can be written in impedance form as:

$$[Z]\{x\} + \{\mathbf{f}\} = \{f\} \quad (4.127)$$

where  $[Z]$  is given by:

$$[Z] = [[K] - [M]\omega^2 + i\omega[C] + i[D]]$$

In order to substitute the nonlinear force by its describing function, it is necessary to assume the hypothesis shown by equations (2.62,2.64,2.66) and also that the external

periodic forcing can be represented in Fourier series as:

$$f_{kl} = \sum_{m=0}^{\infty} f_{kl}^m = \sum_{m=0}^{\infty} F_{kl}^m e^{im\Psi} \quad (4.128)$$

Substituting the internal nonlinear force  $\{\mathbf{f}\}$  by the corresponding describing function equation (2.103) in equation (4.127) yields the  $m$ th harmonic differential equation as:

$$[[Z^m] + [\Theta]^m]\{X^m\} = \{F^m\} \quad (4.129)$$

where  $[Z^m]$  is given by:

$$[Z^m] = [[K] - [M](m\omega)^2 + im\omega[C] + i[D]]$$

Considering  $n$  harmonics in the response, the differential equation of the system can be written as:

$$\begin{bmatrix} [Z^1] + [\Theta]^1 & 0 & 0 & \dots & 0 \\ 0 & [Z^2] + [\Theta]^2 & 0 & \dots & 0 \\ \vdots & 0 & \ddots & & \vdots \\ 0 & 0 & 0 & \dots & [Z^n] + [\Theta]^n \end{bmatrix} \begin{Bmatrix} \{X^1\} \\ \{X^2\} \\ \vdots \\ \{X^n\} \end{Bmatrix} = \begin{Bmatrix} \{F^1\} \\ \{F^2\} \\ \vdots \\ \{F^n\} \end{Bmatrix} \quad (4.130)$$

The quasi-linear theory presented here converts a set of  $n$  nonlinear equations (4.126) to a set of  $n$  nonlinear algebraic equations (4.130). From equation (4.130) it is possible to see that the harmonics equations are uncoupled, which indicates that the response of the structure under harmonic excitation can be obtained iteratively by solving equation (4.130) together with the describing functions that couple the harmonic equation. Equations (4.130,2.99) can be written together in a more compact form as:

$$\{g(y)\} = \{0\} \quad (4.131)$$

where:

$$\begin{pmatrix} \{g^1(y)\} \\ \{g^2(y)\} \\ \vdots \\ \{g^n(y)\} \end{pmatrix} = \begin{pmatrix} ([Z^1] + [\Delta]^1)\{X^1\} \\ ([Z^2] + [\Delta]^2)\{X^2\} \\ \vdots \\ ([Z^n] + [\Delta]^1)\{X^n\} \\ \nu^1(X_k^1 - X_l^1) - \mathcal{F}_{kl}^1 \\ \nu^2(X_k^2 - X_l^2) - \mathcal{F}_{kl}^2 \\ \vdots \\ \nu^n(X_k^n - X_l^n) - \mathcal{F}_{kl}^n \end{pmatrix} \quad (4.132)$$

Equation (4.132) can be solved by using the Newton-Raphson method.

#### 4.5.4 Multi-Harmonic Nonlinear Impedance Coupling using Multi-Harmonic Describing Function (*MUHANORCA*)

Consider the matrix differential equation of motion of the structure with internal nonlinear forces written as:

$$[M]\{\ddot{x}\} + [C]\{\dot{x}\} + i[D]\{x\} + [K]\{x\} + \{\mathbf{f}\} = \{f\} \quad (4.133)$$

Equation (4.133) can be written in impedance form as:

$$[Z]\{x\} + \{\mathbf{f}\} = \{f\} \quad (4.134)$$

where  $[Z]$  is given by:

$$[Z] = [[K] - [M]\omega^2 + i\omega[C] + i[D]] \quad (4.135)$$

In order to substitute the nonlinear force by its multi-harmonic describing function, it is necessary to assume the hypothesis shown by equations (2.62,2.64,2.66) and also

that the external periodic forcing can be represented in Fourier series as:

$$f_{kl} = \sum_{m=0}^{\infty} f_{kl}^m = \sum_{m=0}^{\infty} F_{kl}^m e^{im\Psi} \quad (4.136)$$

Substituting the internal nonlinear force  $\{\mathbf{f}\}$  by the corresponding multi-harmonic describing function equation (2.108) in equation (4.134) yields the  $m_{th}$  harmonic differential equation as:

$$[Z^m]\{X^m\} + \sum_{i=1}^m [\Delta]^{mi}\{X^i\} = \{F^m\} \quad (4.137)$$

Considering  $n$  harmonics in the force and response, the differential equation of the system can be written as:

$$\begin{bmatrix} [Z^1] + [\Delta]^{11} & [\Delta]^{12} & [\Delta]^{13} & \dots & [\Delta]^{1n} \\ [\Delta]^{21} & [Z^2] + [\Delta]^{22} & [\Delta]^{23} & \dots & [\Delta]^{2n} \\ \vdots & & \ddots & & \vdots \\ [\Delta]^{n1} & [\Delta]^{n2} & [\Delta]^{n3} & \dots & [Z^n] + [\Delta]^{nn} \end{bmatrix} \begin{Bmatrix} \{X^1\} \\ \{X^2\} \\ \vdots \\ \{X^n\} \end{Bmatrix} = \begin{Bmatrix} \{F^1\} \\ \{F^2\} \\ \vdots \\ \{F^n\} \end{Bmatrix} \quad (4.138)$$

The quasi-linear theory presented here converts a set of  $n$  nonlinear equations (4.133) to a set of  $n$  nonlinear algebraic equations (4.138). From equation (4.138) it is possible to see that the harmonics equations are coupled, which indicates that the response of the structure under harmonic excitation can be obtained by solving equation (4.130). Equation (4.138) can be written together in a more compact form as:

$$\{g(y)\} = \{0\} \quad (4.139)$$

where:

$$\begin{Bmatrix} \{g^1(y)\} \\ \{g^2(y)\} \\ \vdots \\ \{g^n(y)\} \end{Bmatrix} = \begin{Bmatrix} [[Z^1] + [\Delta]^{11}]\{X^1\} + [\Delta]^{12}\{X^2\} + \dots + [\Delta]^{1n}\{X^n\} - \{\mathcal{F}^1\} \\ [\Delta]^{21}\{X^1\} + [[Z^2] + [\Delta]^{22}]\{X^2\} + \dots + [\Delta]^{2n}\{X^n\} - \{\mathcal{F}^2\} \\ \vdots \\ [\Delta]^{n1}\{X^1\} + [\Delta]^{n2}\{X^2\} + \dots + [[Z^n] + [\Delta]^{nn}]\{X^n\} - \{\mathcal{F}^n\} \end{Bmatrix} \quad (4.140)$$

Equation (4.140) can be solved by using the Newton-Raphson method.

### 4.5.5 Multi-Harmonic Nonlinear Receptance Coupling using Multi-Harmonic Describing Function

Let us assume all the substructures to be connected and the assembled system as presented in section 4.2 . The equation of the Collected Substructure, relating the displacement vector and the force vector for  $n$  harmonics for the displacement and  $m$  harmonics for the force is shown in matrix form as:

$$\begin{pmatrix} x_i^1 \\ x_{\bar{c}}^1 \\ x_{\bar{c}}^1 \\ x_i^2 \\ x_{\bar{c}}^2 \\ x_{\bar{c}}^2 \\ \vdots \\ x_i^n \\ x_{\bar{c}}^n \\ x_{\bar{c}}^n \end{pmatrix} = \begin{bmatrix} H_{ii}^{11} & H_{i\bar{c}}^{11} & H_{i\bar{c}}^{11} & \cdots & H_{ii}^{1m} & H_{i\bar{c}}^{1m} & H_{i\bar{c}}^{1m} \\ \vdots & \vdots & \vdots & \ddots & \vdots & \vdots & \vdots \\ H_{ii}^{n1} & H_{i\bar{c}}^{n1} & H_{i\bar{c}}^{n1} & \cdots & H_{ii}^{nm} & H_{i\bar{c}}^{nm} & H_{i\bar{c}}^{nm} \\ H_{\bar{c}i}^{11} & H_{\bar{c}\bar{c}}^{11} & H_{\bar{c}\bar{c}}^{11} & \cdots & H_{\bar{c}i}^{1m} & H_{\bar{c}\bar{c}}^{1m} & H_{\bar{c}\bar{c}}^{1m} \\ \vdots & \vdots & \vdots & \ddots & \vdots & \vdots & \vdots \\ H_{\bar{c}i}^{n1} & H_{\bar{c}\bar{c}}^{n1} & H_{\bar{c}\bar{c}}^{n1} & \cdots & H_{\bar{c}i}^{nm} & H_{\bar{c}\bar{c}}^{nm} & H_{\bar{c}\bar{c}}^{nm} \\ H_{\bar{c}i}^{11} & H_{\bar{c}\bar{c}}^{11} & H_{\bar{c}\bar{c}}^{11} & \cdots & H_{\bar{c}i}^{1m} & H_{\bar{c}\bar{c}}^{1m} & H_{\bar{c}\bar{c}}^{1m} \\ \vdots & \vdots & \vdots & \ddots & \vdots & \vdots & \vdots \\ H_{\bar{c}i}^{n1} & H_{\bar{c}\bar{c}}^{n1} & H_{\bar{c}\bar{c}}^{n1} & \cdots & H_{\bar{c}i}^{nm} & H_{\bar{c}\bar{c}}^{nm} & H_{\bar{c}\bar{c}}^{nm} \end{bmatrix} \begin{pmatrix} f_i^1 \\ f_{\bar{c}}^1 \\ f_{\bar{c}}^1 \\ f_i^2 \\ f_{\bar{c}}^2 \\ f_{\bar{c}}^2 \\ \vdots \\ f_i^m \\ f_{\bar{c}}^m \\ f_{\bar{c}}^m \end{pmatrix} \quad (4.141)$$

Looking at the Assembled System, the displacement in each point can be written as:

$$\begin{pmatrix} X_I^1 \\ X_C^1 \\ X_{\bar{C}}^1 \\ X_I^2 \\ X_{\bar{C}}^2 \\ X_{\bar{C}}^2 \\ \vdots \\ X_I^n \\ X_{\bar{C}}^n \\ X_{\bar{C}}^n \end{pmatrix} = \begin{bmatrix} H_{II}^{11} & H_{I\bar{C}}^{11} & H_{I\bar{C}}^{11} & \cdots & H_{II}^{1m} & H_{I\bar{C}}^{nm} & H_{I\bar{C}}^{1m} \\ \vdots & \vdots & \vdots & \ddots & \vdots & \vdots & \vdots \\ H_{II}^{n1} & H_{I\bar{C}}^{n1} & H_{I\bar{C}}^{n1} & \cdots & H_{II}^{nm} & H_{I\bar{C}}^{nm} & H_{I\bar{C}}^{nm} \\ H_{\bar{C}I}^{11} & H_{\bar{C}\bar{C}}^{11} & H_{\bar{C}\bar{C}^{11}} & \cdots & H_{\bar{C}I}^{1m} & H_{\bar{C}\bar{C}}^{1m} & H_{\bar{C}\bar{C}}^{1m} \\ \vdots & \vdots & \vdots & \ddots & \vdots & \vdots & \vdots \\ H_{\bar{C}I}^{n1} & H_{\bar{C}\bar{C}}^{n1} & H_{\bar{C}\bar{C}}^{n1} & \cdots & H_{\bar{C}I}^{nm} & H_{\bar{C}\bar{C}}^{nm} & H_{\bar{C}\bar{C}}^{nm} \\ H_{\bar{C}I}^{11} & H_{\bar{C}\bar{C}}^{11} & H_{\bar{C}\bar{C}}^{11} & \cdots & H_{\bar{C}I}^{1m} & H_{\bar{C}\bar{C}}^{1m} & H_{\bar{C}\bar{C}}^{1m} \\ \vdots & \vdots & \vdots & \ddots & \vdots & \vdots & \vdots \\ H_{\bar{C}I}^{n1} & H_{\bar{C}\bar{C}}^{n1} & H_{\bar{C}\bar{C}}^{n1} & \cdots & H_{\bar{C}I}^{nm} & H_{\bar{C}\bar{C}}^{nm} & H_{\bar{C}\bar{C}}^{nm} \end{bmatrix} \begin{pmatrix} F_i^1 \\ F_C^1 \\ F_{\bar{C}}^1 \\ F_I^2 \\ F_{\bar{C}}^2 \\ F_{\bar{C}}^2 \\ \vdots \\ F_I^m \\ F_{\bar{C}}^m \\ F_{\bar{C}}^m \end{pmatrix} \quad (4.142)$$

Assuming that all the harmonics order of the displacement can be arranged in a the set called  $Q_r$  and that all the harmonics order of the force can be arranged in a the set called  $Q_s$ . For the displacement harmonic  $n = q_r$  and for the force harmonic  $m = q_s$ , the Collected

Substructure equation can be written in a more concise form as:

$$\begin{Bmatrix} x_i^{qr} \\ x_{\bar{c}}^{qr} \\ x_{\bar{c}}^{qr} \end{Bmatrix} = \begin{bmatrix} H_{ii}^{qrqs} & H_{i\bar{c}}^{qrqs} & H_{i\bar{c}}^{qrqs} \\ H_{\bar{c}i}^{qrqs} & H_{\bar{c}\bar{c}}^{qrqs} & H_{\bar{c}\bar{c}}^{qrqs} \\ H_{\bar{c}i}^{qrqs} & H_{\bar{c}\bar{c}}^{qrqs} & H_{\bar{c}\bar{c}}^{qrqs} \end{bmatrix} \begin{Bmatrix} f_i^{qs} \\ f_{\bar{c}}^{qs} \\ f_{\bar{c}}^{qs} \end{Bmatrix} \quad (4.143)$$

and the Assembled System equation can also be written in a more concise form as:

$$\begin{Bmatrix} X_I^{qr} \\ X_{\bar{C}}^{qr} \\ X_{\bar{C}}^{qr} \end{Bmatrix} = \begin{bmatrix} H_{II}^{qrqs} & H_{I\bar{C}}^{qrqs} & H_{I\bar{C}}^{qrqs} \\ H_{\bar{C}I}^{qrqs} & H_{\bar{C}\bar{C}}^{qrqs} & H_{\bar{C}\bar{C}}^{qrqs} \\ H_{\bar{C}I}^{qrqs} & H_{\bar{C}\bar{C}}^{qrqs} & H_{\bar{C}\bar{C}}^{qrqs} \end{bmatrix} \begin{Bmatrix} F_I^{qs} \\ F_{\bar{C}}^{qs} \\ F_{\bar{C}}^{qs} \end{Bmatrix} \quad (4.144)$$

The equilibrium conditions can be written as:

$$\begin{aligned} \{F_{\bar{C}}^{qs}\} &= \{F_{\bar{C}}^{qs}\} = \{f_{\bar{c}}^{qs}\} + \{f_{\bar{c}}^{qs}\} \\ \{f_i^{qs}\} &= \{F_I^{qs}\} \end{aligned} \quad (4.145)$$

The compatibility conditions can be written in two forms:

$$\begin{aligned} \{y_{\bar{c}\bar{c}}^{qr}\} &= \{x_{\bar{c}}^{qr}\} - \{x_{\bar{c}}^{qr}\} \\ \{x_i^{qr}\} &= \{X_I^{qr}\} \\ \{x_{\bar{c}}^{qr}\} &= \{X_{\bar{C}}^{qr}\} \\ \{x_{\bar{c}}^{qr}\} &= \{X_{\bar{C}}^{qr}\} \\ \{y_{\bar{c}\bar{c}}^{qr}\} &= -[\mathcal{G}_{\bar{c}\bar{c}}^{qsqr}]^{-1} \{f_{\bar{c}}^{qs}\} \end{aligned} \quad (4.146)$$

or:

$$\begin{aligned} \{y_{\bar{c}\bar{c}}^{qr}\} &= \{x_{\bar{c}}^{qr}\} - \{x_{\bar{c}}^{qr}\} \\ \{x_i^{qr}\} &= \{X_I^{qr}\} \\ \{x_{\bar{c}}^{qr}\} &= \{X_{\bar{C}}^{qr}\} \\ \{x_{\bar{c}}^{qr}\} &= \{X_{\bar{C}}^{qr}\} \\ \{x_{\bar{c}}^{qr}\} - \{x_{\bar{c}}^{qr}\} &= -[\mathcal{G}_{\bar{c}\bar{c}}^{qsqr}]^{-1} \{f_{\bar{c}}^{qs}\} \end{aligned} \quad (4.147)$$

Now using the previous equations (4.141,4.142,4.145,4.146,4.147) it is possible to find a relation between the FRF submatrices of the assembled structure,  $[H_R]$ , in terms of the FRF submatrices of the collected substructures,  $[H_r]$ . The detailed derivation of this relationship

can be found in Appendix D, resulting the following equation:

$$\begin{aligned} \begin{Bmatrix} \{X_I^{qr}\} \\ \{X_C^{qr}\} \\ \{X_C^{qr}\} \end{Bmatrix} &= \begin{pmatrix} \left[ \begin{array}{ccc} [H_{ii}^{qrqs}] & [H_{ic}^{qrqs}] & [H_{ic}^{qrqs}] \\ [H_{ci}^{qrqs}] & [H_{cc}^{qrqs}] & [H_{cc}^{qrqs}] \\ [H_{ci}^{qrqs}] & [H_{cc}^{qrqs}] & [H_{cc}^{qrqs}] \end{array} \right] \\ \left\{ \begin{array}{l} ([H_{ic}^{qrqs}] - [H_{ic}^{qrqs}]) \\ ([H_{cc}^{qrqs}] - [H_{cc}^{qrqs}]) \\ ([H_{cc}^{qrqs}] - [H_{cc}^{qrqs}]) \end{array} \right\} \\ \left[ [H_{cc}^{qrqs}] + [H_{cc}^{qrqs}] - [H_{cc}^{qrqs}] - [H_{cc}^{qrqs}] + [\mathcal{G}_{cc}^{qsqr}]^{-1} \right]^{-1} \left\{ \begin{array}{l} ([H_{ic}^{qrqs}] - [H_{ic}^{qrqs}]) \\ ([H_{cc}^{qrqs}] - [H_{cc}^{qrqs}]) \\ ([H_{cc}^{qrqs}] - [H_{cc}^{qrqs}]) \end{array} \right\}^T \end{pmatrix} \begin{Bmatrix} \{F_I^{qs}\} \\ \{F_C^{qs}\} \\ \{F_C^{qs}\} \end{Bmatrix} \end{aligned} \quad (4.148)$$

where matrix  $[\mathcal{G}_{cc}^{qsqr}]$  is given by:

$$[\mathcal{G}_{cc}^{qsqr}] = \begin{bmatrix} \mathcal{G}_{cc}^{11} & \mathcal{G}_{cc}^{12} & \dots & \mathcal{G}_{cc}^{1qr} \\ \vdots & & \ddots & \vdots \\ \mathcal{G}_{cc}^{qs1} & \mathcal{G}_{cc}^{qs2} & \dots & \mathcal{G}_{cc}^{qsqr} \end{bmatrix}$$

Equation (4.148) can be arranged in a more concise form as:

$$\begin{aligned} \begin{Bmatrix} \{X_I^{qr}\} \\ \{X_C^{qr}\} \end{Bmatrix} &= \begin{pmatrix} \left[ \begin{array}{cc} [H_{ii}^{qrqs}] & [H_{ic}^{qrqs}] \\ [H_{ci}^{qrqs}] & [H_{cc}^{qrqs}] \end{array} \right] \\ \left\{ \begin{array}{l} ([H_{ic}^{qrqs}] - [H_{ic}^{qrqs}]) \\ ([H_{cc}^{qrqs}] - [H_{cc}^{qrqs}]) \end{array} \right\} \\ \left[ [H_{cc}^{qrqs}] + [H_{cc}^{qrqs}] - [H_{cc}^{qrqs}] - [H_{cc}^{qrqs}] + [\mathcal{G}_{cc}^{qsqr}]^{-1} \right]^{-1} \left\{ \begin{array}{l} ([H_{ic}^{qrqs}] - [H_{ic}^{qrqs}]) \\ ([H_{cc}^{qrqs}] - [H_{cc}^{qrqs}]) \end{array} \right\}^T \end{pmatrix} \begin{Bmatrix} \{F_I^{qs}\} \\ \{F_C^{qs}\} \end{Bmatrix} \end{aligned} \quad (4.149)$$

Equation (4.149) is the standard FRF form i.e.:  $\{X\} = [H]\{F\}$ . So that it is possible to conclude that the desired FRF matrix of the assembled system,  $[H]$ , in terms of the FRFs matrix of the substructure, is as follows:

$$[H] = \begin{bmatrix} [H_{ii}^{qrqs}] & [H_{ic}^{qrqs}] \\ [H_{ci}^{qrqs}] & [H_{cc}^{qrqs}] \end{bmatrix} \begin{Bmatrix} ([H_{ic}^{qrqs}] - [H_{ic}^{qrqs}]) \\ ([H_{cc}^{qrqs}] - [H_{cc}^{qrqs}]) \end{Bmatrix} \left[ [H_{cc}^{qrqs}] + [H_{cc}^{qrqs}] - [H_{cc}^{qrqs}] - [H_{cc}^{qrqs}] + [\mathcal{G}_{cc}^{qsqr}]^{-1} \right]^{-1} \begin{Bmatrix} ([H_{ic}^{qrqs}] - [H_{ic}^{qrqs}]) \\ ([H_{cc}^{qrqs}] - [H_{cc}^{qrqs}]) \end{Bmatrix}^T \quad (4.150)$$

This equation is used to obtain the FRF of the assembled structure using the FRFs of the collected substructures. Here,  $\mathcal{G}_{cc}^{qsqr}$  is a function of the harmonic displacement  $Y_{\bar{C}\bar{C}}^{qr}$ , known as the describing function. Therefore the describing function assumes different values at different response amplitudes. The response is determined by solving the system of equations (4.149) simultaneously and interactively.

## 4.6 Concluding Remarks

This Chapter started with the development of a new coupling notation which unifies all the current notations available. Then various coupling methods for analysis of linear and nonlinear structures were reviewed. This was followed by the proposal of a new harmonic nonlinear receptance coupling method, *HANORCA*, using the describing function. This method was later extended to the multi-harmonic nonlinear receptance coupling approach, *MUHANORCA*.

Several other methods were also developed in this work, such as (i) Harmonic Nonlinear Impedance Coupling using Describing Functions, (ii) Multi-Harmonic Nonlinear Impedance Coupling using Multi-Harmonic Balance Method, (iii) Multi-Harmonic Nonlinear Impedance Coupling using High-Order Describing Function and (iv) Multi-Harmonic Nonlinear Impedance Coupling using Multi-Harmonic Describing Function. They were essentially used to improve the basic understanding of the higher-order analysis. The accumulated understanding assisted in the development of the definitive nonlinear coupling method, *MUHANORCA*.

# Chapter 5

## Intelligent Nonlinear Coupling

### Analysis *INCA*<sup>++</sup>

#### 5.1 Introduction

Chapter 4 presented the existing impedance coupling methods and also proposed methods for analysing nonlinear coupled structures. After new methods are developed, they must be evaluated in order to validate and to assess the accuracy of technique involved. This can be achieved either by using analytical or numerical approximate solutions. For the validation of techniques simulating nonlinear responses, numerical approximate solutions, such as the time-marching method with a very fine time-step, are frequently used as a benchmark of the accuracy. In most cases this validation applies in the development of a new software, where a numerical analysis of the exact method and of the new developed method can be obtained.

In engineering education, the initial step in developing programs involves the construction of simple analysis tools to validate the fundamental principles. During this time little attention is paid to common factors such as the implementation details, portability and reusability of the software being developed. On the other hand, the developer also would like to utilise standard functions that are already programmed and checked. Thus, even though one is only testing the principles, it is important to use a language that supports the above common factors, such as FORTRAN which is traditionally used in the engineering environment. After the preliminary stage, the program is usually extended to cope with large models. General-purpose programs are rarely developed by the academic researches

because they are limited to developing the individual contributions within the constraints of the degree programme engaged. Although, from the point of view of the researcher, it is important to validate the method numerically with these small specific programs, the idea behind any research is to apply the method developed to a large physical complex structure, and this is usually accomplished by a reliable general-purpose program. These programs are not easily reshaped to perform modifications that allow researchers to reuse the program, and often the developers are required to redesign and to rebuild their own program to suit their own needs. Although these specifically-developed programs available over the years of research are rarely used outside their original development environment, their published theoretical foundations are often examined and implemented in new contexts by other researchers. However, occasionally these publications, along with others documentation, allow modifications to be made in those specific programs, but a great amount of time is spent on understanding the structure of the program and to maintain the integrity of the original design.

A solution to these problems is to improve the code modularity. An evolutionary software development can be achieved by using object-oriented language (OOL) [14]. Although OOL solves the problem with code modularity, OOL also brings another problem of being numerically inefficient. Usually, programs which will involve a lot of computation should use languages that take advantage of hardware developed for this purpose. Among them, *C* language is considered to be a very efficient language for solving numerical problems. But even this language does not satisfy all the current requirements and future demands. The solution is to apply hybrid methods such as the *C++* programming language [117], which is designed to improve the modularity of the code by supporting object-oriented programming, and at the same time allowing a very efficient numerical performance by remaining almost completely a superset of *C* language, [40].

Recently, there has been a growing interest in applying the object-oriented approach to engineering analysis. For example, Forde *et al.* [41] developed an object-oriented static finite element analysis program. Zimmerman *et al.* [146] showed that object-oriented languages such as Smalltalk are able to handle FEM processing. Scholz [111] describes the benefits of the object-oriented language *C++* for finite element analysis programs. Pidaparti *et al.* [96] developed a object-oriented dynamic finite element analysis program. Menetrey *et al.* [80] developed a finite element program for nonlinear static analysis. Miki *et al.* [85] developed a Smalltalk program to do object-oriented structural and geometric analyses of truss structures.

Due to the iterative and incremental nature of object-oriented languages, the aim here is to design a product that can be easily modified to introduce new analysis procedures, new kinds of solvers or even new kinds of structural components. The software developed called Intelligent Nonlinear Coupling Analysis *INCA<sup>++</sup>* is a completely new program in an Object-Oriented Language using the hybrid language *C++*.

## 5.2 Object-Oriented Language

### 5.2.1 Introduction

The idea behind the Object-Oriented Language is that the object-oriented approach adapts the computer to the problem instead of trying to mould the problem into something familiar to the computer. A useful way to understand this idea is to look at some aspects of programming in different ways. The object-oriented approach requires that the user to develop a program in its own terms using all the key features available in the language. Following this rule makes it easier to develop the program in OOL and to keep the solution under control rather than developing the program in a procedural language that keeps the solution in the terms of the computer. This approach permits the use of artificial intelligent techniques such as the event-driven architectures used extensively in modern word-processing and spreadsheet applications, and knowledge-based expert systems [40].

The basic concept of the event-driven approach is that actions taken by the user result in events. Applications obtain the events by continual extraction of events from an event queue. This application responds to each event with the execution of an associated action.

The knowledge-based technology has the ability to perform a forward and backward chain of operations to provide the missing data for the task to be completed.

### 5.2.2 Object Model

A model is a concept in computer science that consists of various elements. If a model is composed of the major known elements which can be described as abstraction, encapsulation, modularity, and hierarchy, it is called an Object Model. If all the basic elements are used at the same time, the final model is an Object Model with Object-Oriented Design.

### 5.2.3 Basic Elements of Object Model

An object-oriented language means a programming language that supports the basic elements of the Object Model. If any of these elements are missing in the program, the level of control over the complexity of the problem is reduced.

These elements are explained in the following sections. To aid understanding of these elements, some examples have been given related to the *INCA*<sup>++</sup> software.

#### 5.2.3.1 Abstraction

Abstraction describes the process of abstracting a real-world entity into a representation in the computer. The result is the creation of a new data type called "class" that behaves just like any other data type which is already defined into the language such as an integer, float, etc. Deciding the right set of abstractions for a given plan is usually the central problem in object-oriented program design.

An example of abstraction can be a physical structure represented by the abstraction class **Structure**. Every physical system can now have a mathematical representation inside the computer using the class **Structure**. The inside view of the class **Structure** is composed of DOFs, nodes, elements, loads, etc. From the outside view, a class **Structure** is just a class that can answer any questions which are asked, such as the displacement in a specific DOF or the stress over all the elements, frequency response function when excited in DOF1 and measured in DOF2, etc.

#### 5.2.3.2 Object

A single object is an example of a class. In other words, when creating a variable of a data type, we are creating an object. So it is possible to say that variables are now called objects. Each object is an entity that exhibits some well-defined behaviour, having a state and a unique identity. Using the type already defined in the language a good example could be a definition of three different integer variables such as follows:

```
integer A,B,C;
```

where A,B and C are objects of type integer.

In the same way using the class **Structure** that was proposed in the last section it is possible to define three different structures:

```
Structure D,E,F;
```

where D, E and F are objects of type **Structure**.

### 5.2.3.3 Encapsulation

In procedural language the main point is concentrated in the subroutines whereas in object-oriented language the focus is in the objects.

Encapsulation organises the variables, hides the complexity of the inside view of the objects and gives internal control over the object. Encapsulation teaches the objects how to handle messages and gives it structure and behaviour. Encapsulation also serves to distinguish between the interface of a class and its implementation. The interface describes what the class does, and the implementation defines how the class works.

The interface of the class consist of two sets of elements, Attributes and Methods:

- **Attributes:** sets of variables that belong to the object. Example of attributes of a class **Structure** can be nodes, elements, stiffness matrix, mass matrix, eigenvalue diagonal matrix, eigenvector full matrix, load list, etc.
- **Methods:** operations that an object is able to execute. An example could be the following method:

```
giveStiffnessMatrix();
```

This method can be used by another class when sending a message to a specific class **Structure**. For example imagine the stiffness matrix of the object **Structure D** defined in section (5.2.3.2) is required. The way to obtain it is to send the following message:

```
D.giveStiffnessMatrix();
```

The way to read this message is: "**Structure D**, give me your stiffness matrix".

The implementation is the way in which the methods of the class execute the message using a group of commands. An example of the implementation could be how the method *giveStiffnessMatrix* gets the stiffness matrix. In this case, the implementation is a group of commands used to query the user to feed in the stiffness matrix via the keyboard, or a group of commands to enter the name of the file where the stiffness matrix is stored and them to read from this file. Imagine another example related with the coupling procedure where the structure is composed of some substructures. In this case the method can be composed of some commands that first send a message to each substructure asking for its

stiffness matrix. With the matrix of each substructure thus obtained, the method assembles the global stiffness matrix and returns it. It is important to notice that the way the method processes the message *giveStiffnessMatrix* is not relevant for the class sending this message. The class sending the message just needs the contents of the global stiffness matrix.

#### 5.2.3.4 Modularity

Modularity consists of a physical set of packages of logically-related classes, producing a system physical architecture. The use of modules is essential to manage complexity in large problems. In C++, it is possible to say that there is a convention for two modules, the module interface where the files has the extension *.h*, known as header files, and for the module implementation where the files have the extension *.cpp*. The dependencies among files can then be stated by using the `#include` macro. An example of a module could be a module called *FRFMethods* which is composed of all the FRF methods related to coupling procedures such as Impedance Method, Receptance Method, Nonlinear Receptance method, etc.

#### 5.2.3.5 Hierarchy

Hierarchy is the idea of defining a new class from another class already defined using inheritance. Inheritance defines relationship among classes where one class shares the structure or behaviour defined in one or more classes. Typically, this new class enhances or redefines the existing structure and behaviour of its superclasses. Consider all the approaches related to coupling procedures. A generalised class of *FRFMethods* will describe our abstraction of coupling approaches. However, different approaches demand different specialised coupling procedures. For instance, the Impedance approach needs to have the impedance matrix of all substructures whereas it is completely different in the Receptance Coupling Approach which requires the assembly of a special matrix composed of Frequency Response Functions. In this example, the Impedance Approach will be represented by a class called **Impedance** that could have a method called *giveImpedance()* and the Receptance Coupling Approach will be represented by a class called **Receptance** that could have a method called *giveH()*. On the other hand, all approaches need to know which are the connection coordinates and the internal coordinates. The methods that could represent these messages could be *getCoonectioCoordinates()* and *getInternalCoordinates()*. Therefore those methods

that are common to all procedures can be defined in the superclass called `{FRFMethod}` as shown in the following definition:

```
class FRFMethod{
:
  getCoonectionCoordinates();
  getInternalCoordinates();
:
}
```

An example of inheritance from the class `FRFMethod` is the `Impedance` class and the `Receptance` class as shown from the following definition:

```
class Impedance : public FRFMethod{
:
  giveImpedance();
:
}
class Receptance : public FRFMethod{
:
  giveH();
:
}
```

### 5.2.3.6 Polymorphism

Polymorphism is a concept in type theory where a single name may denote an appropriate behaviour of a derived class among many different derived classes that are related by some common superclass. This means that methods in different classes with completely different operations can share the same name. For the superclass `FRFMethod` and the subclasses `Impedance` and `Receptance` it is possible to have the same message to execute a specific task. For example in order to have the solution at a particular frequency, the message needed to execute this task can be a method called *solveYourselfAt*. Although the message is the

same for both classes, the operations inside each method are completely different from each other. The message *solveYourselfAt* in each class is shown in the following definition:

```
class FRFMethod{
:
virtual solveYourselfAt();
:
}

class Impedance : public FRFMethod{
:
assembleYourselfAt(){
:
giveImpedance();
:
}
:
}

class Receptance : public FRFMethod{
:
assembleYourselfAt(){
:
giveH();
:
}
:
}
```

## 5.2.4 Advanced Concept

Programming in OOL means that at least all the basic concepts are used. However, an intrinsic inconvenience from the procedural programming still remains when programming only with the basics concepts. It is concerned with the fact that a code is designed as a sequence of operations and all the operations are dependent on the correct previous executions of the methods. To overcome this problem, another element is introduced in the Object Model, the concept of non-anticipation. This concept implies that the content of a method should not be dependent on previous assumptions of the state of the program.

This can be better seen when comparing the standard concept against the non-anticipation concept. In the standard approach if the connection coordinates necessary during the coupling are required, the programmer should call up a procedure which will manage to obtain this data, such as:

```
getConnectionCoordinates();
```

Later on, if the same data is required again during the program, another procedure that would just return these coordinates could be called for:

```
return ConnectionCoordinates();
```

This decision avoids wasting time getting these variables again, but it tends to create difficulties in future extensions. Alternatively, if the programmer does not assume anything about the state of the variable, only one message would ever need to be sent for all situations:

```
giveConnectionCoordinates();
```

The code inside this method should contain a simple test that checks whether the variable already exists or not. If the variable does not exist, get the variable and return it or, if the variable exist, just return it. The following code describes this situation:

```
ObjectList *Coupling::giveConnectionCoordinates(){
    if(!ConnectionCoordinates)getConnectionCoordinates();
    return ConnectionCoordinates;
}
```

## 5.2.5 Achieving Object Model

A good object model can be best achieved when the development process is divided into phases known as Object-Oriented Analysis, Object-Oriented Design and Object-Oriented Programming.

Object-Oriented Analysis is the phase where the nebulous requirements of the experts in the problem are transferred into a description of the task to be solved by the programmer.

Object-Oriented Design is the phase where the programmer must start defining classes and modules listing all the operations and their relationships to other classes.

Object-Oriented Programming is the phase where the Object Model is physically implemented. The classes and methods are coded, tested and integrated with each other.

After completing these phases, the programmer's developing experience can usually result in improvements and modifications to the model through further iterations of the process.

When developing a general program, the object model can be better understood with the help of a visual tools. The Booch notation [14, 138] is an example of visual tool used for development of software and to produce automatic documentation of the program. A brief summary of the Booch notation is shown in Appendix F. The Booch method presents a set of steps which are applied iteratively and incrementally to pieces of the system. This is desirable since it is possible to analyse just small parts, design them and code them, and then make this an iterative cycle and incrementally enhance the strategies adopted during the design.

### 5.3 Specifications of *INCA<sup>++</sup>*

The development of the Object-Oriented Analysis of the *INCA<sup>++</sup>* is performed by first defining all the required specifications. The general requirement is to produce a software in order to be able to perform static and dynamic analyses of linear and nonlinear structures in time and frequency domains based on current and emerging computer technology. The software should also provide support for rapid development of new methods. The specific requirements are now concerned with the physical problem to be analysed. The physical structure can be composed of substructures which are represented by the discrete system. The linear and nonlinear structural dynamic coupling techniques are applied to obtain the assembled structure. The input data can be eigenvalues, eigenvectors, mass, stiffness and damping matrices, and frequency response functions. A structure will have a name, where all of the input and output data of the structure will be related to its name. The structure is defined by the elements of the spatial model, modal model and response model. The spatial model is defined with mass, stiffness and damping matrices, the modal model is

defined with eigenvalues, and eigenvectors and the response model is defined by frequency response functions. After defining a structure with a specific model, the program should be able to produce all the remaining elements for working with the other models.

The aim of the first phase is to produce an intermediate release *INCA<sup>++</sup>*, which will provide the desired tool for checking and comparing different approaches for different inputs. The second phase is to add a post-processor in the program in order to show the results obtained from the calculations. The last phase is to add a pre-processor that will allow a visual mode of entering all the data involved in the procedures. During this work, the objective was to produce only the first phase.

A point to be considered in the Object Model related to the coupling procedure is that the class **Structure** can be composed of  $n$  classes **Structure** and any of these  $n$  classes **Structure** can be again composed of  $n$  classes **Structure** as shown in Figure 5.1. Another point that must be decided is the way to start developing the software. A software

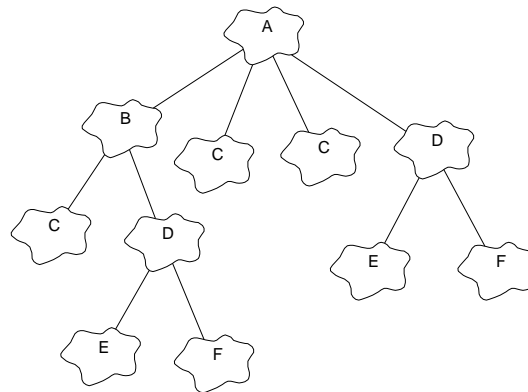


Figure 5.1: Example of structure A composition

can be developed by using some very well-checked libraries that are carefully developed for all possible general-purpose cases. Therefore the software is the last product to be developed since all the libraries must be very well widely developed first. This kind of development is called "bottom-up". Another approach is to develop only the software necessary for the program. This kind of development is called "top-down", and experts in the development field claim it to be more efficient because only what it is really required is developed [14]. Therefore the "top-down" development procedure was adopted here.

## 5.4 First Design of *INCA<sup>++</sup>* Object Model

The object-oriented system is a programming environment in which the fundamental processing model is to send a message to an object rather than using the more traditional approach of calling a procedure to operate on some data. This approach qualitatively enhances the design, creation, and maintenance of a software system. The great advantage achieved from this language is the modularity.

Every entity in engineering analysis is considered as an object, each object is an instance of each class, and these classes have a class hierarchy. All the knowledge is divided into small parts, and they are stored in pertinent classes. Therefore the primary part of the research involves the development of the class hierarchy and the data structure in each class and specifying the behaviour of each class. The class hierarchy and the data structures are static representations of the knowledge, whereas methods by which objects respond to messages are dynamic representations of the knowledge.

When dealing with discrete systems, various basic terms come to mind, such as coordinates, nodes, elements, degrees of freedom, load, force, displacement, etc. The first step is to specify all these entities. The next step is to decide which entity should be created as an object and what the tasks of this object should be. These are the most difficult questions to be answered. Since it is not necessary to decide everything in one step, since another characteristic of the language is to support iterative approach, the optimum procedure is to define the obvious objects like DOF, node, element, structure, and progressively continue making the decisions about the less-obvious objects when necessary.

An important point to remember concerns making the code readable. A significant help towards understanding the code better is to choose the right names for the classes, objects and methods. These names should be immediately clear enough so that just reading the name, it is possible to understand the abstraction, concept or picture represented by the class, object or messages.

Another decision concerns where to start and what exactly is to be developed. It is obvious that certain basic objects will be necessary to organise and classify the input data and the data to be calculated. Such basic objects can be highlighted as an array, single-linked-list and double-linked-list. Sometimes using an array instead of a single linked list or double linked list will work faster, use less memory, among other advantages. From previous experience, it has become clear that whether the class to be developed is related with the input or output data, it is not so important if the task takes one or two seconds

more to do using either the array or the single-linked list or the double linked-list. Hence it is more important to know where and when it will be necessary to use all of these basic classes rather than to start developing all of them and trying to guess which to use. Since the program can be enhanced progressively after checking where it should be improved, another decision was to use the entire data dictionary as a double-linked-list.

From the specification, the first design of the class `Structure` is shown in Figure 5.2.

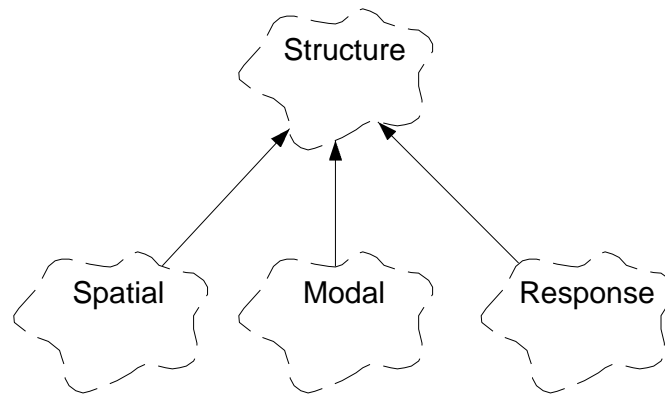
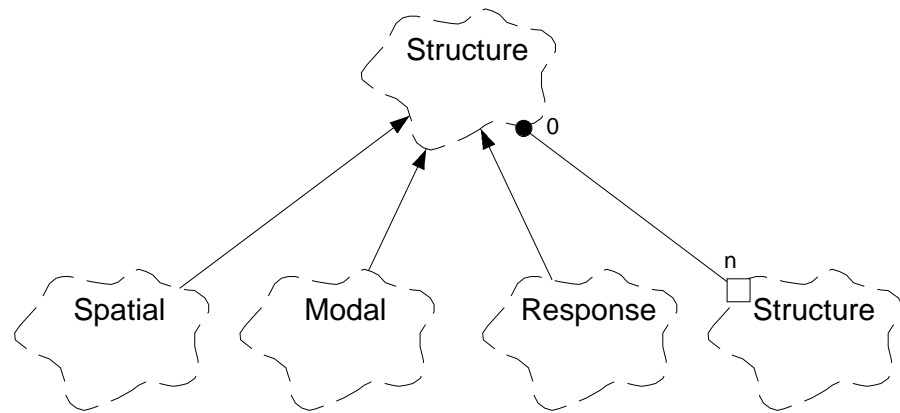


Figure 5.2: Class Structure

The class `Structure` will have all the attributes that define a structure model such as elements, nodes, dynamics characteristics, etc. Some other less-obvious classes are defined as `Spatial`, `Modal` and `Response`. The class `Spatial` is an instance of class `Structure` and is created with the spatial characteristics of the structure model (stiffness, mass and damping matrix). The class `Modal` is an instance of class `Structure` and is created with the modal characteristics of the structure model (eigenvalues and eigenvectors). The class `Response` is an instance of class `Structure` and is created with the response characteristics of the structure model (frequency response functions). The idea of defining these less-obvious classes came when determining how the class `Structure` should choose which function it will use. For example, to generate a frequency response function, the class `Structure` could use the spatial properties or use the modal properties or even get it from a file. But if the structure is defined as `Modal` class, the process of calculation is fixed and the frequency response function will be calculated using the modal properties.

Another point mentioned in the specifications concerned the structure composition showed in Figure 5.1. After reviewing how to introduce this specification in the `Structure Model`, a solution was found whereby the class `Structure` requires a list of reference of `Structure` classes, as the solution shown in Figure 5.3 suggests: From this example it is

Figure 5.3: Enhanced **Structure** class

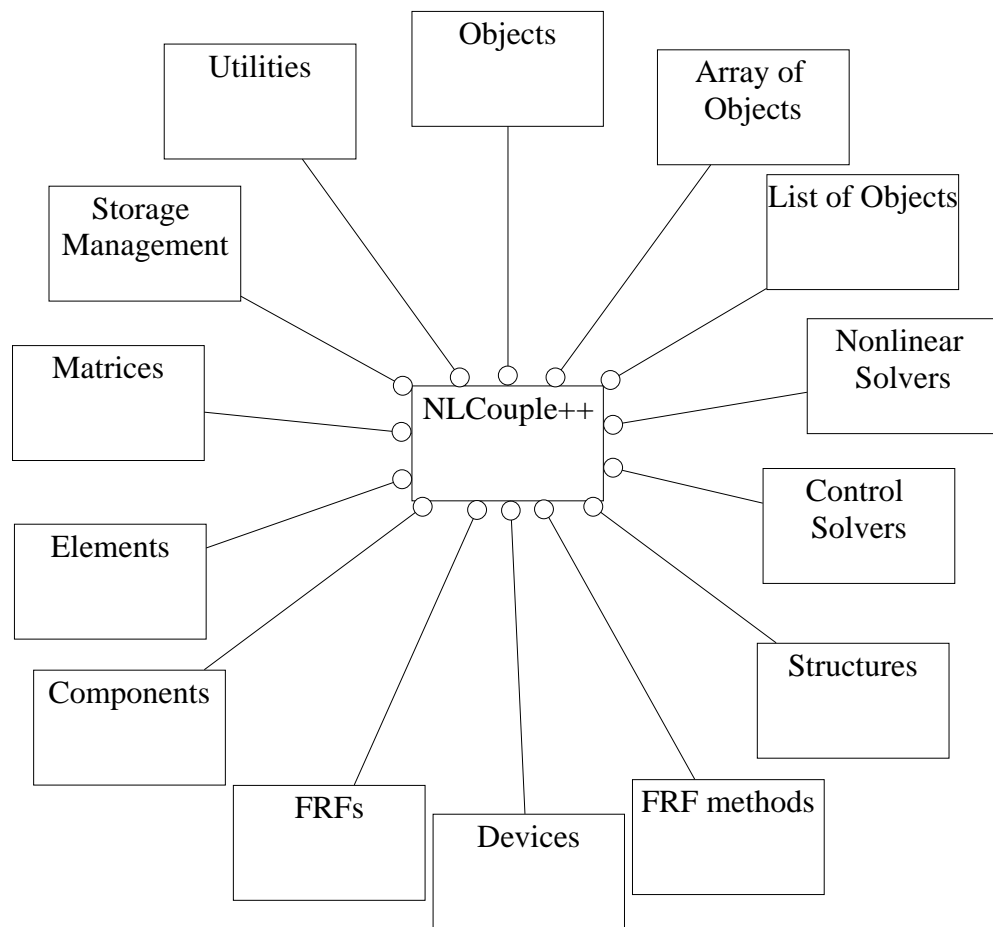
possible to start considering the advantages of Object-Oriented Language. As previously described, since the language supporting the iterative approach, it is possible to develop the first **Structure** Model, shown in Figure 5.2, and then to enhance that model with the introduction of this new specification, shown in Figure 5.3.

Another consideration arises in connection with the notation, that after applying the Booch notation, Figures 5.2,5.3, we can more easily capture the overall picture.

The modules of the program can be seen in Figure 5.4 and a list of the significant classes are sketched in the hierarchy tree shown in Figure 5.5. The latest release of *INCA*<sup>++</sup> is a program written in *C++*, designed to promote software reuse and minimise system maintenance. This release can be used to calculate the dynamic response of a structure in the time domain and in the frequency domain. In the time domain the integration method used was Runge-Kutta. In the frequency domain the methods available for linear analysis are the linear impedance method (*LI*) and the linear receptance coupling method (*LIRCA*). For nonlinear analysis the methods available are the nonlinear impedance (*NLI*) and the multi-harmonic nonlinear receptance coupling approach (*MUHANORCA*), both using the multi-harmonic describing function to represent the nonlinearity.

The gyroscopic effect required for analysis of rotor-dynamic structures is already implemented.

The joints available in the program are rigid connection, linear spring, viscous damping, nonlinear cubic stiffness, coulomb friction, hysteretic damping using the macro/micro slip friction and polynomial.

Figure 5.4: Modules of  $INCA^{++}$

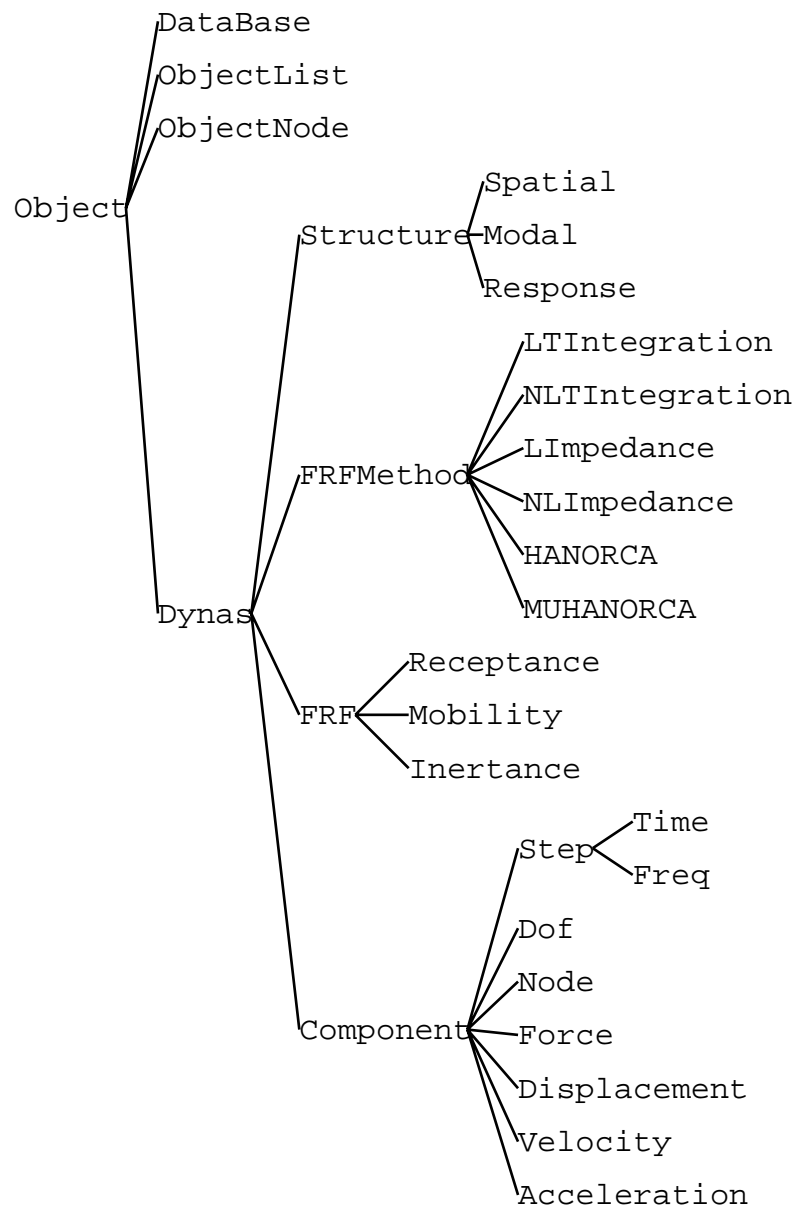


Figure 5.5: Hierarchy tree

# Chapter 6

## Numerical Case Studies of Coupled Structures using *INCA*<sup>++</sup>

### 6.1 Introduction

The release of *INCA*<sup>++</sup> software prepared for this thesis has been validated using different sets of simulated data. It is not intended here to show all the validation cases studied, but instead to show the cases that have all the key features already tested and implemented. A detailed simple case can be seen in Appendix E.

### 6.2 Linear Numerical Simulation

This case shows a linear application where the substructures are connected by using all the linear connections implemented in the software. The following simulation consists of obtaining an equation of the assembled structure composed of three substructures, with a linear spring element and a viscous damping element between ground  $g$  and coordinate  $x_1$ ,  $x_2$  and  $x_6$ ,  $x_4$  and  $x_{10}$ , with a rigid element between coordinates  $x_3$  and  $x_9$ ,  $x_6$  and  $x_8$ ,  $x_8$  and  $x_9$ ,  $x_{11}$  and ground  $g$ . The Collected Substructure and Assembled System can be seen in figures (6.1) and (6.2)

This example has two internal coordinates  $x_5, x_7$ , ten pairs of connection coordinate  $(g, x_1)$ ,  $(g, x_1)$ ,  $(x_2, x_6)$ ,  $(x_2, x_6)$ ,  $(x_4, x_{10})$ ,  $(x_4, x_{10})$ ,  $(x_3, x_9)$ ,  $(x_6, x_8)$ ,  $(x_8, x_9)$ ,  $(x_{11}, g)$ , the response is required in two connection coordinates  $x_4, x_{10}$  and one internal coordinate  $x_5$ , and one excitation at the connection coordinate  $x_6$  as shown in the groups,

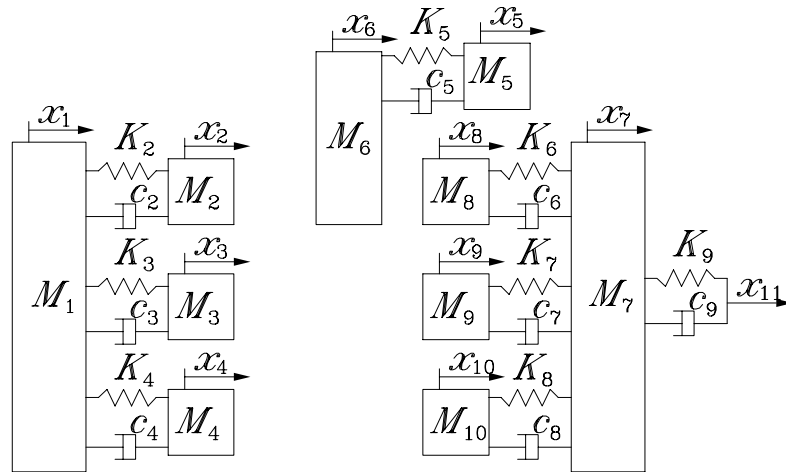


Figure 6.1: Collected Substructure

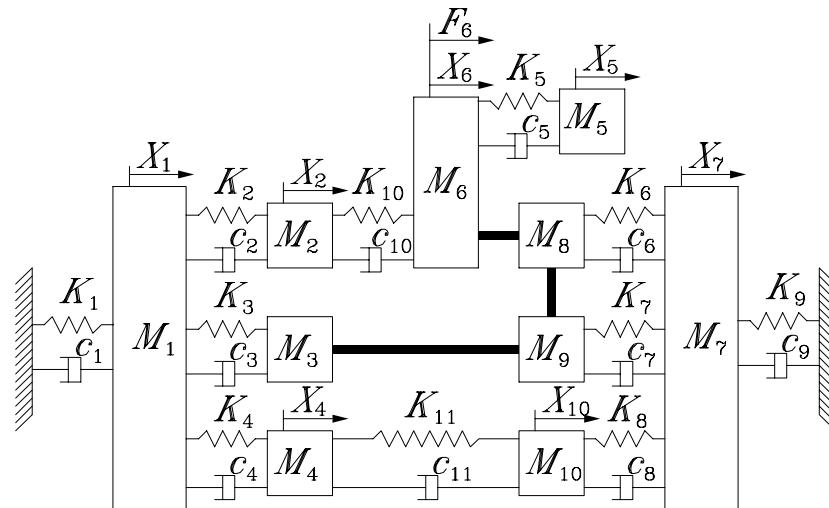


Figure 6.2: Assembled Structure

$$\begin{aligned}
i &= \{5, 7\} \\
\bar{c} &= \{1, 1, 2, 2, 4, 4, 6, 8, 9, 11\} \\
\tilde{c} &= \{g, g, 6, 6, 10, 10, 8, 9, 3, g\} \\
c &= \{1, 2, 4, 6, 10\} \\
c_d &= \{4, 10\} \\
i_d &= \{5\} \\
c_f &= \{6\} \\
i_f &= \{\}
\end{aligned} \tag{6.1}$$

The physical characteristics of the system are taken to be

$$\begin{aligned}
m1 &= 5 \text{ kg} & m2 &= 0.3 \text{ kg} & m3 &= 3 \text{ kg} & m4 &= 4 \text{ kg} \\
m5 &= 1 \text{ kg} & m6 &= 3 \text{ kg} & m7 &= 5 \text{ kg} & m8 &= 1 \text{ kg} \\
m9 &= 1 \text{ kg} & m10 &= 1 \text{ kg} & & & & \\
k1 &= 9.10^6 \text{ N/m} & k2 &= 3.10^6 \text{ N/m} & k3 &= 5.10^6 \text{ N/m} & & \\
k4 &= 4.10^6 \text{ N/m} & k5 &= 3.10^6 \text{ N/m} & k6 &= 2.10^6 \text{ N/m} & & \\
k7 &= 4.10^6 \text{ N/m} & k8 &= 5.10^6 \text{ N/m} & k9 &= 9.10^6 \text{ N/m} & & \\
k10 &= 4.10^6 \text{ N/m} & k11 &= 4.10^5 \text{ N/m} & & & & \\
c1 &= 3 \text{ Nm/s} & c2 &= 1 \text{ Nm/s} & c3 &= 1 \text{ Nm/s} & & \\
c4 &= 2 \text{ Nm/s} & c5 &= 4 \text{ Nm/s} & c6 &= 3 \text{ Nm/s} & & \\
c7 &= 2 \text{ Nm/s} & c8 &= 1 \text{ Nm/s} & c9 &= 4 \text{ Nm/s} & & \\
c10 &= 5 \text{ Nm/s} & c11 &= 5 \text{ Nm/s} & & & &
\end{aligned}$$

Applying the *HANORCA* method, a set of linear algebraic equations are obtained and the displacement of this Assembled System can be calculated by solving these equations. The coupled results of the coordinates  $X4, X5$  and  $X10$  can be seen in figures (6.3,6.4,6.5)

### 6.3 Simulation using *HANORCA*

These simulations consist of obtaining a harmonic response equation of the assembled structure composed of three substructures, with one nonlinear element between coordinates  $x4$

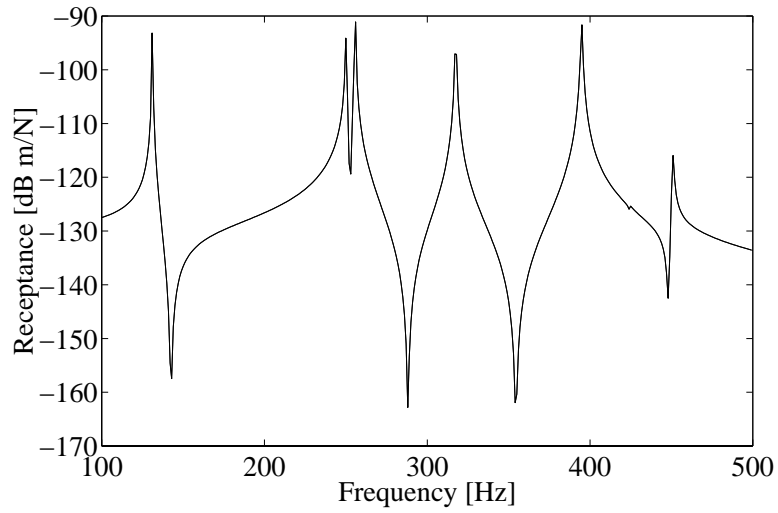


Figure 6.3: Displacement in coordinate X4

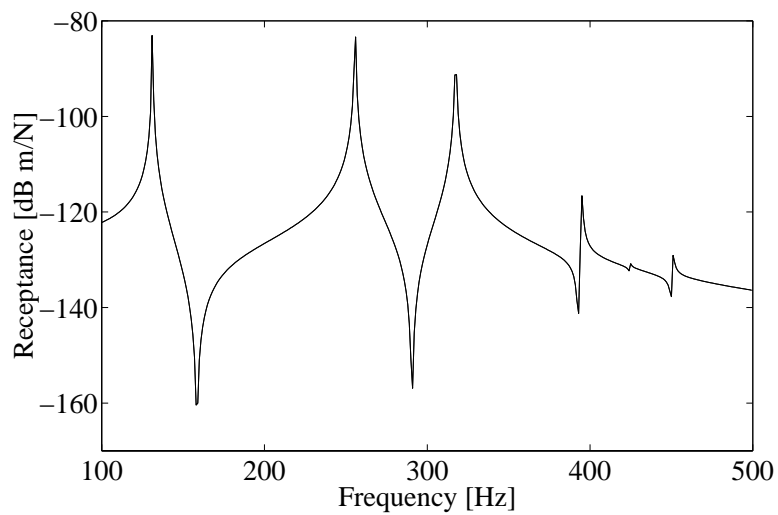
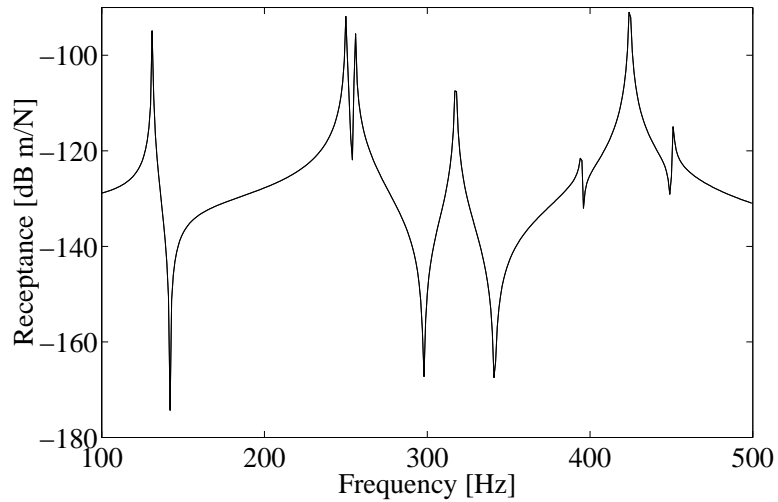


Figure 6.4: Displacement in coordinate X5

Figure 6.5: Displacement in coordinate  $X_{10}$ 

and  $x_{10}$ , with coordinates  $x_3$  and  $x_9$ , and  $x_2, x_6$  and  $x_8$  rigidly connected. The Collected Substructure and Assembled System can be seen in figures (6.1),(6.2)

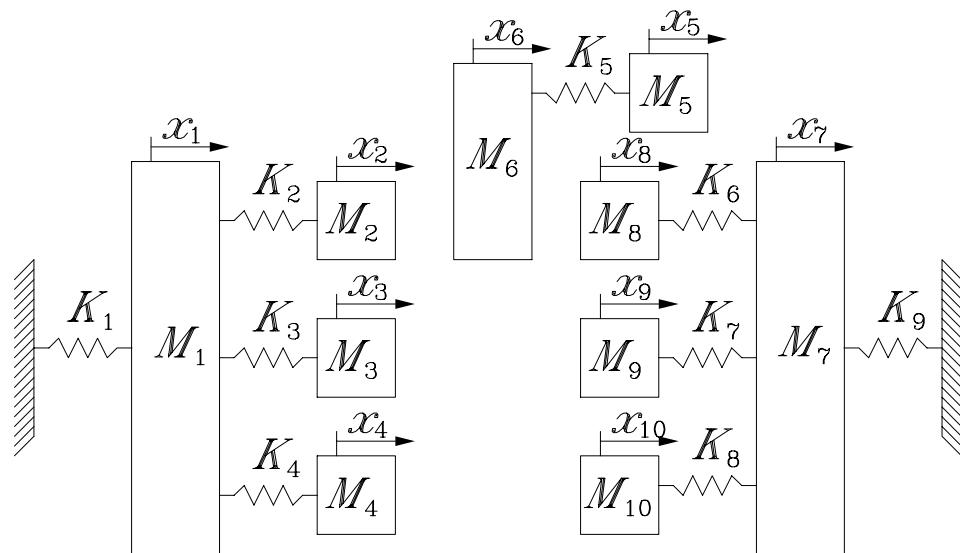


Figure 6.6: Collected Substructure

This example has four pairs of connection coordinates  $(x_2, x_6)$ ,  $(x_6, x_8)$ ,  $(x_3, x_9)$ ,  $(x_4, x_{10})$  and three external coordinates as shown in the groups:

$$i = \{1, 5, 7\}$$

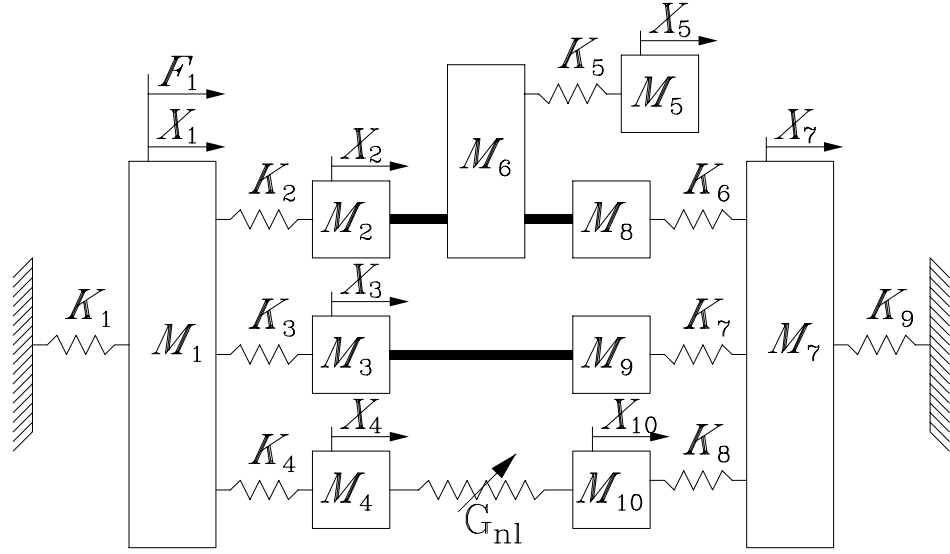


Figure 6.7: Assembled Structure

$$\begin{aligned}
 \bar{c} &= \{2, 6, 3, 4\} \\
 \tilde{c} &= \{6, 8, 9, 10\} \\
 c &= \{2, 3, 4, 10\} \\
 c_d &= \{4, 10\} \\
 i_d &= \{\} \\
 c_f &= \{\} \\
 i_f &= \{1\}
 \end{aligned} \tag{6.2}$$

The physical characteristics of the system are taken to be:

$$\begin{aligned}
 m1 &= 5 \text{ kg} & m2 &= 1 \text{ kg} & m3 &= 1 \text{ kg} & m4 &= 1 \text{ kg} \\
 m5 &= 1 \text{ kg} & m6 &= 3 \text{ kg} & m7 &= 5 \text{ kg} & m8 &= 1 \text{ kg} \\
 m9 &= 1 \text{ kg} & m10 &= 1 \text{ kg}
 \end{aligned}$$

$$\begin{aligned}
 k1 &= 9.10^6 \text{ N/m} & k2 &= 2.10^6 \text{ N/m} & k3 &= 5.10^6 \text{ N/m} \\
 k4 &= 4.10^6 \text{ N/m} & k5 &= 1.10^6 \text{ N/m} & k6 &= 1.10^6 \text{ N/m} \\
 k7 &= 6.10^6 \text{ N/m} & k8 &= 4.10^6 \text{ N/m} & k9 &= 10.10^6 \text{ N/m} \\
 G_{nl} &= 4.10^5 + \frac{3}{2} * 1.10^5 * (x_4 - x_{10})^2
 \end{aligned}$$

Using the groups in equation(6.3), it is possible to define the following submatrices

$$H_{\bar{c}\bar{c}} = \begin{bmatrix} H_{22} & 0 & H_{23} & H_{24} \\ 0 & H_{66} & 0 & 0 \\ H_{32} & 0 & H_{33} & H_{34} \\ H_{42} & 0 & H_{43} & H_{44} \end{bmatrix} \quad (6.3)$$

$$H_{\bar{c}\bar{c}} = \begin{bmatrix} H_{66} & 0 & 0 & 0 \\ 0 & H_{88} & H_{89} & H_{810} \\ 0 & H_{98} & H_{99} & H_{910} \\ 0 & H_{108} & H_{109} & H_{1010} \end{bmatrix}$$

$$H_{\bar{c}\bar{c}} = \begin{bmatrix} 0 & 0 & 0 & 0 \\ H_{66} & 0 & 0 & 0 \\ 0 & 0 & 0 & 0 \\ 0 & 0 & 0 & 0 \end{bmatrix}$$

$$H_{c_d\bar{c}} = \begin{bmatrix} H_{42} & 0 & H_{43} & H_{44} \\ 0 & 0 & 0 & 0 \end{bmatrix}$$

$$H_{c_d\bar{c}} = \begin{bmatrix} 0 & 0 & 0 & 0 \\ 0 & H_{108} & H_{109} & H_{1010} \end{bmatrix}$$

$$H_{i_f\bar{c}} = \begin{bmatrix} H_{12} & 0 & H_{13} & H_{14} \end{bmatrix}$$

$$H_{i_f\bar{c}} = \begin{bmatrix} 0 & 0 & 0 & 0 \end{bmatrix}$$

The equation of the Assembled System relating both the desired connection and excitation points can be determined by substituting equations (6.3) into equation(4.118), leading to the following equation,

$$\begin{Bmatrix} X_4 \\ X_{10} \end{Bmatrix} = \left( \begin{bmatrix} H_{14} \\ 0 \end{bmatrix} - \begin{Bmatrix} H_{42} & 0 & H_{43} & H_{44} \\ 0 & -H_{108} & -H_{109} & -H_{1010} \end{Bmatrix} [B]^{-1} \begin{Bmatrix} H_{12} \\ 0 \\ H_{13} \\ H_{14} \end{Bmatrix} \right) \{F_1\} \quad (6.4)$$

where:

$$[B] = \begin{bmatrix} H_{22} + H_{66} & -H_{66} & H_{23} & H_{24} \\ -H_{66} & H_{66} + H_{88} & H_{89} & H_{810} \\ H_{32} & H_{98} & H_{33} + H_{99} & H_{34} + H_{910} \\ H_{42} & H_{108} & H_{43} + H_{109} & H_{44} + H_{1010} + \frac{1}{G_{nl}} \end{bmatrix}$$

The displacement response of the Assembled System is obtained by solving the nonlinear algebraic simultaneous equation (6.5) using the Newton-Raphson method. Equation (6.5) is solved for the linear case and for the nonlinear case with forces varying from  $2.5 * 10^5 N$  to  $2.0 * 10^6 N$  with an increment of  $2.5 * 10^5 N$ . The receptance  $\alpha_{41}$  and  $\alpha_{101}$  can be seen in Figures 6.8,6.9 respectively.

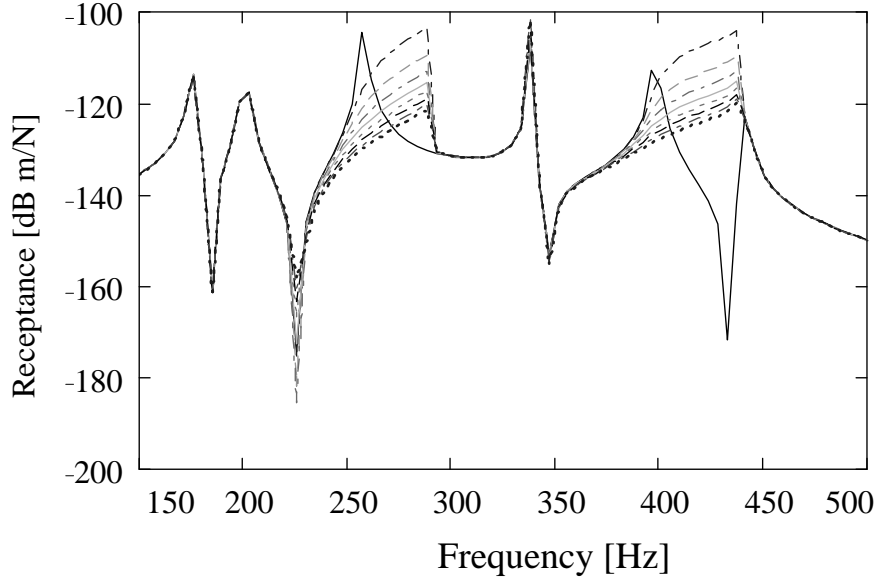


Figure 6.8: Receptance  $\alpha_{41}$

## 6.4 Simulation using *MUHAIM*

This simulated case utilises the Multi-Harmonic Impedance approach. The simulation consists of obtaining an equation for the Assembled Structure of Figure 6.10 with one nonlinear hysteretic element between ground and coordinate  $X1$ . The model used to represent the nonlinear hysteretic element is the Ren's model previously presented in section 3.3.3.4.

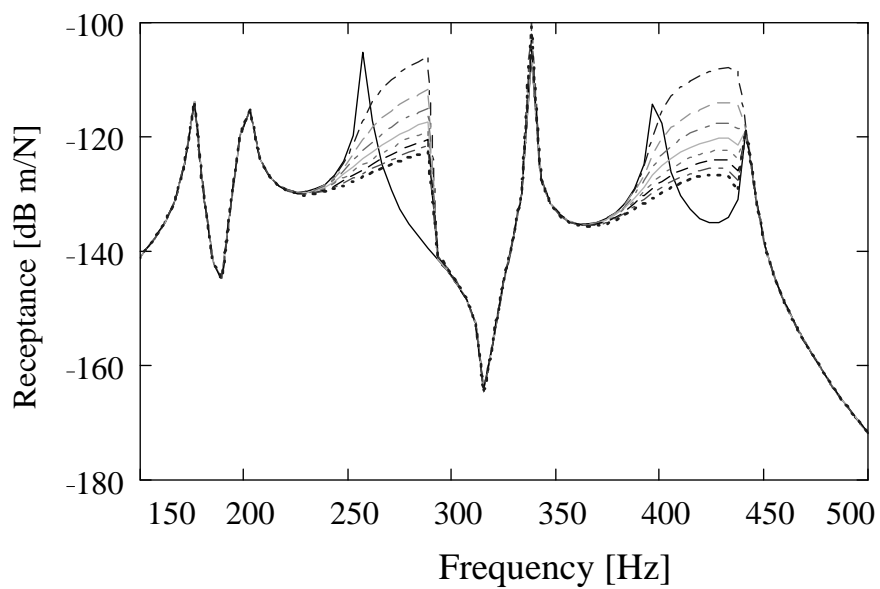
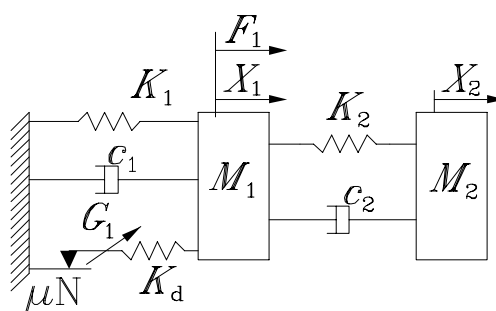
Figure 6.9: Receptance  $\alpha_{101}$ 

Figure 6.10: Assembled Structure

The physical characteristics of the system are taken to be:

$$\begin{aligned} m1 &= 1 \text{ kg} & m2 &= 1 \text{ kg} \\ c1 &= 4 \text{ Nm/s} & c2 &= 4 \text{ Nm/s} \\ k1 &= 4.10^4 \text{ N/m} & k2 &= 4.10^4 \text{ N/m} \\ G_1 &= \text{macroslip model} \begin{cases} K_d = 4.10^4 \text{ N/m} \\ \mu N = 1 \text{ to } 250 \text{ N} \end{cases} \end{aligned}$$

The displacement response of the Assembled System is obtained by solving the nonlinear algebraic simultaneous equation (4.138) using the Newton-Raphson method. This result is compared to the solution obtained from the time integration, considered as the exact solution.

Figure 6.11 shows a comparison of the receptance  $\{H_{11}^{11}\}^1$  calculated using equation (4.138) assuming the first harmonic  $\{X\}^1$ , the receptance  $\{H_{11}^{11}\}^3$  calculated using equation (4.138) assuming the first and third harmonics  $\{X\}^1$  and  $\{X\}^3$ , the receptance  $\{H_{11}^{11}\}^5$  calculated using equation (4.138) assuming the first, third and fifth harmonics  $\{X\}^1$ ,  $\{X\}^3$  and  $\{X\}^5$ , and the receptance  $\{H_{11}^{11}\}^t$  calculated using time integration.

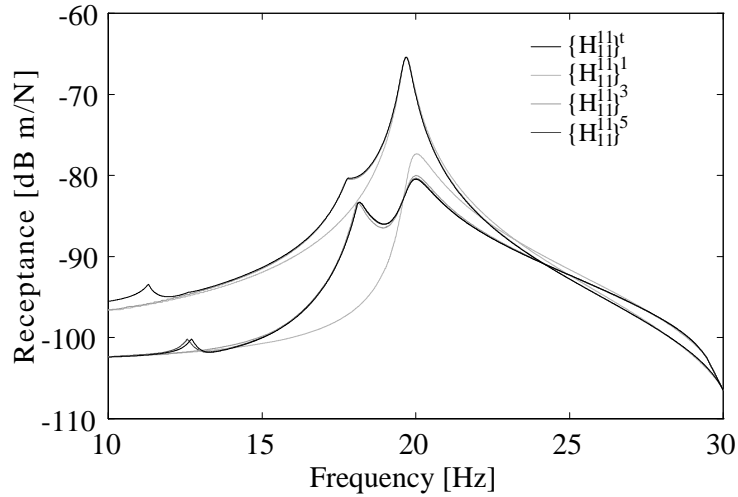
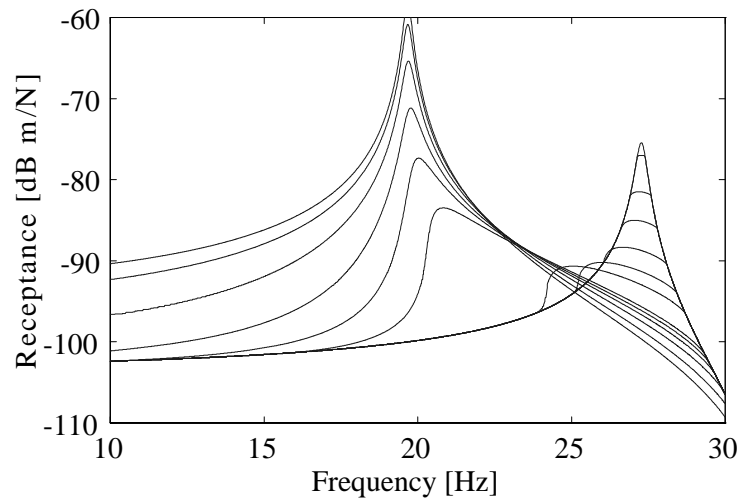
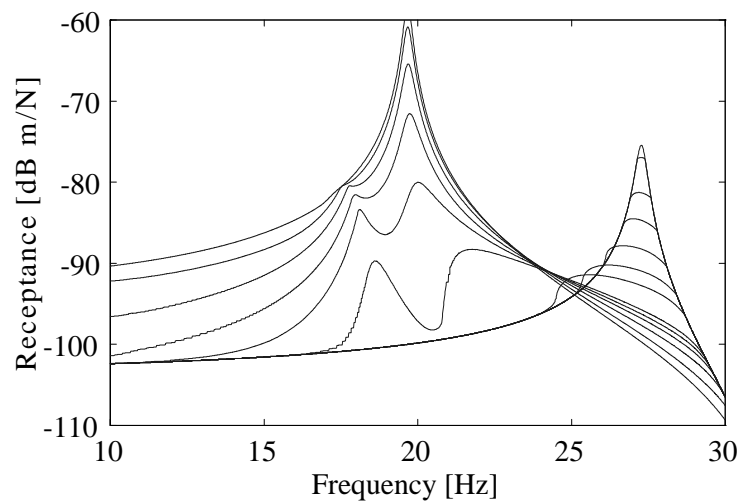
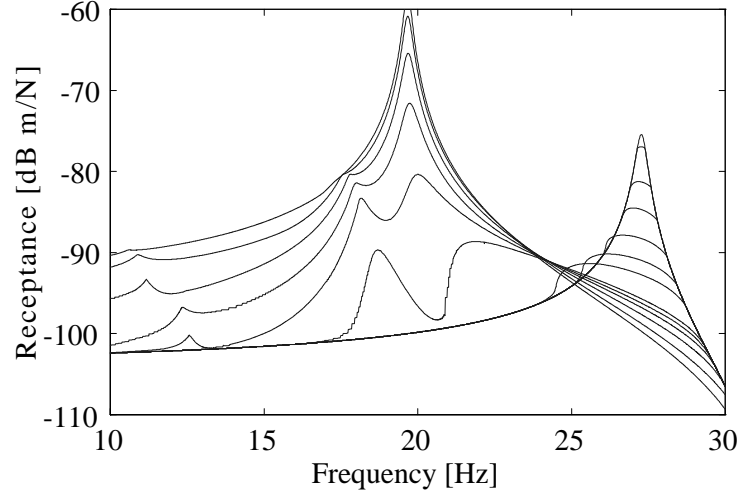


Figure 6.11: Influence of the number of harmonic terms on the frequency response for  $\mu.N=5$  and  $\mu.N=7.5$

The frequency response functions  $\{H_{11}^{11}\}^1$ ,  $\{H_{11}^{11}\}^3$  and  $\{H_{11}^{11}\}^5$  for various levels of force  $\mu N$  varying from 1 to 250N are shown in Figures 6.12, 6.13 and 6.14.

Figure 6.12: Frequency Response  $\{H_{11}^{11}\}^1$ Figure 6.13: Frequency Response  $\{H_{11}^{11}\}^3$

Figure 6.14: Frequency Response  $\{H_{11}^{11}\}^5$ 

## 6.5 Simulation using *MUHANORCA*

This simulated case uses the *MUHANORCA* approach. The simulation consists of obtaining an equation for the Assembled Structure composed of three substructures, with a linear spring and viscous damping elements connecting coordinate 2 with 6 and 4 with 10, with one nonlinear hysteretic element between ground  $g$  and coordinate 6, and rigid connections between coordinates 6 and 8, 4 and 10. The Collected Substructure and Assembled System can be seen in figures (6.15) and (6.16)

This example has seven pairs of connection coordinates  $(x_2, x_6)$ ,  $(x_2, x_6)$ ,  $(x_3, x_9)$ ,  $(x_4, x_{10})$ ,  $(x_4, x_{10})$ ,  $(x_6, x_8)$  and  $(x_6, g)$ , and three external coordinates as shown in the groups:

$$\begin{aligned}
 i &= \{1, 5, 7\} & c_d &= \{6\} \\
 \bar{c} &= \{2, 2, 3, 4, 4, 6, 6\} & i_d &= \{\} \\
 \tilde{c} &= \{6, 6, 9, 10, 10, 8, g\} & c_f &= \{6\} \\
 c &= \{2, 3, 4, 10\} & i_f &= \{\}
 \end{aligned} \tag{6.5}$$

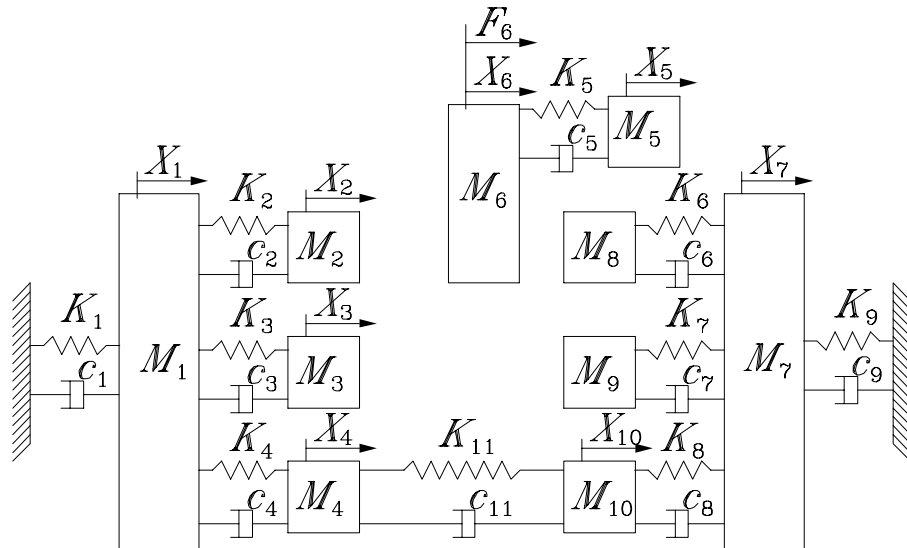


Figure 6.15: Collected Substructure

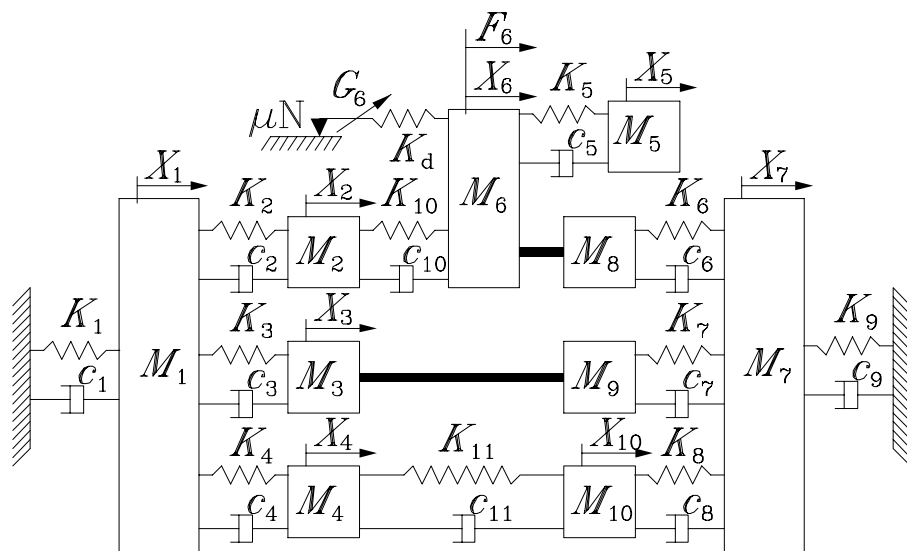


Figure 6.16: Assembled Structure

The physical characteristics of the system are:

$$m1 = 5 \text{ kg} \quad m2 = 0.3 \text{ kg} \quad m3 = 3 \text{ kg} \quad m4 = 4 \text{ kg}$$

$$m5 = 1 \text{ kg} \quad m6 = 3 \text{ kg} \quad m7 = 5 \text{ kg} \quad m8 = 1 \text{ kg}$$

$$m9 = 1 \text{ kg} \quad m10 = 1 \text{ kg}$$

$$k1 = 3.10^3 \text{ N/m} \quad k2 = 2.10^4 \text{ N/m} \quad k3 = 5.10^3 \text{ N/m}$$

$$k4 = 4.10^3 \text{ N/m} \quad k5 = 4.10^4 \text{ N/m} \quad k6 = 2.10^4 \text{ N/m}$$

$$k7 = 6.10^3 \text{ N/m} \quad k8 = 4.10^3 \text{ N/m} \quad k9 = 3.10^3 \text{ N/m}$$

$$k10 = 4.10^2 \text{ N/m} \quad k11 = 4.10^3 \text{ N/m}$$

$$c1 = 3.10^3 \text{ Nm/s} \quad c2 = 8 \text{ Nm/s} \quad c3 = 2 \text{ Nm/s}$$

$$c4 = 1 \text{ Nm/s} \quad c5 = 4 \text{ Nm/s} \quad c6 = 8 \text{ Nm/s}$$

$$c7 = 2 \text{ Nm/s} \quad c8 = 1 \text{ Nm/s} \quad c9 = 9 \text{ Nm/s}$$

$$c10 = 5 \text{ Nm/s} \quad c11 = 5 \text{ Nm/s}$$

$$G_6 = \text{macroslip model} \begin{cases} K_d = 1.10^5 \text{ N/m} \\ \mu N = 5 \text{ N} \end{cases}$$

$$F_6 = 100 \text{ N}$$

The displacement response of the Assembled System is obtained by solving the nonlinear algebraic simultaneous equation (4.149) using the Newton-Raphson method. Figure 6.17 shows a comparison of the receptance  $\{H_{11}^{11}\}^1$  calculated considering the first harmonic  $\{X\}^1$ , the receptance  $\{H_{11}^{11}\}^3$  calculated considering the first and third harmonics  $\{X\}^1$  and  $\{X\}^3$ , the receptance  $\{H_{11}^{11}\}^5$  calculated considering the first, third and fifth harmonics  $\{X\}^1$ ,  $\{X\}^3$  and  $\{X\}^5$ , and the receptance  $H_{11}^t$  calculated using the time integration method.

Figure 6.18 shows a comparison of the receptance  $\{H_{11}^{31}\}^3$  calculated considering the first and third harmonics  $\{X\}^1$  and  $\{X\}^3$ , the receptance  $\{H_{11}^{31}\}^5$  calculated considering the first, third and fifth harmonics  $\{X\}^1$ ,  $\{X\}^3$  and  $\{X\}^5$ , and the receptance  $H_{11}^t$  calculated using time integration method. Figure 6.19 shows the receptance  $\{H_{11}^{51}\}^5$  calculated considering the first, third and fifth harmonics  $\{X\}^1$ ,  $\{X\}^3$  and  $\{X\}^5$ .

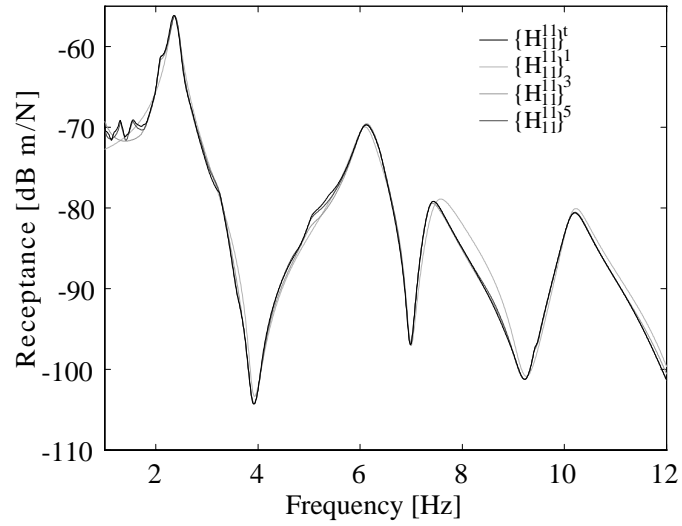
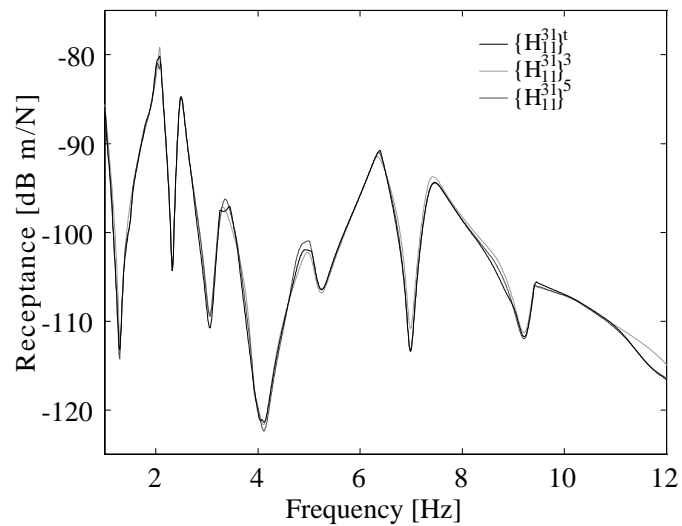
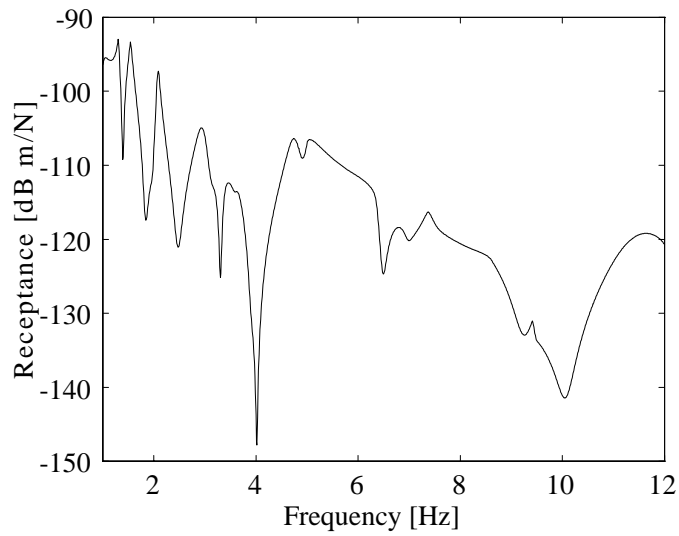


Figure 6.17: Influence of the number of harmonic terms on the FRF

Figure 6.18: Comparison of  $\{H_{31}^{31}\}^3$ ,  $\{H_{31}^{31}\}^5$  and  $H_{31}^t$

Figure 6.19: Frequency Response  $\{H_{31}^{51}\}^5$ 

## 6.6 Concluding Remarks

This chapter highlights the application of the analysis methods developed in this thesis to structural dynamics by numerical simulation. The developed methods using the describing function are found to be very accurate when compared with existing time integration methods. Quantitative comparisons of computer costs between the multi-harmonic nonlinear receptance coupling approach and the time integration method reveal that there is a well defined advantage of the former over the latter.

# Chapter 7

## Experimental Case Studies

### 7.1 Introduction

In this chapter, the nonlinear coupling procedure developed in Chapter 4 is applied to two real structures. One structure is obtained by coupling a clamped beam with two nonlinear cubic stiffness joints as shown in Figure 7.14. The other structure is a Rotor Kit RK4 from Bentley Nevada with some modifications in the original supports in order to exhibit a clear nonlinear stiffness behaviour as presented in Figure 7.52. All the FRF data measured from the nonlinear structures were obtained by a sinusoidal excitation with a special control of the force where the level of the fundamental force is kept constant and the level of the harmonics is kept zero for all the frequencies measured. This technique is discussed in the following sections.

### 7.2 FRF Measurements on Nonlinear Structures

The frequency domain analysis of linear structures is characterised by a set of unique frequency response functions which can be defined as frequency-dependent quantities calculated from the ratio between a harmonic displacement response and the harmonic driving force. For nonlinear structures, the frequency response function has two principal differences compared with the definition for a linear system. The first is that the total response of a nonlinear system in the time domain is represented by a sequence of frequency response functions in the frequency domain in contrast to only one function in the linear case. The stronger the nonlinearities are, the more frequency response functions are needed to represent the total response. On the other hand, for a wide class of nonlinear systems, most of

the dominant effects are contained in the so-called first-, second- and third-order frequency response functions and these are often sufficient to characterise the system quite accurately [108, 133]. The second difference is that each frequency response function is a multi-variable function, even for a system under single input and single output. This feature increases the difficulty of the analysis of nonlinear structures.

Frequency response functions have been successfully measured for many years in a wide variety of modal testing applications using different types of excitation to drive the test structure. Although the measured frequency response functions of linear structures are independent of the choice of the excitation technique, most engineering structures are often found to exhibit the problem that the overall structure response is nonlinearly dependent on the level and the kind of excitation. An appropriate excitation technique should be selected in order to study a nonlinear system. There are mainly three types of excitation method widely used in vibration analysis: periodic, random and transient, and they are each discussed below.

### **7.2.1 Sine Excitation**

Sine excitation is one of the most periodic commonly-applied excitation techniques to obtain frequency response functions because of its uniqueness and precision characteristics. This frequency response function is obtained by using steady-state harmonic excitation. For each frequency, a force is applied which consists of a constant-amplitude sine wave. The displacement response is allowed to reach a steady-state condition and the spectral analysis of the excitation and the response is calculated. For linear structures, when the input is a sinusoid, the response is also a sinusoid with the same frequency as the excitation but with a different magnitude and phase. Thus, for a linear case, just one component of the frequency spectrum is extracted at each frequency point. However, for nonlinear systems, even when the input is a pure sinusoid, the response is composed of a number of frequency components, such as harmonics and intermodulation frequencies. In this case, the first and higher frequency response functions can be calculated using the ideal mathematical definition related with the Volterra series or the measured approximated frequency response function defined in several different ways, both presented in Chapter 2. The latter, if correctly defined, can still contain useful information about the behaviour of the system.

The great advantage of a sinusoidal excitation is related with its frequency-selective nature. In this case, the level of the input force can be accurately controlled, a feature

which becomes very important in the successful evaluation of frequency response functions of nonlinear structures [116] due to the fact that harmonic excitation reveals the distortions of the FRFs in the resonance regions for different levels of force. Harmonic excitation also reveals the subharmonic and superharmonic responses that are clear manifestations of nonlinear behaviour. Furthermore, the measurements can be concentrated where they are required, having a different frequency increment in different frequency ranges. For instance, near resonances and antiresonances, the FRFs exhibit rapid changes and a fine frequency increment is recommended. On the other hand, away from resonances and antiresonances, the variation is very slow and a wider frequency gap can be used instead. In addition, the signal-to-noise ratio is generally good because once the energy is concentrated at one frequency, the response in the same frequency and in the harmonics and intermodulations can be averaged out through an integration process.

Two different conditions can be used to obtain frequency response functions of nonlinear systems. The first one is by keeping the amplitude of the force level constant at all the different excitation frequencies. This technique allows us to observe the distortion of the frequency response functions such as the "jump" phenomenon as the input level is increased. The second one is by keeping the amplitude of the response level constant at different excitation frequencies. Here, the frequency response function obtained looks like the frequency response function of a linear system. This allows us to apply standard modal analysis techniques to obtain some linearised characteristics of the system.

The main drawback of the sinusoidal excitation technique is that the time spent to obtain a typical frequency response function is greater than that required by the other commonly-used techniques. This is related to the fact that the excitation is performed on a frequency-by-frequency basis and, at each frequency, a delay is imposed in the measurement in order to allow the system to achieve the required steady-state response before starting measurements. Occasionally, however, the correct measurement of the frequency response is more important than the time spent during the procedure. Normally, when the objective is to improve the analytical model using the correlation of the analytical data with the test data, the more accuracy obtained in the FRF measured, the better is the derived analytical model.

## 7.2.2 Random Excitation

Random excitation is widely used in linear structural dynamic tests because of the characteristics of random signals of containing energy over a wide range of frequencies simultaneously, thus enabling the random excitation to have a potential time-saving in obtaining the frequency response functions. The random signal is a continuous signal which never repeats itself and whose amplitude can only be predicted in terms of statistical terms.

The process of measuring frequency response functions begins with the sampling of the random force and the response in the time domain at discrete points in time. The original signals are continuous in time but the sampled time history signals are finite in length and are nonperiodic. These sampled time history signals are converted to the frequency domain by applying Fourier analysis. The use of Fourier analysis places restrictions, for example the nonperiodic sample time history signals are considered periodic and as a result, a leakage problem occurs in the estimation of the frequency response functions. However, this effect can be minimised by using weighting functions, such as a Hanning window, before the Fourier analysis is performed. After the signal is processed, the required frequency response function of the structure is derived by an appropriate combination of a number of force and response spectra. The limitation is related with the constraints imposed by the conventional methods of Fourier analysis for equally-spaced points in the frequency domain and the limited number of points available. In this case, the points cannot be concentrated around the resonances and antiresonances as can be done in the case of sinusoidal excitation. On the other hand, the points can be shaped to fit the frequency range of interest by filtering and modulating the original broad band signal. Thus the system is not excited by frequencies outside the analysis bandwidth, giving a better dynamic range in the analysis.

For nonlinear systems, the frequency response function obtained by using random excitation appears to be undistorted and similar to that of a linear system. This is due to the averaging effect of using the random excitation. Although the FRFs do not show any distortions, different FRFs will be obtained for different input levels, resulting in input dependency. This technique is also extended to obtain higher-order FRFs [48, 123, 89]. In addition, although the procedure does not seem to produce higher-order FRFs of good quality, the FRFs are improved by applying a linear global fitter that fits a linear model to the obtained data [49].

### 7.2.3 Impact Excitation

Transient, as impact, excitation is a very popular and convenient excitation technique for mechanical structures. This popularity is mainly due to the simplicity of the excitation method which makes it very adaptable to a wide range of testing conditions. Impact excitation can be produced by using an instrumented hammer with a force transducer on which an impact tip is mounted. When the structure is excited by the hammer, energy is transferred to the structure in a very short period of time. The process of measuring frequency response functions begins with the sampling of force and the response time history signals due to the impact. Once again, the time histories are converted to the frequency domain by applying Fourier analysis. Because of the constraints imposed from the Fourier analysis, a leakage problem can occur, usually in the response signal. If the response does not decay almost to zero by the end of the sampling period, the exponential window is applied to reduce the leakage. Then the frequency response is obtained by dividing the spectrum of the response by the spectrum of the force.

The shape of the force signal depends on the type of hammer tip, the mass of the hammer and the dynamic characteristics of the structure under investigation. As the frequency bandwidth of the force spectrum is determined by the duration of the impulse, these characteristics will determine the upper cutoff frequency of the excitation signal. The stiffer the hammer tip and the structure are, the shorter the pulse, and the wider the frequency span. Extra mass on the hammer lengthen the force pulse and therefore lowers the cutoff frequency as well as increasing the excitation force level. The advantages of the impact test are related with the short time spent to obtain the frequency response function due to only few averages being needed and to it being very easy to use in the field. However, the disadvantage of impact excitation comes from the fact that the excitation bandwidth has a limited control, low input energy and a low signal-to-noise ratio.

Unfortunately, an impact force can rarely be used for nonlinear structures because of inconsistency in the duration and force of the impacts and the low RMS signal levels produced due to the brief duration of the active input. This means that the level of energy applied can be very difficult to control and the high peak levels can overdrive the system and exaggerate its nonlinear response. In addition, the low RMS value can result in poor signal-to-noise ratios of the measured signals. However, it has been already applied to identify simple localised nonlinearities [42] and has been used to measure second-order FRFs of nonlinear structures by using a special electric impact hammer [21, 22].

### **7.2.4 Discussion of Different Excitation Techniques**

As mentioned earlier, there are a number of excitation techniques available nowadays for vibration tests on structures, among them the three main types of excitation were presented. Each of these methods has its advantages and disadvantages, and the choice becomes more important when having to analyse nonlinear structures.

For linear structures, since all kinds of excitation should give the same unique FRF, the choice of the excitation, among other things, is related with the test application, time available for the analysis and data quality required. For nonlinear structures, it is important to realise that these structures respond in different ways to different types of excitation. Therefore the choice of excitation is dependent on the analysis required of the structure. If the main concern is first to understand and to diagnose structural vibration characteristics, then impact excitation can be considered. Because of its characteristics of simplicity and adaptation, the impact test provides a simple and fast way to understand what a given structure is doing dynamically. When the dynamic modelling of the nonlinear structures is the main interest, the primary concern will be to extract a linear model of the system that will behave dynamically as similar as possible to the nonlinear system. Random excitation can be an efficient technique in this case because of its characteristics of considering the effects of nonlinearities as a systematic error in the output. Therefore the frequency response function obtained will give a "best" linear approximation to the system. On the other hand, if the main concern is to investigate nonlinearities, how the spatial, modal or response model of a nonlinear structure will change for different vibration response levels, the sinusoidal excitation technique is the most appropriate procedure, because of the well controlled input force level. In this study only the sinusoidal excitation is applied.

### **7.2.5 Practical Considerations of Measuring FRF properties of Nonlinear Structures**

As discussed above, in the case where the frequency response functions of nonlinear structures for different vibration response levels are going to be measured, sinusoidal excitation is strongly recommended. However, the choice of the excitation is only the first step to obtain the frequency response function. There are still a number of possible practical problems which need to be carefully considered in order to achieve a successful frequency response measurement.

Most FRF measurements using sinusoidal excitation require a function generator to generate a sinusoidal voltage, the attachment of a single electrodynamic shaker to drive the test structure, a power amplifier that applies the sinusoidal voltage from the function generator to the shaker, a flexible stinger to transmit the excitation force to the structure, a force transducer measuring the input force and multiple accelerometers to measure the structural responses. The excitation and response signals are acquired and then processed by using a digital spectrum analyser to perform the FRF calculations. In theory, acquiring the FRF using the described measurement system should be straightforward. However, in practice, to ensure good measurements of structural frequency response functions requires consideration of many aspects of the whole measurement system. Many types of error related with the transducers, signal conditioning, boundary conditions, shakers, power amplifier and stingers can affect the accuracy of the measurements. Choosing the right measurement system is an important part of the pre-test planning. After obtaining some FRFs of the structure under test, it is also good practice to perform simple checks for common errors related with instrument installation, excitation location, excitation installation and response measurements [31].

The connection between the exciter and the structure through the use of the stinger can be a source of errors. Ideally, the stinger should have a high axial stiffness but be very flexible in the transverse directions. In practical situations, this can be difficult to achieve and the stinger will generally present some stiffness in its transverse directions, introducing secondary forms of unwanted excitations such as bending moments and shear forces, which will act on the force transducer and the structure. This will cause errors in the measured FRFs. Various studies related with the analytical modelling of this problem [54, 60] as well as some solutions [3, 15, 71] can be found. This problem usually can be minimised by an appropriate dimensioning of the stinger [3, 60].

The interaction between the shaker and the structure can be another source of error. Errors attributed to the impedance mismatch between the shaker and the structure can often be eliminated or significantly reduced by studying the interaction between the shaker and the structure [79, 93, 99], and then deciding on an appropriate choice for the shaker. In summary, the shaker should be chosen such that the mass and stiffness characteristics are negligible with respect to the generalised mass and stiffness characteristics of the structure under test.

Another problem related with the shaker is that the force input to a system near a system resonance can vary considerably. In theory, when a sinusoidal voltage is applied to

the shaker via an amplifier, the shaker should generate a similar simple harmonic force in the force transducer. This is due to the fact that although the magnetic field of the shaker is nonlinear, it is assumed linear for small amplitudes of vibration of the armature. However, in practice, when the structure under test resonates, the displacements are relatively large and the reaction force between the exciter and the structure tends to become very small. At this resonant condition the armature movement is in the nonlinear magnetic field and higher harmonics will be present in the input force [124]. It should be stressed that if the structure under test is linear then in theory the frequency response function is independent of the variation in the input force spectrum. However, reliable experimental results can be obtained by applying the techniques for filtering out unwanted harmonics [31]. Many commercial instruments include this feature. On the other hand, if the structure is nonlinear, this problem is accentuated because of the interaction of the shaker and the structure. Other harmonics can also be predominant in the input force due to the nonlinear response of the structure. Therefore the measured FRF obtained with this force could result in problems when used in analytical procedures [129]. Indeed, all the theoretical work concerning the harmonic forced response of nonlinear systems assumes a simple harmonic excitation with a constant force level as a input force. Hence the external force should be tuned to ensure a constant pure harmonic excitation force. This requires a robust nonlinear force control algorithm. In other words, the algorithm should not fail by estimating a wrong excitation force that will damage either the measurement equipment or the structure.

There is an additional difficulty in achieving uni-directional excitation: undesirable excitation in the other directions. Around resonance this problem becomes more acute. To overcome this problem, the shaft can be excited in two directions. The first shaker is in the direction of desired excitation. The second shaker excites in the perpendicular direction. By applying an acceleration control algorithm, any acceleration in the perpendicular direction can be minimised. The basic acceleration control algorithm is the same as the force control algorithm. Both control algorithms are developed in the next sections.

### 7.2.6 Nonlinear Force Control Algorithm

The nonlinear force algorithm can be derived by first representing the voltage applied in the shaker armature,  $\mathbf{v}$ , and the force in the transducer,  $\mathbf{f}$ , as Fourier series:

$$\mathbf{v} = \sum_{m=0}^{\infty} \mathbf{v}^m = \sum_{m=0}^{\infty} \mathbf{v}^m e^{im\Psi} \quad (7.1)$$

$$\mathbf{f} = \sum_{m=0}^{\infty} \mathbf{f}^m = \sum_{m=0}^{\infty} \mathcal{F}^m e^{im\Psi} \quad (7.2)$$

Considering  $n$  harmonic components in the force, the coefficients in equations (7.1,7.2) can be written in matricial form as

$$\mathbf{v} = \begin{Bmatrix} \mathbf{v}^1 \\ \mathbf{v}^2 \\ \vdots \\ \mathbf{v}^n \end{Bmatrix} \quad \mathbf{f} = \begin{Bmatrix} \mathcal{F}^1 \\ \mathcal{F}^2 \\ \vdots \\ \mathcal{F}^n \end{Bmatrix} \quad (7.3)$$

The relation between the required force in the force transducer,  $\mathbf{f}$ , and the adjusted harmonic input voltage signal,  $\mathbf{v}$ , at frequency,  $\omega$ , in the shaker armature can be expressed via an unknown functional relationship,  $\mathbf{F}$ , as:

$$\mathbf{f} = \mathbf{F}(\mathbf{v}, \omega) \quad (7.4)$$

If  $(\mathbf{v}_d, \mathbf{f}_d)$  is the solution which satisfies equation (7.4), then:

$$\mathbf{f}_d - \mathbf{F}(\mathbf{v}_d, \omega) = 0 \quad (7.5)$$

Equation (7.5) can be solved by the Newton-Raphson method described in section (2.7). This method gives a very efficient means of converging to a solution, given a sufficiently good initial guess. Therefore, it is desirable to find a good initial guess that can be used to find the solution and at the same time avoid the problem of estimating a wrong excitation force that will damage either the measurement equipment or the structure. Test experience showed that a good initial guess is the first harmonic solution. Thus, instead of finding a solution for a set of nonlinear system of equations, the problem is reduced to a one-dimensional nonlinear equation where the only concern is to first find a voltage  $(\mathbf{v})_1$  and ignore the higher harmonics. It is interesting to point out that for the first harmonic only the amplitude is controlled, whereas for the remaining harmonics, both the amplitude and phase must be controlled.

The first hypothesis assumed is that the solution is bracketed in the range of the function generator voltage. A solution is said to be bracketed in the interval  $(a, b)$  if  $f(a)$  and  $f(b)$  have opposite signs. Then a quick check is performed to secure that the solution is really bracketed.

There is not much theory available as to how to determine this bracketing. If it is assumed that the function is continuous, then at least one root must lie in that interval. The procedure adopted is: given an initial guess, take positive and negative steps of increasing size until the root is bracketed.

Once it is known that an interval contains the solution, several classical procedures are available to locate it precisely. The bisection method is one that cannot fail as long as the solution is bracketed. The problem with the bisection method is slow convergence. The Newton-Raphson method is one that has a poor global convergence but can locate the solution precisely after having a good initial guess. A fail-safe algorithm is the one that combines the bisection method and the Newton-Raphson method. The hybrid algorithm takes a bisection step whenever Newton-Raphson would take a solution out of the brackets, or whenever Newton-Raphson is not reducing the size of the brackets rapidly enough.

After obtained the harmonic solution, the resulting solution is used as an initial guess for the Newton-Raphson method using now all the nonlinear equations. Before applying the Newton-Raphson method, a check is carried out to evaluate the  $n$  important harmonics that should be controlled. When the solution is found assuming the  $n$  harmonics, since the structure is nonlinear new harmonics may now need to be controlled. A new check is performed to assess whether the new harmonics have become relevant. If it is found that some new harmonics should be controlled, they are added to the previous set and the Newton-Raphson solution is repeated. When it reaches the solution, the frequency is then incremented and this solution is now used as the next guess to find the new bracketed interval.

The implementation is presented in an algorithm form below:

1. Initial guess for driving voltage

$$v = \left\{ \begin{array}{c} \mathcal{V}^1 \\ \mathcal{V}^2 \\ \vdots \\ \mathcal{V}^n \end{array} \right\}$$

2. Find lower and higher voltages  $\mathcal{V}_l^1$  and  $\mathcal{V}_h^1$  that bracket the solution  $\mathcal{F}_l^1$  and  $\mathcal{F}_h^1$ .
3. Using the one-dimension Newton-Raphson method combined with the Bisection method, find the solution of the function bracketed between  $\mathcal{V}_l^1$  and  $\mathcal{V}_h^1$
4. Create a set of harmonics to be controlled .

5. Using as the initial guess to the solution from the step 3, find the solution by the multi-dimension Newton-Raphson method.
6. Check the harmonics to be controlled to establish, if there are any new harmonics, update the harmonics set and go back to step 5.
7. Increment the frequency.
8. Update the initial guess of step 1 with the solution of the step 5 and start the procedure again on step 1.

### 7.2.7 Acceleration Control Algorithm

The acceleration control algorithm can be derived by first representing the voltage applied in the shaker armature,  $\mathbf{v}$ , and the measured acceleration,  $\ddot{x}$ , in frequency domain as :

$$\mathbf{v} = \mathcal{V}e^{i\Psi} \quad (7.6)$$

$$\ddot{x} = \ddot{X}e^{im\Psi} \quad (7.7)$$

The relation between the required acceleration in the accelerometer,  $\ddot{x}$ , and the adjusted harmonic input voltage signal,  $\mathbf{v}$ , at frequency,  $\omega$ , in the shaker armature can be expressed via an unknown functional relationship,  $\mathbf{F}$ , as:

$$\ddot{x} = \mathbf{F}(\mathbf{v}, \omega) \quad (7.8)$$

If  $(\mathbf{v}_d, \ddot{x}_d)$  is the solution which satisfies equation (7.8), then:

$$\ddot{x}_d - \mathbf{F}(\mathbf{v}_d, \omega) = 0 \quad (7.9)$$

Equation (7.9) can be solved by the Newton-Raphson method described in section (2.7). It is interesting to point out that the amplitude and phase of the harmonic component  $(\mathcal{V})_1$  must be controlled.

The implementation is presented in an algorithm form below:

1. Initial guess for driving voltage

$$\mathbf{v} = \mathcal{V}^1$$

2. Using the initial guess, find the solution by using the Newton-Raphson method.

3. Measure FRFs in the perpendicular direction.
4. Increment the frequency.
5. Update the initial guess of step 1 with the solution of the step 2 and start the procedure again on step 1.

### 7.3 Experimental Setup

The overall setup for both test rigs can be seen in Figures 7.1 and 7.2. The experimental setup for both structures tested consisted of a shaker connected via a push-rod to a B&K 8200 force transducer which was used to measure the input force to the structure. All the resulting responses at selected points were measured using the ENDEVCO 2222C lightweight accelerometers which were attached to the structure using beeswax.

Two frequency response analysers were used to measure FRFs of the structures. The first one, the Beran 402 Frequency Response Analyser, was used to measure the linear FRFs of Test Rig I. The second one, a "virtual analyser" developed during this project, was used to obtain FRFs when a special parameter is required to be controlled. The virtual analyser consisted of a Pentium 200MHz computer, a National Instruments card AT-MIO-64E-3, an HP 33120A function generator and the *INCA*<sup>++</sup> software. This virtual analyser was used to obtain the linear FRFs of the Test Rig II and also to obtain the FRFs of both nonlinear structures. Both analysers can be seen in Figure 7.1. The block diagram of the linear and nonlinear experimental setup of Test Rig I using both analysers can be seen in Figures 7.3 and 7.4, respectively. The block diagram of the linear and nonlinear experimental setup of Test Rig II using the virtual analyser can be seen in Figures 7.5 and 7.6, respectively.

The a National Instruments card AT-MIO-64E-3 has 64 analogue input channels and two analogue outputs. The analogue output channel is used as an arbitrary waveform generator where the waveform generated can be updated on the fly when the card is driven by an external clock. The external clock used is via the HP 33120A function generator which has the capability of changing the clock rate of the square output signal without discontinuity. This requirement is essential because if there is a burst between the waveforms generated, a long settling time is again required for the structure to achieve the steady-state response.

The *INCA*<sup>++</sup> software employs a correlation technique to calculate the amplitude and phase components of the fundamental and harmonics of excitation force and response

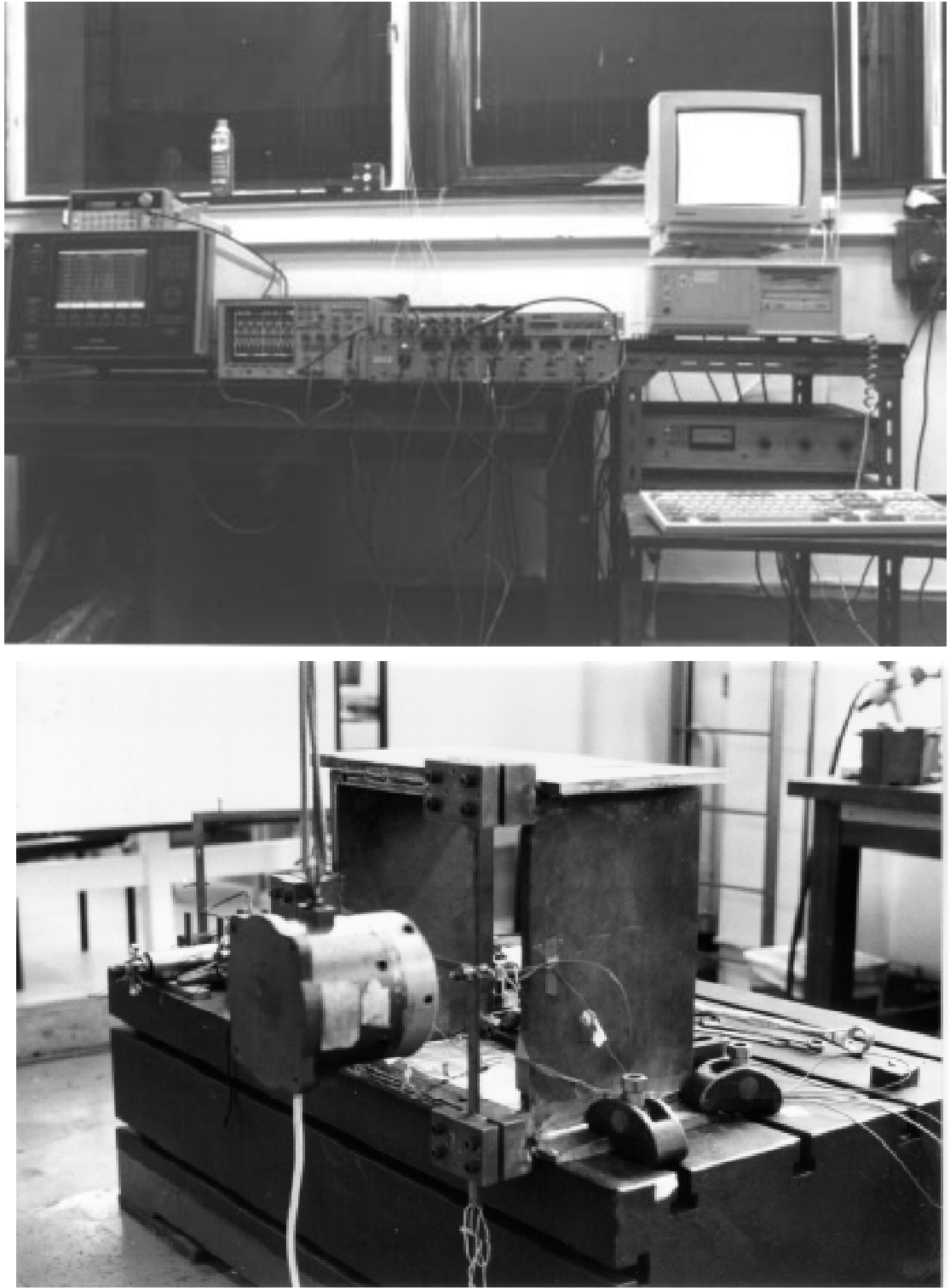


Figure 7.1: Overall setup Test Rig I

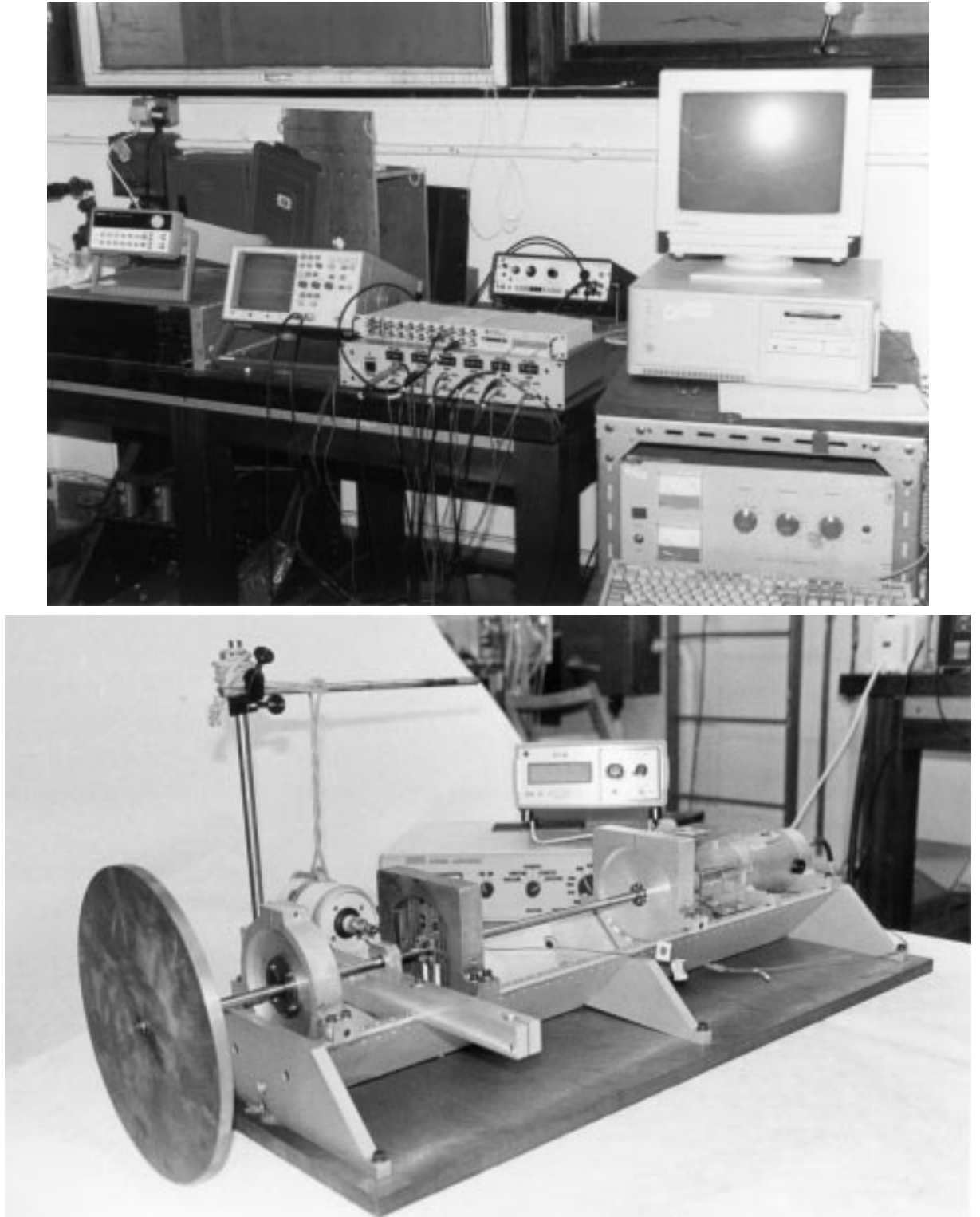


Figure 7.2: Overall setup Test Rig II

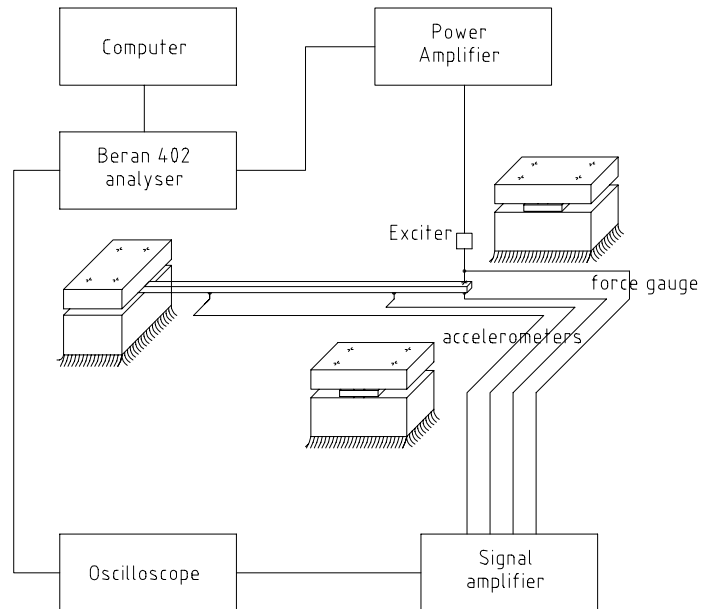


Figure 7.3: Block diagram of the linear experimental setup Test Rig I

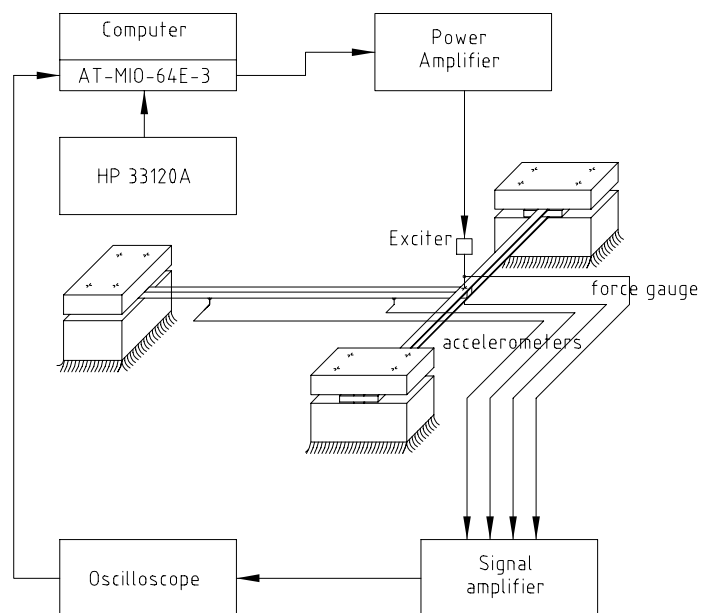


Figure 7.4: Block diagram of the nonlinear experimental setup Test Rig I

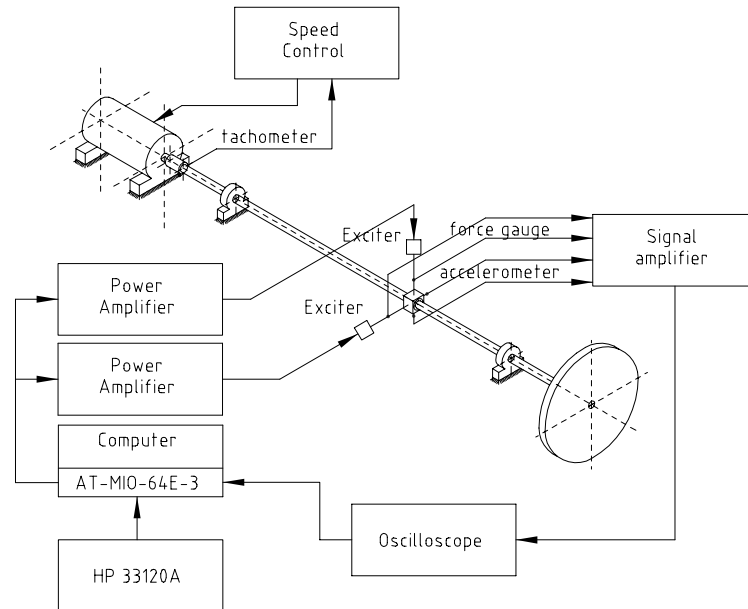


Figure 7.5: Block diagram of the linear experimental setup Test Rig II

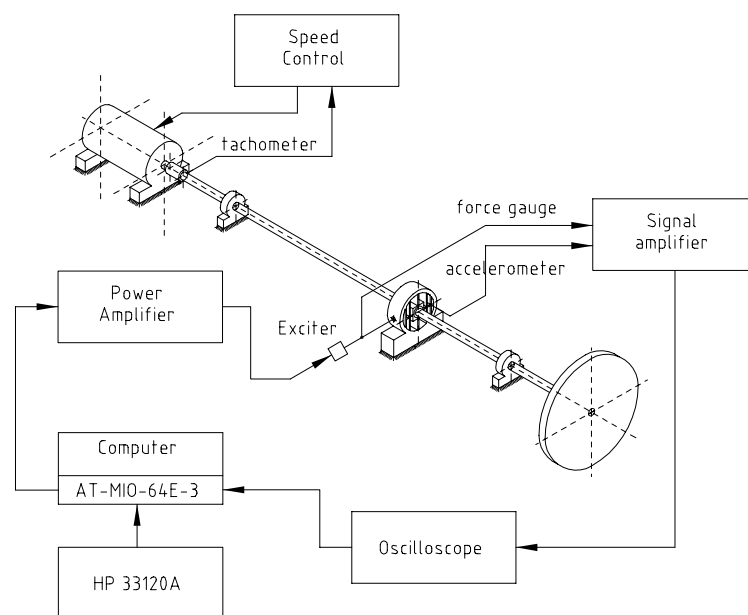


Figure 7.6: Block diagram of the nonlinear experimental setup Test Rig II

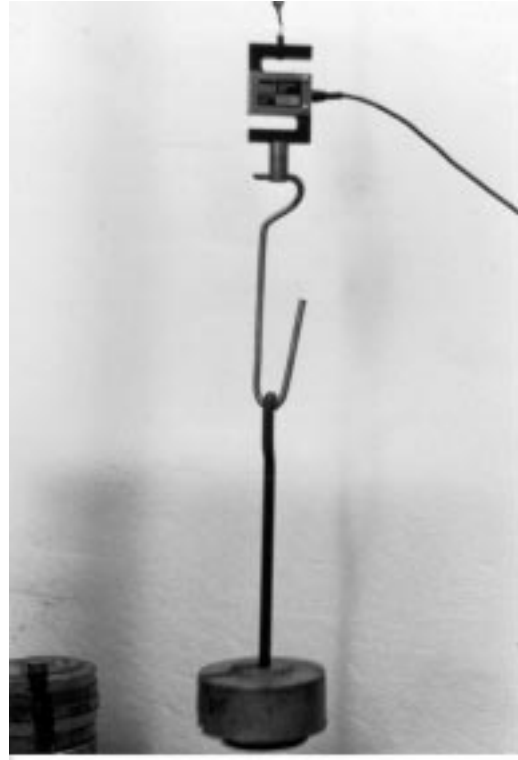
signals. This technique requires a synchronisation between the excitation and the response, which is obtained by having both the system acquisition and the arbitrary wave form generator of the National Instruments card, driven by one single external clock via the HP 33120A function generator.

Before any measurements were made, the overall system measurement sensitivity was calibrated for both the static test and the dynamic test. The static test refers to obtaining the relationship between static loading and structure deformation while the dynamic test involves the measuring structure's FRFs. The displacement for the static test was obtained by a Solartron DF9150 LVDT transducer and the force was obtained by a Saxeway J7100-500N load cell with a Fylde FE-492-BBS bridge conditioner. The LVDT was calibrated against a dial gage and the setup calibration can be seen in Figure 7.7(a). The load cell was calibrated against a set of standard masses and the setup calibration can be seen in Figure 7.7(b).

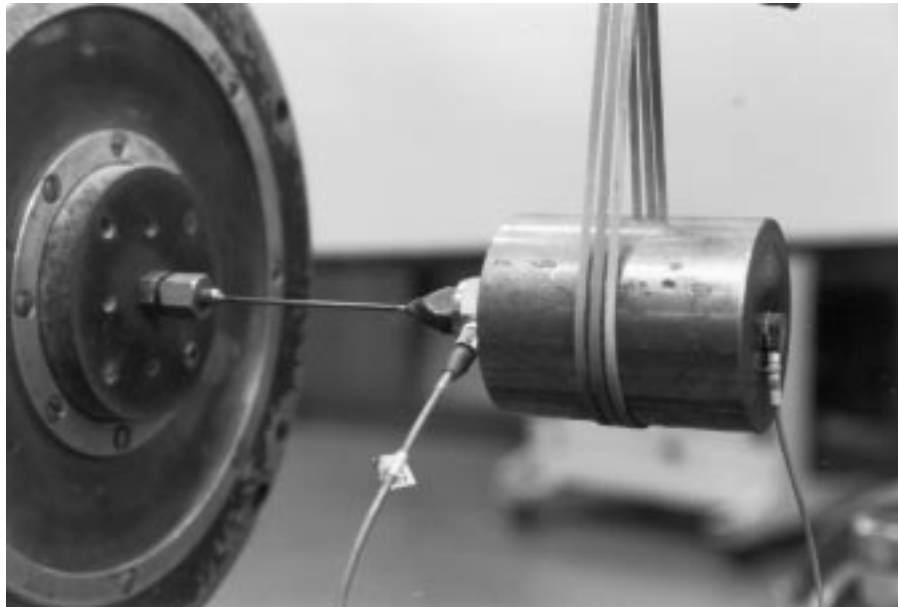
Since all the FRFs of the nonlinear structures were measured using force control, it was necessary firstly to check that the sensitivity of the force transducer was the same as that specified by the manufacturer. Such a measurement is quite difficult to achieve and usually the sensitivity of the force transducer is trusted from the calibration chart given by the manufacturer and is checked against other transducer force considered in good condition. Then the FRFs were calibrated by using the ratio calibration technique [31]. The accelerometers and proximity sensors were attached to a freely-suspended mass which was excited by shaker in the same way as measurements would be made on the structure itself, as shown in Figure 7.7(c). Therefore the sensitivity of the force transducer given by the manufacturer was used and a correction scale factor for the accelerometer was adjusted such that the FRF level obtained over a frequency range is equal to the reciprocal of the mass of the calibration block.



(a) LVDT calibration



(b) Load Cell calibration



(c) FRF Calibration

Figure 7.7: Calibration Setup

## 7.4 Experimental Test Rig I

### 7.4.1 Test Rig Model

The Test Rig I was made of a continuous system having a local nonlinear cubic stiffness, as shown in Figure 7.8. It consists of a uniform beam, *A*, of 420 mm length with a cross

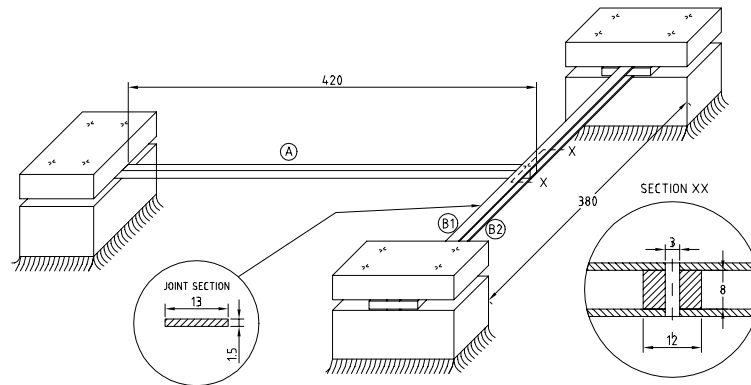


Figure 7.8: System configuration

section of 12mm by 8mm, which was clamped at one end and supported at the other end by two clamped-clamped beams, *B1* and *B2*, of 380mm length with a cross section of 13mm by 1.5mm. The stiffness of the beam *A* is linear and the local nonlinear cubic stiffness is produced by two clamped-clamped beams, *B1* and *B2*, due to the increase of the longitudinal tension under large amplitude of vibrations. Three accelerometers and one force-measuring transducer were attached along the beam. The first, second and third accelerometers were placed at 6mm, 82mm and 308mm respectively from the free end of the beam. The force transducer was located at 6mm from the free end of the beam. Both beams, *B1* and *B2*, modelled as the nonlinear joint, were clamped to the beam *A* at the place of intersection as shown in Figure 7.8. They are bolted together on one side by the force transducer and on the other side by a block mass with a thread. A detailed photograph can be seen in Figure 7.14.

### 7.4.2 Linear Test Rig I Assembly

The linear assembly rig is identical to the rig shown in Figure 7.8 except for the beams, *B1* and *B2*, which were removed. The linear test rig setup is shown in Figure 7.9.

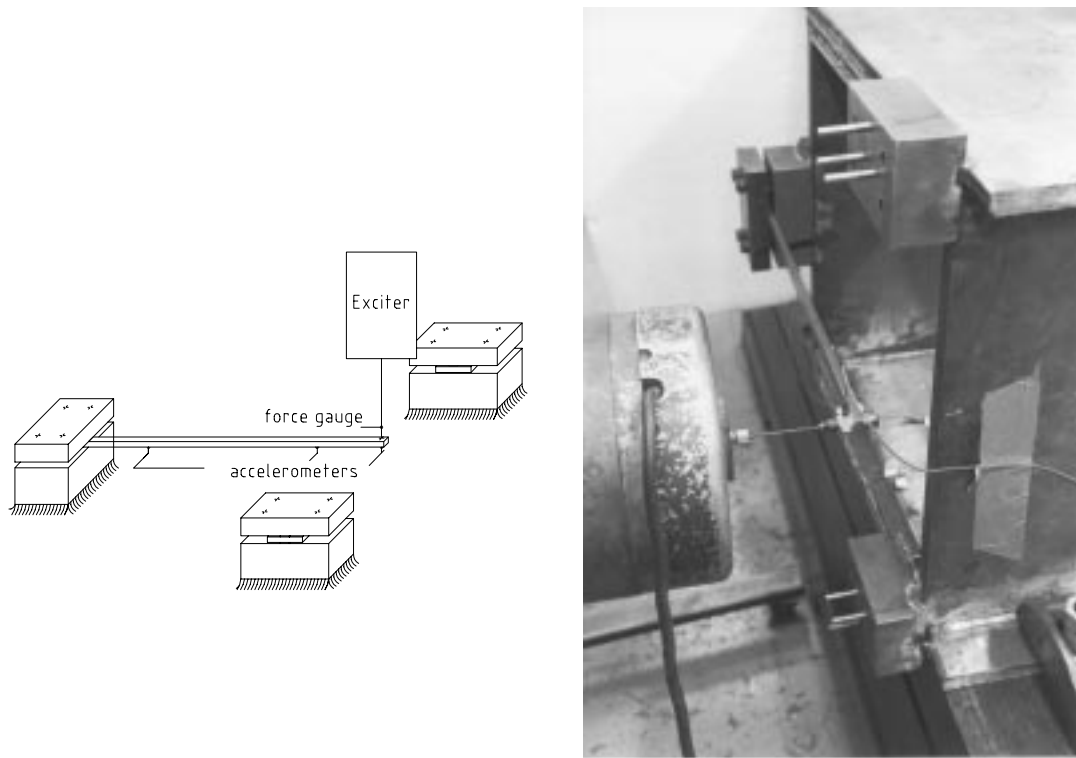


Figure 7.9: Linear Test Rig I assembly

### 7.4.3 Measured and Updated FRF of Linear Test Rig I Assembly

Due to different stiffness conditions which apply to the analytical and experimental configurations, an updated analytical model was used to represent the linear clamped beam as shown in Figure 7.10.

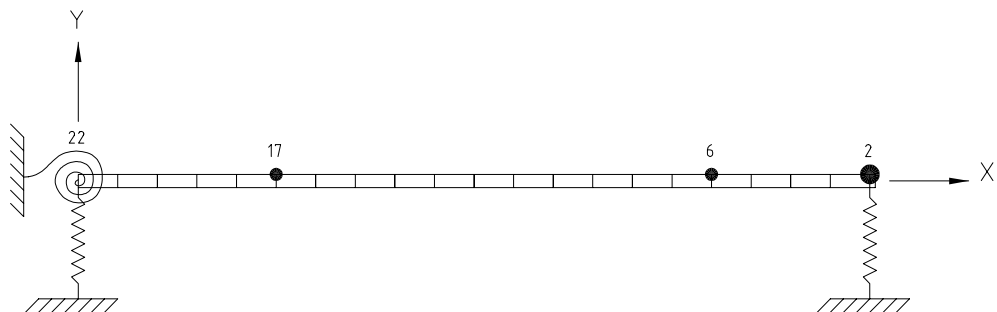


Figure 7.10: Analytical linear model test rig I

The beam was modelled using Timoshenko beam elements with the updated values of

elasticity modulus of  $1.96E11 \text{ N/m}^2$  and density of  $7900 \text{ kg/m}^3$ . The updated translational and rotational springs used to model the clamped joint were  $20E6 \text{ N/m}$  and  $1E4 \text{ N.m/rad}$  respectively. The updated mass and moment of inertia used in nodes 6 and 17 were  $1 \text{ g}$  and  $3.8E - 8 \text{ Kg m}^2$ , respectively. The updated mass and moment of inertia used in node 2 were  $37 \text{ g}$  and  $9.6E - 6 \text{ Kg m}^2$ , respectively. The mass of the shaker was  $46 \text{ kg}$  and the updated spring of the shaker used in node 2 was  $250 \text{ N/m}$ .

Three FRFs,  $H_{11}$ ,  $H_{21}$  and  $H_{31}$ , were measured by *INCA++* software using the BERAN 402 frequency response analyser. The frequency range was from 20 Hz to 1500 Hz and the excitation frequency was increased by steps of 0.01 Hz. For all three FRFs, excitation was at node 2 and responses were measured at nodes 2, 6 and 17 respectively.

The measured and updated frequency response functions of the linear structure for the three positions along the beam are shown in Figures 7.11,7.12,7.13.

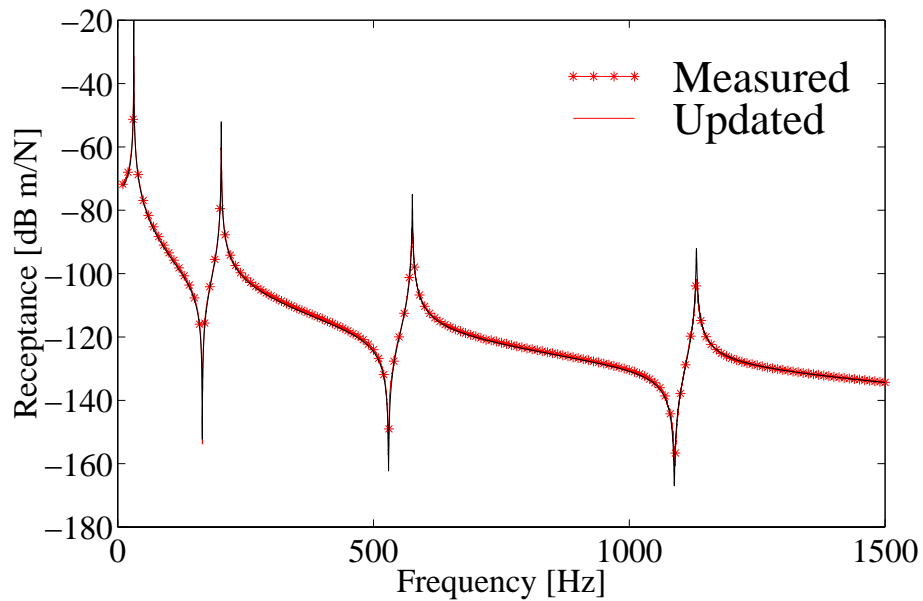
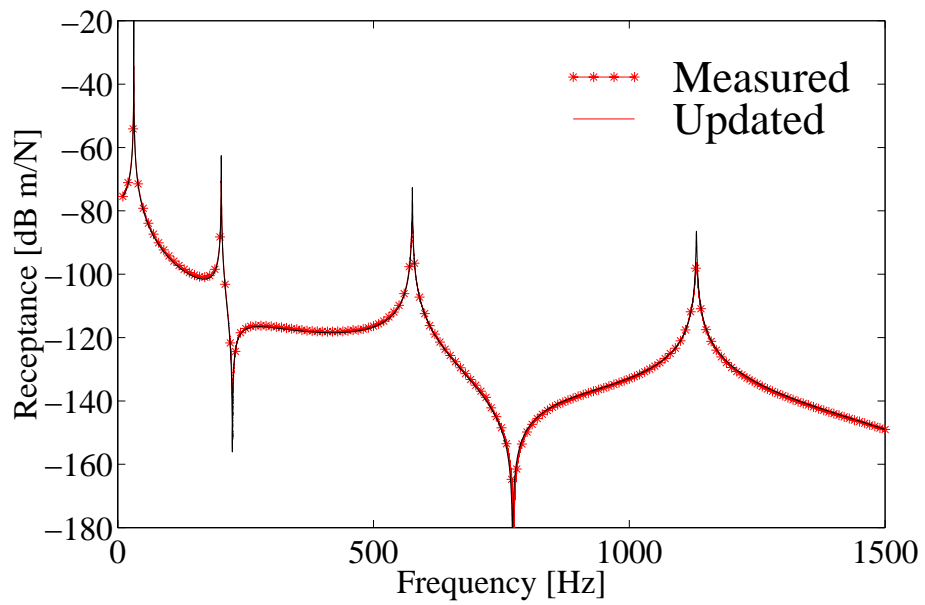
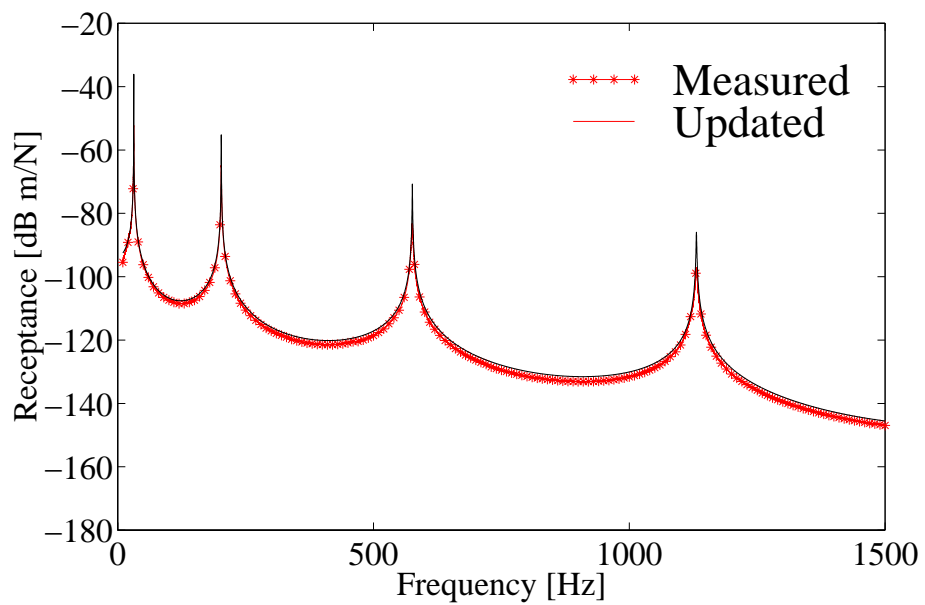


Figure 7.11: Frequency Response Function  $H_{11}$

Figure 7.12: Frequency Response Function  $H_{21}$ Figure 7.13: Frequency Response Function  $H_{31}$

#### 7.4.4 Nonlinear Test Rig Assembly

This test rig was designed to have the first mode with nonlinear behaviour and at the same time to have a very small influence of the rotational degree of freedom. This allows us to predict the behaviour of the first mode using only translational measurements. The nonlinear test rig assembly is presented in Figure 7.14.

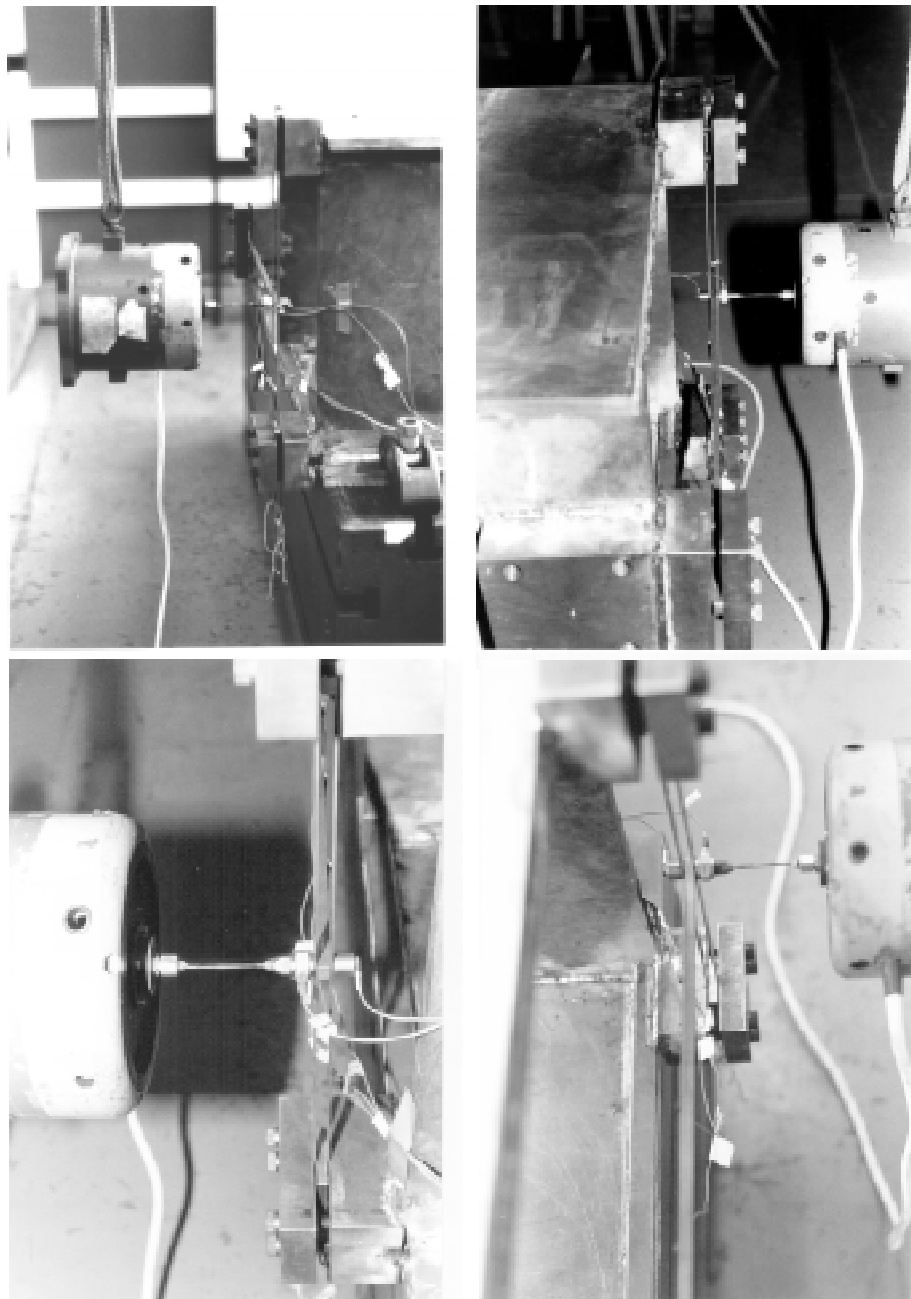


Figure 7.14: Test Rig I assembly

### 7.4.5 Experimental properties of the joints

The properties of the nonlinear joints were obtained by first performing a static test. After the static test was done, a curve of the type  $k_1 * x + k_2 * x^3$  was fitted and the parameters  $k_1 = 6500 \text{ N/m}$  and  $k_2 = 11800E5 \text{ N/m}$  were obtained. The same beam was modelled in ANSYS and the relationship between force and deformation for all these cases is shown in Figure 7.15.

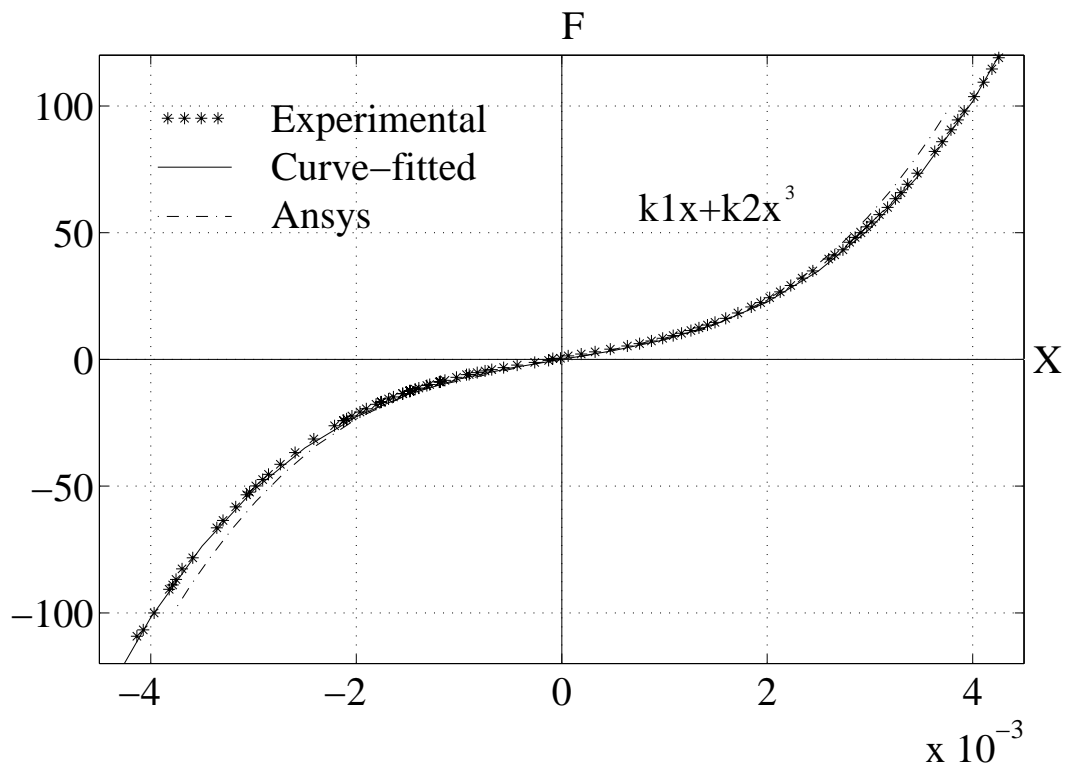


Figure 7.15: Relationship between loading and deformation

### 7.4.6 First Assembly Model Test Rig I

The first analytical model used to represent the nonlinear dynamic test rig is shown in Figure 7.16.

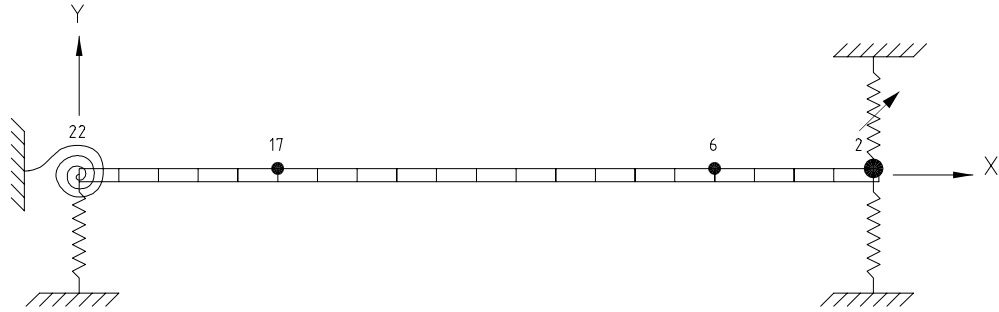
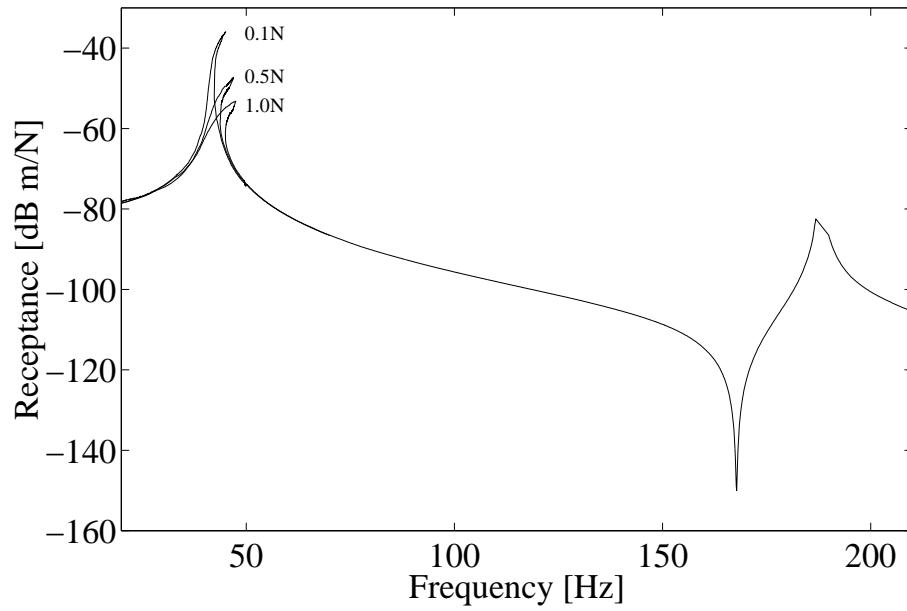
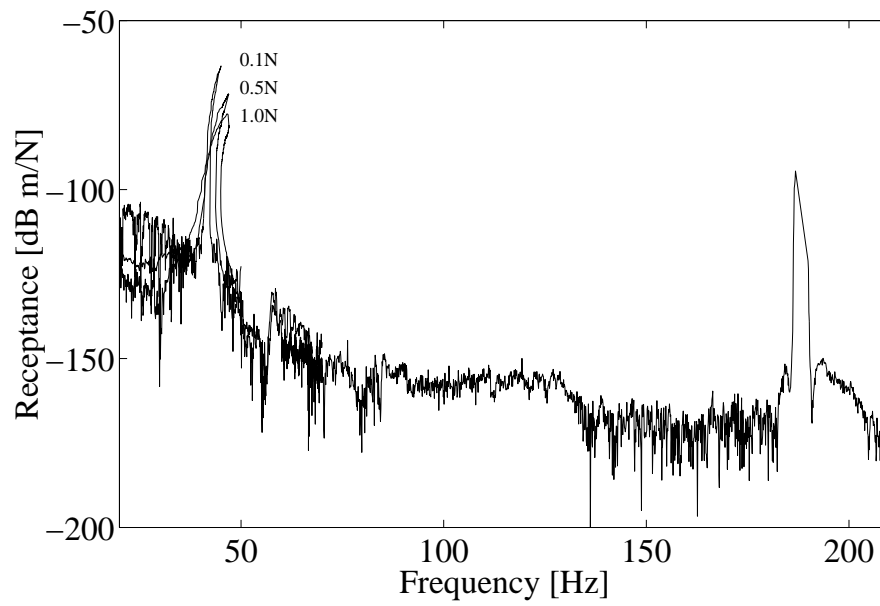


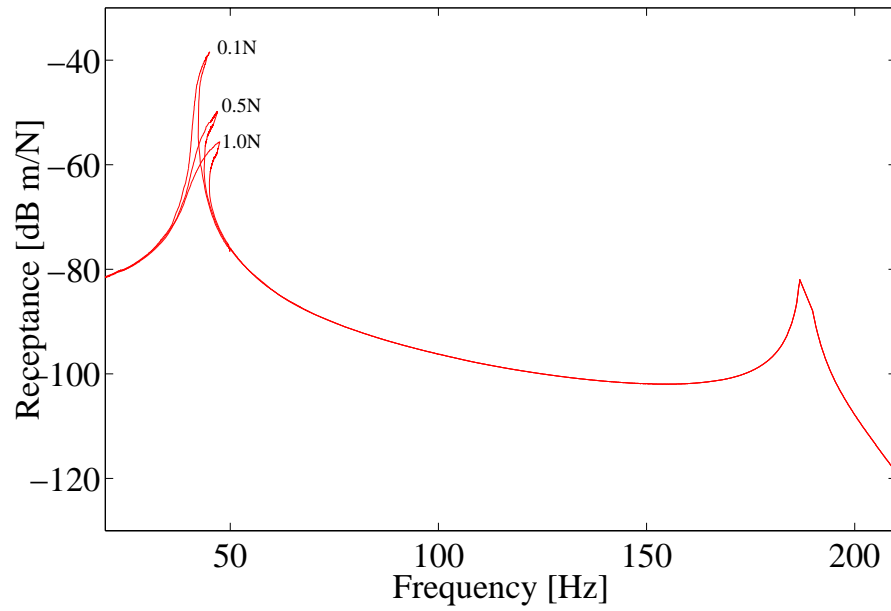
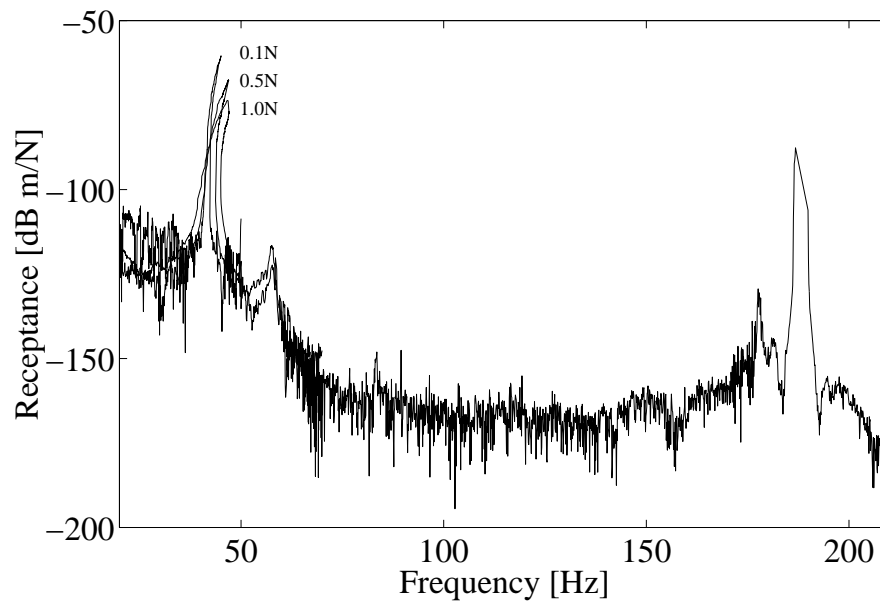
Figure 7.16: Analytical model Test Rig I

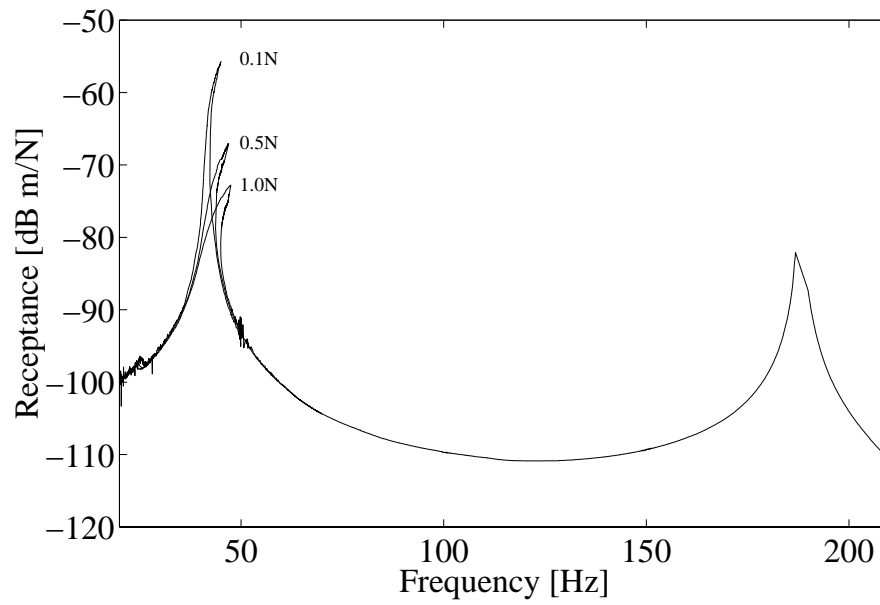
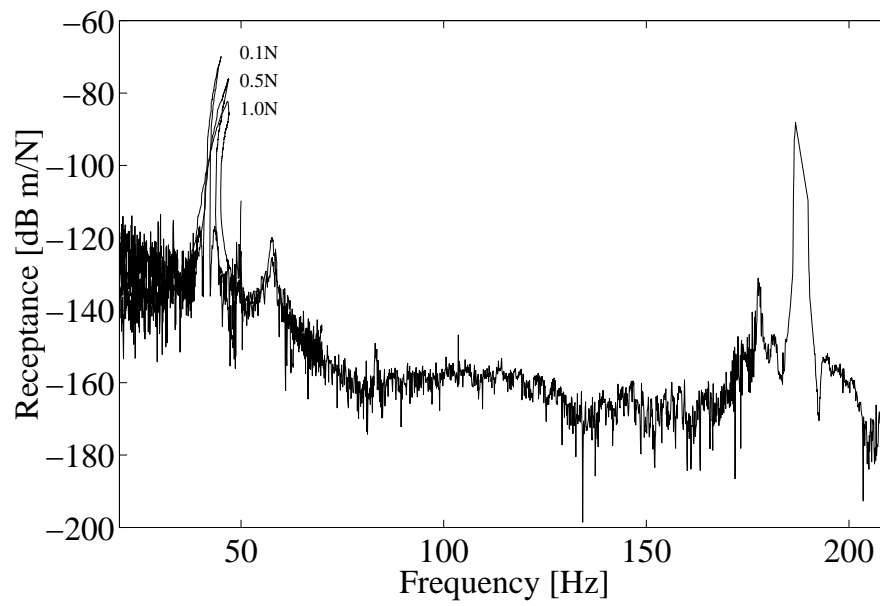
The nonlinear beams,  $B1$  and  $B2$ , shown in Figure 7.8 were modelled here as a concentrated nonlinear spring with mass. This model was used to predict the behaviour of the first mode using only translational FRFs obtained experimentally. The only parameter that had to be updated was the mass of the nonlinear beams to be used in the model. The updated concentrated mass at node 2 used to represent the nonlinear beams was 48 g.

### 7.4.7 Measured FRFs of Test Rig I

The fundamental frequency response functions  $H_{11}^{11}$ ,  $H_{21}^{11}$  and  $H_{31}^{11}$  and the higher-order frequency response functions  $H_{11}^{31}$ ,  $H_{21}^{31}$  and  $H_{31}^{31}$  were measured by the *INCA++* software using the virtual frequency response analyser presented in section 7.3. The frequency range was from 20 Hz to 210 Hz. The excitation frequency was increased by steps of 0.1 Hz way from the resonance region and by steps of 0.01 Hz around the natural frequencies. The excitation force level was 0.1N, 0.5N and 1N. Figure 7.17 shows the FRF  $H_{11}^{11}$  and figure 7.18 shows the FRF  $H_{11}^{31}$  both measured from point 2. Figure 7.19 shows the FRF  $H_{21}^{11}$  and figure 7.20 shows the FRF  $H_{21}^{31}$  both measured from point 6. Figure 7.21 shows the FRF  $H_{31}^{11}$  and figure 7.22 shows the FRF  $H_{31}^{31}$  both measured from point 17.

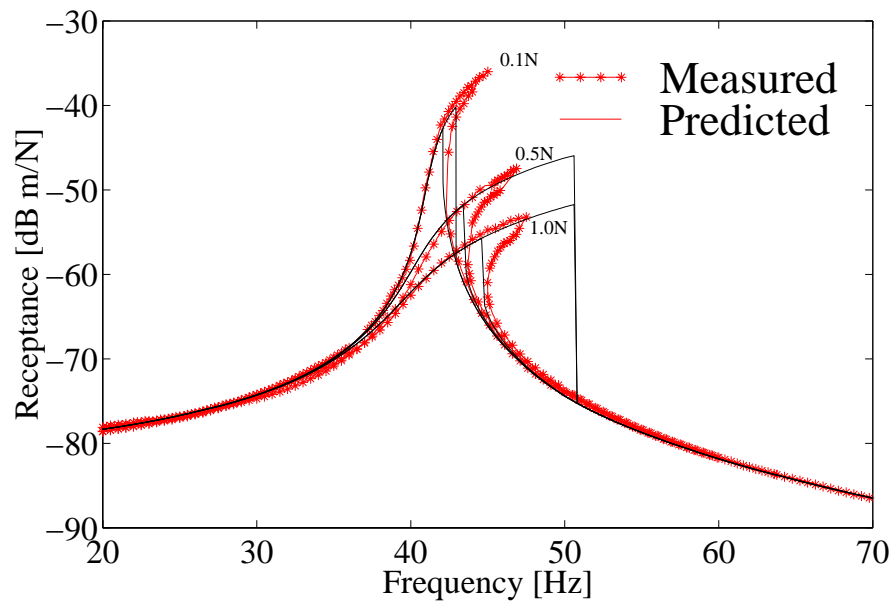
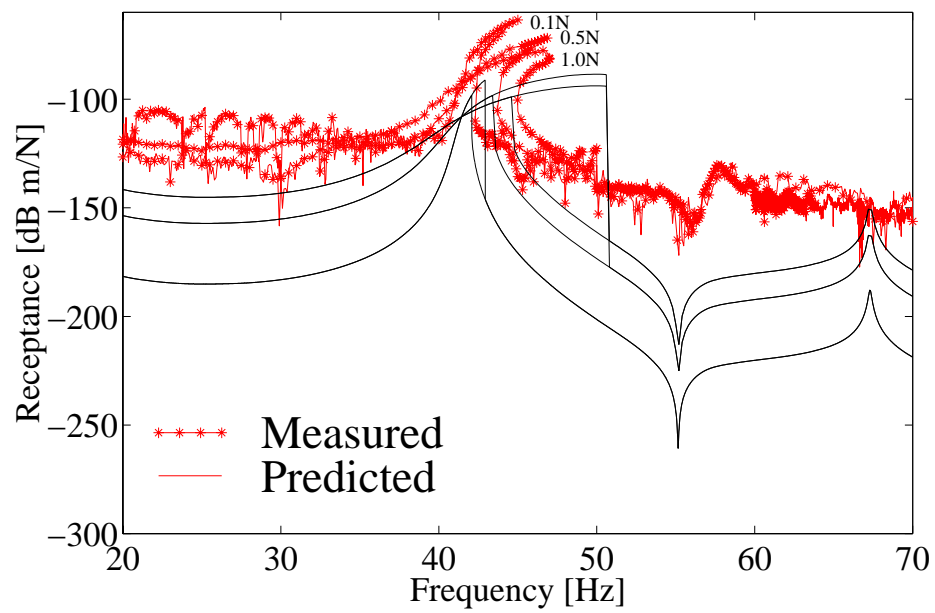
Figure 7.17: Measured Frequency Response  $H_{11}^{11}$ Figure 7.18: Measured Frequency Response  $H_{11}^{31}$

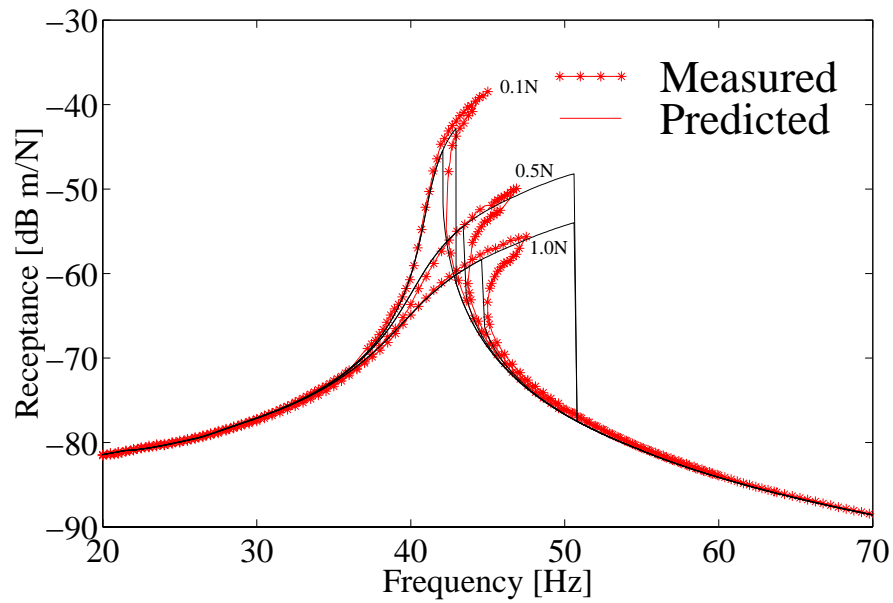
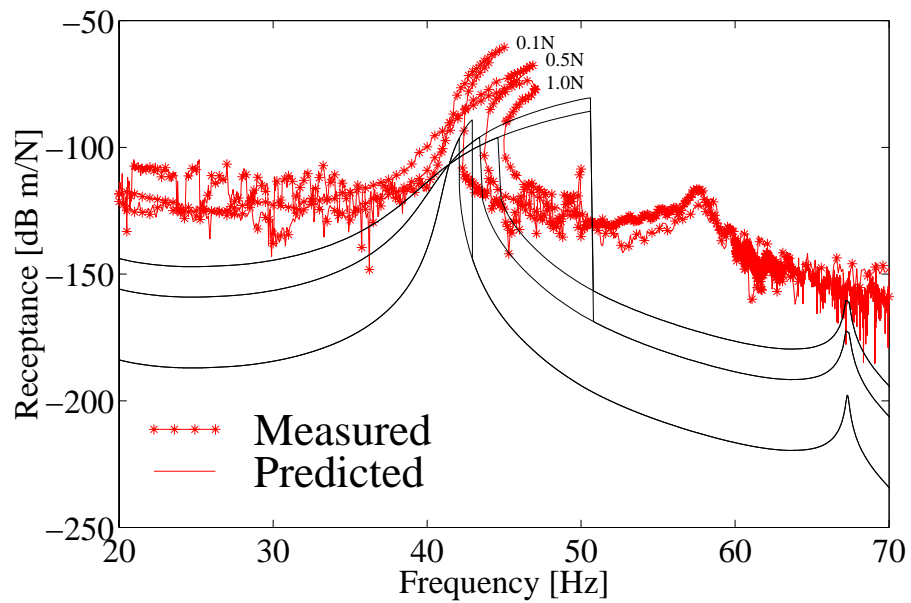
Figure 7.19: Measured Frequency Response  $H_{21}^{11}$ Figure 7.20: Measured Frequency Response  $H_{21}^{31}$

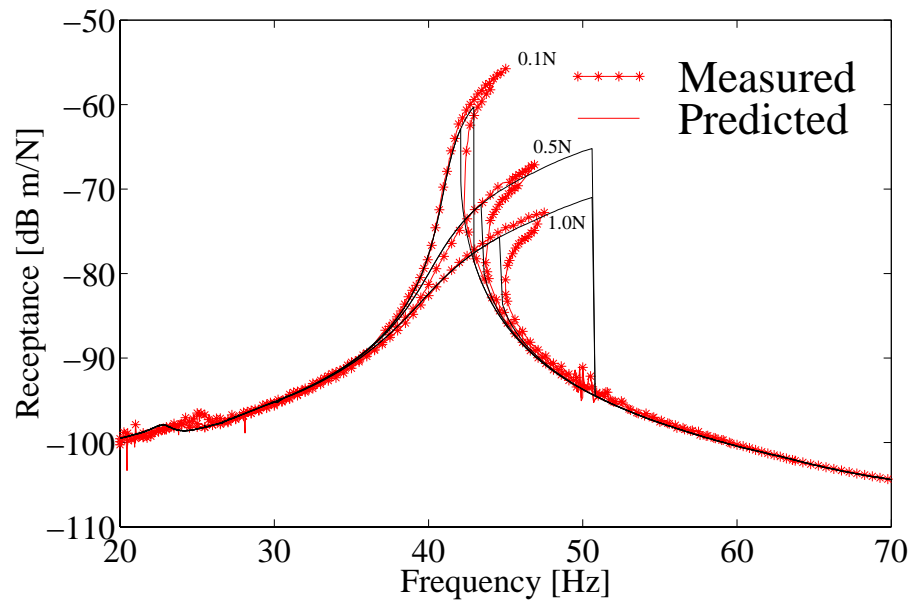
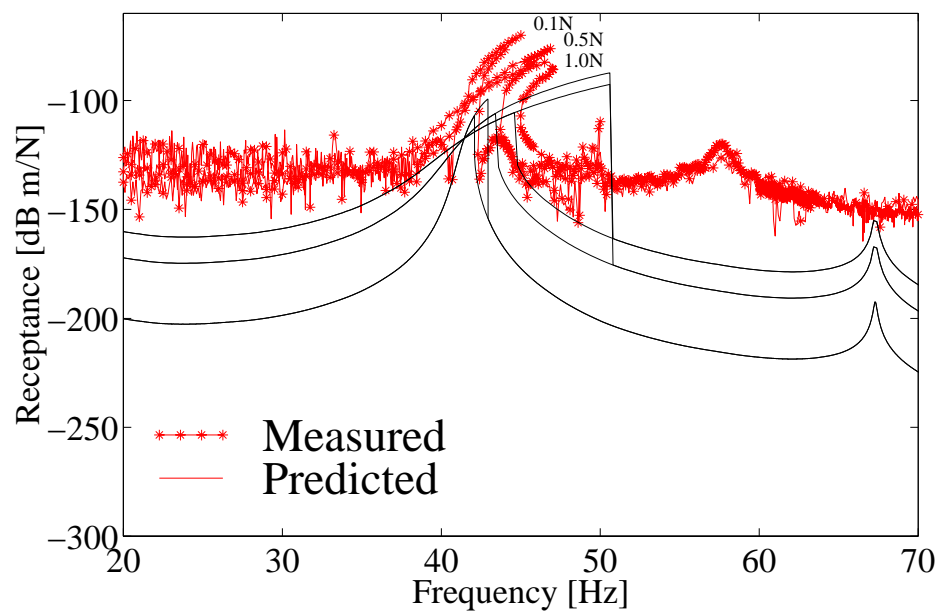
Figure 7.21: Measured Frequency Response  $H_{31}^{11}$ Figure 7.22: Measured Frequency Response  $H_{31}^{31}$

### 7.4.8 Measured and Predicted Coupling FRFs using First Assembly Model Test Rig I

Using the joint parameters obtained in section 7.4.5 in the first analytical model presented in section 7.4.6, the frequency response functions  $\{H_{11}^{11}\}^3$ ,  $\{H_{11}^{31}\}^3$  and  $\{H_{11}^{51}\}^3$  for forces of 0.1N, 0.5N and 1N were predicted by the *INCA++* software using the *MUHANORCA* method. Figure 7.23 shows the FRF  $\{H_{11}^{11}\}^3$  data measured from point 2 within a certain frequency range and the corresponding predicted FRF data. Figure 7.24 shows the FRF  $\{H_{11}^{31}\}^3$  measured from point 2 and the corresponding FRF predicted data. Figure 7.25 shows the FRF  $\{H_{21}^{11}\}^3$  measured from point 6 and the corresponding FRF predicted data. Figure 7.26 shows the FRF  $\{H_{21}^{31}\}^3$  measured from point 6 and the corresponding FRF predicted data. Figure 7.27 shows the FRF  $\{H_{31}^{11}\}^3$  measured from point 17 and the corresponding FRF predicted data. Figure 7.28 shows the FRF  $\{H_{31}^{31}\}^3$  measured from point 17 and the corresponding FRF predicted data.

Figure 7.23: Frequency Response  $\{H_{11}^{11}\}^3$ Figure 7.24: Frequency Response  $\{H_{11}^{31}\}^3$

Figure 7.25: Frequency Response  $\{H_{21}^{11}\}^3$ Figure 7.26: Frequency Response  $\{H_{21}^{31}\}^3$

Figure 7.27: Frequency Response  $\{H_{31}^{11}\}^3$ Figure 7.28: Frequency Response  $\{H_{31}^{31}\}^3$

### 7.4.9 Discussion of Results

The first analytical model presented in section 7.4.6 succeeded in predicting the dynamic behaviour of the first mode using only translational measurements. The predicted assembly first-order FRFs obtained agreed extremely well with those measured on the assembled structure—see Figures 7.23, 7.25 and 7.27. On the other hand, for the higher-order FRFs, the amplitudes of the measured FRFs were shifted from the predicted ones, and this suggested that a systematic error could have occurred in the measurements.

Good results cannot be expected when predicting the second mode using the first analytical model as shown by the predicted FRF  $\{H_{11}^{11}\}^3$  for a force level of  $0.1N$  in Figure 7.29. This can be explained by the fact that the rotational degree of freedom, not included in

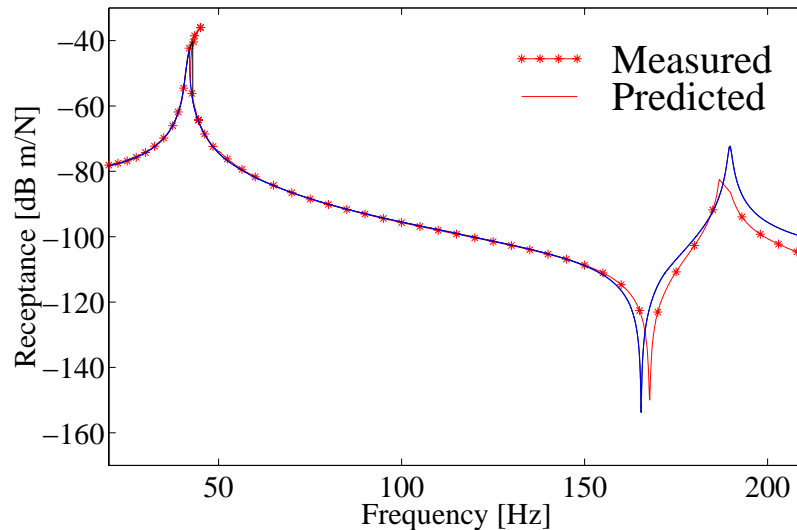


Figure 7.29: Frequency Response  $\{H_{11}^{11}\}^3$

this model, is important for the prediction of the second mode. In addition, it is possible to conclude from the measurements that the second mode is almost linear. From a comparison of the amplitudes of vibration of the first and second modes at node 2, the level of the receptance where the nonlinearity starts to exert an influence is around  $-70\text{dB}$  and the response of the second mode is lower than that value, as seen in Figure 7.23. Thus, the source of error is probably coming from the lack of the rotational degree of freedom not included in this model, and not from the nonlinear behaviour of the joint. To improve the prediction around the second mode, a better analytical model representing the linear behaviour of the nonlinear beams,  $B1$  and  $B2$ , must be used. It is going to be done in the next section.

For cubic stiffness nonlinearity, mathematics shows that there are three response solutions for some frequencies. The conventional idea is that two response solutions are stable and one that is unstable. The two stable solutions are usually obtained by measuring the response from frequency sweeps up and down. According to the conventional idea, the unstable one is impossible to measure. No other known recorded results show the measurements of the unstable solution. Therefore it was a surprise to be able to "measure" all three cases.

A reasonable explanation is as follows. The assembly structure can be considered as a sum of two substructures: the nonlinear structure itself and the shaker-push-rod system. Although the former has the unstable response, when put together, the assembly is stable. Therefore using the transducer force between both substructures and the accelerometer in the nonlinear substructure, it is possible to measure a stable response of the assembly which corresponds to the unstable response of the nonlinear substructure.

#### 7.4.10 Second Assembly Model Test Rig I

In order to improve the prediction of the coupled structure behaviour in the frequency range measured, a second analytical model was used to represent the nonlinear test rig and is shown in Figure 7.30.

This assembly model consists of two substructures coupled to each other at node 2. The first substructure composed of the beam *A* is modelled as a linear clamped-free beam, discretised as 21 2D Timoshenko beam elements. The second substructure, composed of the beams *B1* and *B2*, is modelled as two parallel linear clamped-clamped beams each one discretised with 20 2D Timoshenko beam elements. The nonlinear behaviour of the substructure is modelled as a concentrated nonlinear massless spring joint. The assembly structure was updated by changing only parameters from the second substructure, once the first substructure was already updated in section 7.4.3. This is equivalent to updating the linear behaviour of the nonlinear beams. The linear response of the assembled structure was measured assuming that for low amplitudes of vibration, without controlling the force, the FRF measured is the closest linear representation of the linear dynamic behaviour.

The beams were modelled with the updated values of elasticity modulus of  $2.3E11 \text{ N/m}^2$  and density of  $7800 \text{ kg/m}^3$ . The stiffnesses of the translational spring in the y direction and the rotational spring in relation to the x axis used to model the clamped condition in both ends of the beams were  $1E6 \text{ N/m}$  and  $500 \text{ Nm/rad}$ , respectively. In order to represent the

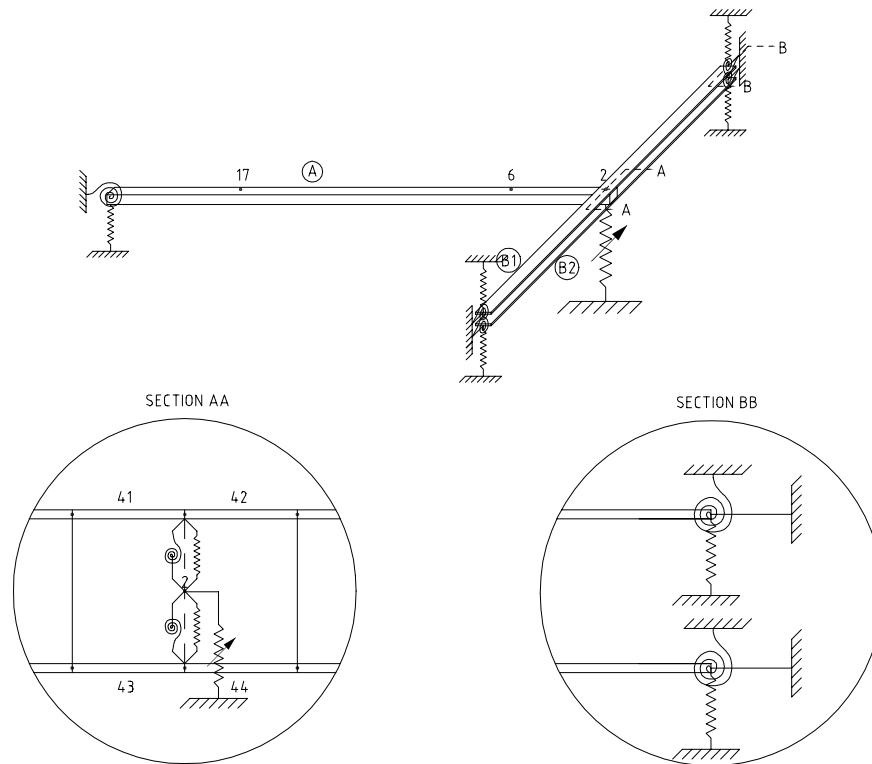
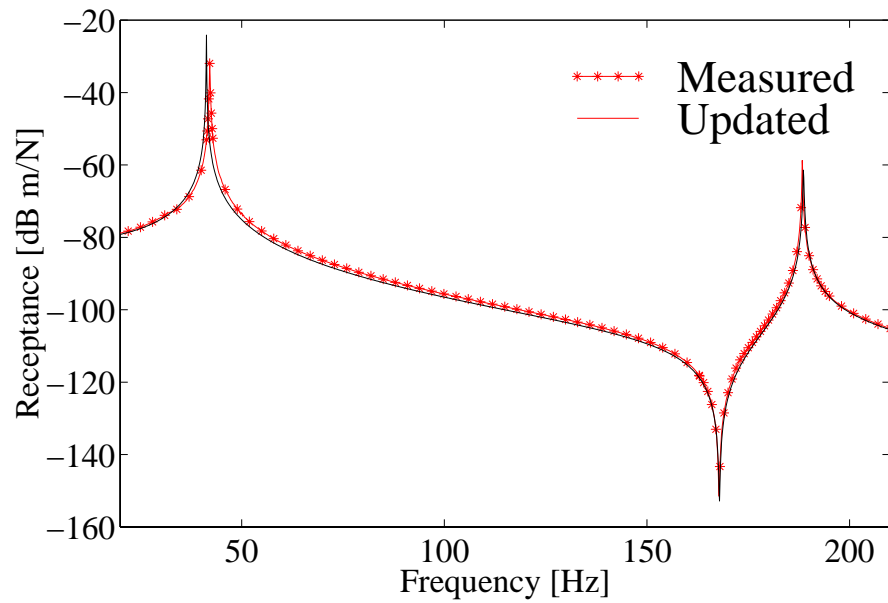
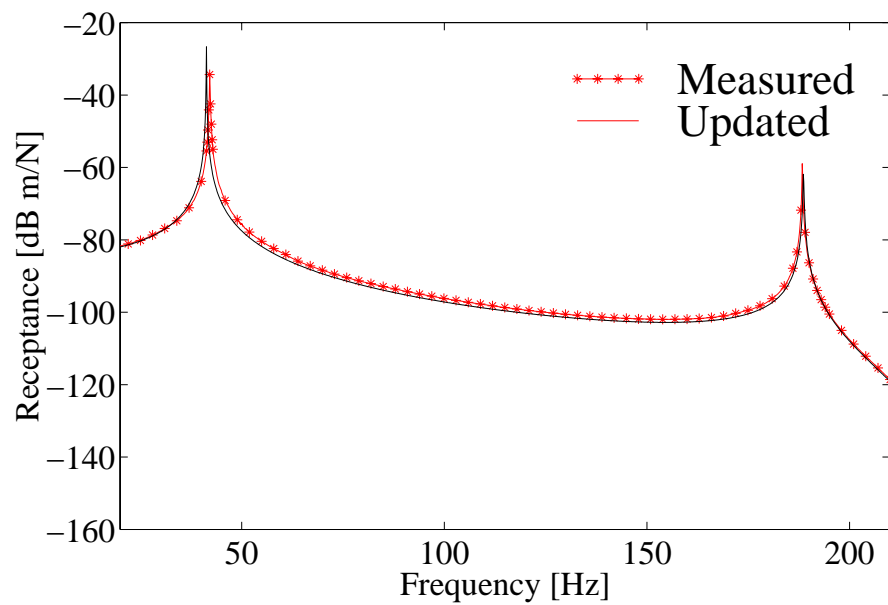
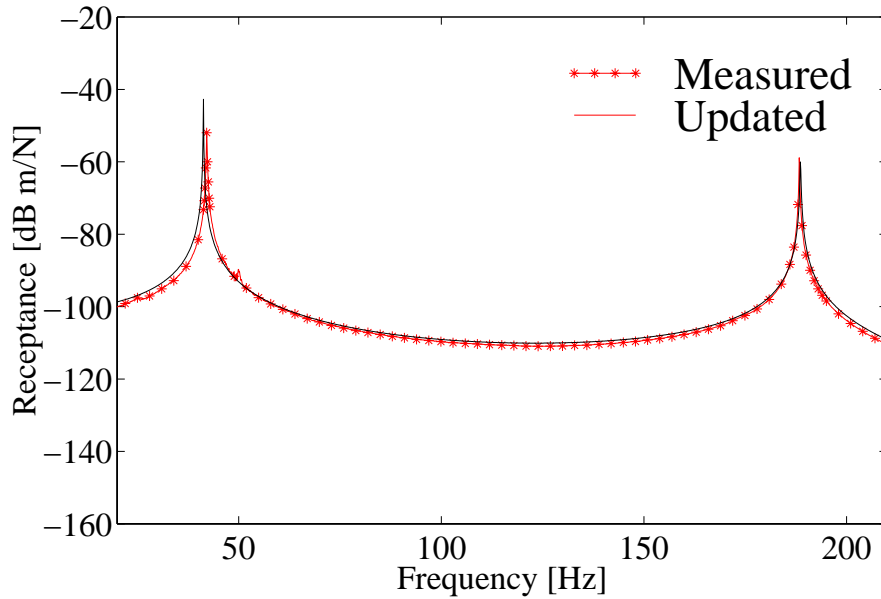


Figure 7.30: Second analytical model Test Rig I

boundary conditions imposed by clamping the nonlinear beams to both sides of the linear beam, the stiffnesses of the beam elements 45,46,47 and 48 were increased by increasing the section area. The updated value of the area is  $4.3E - 5 \text{ m}^2$ . The bolt that connects the linear beam with the nonlinear beam was modelled using translational and rotational springs. The updated value for the translational spring stiffness was  $2.2E6 \text{ N/m}$  and the rotational spring,  $9 \text{ Nm/rad}$ . The updating was repeated until the following two conditions were met. First, the anti-resonance and resonance of the second mode were in good agreement with the experimental FRF. Second, the reciprocal of an element of the flexibility matrix (which has been measured) must be  $6500 \text{ N/m}$  (7.4.5). This element is related to node 2 and its excitation and response in the y-direction. No attempt was made to update the model to match the the natural frequency of the first mode because of its strong nonlinearity.

The result of the updated linear assembly structure for nodes 2, 6 and 17 can be seen in figures (7.31,7.32,7.33).

Figure 7.31: Frequency Response  $\{H_{11}\}$ Figure 7.32: Frequency Response  $\{H_{21}\}$

Figure 7.33: Frequency Response  $\{H_{31}\}$ 

#### 7.4.11 Measured and Predicted Coupling FRFs using Second Assembly Model Test Rig I

After updating the linear model of the substructure 2, all the FRFs that were not measured for substructures 1 and 2 but were required to obtain the coupled system's response in nodes 2,6 and 17 were analytically calculated from the updated models. For example, at node 2, three FRFs from each substructure were required namely,  $H_{yy}$ ,  $H_{y\theta_z}$ , and  $H_{\theta_z\theta_z}$ .  $H_{yy}$  from the first substructure was measured while the other two were obtained from the updated model. For the second substructure all the required linear FRFs were obtained from the updated model. Once all the FRFs were obtained, the *INCA++* software using the *MUHANORCA* method was applied with the nonlinear joints parameters obtained in section 7.4.5.

The predicted frequency response functions  $\{H_{11}^{11}\}^5$ ,  $\{H_{11}^{31}\}^5$  and  $\{H_{11}^{51}\}^5$  for a force of 0.1N, 0.5N and 1N were calculated. Figure 7.34 shows the FRF  $\{H_{11}^{11}\}^3$  measured from point 2 and the corresponding predicted FRF data. Figure 7.36 shows the FRF  $\{H_{11}^{31}\}^3$  measured from point 2 and the corresponding predicted FRF data. Figure 7.38 shows the FRF  $\{H_{21}^{11}\}^3$  measured from point 6 and the corresponding predicted FRF data. Figure 7.35 shows the FRF  $\{H_{21}^{31}\}^3$  measured from point 6 and the corresponding predicted FRF data. Figure 7.37 shows the FRF  $\{H_{31}^{11}\}^3$  measured from point 17 and the corresponding

predicted FRF data. Figure 7.39 shows the FRF  $\{H_{31}^{31}\}^3$  measured from point 17 and the corresponding predicted FRF data.

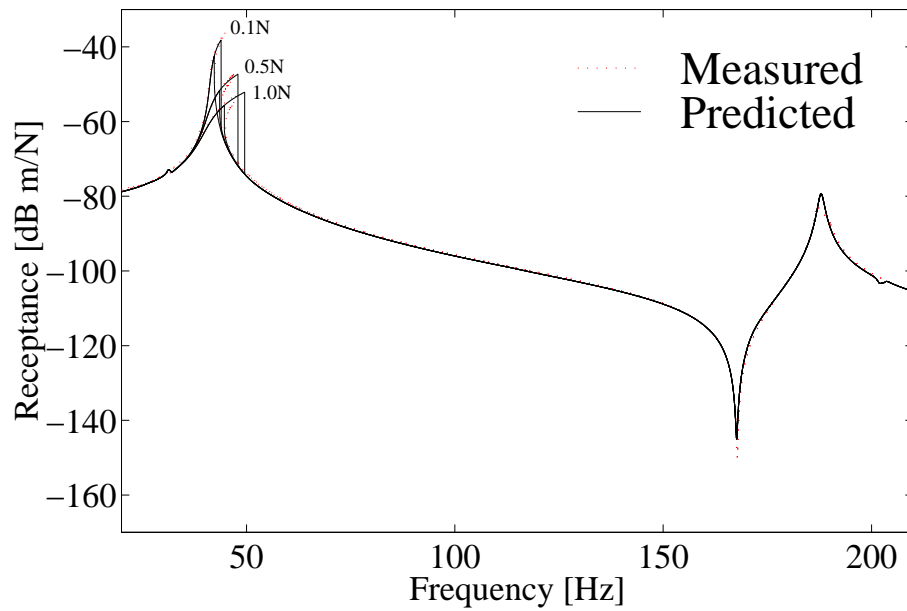


Figure 7.34: Frequency Response  $\{H_{11}^{11}\}^3$

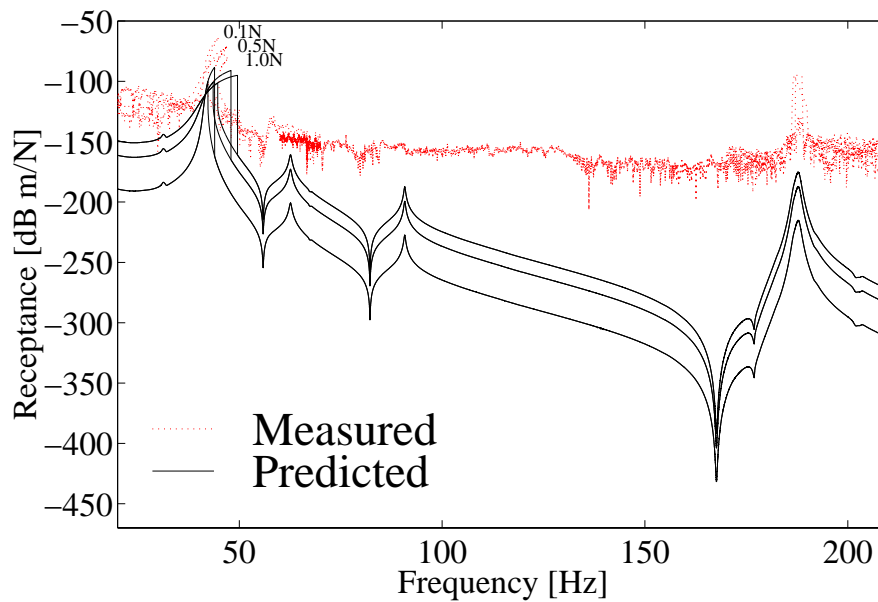
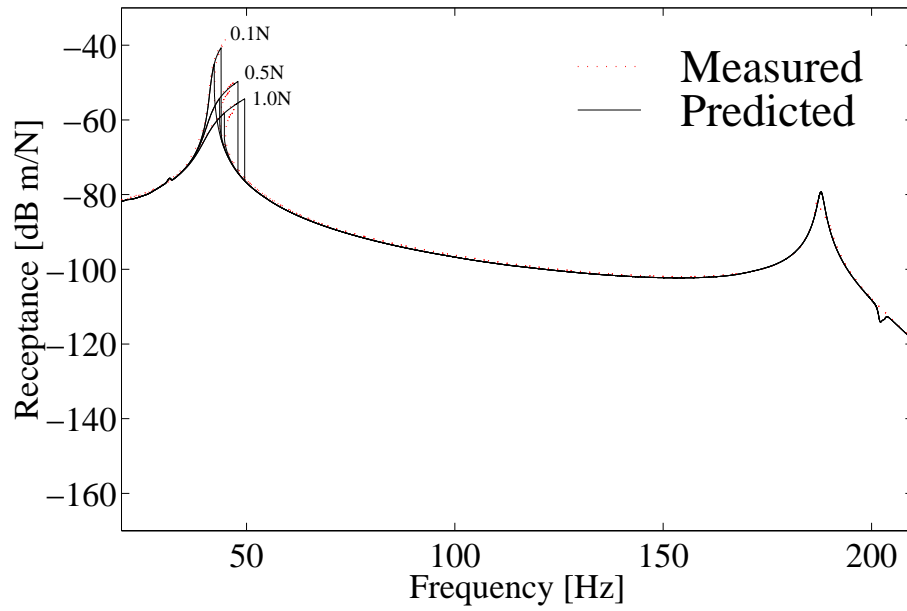
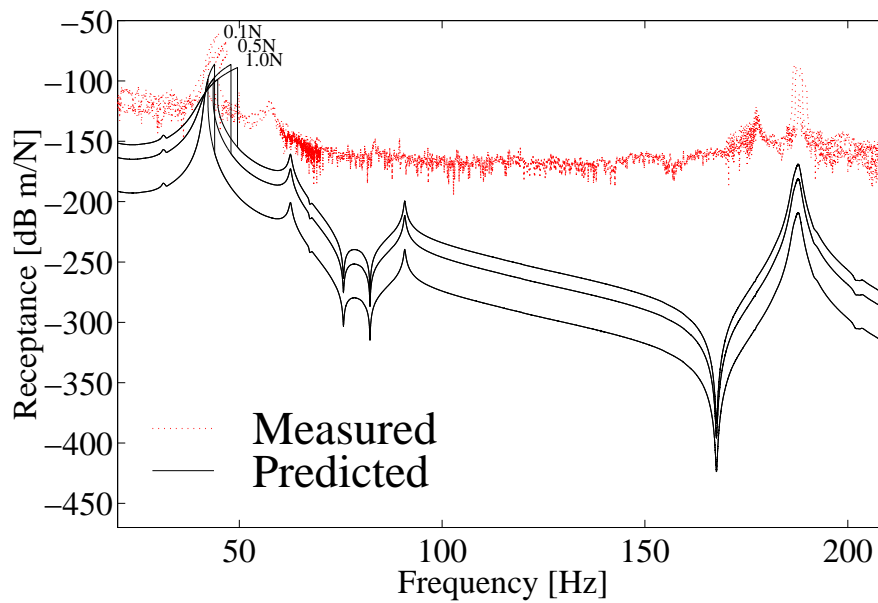
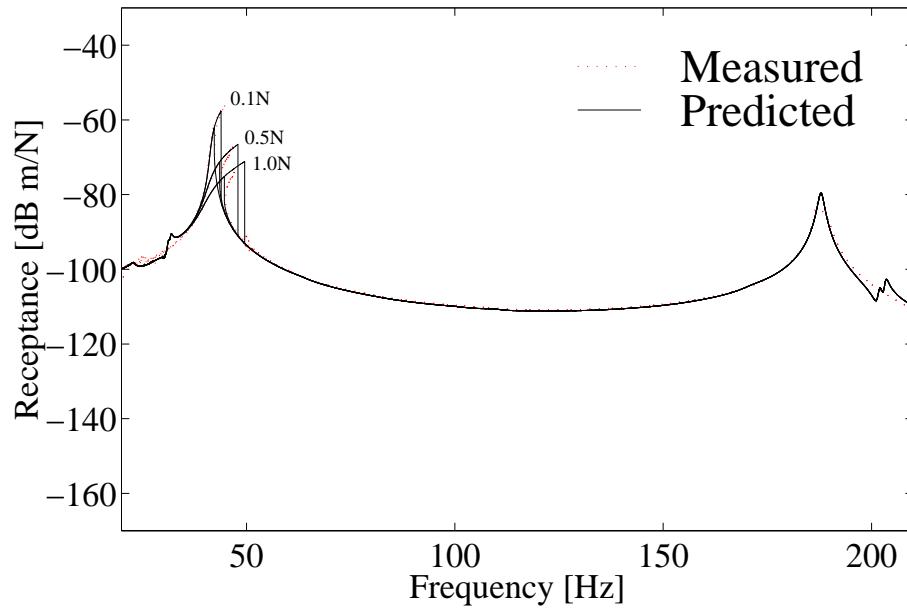
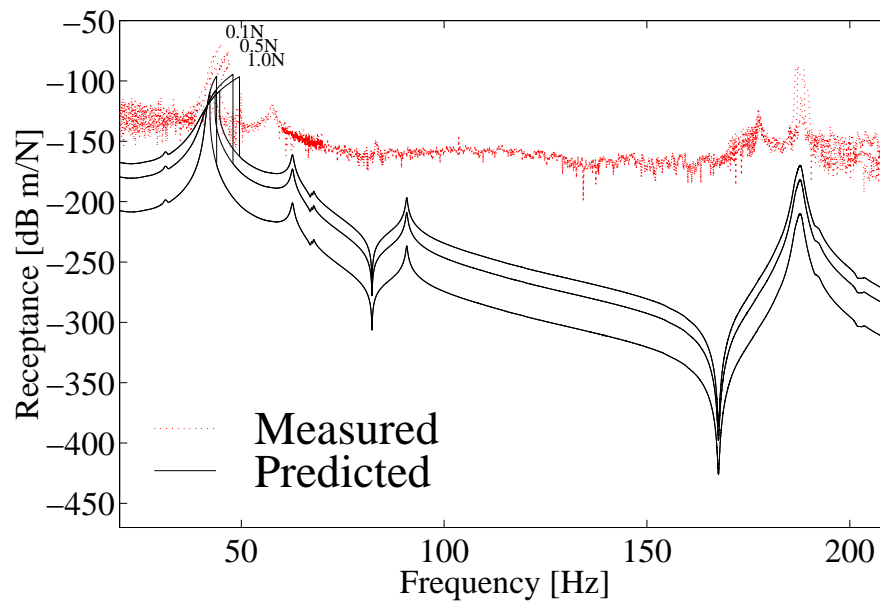


Figure 7.35: Frequency Response  $\{H_{11}^{31}\}^3$

Figure 7.36: Frequency Response  $\{H_{21}^{11}\}^3$ Figure 7.37: Frequency Response  $\{H_{21}^{31}\}^3$

Figure 7.38: Frequency Response  $\{H_{31}^{11}\}^3$ Figure 7.39: Frequency Response  $\{H_{31}^{31}\}^3$

### **7.4.12 Discussion of Results**

This model was able to represent the dynamic behaviour of the coupled structure in the frequency range measured. The predicted nonlinear behaviour was calculated by using the measured FRFs and the analytical FRFs obtained from the updated models. The analytical FRFs were used in substitution of the FRFs that were not measured but were required in the coupling procedure. Various updated models were obtained for the cantilever beam but the result predictions were not good because although it has a good representation of the dynamic behaviour for the frequency range measured, the natural frequencies were close but not close enough. Small shifts in the resonance and anti-resonance imply in errors in the prediction. The predicted assembly first-order FRFs obtained for the frequency range including the first and second mode agree well with those measured in the assembled structure. These good results were obtained since the model updated for the cantilever beam was able to have resonance and anti-resonance very close to the measured physical model. On the other hand, for the higher-order FRFs the result did not improve and is still shifted. As discussed before, it is possible that a systematic error occurred in the measurements. From the predicted higher order FRFs is possible to observe that the level of the harmonic response is very small which implies that for the cubic stiffness nonlinearity the influence of these higher harmonics is very small.

## 7.5 Experimental Test Rig II

### 7.5.1 Test Rig II

The Test Rig II is based on the RK4 Rotor Kit from BENTLY NEVADA which consists of a mechanical base with a motor controlled by a direct-current motor speed. The shaft of the motor is coupled to a long shaft supported at both ends by journal bearings. Each bearing is attached to a bearing block. There is a possibility of two balance wheels and up to six proximity probes controlled by a proximator assembly. The RK4 test rig can be seen in Figure 7.40.

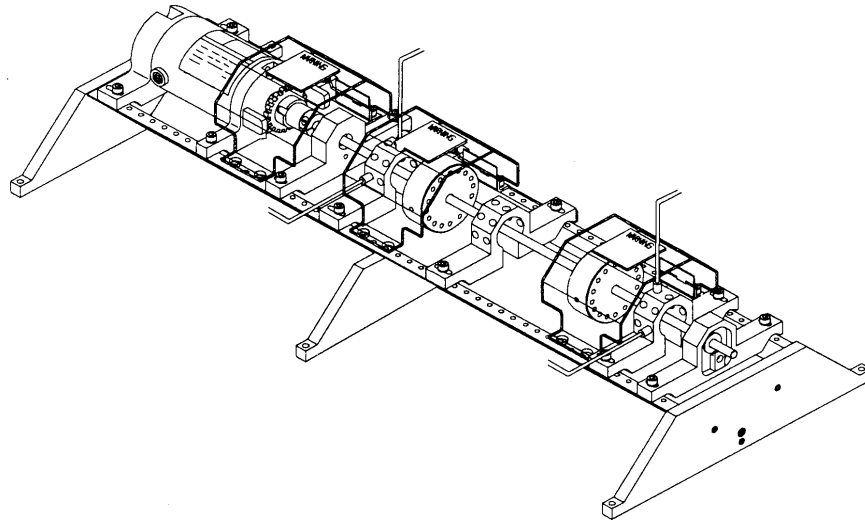
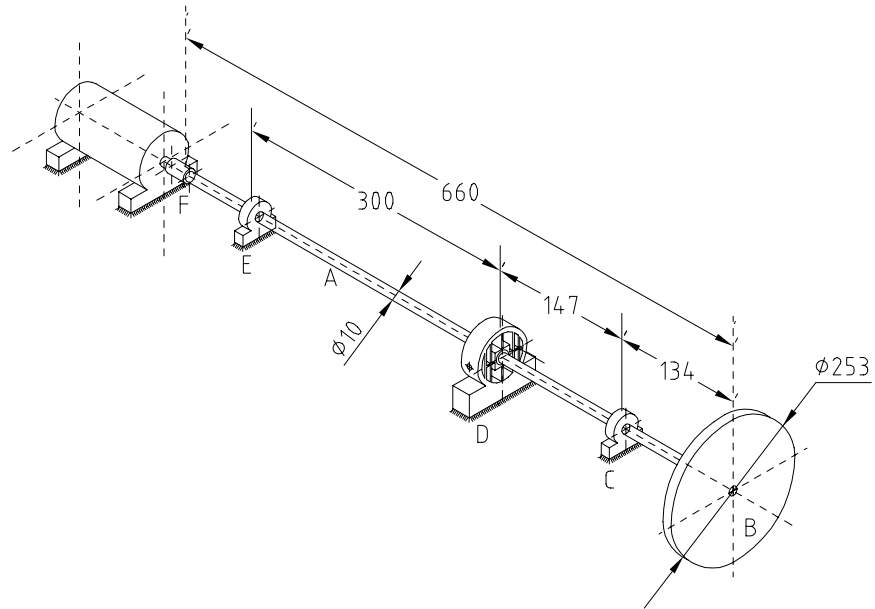


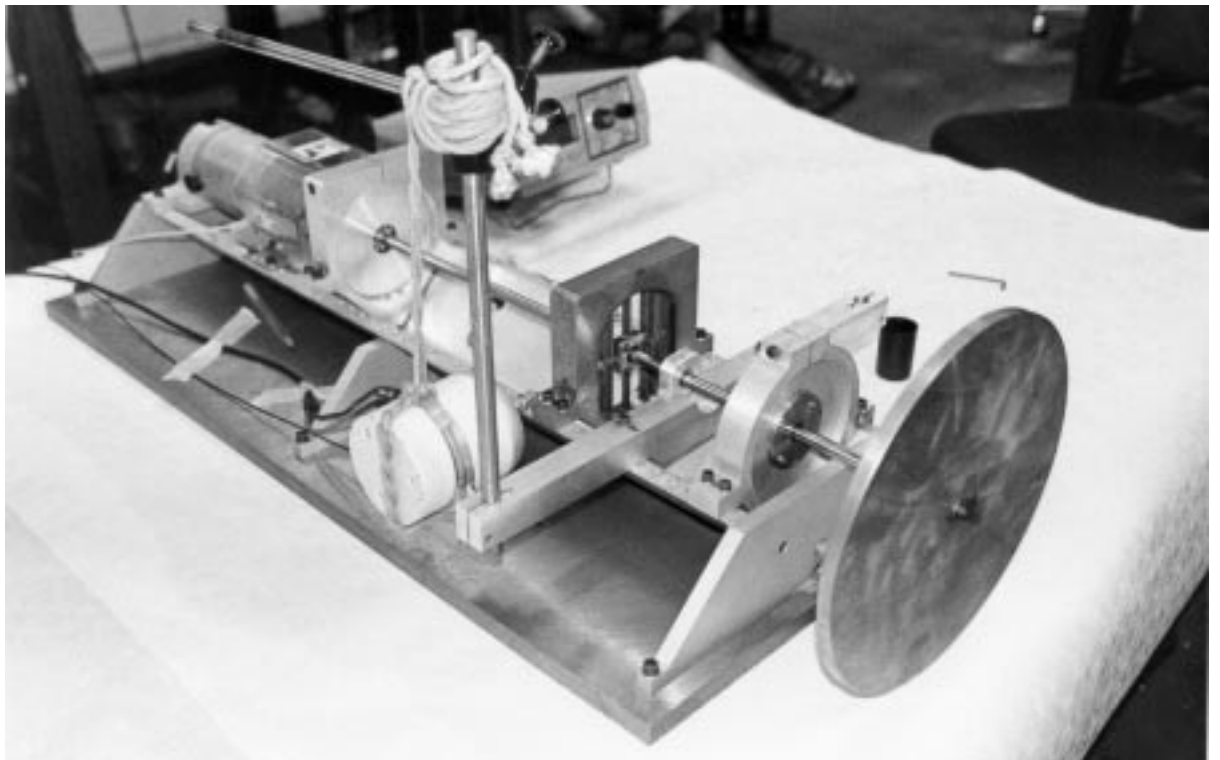
Figure 7.40: RK4 Rotor Kit

### 7.5.2 Modified Test Rig II

The Modified Test Rig II was made of a continuous system having a local nonlinear polynomial stiffness, as shown by component *D* in Figure 7.41. It consists of a uniform shaft, *A*, of 660 mm length with a circular cross section of 10mm. This shaft *A* is supported by bearings at three locations. Each bearing has a special bearing housing, *C*, *D* and *E*. Bearing housings *C* and *E* are rigid and the *D* is nonlinear. The design and photograph of the rigid bearing block *C* and *E* can be seen in Figure 7.42 and Figure 7.43 respectively.



(a) Diagram



(b) Photograph

Figure 7.41: System configuration

The design and photograph of the nonlinear bearing housing  $D$  can be seen in Figure 7.44 and 7.45 respectively. Shaft  $A$  has a disk  $B$  of a diameter of 150mm and a thickness of 10mm attached at one end and a motor coupled by a special joint  $F$  at the other end. The rotor, the first bearing, the second bearing and the third bearing are placed at 4mm, 134mm, 281mm and 581mm respectively from the end of the shaft that has the disk. The stiffness of the shaft,  $A$ , is linear and the local nonlinear polynomial stiffness is produced by the special bearing housing,  $D$ .

### 7.5.3 Linear Test Rig Assembly

The linear assembly rig is identical to the rig shown in Figure 7.41 except for the nonlinear bearing housing,  $D$ , which was removed. Four accelerometers and two force-measuring transducers were attached along the shaft. Two accelerometers were placed at the disk  $B$  at  $y$  and  $z$  directions respectively. The other two accelerometers and the two force transducer were placed at 281mm from the free end of the beam at  $y$  and  $z$  directions. The linear test rig setup is shown in Figure 7.46.

### 7.5.4 Measured and Updated FRF of Linear Test Rig II Assembly

Due to different stiffness conditions which apply to the analytical and experimental configurations, an updated analytical model, Figure 7.47, was used to represent the physical system. The shaft was modelled using Timoshenko beam elements with the updated values of elasticity modulus of  $2.1E11 \text{ N/m}^2$  and density of  $7800 \text{ kg/m}^3$ . The translational springs used to model the rigid bearing housing in  $x$  and  $y$  direction, in node 8 and 34, were  $7.5E6 \text{ N/m}$ . The rotational springs,  $\theta_y$  and  $\theta_z$ , used to model the influence of the shaker-push-rod system were  $6.5E2 \text{ N/m}$  and  $3.2E2 \text{ N/m}$  respectively. The updated mass and moment of inertia used to model the bearings in nodes 8 and 34 were  $10 \text{ g}$  and  $1E-6 \text{ Kgm}^2$  respectively. A special adapter,  $F$ , was designed to allow a continuous excitation of the system when the shaft is rotating. The updated masses,  $m_y$  and  $m_z$ , used to model the mass influence of the subsystem composed of adapter,  $F$ , push rod and shaker in node 14, were  $60 \text{ g}$  and  $80 \text{ g}$  respectively. The updated moments of inertia,  $I_{yy}$  and  $I_{zz}$ , used in node 14 were  $1E-6 \text{ Kgm}^2$ . The updated masses,  $m_y$  and  $m_z$ , in mode 31 used to model the mass influence of the coupling joint used between the motor and the shaft were  $20 \text{ g}$ . The updated

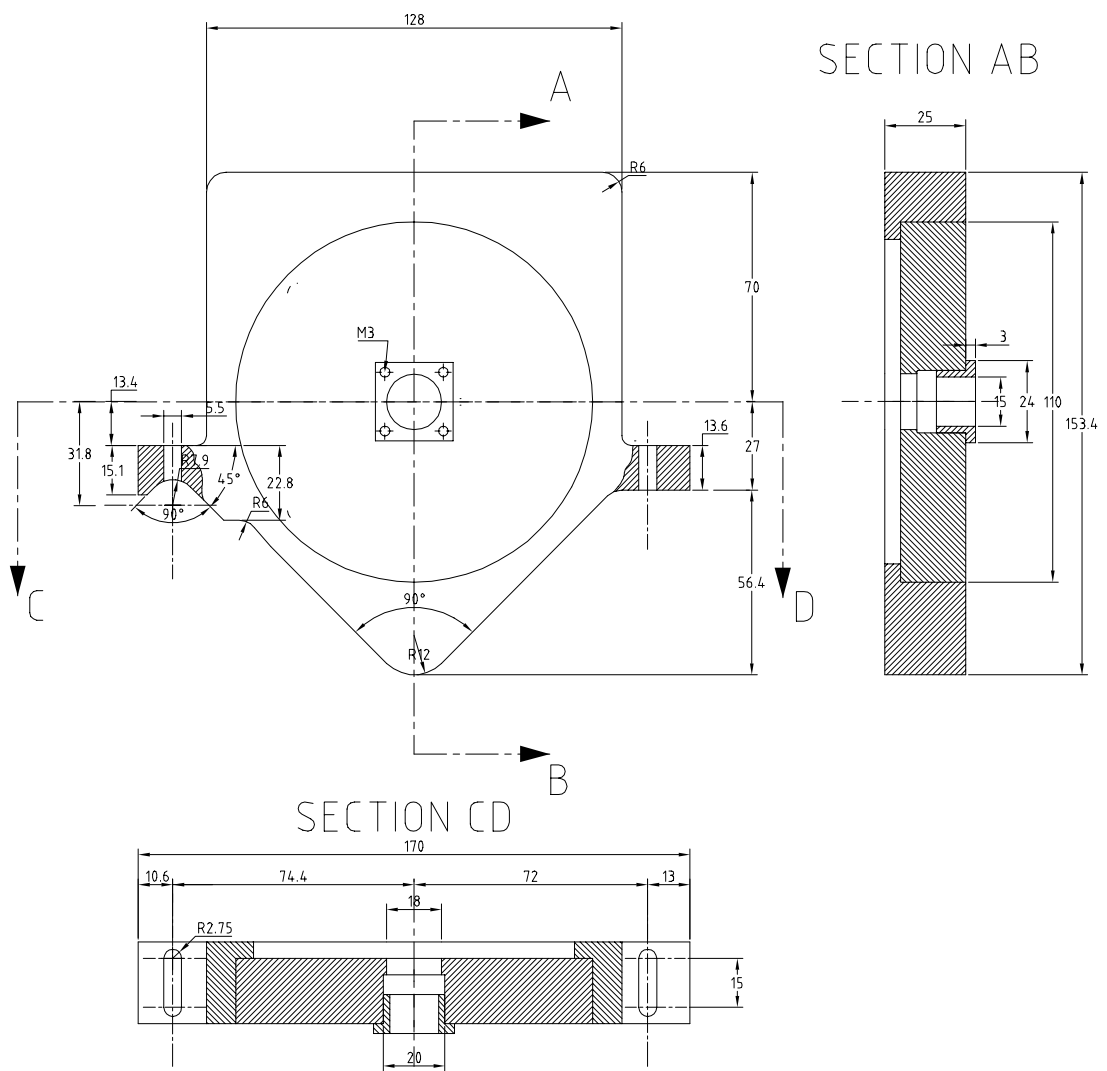


Figure 7.42: Rigid bearing housing design

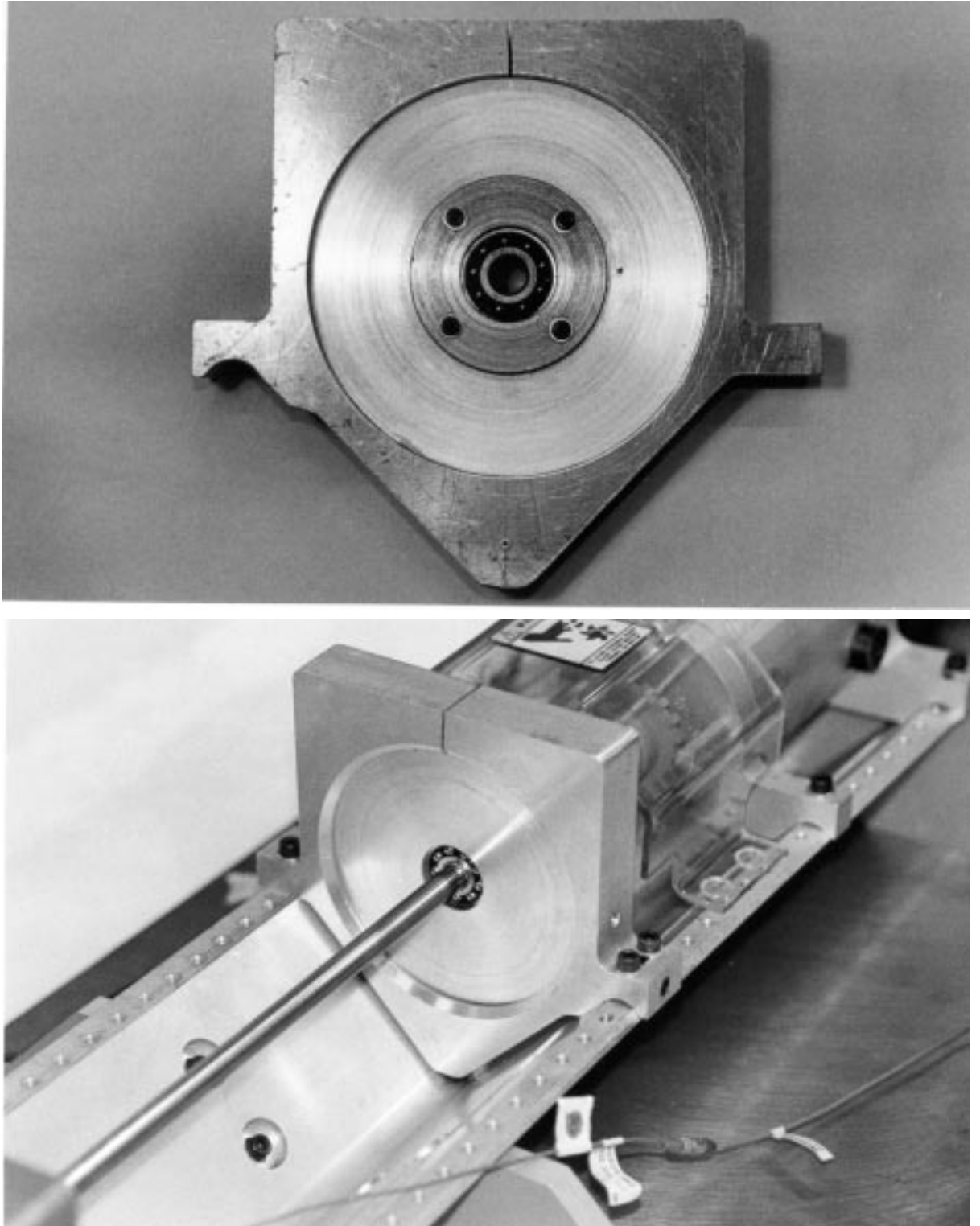


Figure 7.43: Rigid bearing housing photograph

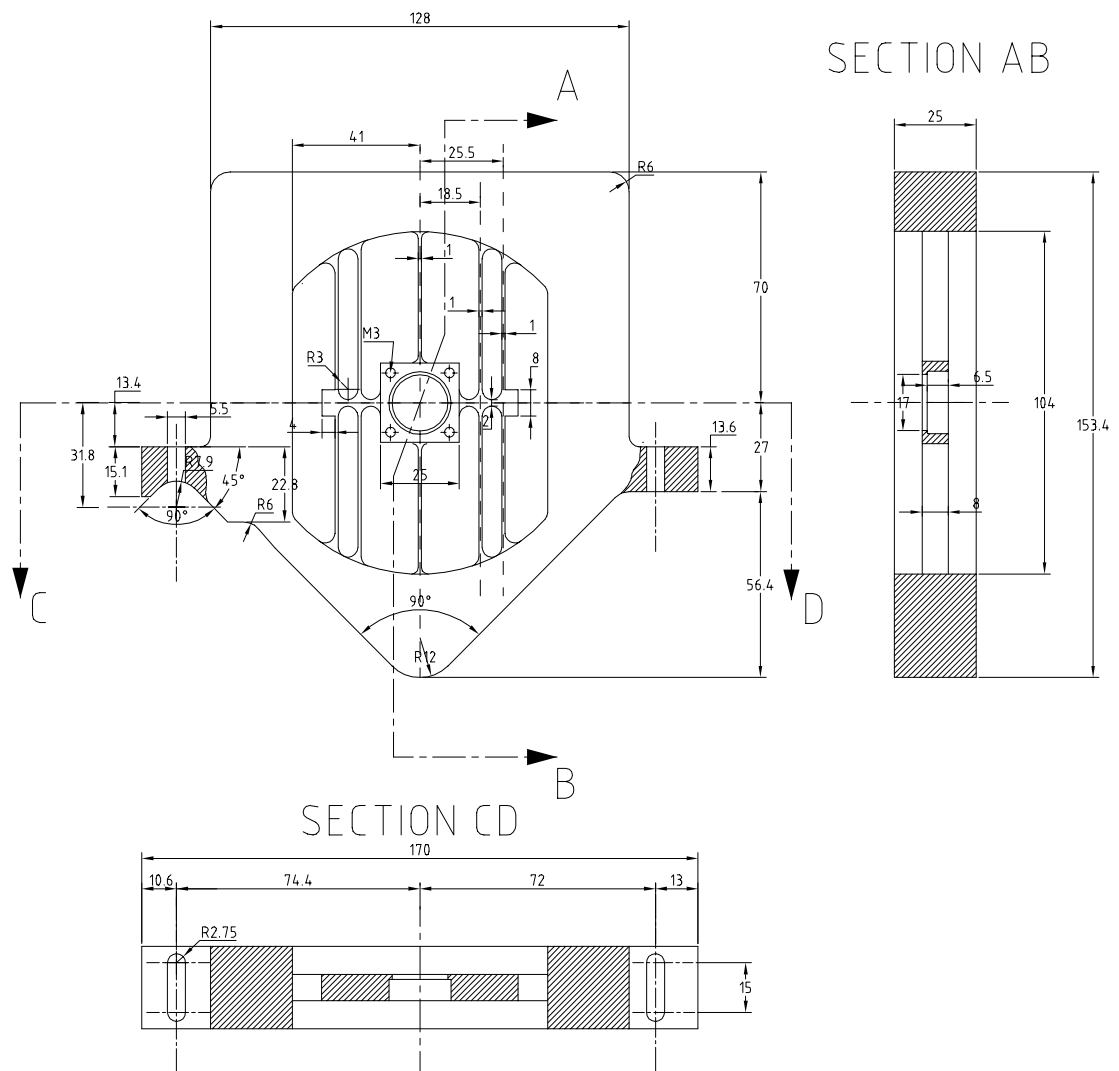


Figure 7.44: Nonlinear bearing housing design

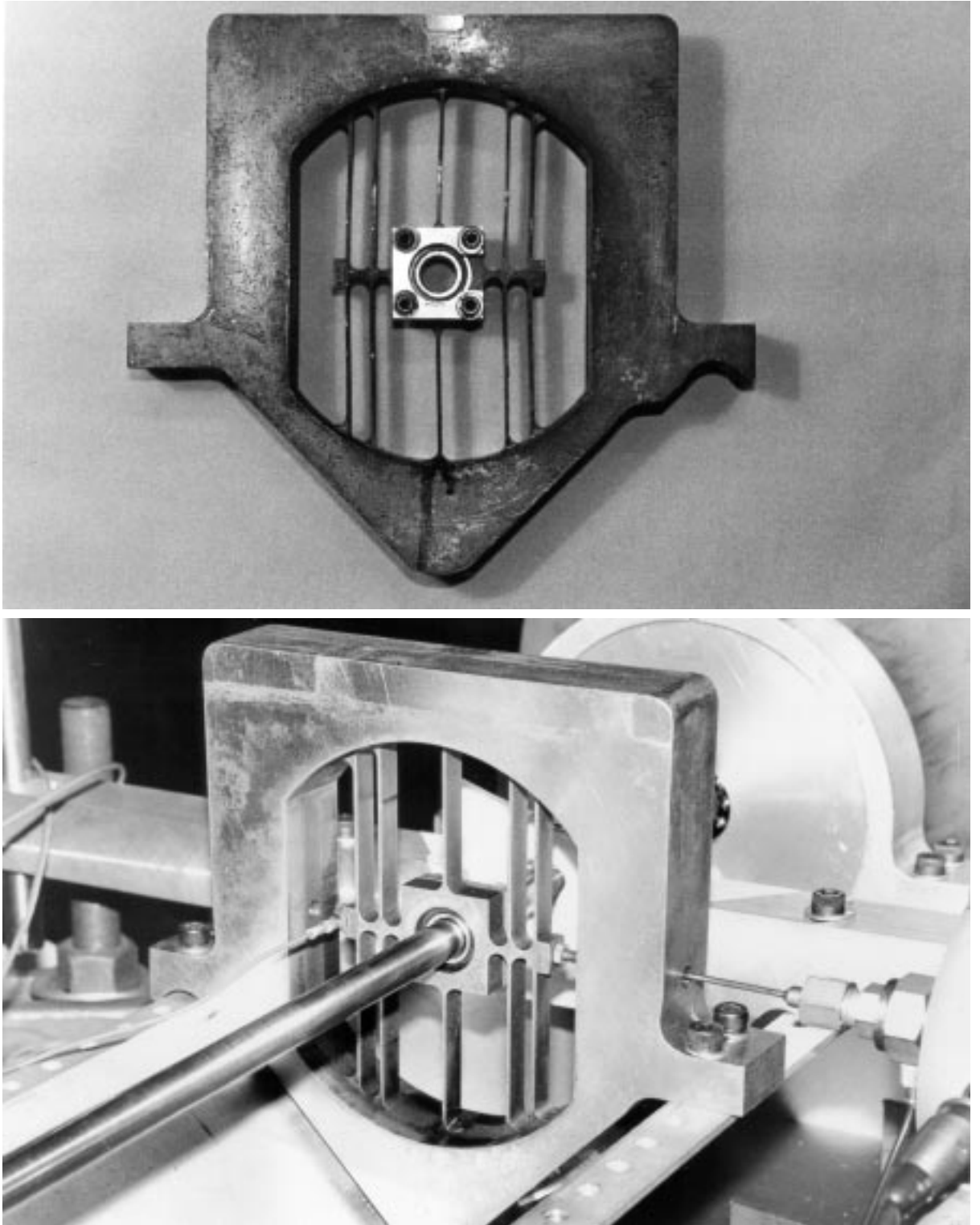
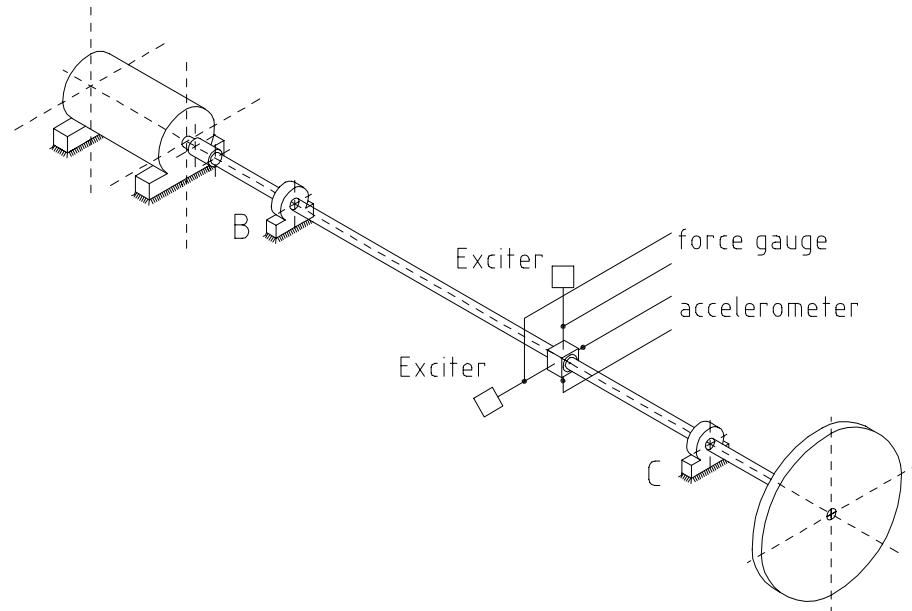
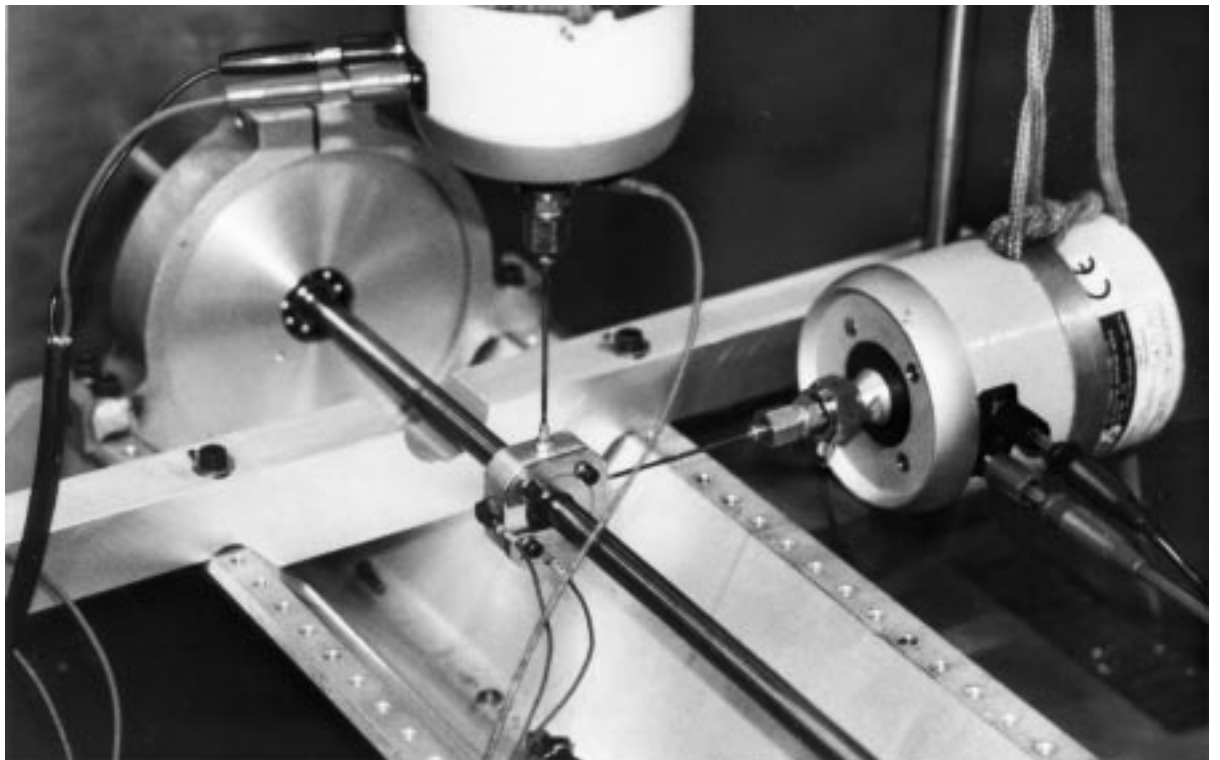


Figure 7.45: Nonlinear bearing housing photograph



(a) Diagram



(b) Photograph

Figure 7.46: Linear Test Rig II assembly

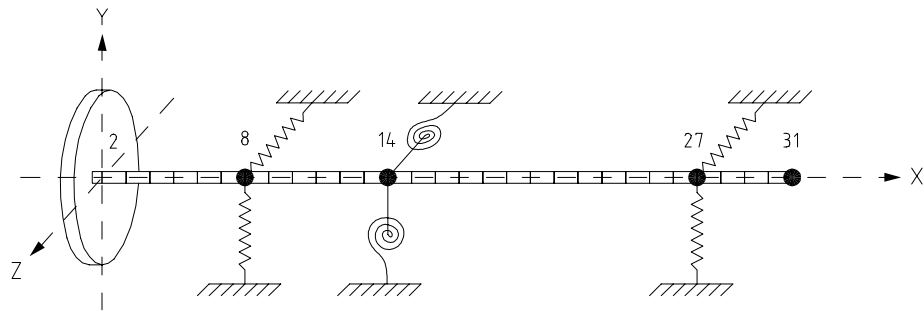
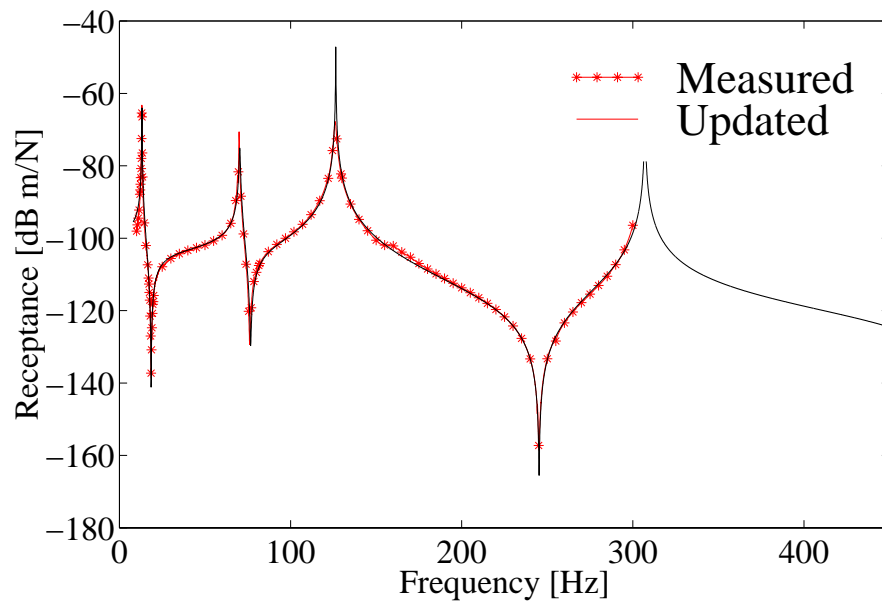
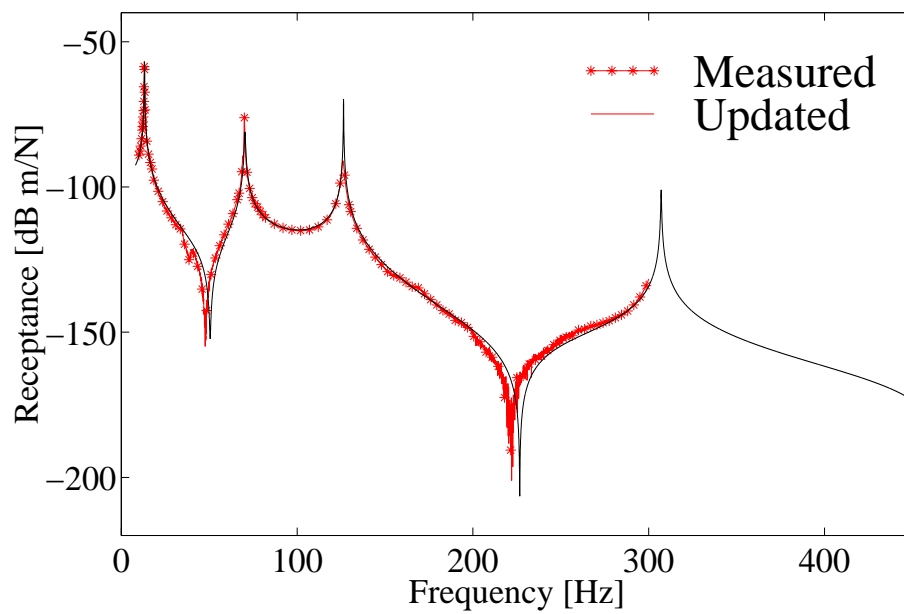
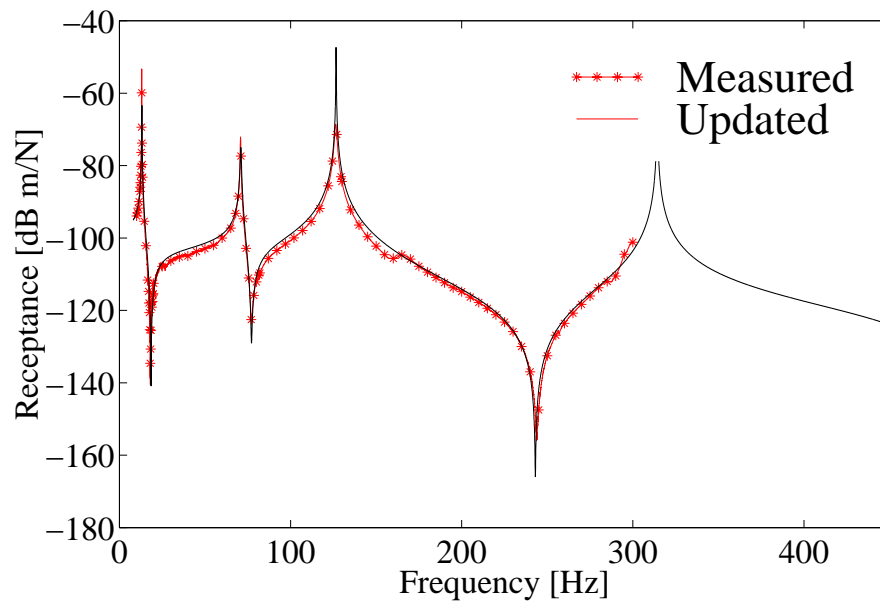
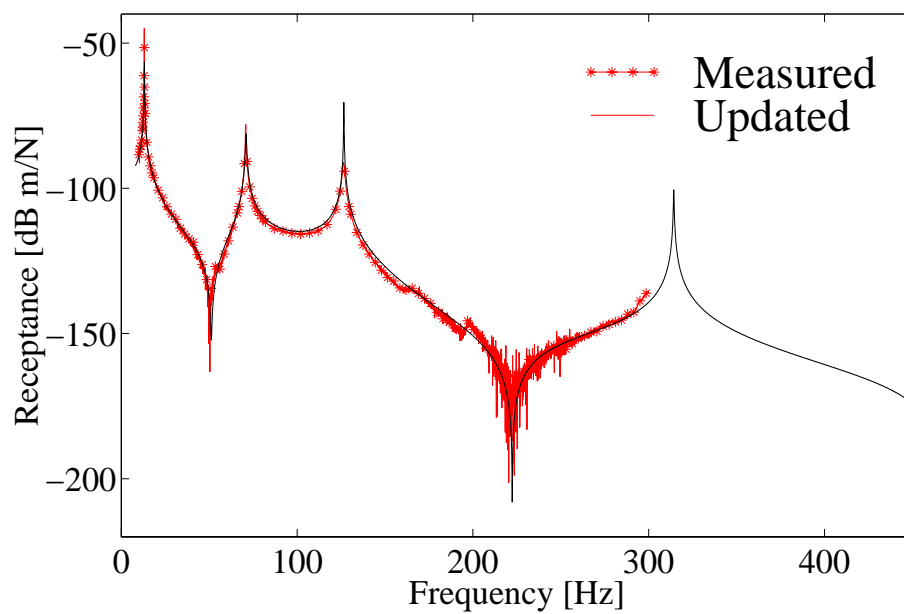


Figure 7.47: Analytical linear model Test Rig II

mass of the disk in node 2 was  $3.18 \text{ Kg}$ . The updated moments of inertia of the disk in node 2,  $I_{yy}$ ,  $I_{zz}$  and  $I_{xx}$ , were  $1.57E - 2 \text{ Kgm}^2$ ,  $1.52E - 2 \text{ Kgm}^2$  and  $3.1 \text{ Kgm}^2$  respectively.

Four FRFs,  $H_{11}$ ,  $H_{21}$ ,  $H_{33}$  and  $H_{43}$  were measured by *INCA++* software using the virtual frequency response analyser and are shown in Figures 7.48,7.49,7.50 and 7.51. The frequency range was from 8 Hz to 300 Hz. The excitation frequency was increased by steps of 0.01 Hz. For two FRFs,  $H_{11}$ ,  $H_{21}$ , the excitation was in  $z$  direction at node 14 and responses were measured in  $z$  direction at nodes 14 and 2 respectively. The other two FRFs,  $H_{33}$ ,  $H_{43}$ , the excitation was in  $y$  direction at node 14 and responses were measured in  $y$  direction at nodes 14 and 2 respectively.

Figure 7.48: Frequency Response Function  $H_{11}$ Figure 7.49: Frequency Response Function  $H_{21}$

Figure 7.50: Frequency Response Function  $H_{33}$ Figure 7.51: Frequency Response Function  $H_{43}$

### 7.5.5 Nonlinear Test Rig Assembly

This test rig was designed to have nonlinear behaviour in the  $z$  direction and linear behaviour in the  $y$  direction. This was achieved by using the specially designed nonlinear bearing housing previously shown in picture 7.45. The nonlinear test rig assembly is presented in Figure 7.52.

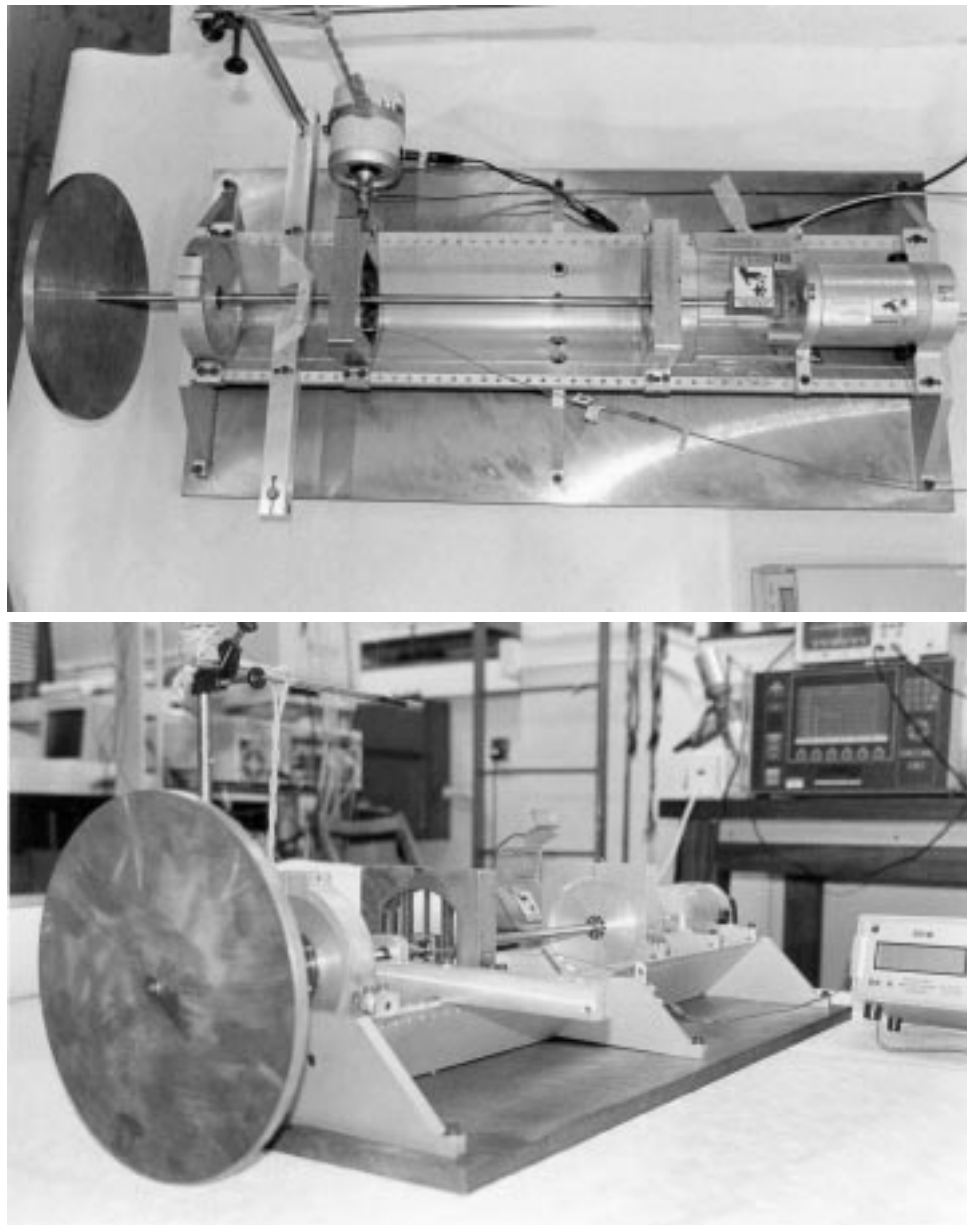


Figure 7.52: Test Rig II assembly

### 7.5.6 Analytical properties of the joints

The analytical properties of the nonlinear joints were obtained by first doing a static test. Although it was project to have a cubic stiffness nonlinearity and the precision of the process of the wire cutter utilised to obtain the desired nonlinearity, it turn out to be a polynomial nonlinearity as shown in the Figure 7.53. The reason was that the material utilised to machine the bearing housing had some pre-stress and a stress release should be done a priori. Instead of machining a new bearing housing with cubic stiffness nonlinearity, it was decided to use this one by implementing this new polynomial nonlinearity in the *INCA++* software. housing. After the static test was completed, a curve of the type  $k_1 * x + k_2 * x^2 + k_3 * x^3$  was fitted and the parameters  $k_1 = -5E4 \text{ N/m}$ ,  $k_2 = -3.8E5 \text{ N/m}$  and  $k_3 = 1.09E11 \text{ N/m}$  were obtained. The relationship between force and deformation for these cases is shown in Figure 7.53. The static test setup can be seen in figure 7.54.

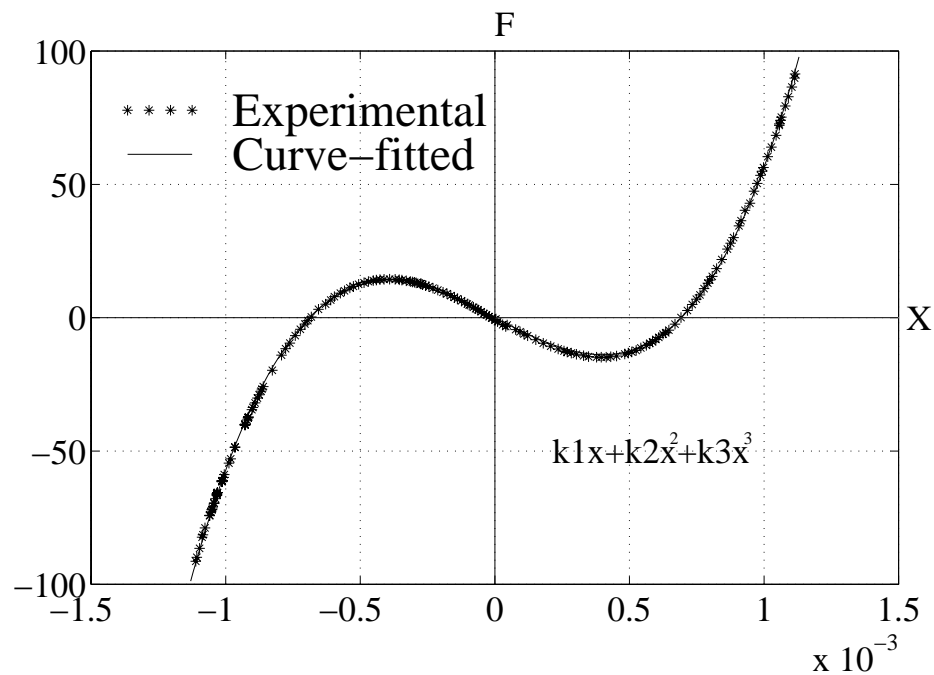


Figure 7.53: Relationship between loading and deformation

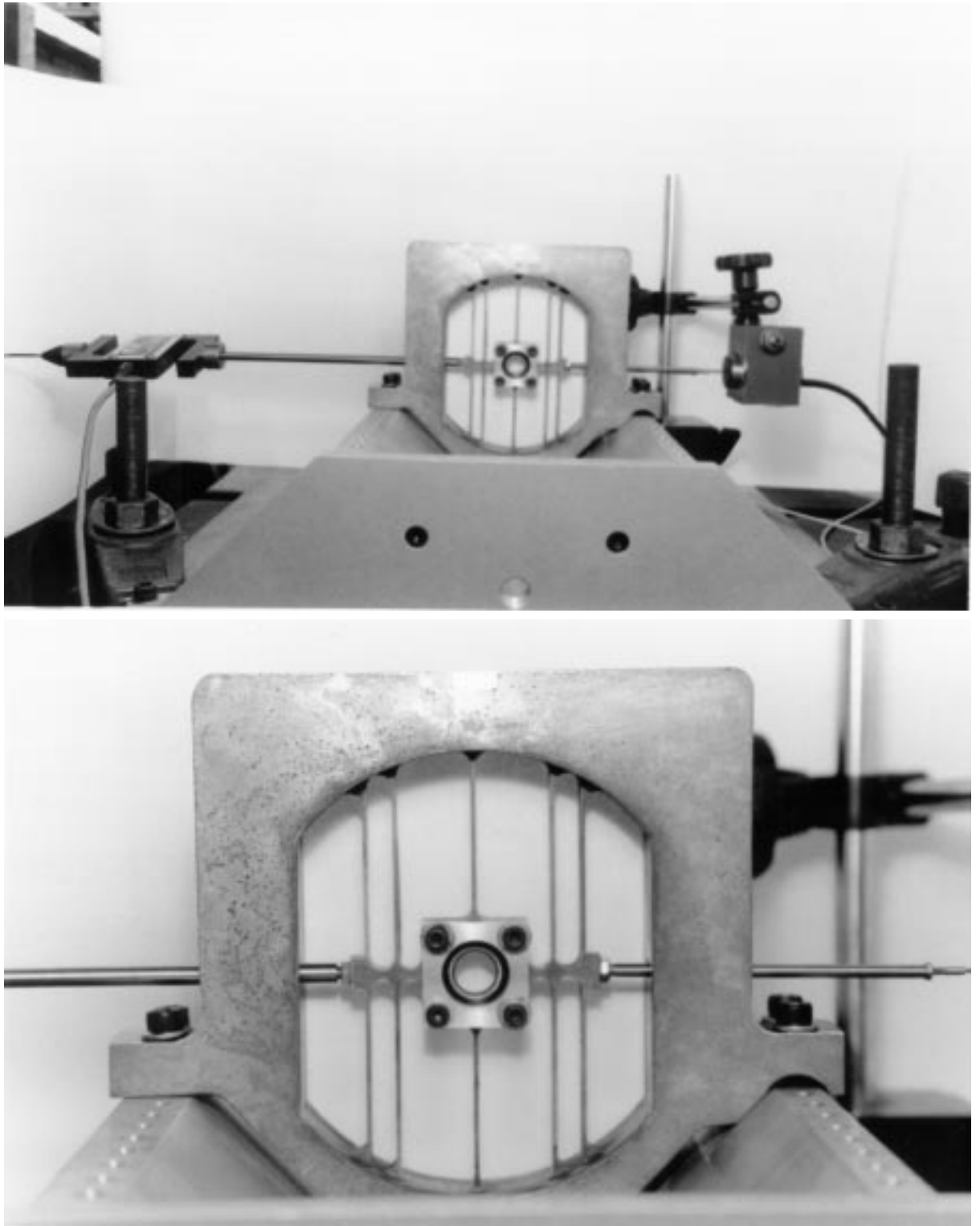


Figure 7.54: Static test setup

### 7.5.7 Assembly Model Test Rig II

The analytical model used to represent the nonlinear dynamic test rig is shown in Figure 7.55.

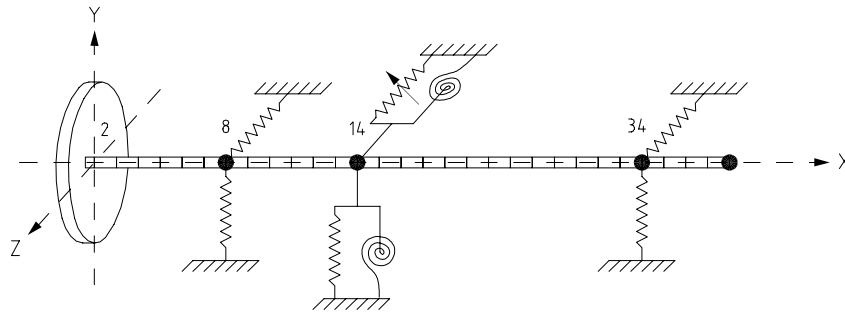
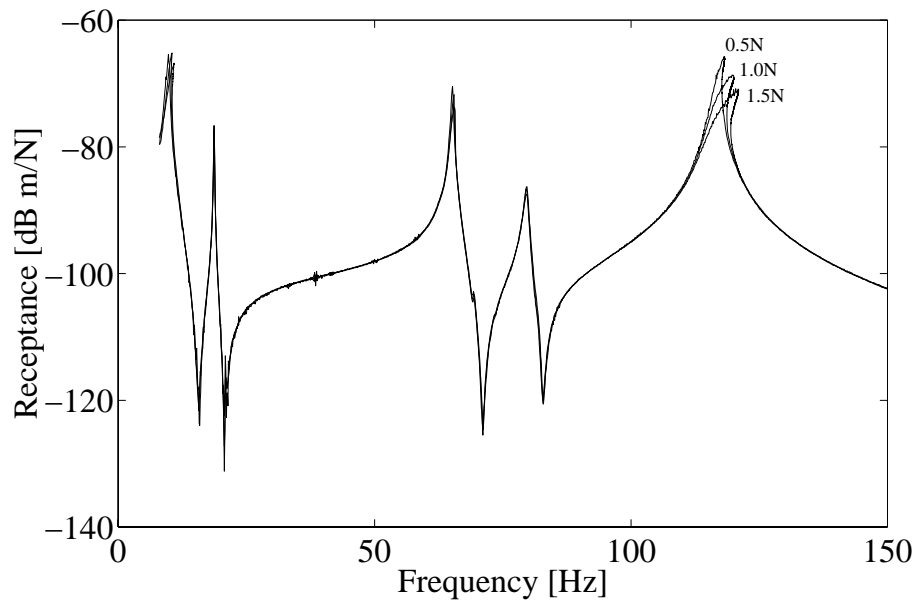
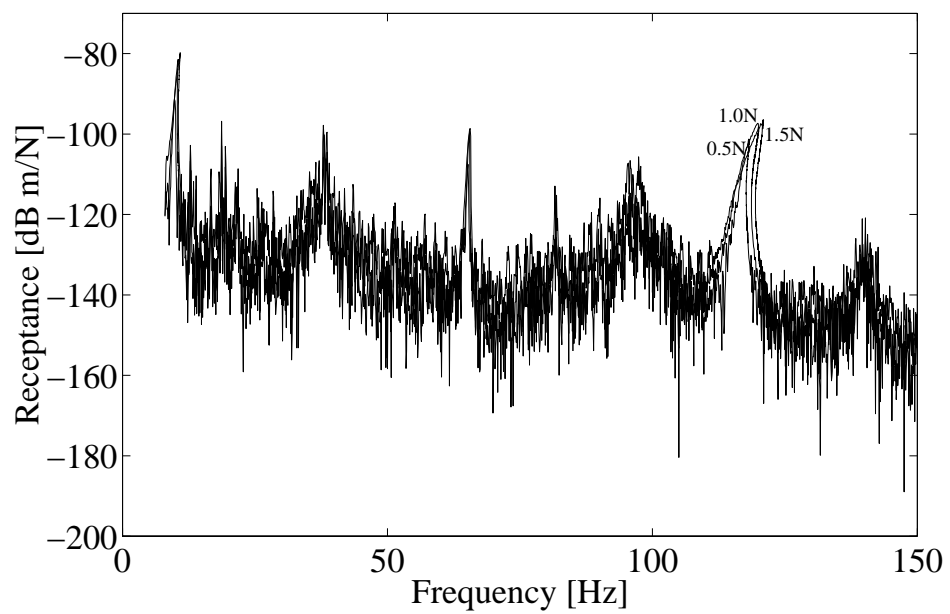


Figure 7.55: Analytical assembly model Test Rig II

This model was used to predict the nonlinear dynamic behaviour of system. The nonlinear bearing housing,  $C$ , shown in Figure 7.41 were modelled here as a concentrate nonlinear spring with mass.

### 7.5.8 Measured FRFs of Test Rig II

The frequency response functions  $H_{11}^{11}$  and  $H_{11}^{31}$  were measured by the *INCA++* software using the virtual frequency response analyser presented in section 7.3. The frequency range was from 8 Hz to 150 Hz. The excitation frequency was increased in steps of 0.1 Hz way from the resonance region and in steps of 0.01 Hz around the natural frequencies. The excitation force level was 0.5N, 1.0N and 1.5N . The rotation speed of the rotor was 500 *rpm*. Figure 7.56 shows the FRF  $H_{11}^{11}$  and figure 7.57 shows the FRF  $H_{11}^{31}$ .

Figure 7.56: Measured Frequency Response  $H_{11}^{11}$ Figure 7.57: Measured Frequency Response  $H_{11}^{31}$

### 7.5.9 Measured and Predicted Coupling FRFs using Assembly Model Test Rig II

After updating the linear behaviour of the Test Rig II using the analytical model presented in section 7.5.4, all the FRFs required to obtain the coupled system's response in nodes 14 were analytically calculated from the updated models and the nonlinear joints parameters required were obtained from section 7.5.6. Three new parameters have to be updated in order to predicted the FRFs of the assembled system. These are namely, the stiffness of the housing bearing in  $y$  direction with the final value of  $1E6 N/m$  and the rotation stiffness in  $\theta_y$  and  $\theta_x$  directions with the final value of  $600 Nm/rad$ .

The frequency response functions  $\{H_{11}^{11}\}^3$ , and  $\{H_{11}^{31}\}^3$  for a force of 0.5N, 1.0N and 1.5N were predicted by the *INCA++* software using the *MUHANORCA* method. Figure 7.58 shows the FRF  $\{H_{11}^{11}\}^3$  data measured from point 14 in  $z$  direction for a force level of 0.5N within a certain frequency range and the corresponding FRF predicted data. Figure 7.59 shows the FRF  $\{H_{11}^{31}\}^3$  measured from point 14 in  $z$  direction for a force level of 0.5N and the corresponding FRF predicted data. Figure 7.60 shows the FRF  $\{H_{11}^{11}\}^3$  data measured from point 14 in  $z$  direction for a force level of 1N within a certain frequency range and the corresponding FRF predicted data. Figure 7.61 shows the FRF  $\{H_{11}^{31}\}^3$  measured from point 14 in  $z$  direction for a force level of 1.0N and the corresponding FRF predicted data. Figure 7.62 shows the FRF  $\{H_{11}^{11}\}^3$  data measured from point 14 in  $z$  direction for a force level of 1.5N within a certain frequency range and the corresponding FRF predicted data. Figure 7.63 shows the FRF  $\{H_{11}^{31}\}^3$  measured from point 14 in  $z$  direction for a force level of 1.5N and the corresponding FRF predicted data.

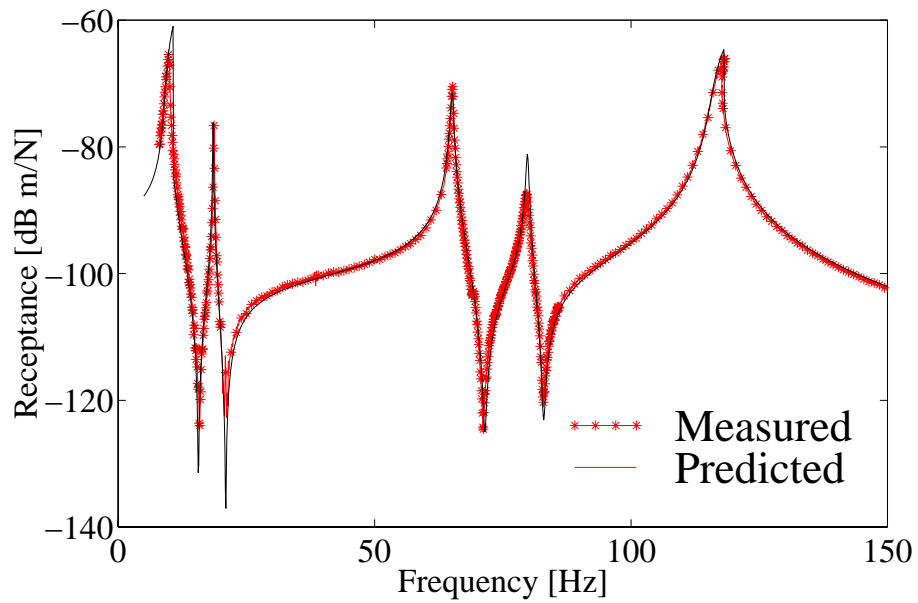


Figure 7.58: Frequency Response  $\{H_{11}^{11}\}^3$  for  $0.5N$

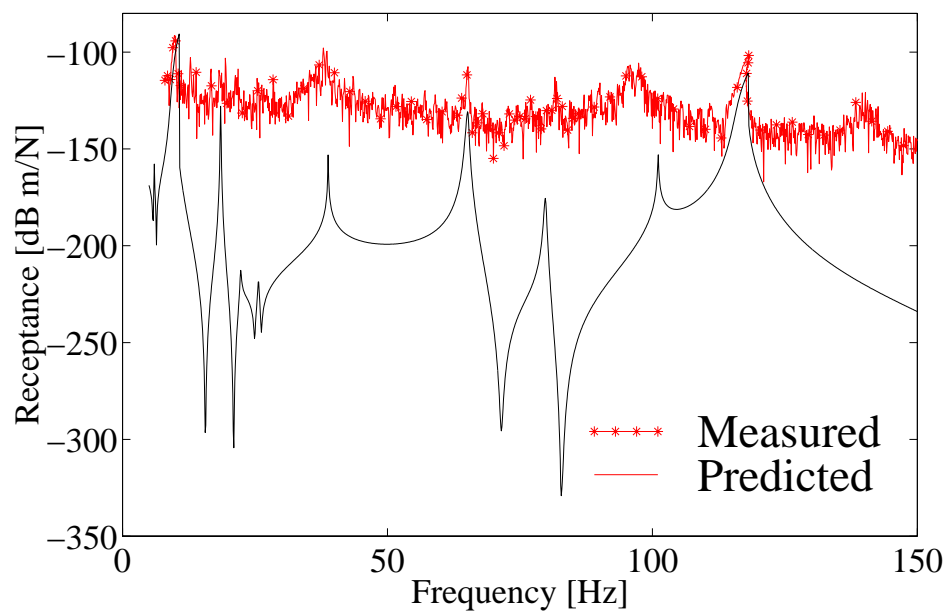
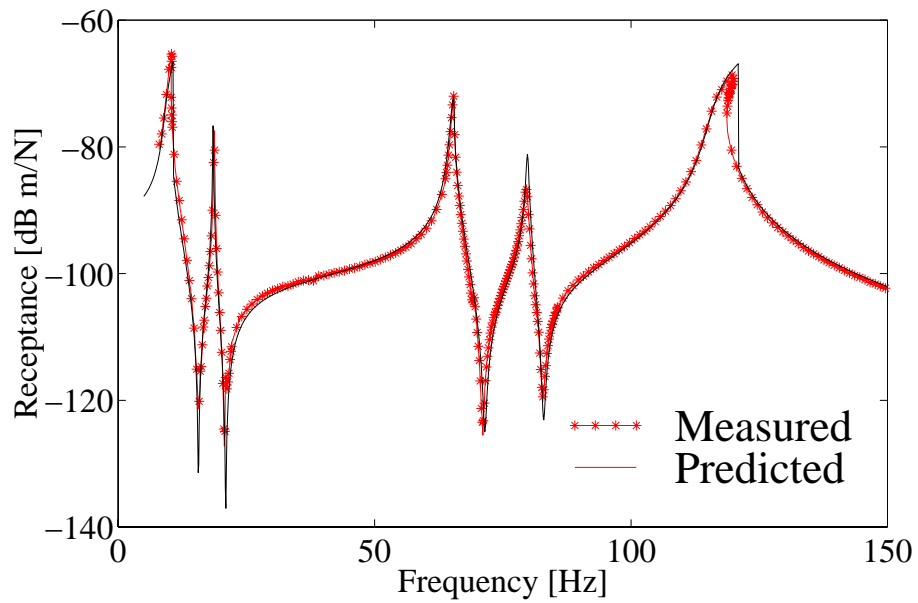
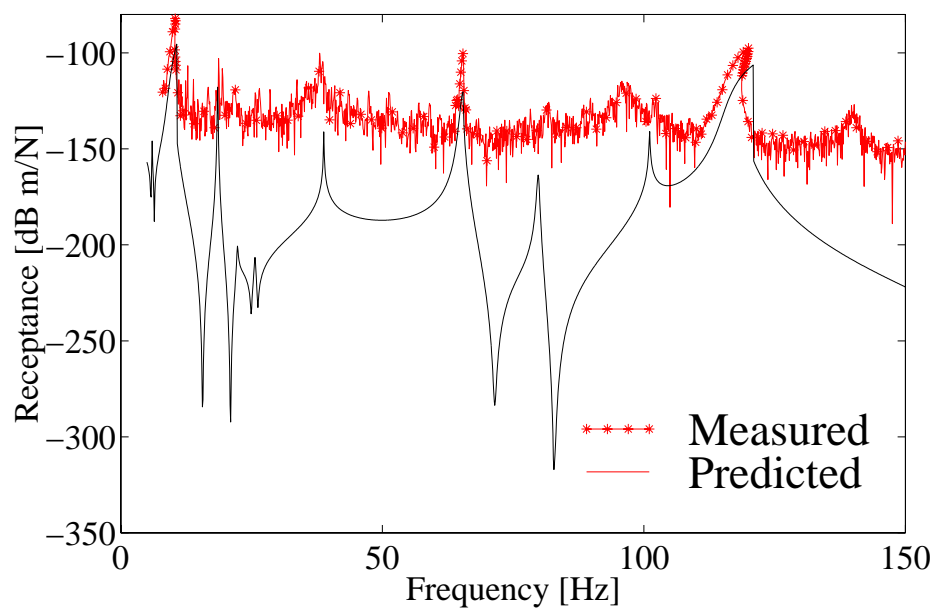
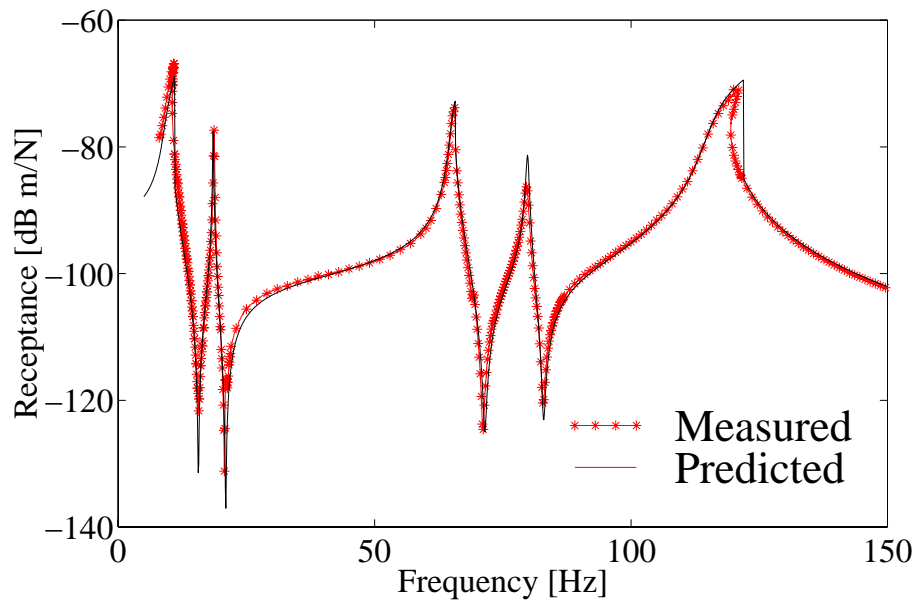
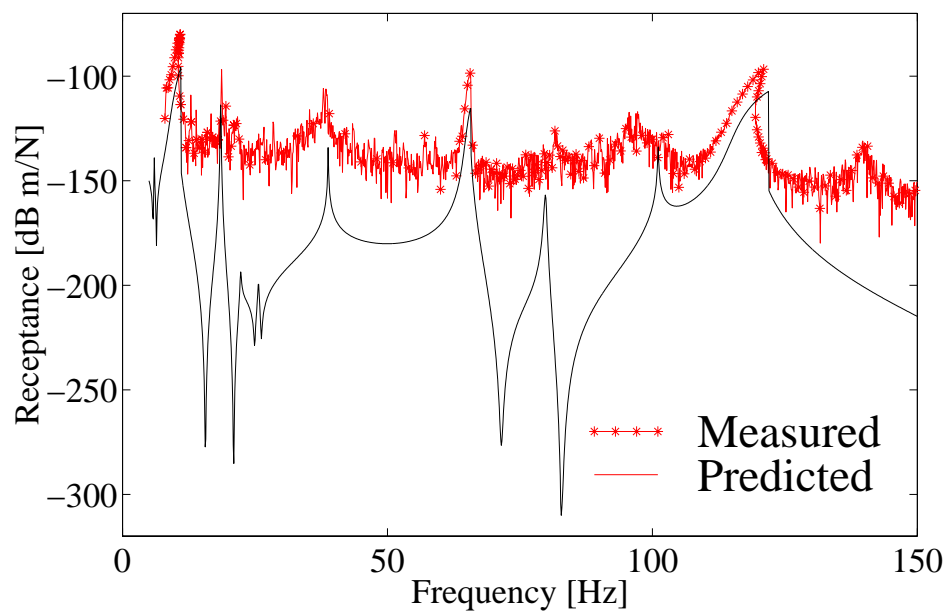


Figure 7.59: Frequency Response  $\{H_{11}^{31}\}^3$  for  $0.5N$

Figure 7.60: Frequency Response  $\{H_{11}^{11}\}^3$  for  $1.0N$ Figure 7.61: Frequency Response  $\{H_{11}^{31}\}^3$  for  $1.0N$

Figure 7.62: Frequency Response  $\{H_{11}^{11}\}^3$  for  $1.5N$ Figure 7.63: Frequency Response  $\{H_{11}^{31}\}^3$  for  $1.5N$

### 7.5.10 Discussion of Results

This analytical model presented in section 7.5.7 was able to represent the dynamic behaviour of the coupled structure in the frequency range measured. It is possible to observe from the measurements that the first and second natural frequencies have a very strong gyroscopic effect splitting each natural frequency in two, known as forward and backward whirl. In addition it is possible to conclude from the measurements that the forward whirl are linear and backward whirl are nonlinear. From a comparison of the amplitude of vibration on the forward and backward whirl of the first and second modes with the third mode at node 14, the level of the receptance where the nonlinearity starts to exert an influence is around -80dB and the response of both forward whirls are lower than -80Db and the response of both backward whirls are higher than -80Db as seen in Figure 7.56.

The predicted assembly first-order FRFs obtained agree well with those measured in the assembled structure. For the higher-order FRFs, although the result presented the same shifting problem noticed in the first test rig, discussed in section 7.4.12, it is less marked, which makes it possible to be correlated with a systematic error occurred in the measurements. Another interesting point to be noticed is related to the fact that that the level of the harmonic response is very small, which implies that for this polynomial stiffness nonlinearity the influence of higher harmonics is very small.

### 7.5.11 Conclusions

Application of the nonlinear FRF-based coupling technique, *MUHANORCA*, to two different practical structures has been examined in this chapter. One was a stationary structure and the other one was a rotating structure. The limitations and difficulties of some of the problems encountered during these experiments have been discussed.

The problems related with the predictions using updating models and experimental data were examined. It has been demonstrated that when a very good updated model is obtained, small differences in resonance and anti-resonances imply large errors in the prediction. In order to overcome these inconsistencies, it was decided to use synthesised FRFs for the analysis of the Test Rig II which were calculated using the updated model. During the updating analysis, two difficulties were encountered. The first one was identifying the right parameter to updated and the second was finding its sensitive region.

For the first-order FRFs, the overall shape of the predicted FRFs match the measured counterparts very well. However, for the higher-order FRFs, the difference between the pre-

dicted and measured FRFs of the assembly structure is much more significant. It is believed that the true FRF cannot be measured as the high level of noise overwrites the dynamic behaviour of the structure. Therefore for low amplitudes of vibration, the measurements are constrained to noise. For large amplitudes of vibration, the measurements follow the overall trend quite well, as the resonances are reasonably well captured.

A very interesting result was the possibility of measuring FRF in the unstable area, although it was thought impossible. A reasonable explanation of this fact is that although the nonlinear structure itself has the unstable response, the structure composed of the shaker plus the nonlinear structure is now stable.

The *MUHANORCA* method developed has been successfully verified for the stationary and rotational structures.

# Chapter 8

## Conclusion and Future work

### 8.1 Introduction

The aim of the work reported in this thesis has been to extend the scope of structural dynamic coupling procedures to nonlinear structures by developing a nonlinear coupling approach. The general conclusions of the research are presented in the following sections. One section is devoted to the nonlinear coupling methods developed, the refinements implemented and the accuracy which can be obtained in the coupling analysis when using higher-order harmonics in the response. Another section is dedicated to the experimental measurement of frequency response functions of nonlinear structures. In the last section some suggestions for further work are presented.

### 8.2 Conclusions on the Nonlinear Receptance Coupling Technique

In considering the dynamic response of many engineering structures, it is necessary to obtain a good predictive model, either for structural modification purposes (optimisation) or for structural response behaviour prediction under different input conditions. However, a suitable mathematical model of a complex structure is very difficult to obtain due to the fact that most practical engineering structures possess a degree of nonlinearity. To solve this problem, a complex structure can be subdivided into components that are treated separately to produce subsystem models that are then coupled by various connection elements to obtain a model of the complete structure. Unlike many other structural elements, it is

the connection elements that usually contain the nonlinear behaviour. In some cases, they are treated as linear joints, either because the degree of nonlinearity is small and therefore insignificant in the frequency range of interest or because a more accurate analysis procedure is not available. In other cases, the effect of the nonlinearity may become so significant that it has to be taken into account in the dynamic analysis in order to achieve the necessary accuracy from the analytical model.

In order to meet this need, a new nonlinear harmonic receptance coupling method that handles the connection elements as linear or nonlinear joint connections, *HANORCA*, has been developed in this work. This method retains the overall computational and numerical efficiency of the linear method proposed by Jetmundsen, Bielawa and Flannelly [63]. In addition, several refinements were introduced to achieve better efficiency. The implementation of the refinements helped to obtaining fast and reliable results for the prediction of complex assembled structures. Then this method was extended to a multi-harmonic nonlinear receptance coupling approach, *MUHANORCA*. The *MUHANORCA* method is based on the premise that the nonlinear joint has already been identified and that response models of the others substructures that comprise the whole assembly are available. These response models can be obtained either from analytical or experimental data.

Depending on which kinds of nonlinearity are present in the structure, the higher frequency components of the response (to a simple harmonic excitation) may sometimes be as important as the fundamental frequency response component. Therefore, a satisfactory level of model accuracy can only be obtained if higher-order FRFs are included in the analysis. As a result, the first-order nonlinear coupling method (which considers only the fundamental components of the response) was extended to a higher-order nonlinear coupling method. By extending the first-order nonlinear coupling to higher order nonlinear coupling, the first-order describing function was also extended to higher-order describing functions.

Both numerical studies and experimental investigations have been carried out to assess the effectiveness of the method. When comparing predicted and measured FRFs, it can be seen that both the variation in natural frequency as a function of input level, and the jump phenomena at resonance, are well predicted. As demonstrated by both studies, successful prediction of the coupled frequency response behaviour of a linear system with local nonlinear joints can be achieved provided that the describing function of the nonlinear joints are properly identified.

The nonlinear coupling algorithm developed in this work is very efficient because it requires only the inversion of matrices referred to the connection coordinates. This

advantage becomes even more significant when using all the refinements developed. The algorithm used to solve the nonlinear set of equations worked very well for all problems studied. The main difficulty to be overcome was how to find a new initial guess when the method failed to give a solution. The initial guess is very case-dependent and depends mainly on the type of nonlinearity present. For each different joint, a different strategy was adopted to find a good initial guess.

The other coupling methods developed in this work, such as (i) Harmonic Nonlinear Impedance Coupling using Describing Functions, (ii) Multi-Harmonic Nonlinear Impedance Coupling using Multi-Harmonic Balance Method, (iii) Multi-Harmonic Nonlinear Impedance Coupling using High-Order Describing Function and (iv) Multi-Harmonic Nonlinear Impedance Coupling using Multi-Harmonic Describing Function were essentially used to improve the basic understanding of the higher-order analysis and to assist in the development of the definitive nonlinear coupling method, *MUHANORCA*. Although these previous methods are not so efficient, they are very simple to program and to understand, and therefore they can be used to perform analytical simulations when the spatial properties are available.

A unified coupling notation was proposed and used in all the methods developed during this work. This notation unifies all the current different notations available.

With the help of stepped-sine excitation, a better understanding of the effect of nonlinearity on the frequency response function data measured has been obtained. A practical difficulty was identified when measuring frequency response functions of a nonlinear structure at high levels of force. A true frequency response function of a nonlinear structure subject to a simple harmonic excitation is very difficult to obtain in practice around resonance due to the higher harmonics becoming more significant in the input force. If such measured results are used to compare with a predicted analytical frequency response function, much care must be taken. In this research, a nonlinear force control algorithm was developed to overcome this difficulty. Although the method is quite time-consuming, it gives very good results.

The difficulty in achieving uni-directional excitation was overcome by exciting the structure in two orthogonal directions. The first shaker was aligned in the direction of the desired excitation. The second shaker excited in the perpendicular direction. Any acceleration in the perpendicular direction was minimised by applying an acceleration control algorithm. The acceleration control algorithm is an extension of the force control algorithm.

It has previously been thought impossible to measure all three levels of the FRF in the special region around resonance where, for some nonlinearities, there is no unique solution.

Conventionally, the upper and lower responses are attainable but not the intermediate one. However, in this work it has been possible to measure all three. It seems that although the nonlinear structure on its own has the unstable region, the addition of shaker to the structure stabilises the response in that region.

### 8.3 Contributions

Here we present a summary list of the main contributions delivered by this research:

- A notation for the structures and coordinates involved in the coupling procedure that allows coupling several components at the same time has been developed.
- A Nonlinear Receptance Coupling Approach (*HANORCA*) for the fundamental harmonic response component has been proposed, and some numerical improvements in *HANORCA* related to time-consumption made.
- A multi-harmonic analysis was also discussed and the Describing Function method extended to higher-order harmonics, (*HODEF*).
- A new Multi-Harmonic Describing Function, (*MUHADEF*), was proposed and a new generalised Multi-Harmonic Nonlinear Receptance Coupling Approach, (*MUHANORCA*), was developed. These approaches enable us to couple linear and nonlinear structures with different types of joint, where the describing functions of all the nonlinear joint elements are specified. The method is general and can be widely applied. The Multi-Harmonic Nonlinear Receptance Coupling Approach was obtained as a result of the development and study of other three quasi-linearisation approaches, the Multi-Harmonic Nonlinear Impedance Coupling using Multi-Harmonic Balance Method, the Multi-Harmonic Nonlinear Impedance Coupling using High-Order Describing Function and the Multi-Harmonic Nonlinear Impedance Coupling using Multi-Harmonic Describing Function.
- An intelligent coupling analysis program, *INCA<sup>++</sup>*, that can couple several linear or nonlinear structures at the same time using rigid, linear or nonlinear connection elements and for different analytical methods, has been developed. This program provides the necessary numerical evaluation for the validation of the developed analytical methods.

- Numerical results obtained by the developed method were validated with the response obtained by the time-integration method, here considered to be the exact result [36, 38, 37].
- An experimental evaluation were carried out successfully on two test cases.
- A robust nonlinear force control algorithm to ensure a constant pure harmonic excitation force was developed.
- An acceleration control algorithm to minimise excitation in the orthogonal direction was developed.
- A "virtual analyser" to obtain FRFs from harmonic excitation utilising the correlation technique was developed.

## 8.4 Prospects

The study undertaken in this thesis has achieved its original objectives, and in the process has identified a number of further developments that would be of interest in future work in the field of Nonlinear Coupling analysis. Some general suggestion are outlined below.

- Applications of the method developed to more complicated structures having different nonlinearities.
- The procedure used to find the initial guess for the nonlinear force control can be used as the initial guess for the Newton-Raphson method used in the nonlinear coupling procedure.
- Alternatives algorithm to bracket the solution in the nonlinear force control must be investigate.
- Minimisation techniques for finding a minimum of a functions should be investigated as alternatives to the multidimensional root applied in the nonlinear coupling procedure.
- Application of numerical techniques which enable the calculation of the analytical FRF in the unstable region.

# Bibliography

- [1] M.L. Adams.  
Nonlinear dynamics of flexible multi-bearing rotors.  
*Journal of Sound and Vibration*, 71(1):129–144, 1980.
- [2] H. Ahmadian, J.E. Mottershead, and M.I. Friswell.  
Joint modelling for finite element model updating.  
In *14th IMAC*, pages 591–596, 1996.
- [3] I.A. Anderson.  
Avoiding stinger rod resonance on small structures.  
In *8th IMAC*, pages 673–678, 1990.
- [4] Nobari A.S.  
*Identification of the dynamic characteristics of structural joints*.  
PhD thesis, Department of Mechanical Engineering, Imperial College, Exhibition  
Road, London, SW7 3DU, 1992.
- [5] J.P. Bandstra.  
Comparison of equivalent viscous damping and non-linear damping in discrete and  
continuous vibrating systems.  
*ASME Journal of Vibration, Acoustics, Stress and Reliability in Design*, 105:382–392,  
1983.
- [6] K. J. Bathe.  
*Finite Element Procedures in Engineering Analysis*.  
Prentice-Hall, Englewood Cliffs, New Jersey, 1982.
- [7] S.A. Billings and K.M. Tsang.  
Spectral analysis for nonlinear systems, part i: Parametric nonlinear spectral analysis.  
*Mechanical Systems and Signal Processing*, 3(4):319–339, 1989.
- [8] S.A. Billings, K.M. Tsang, and G.R. Tomlinson.

- Spectral analysis for nonlinear systems, part iii: Case study examples.  
*Mechanical Systems and Signal Processing*, 4(?):3–21, 1990.
- [9] A.C. Bindemann and A.A. Ferri.  
Large amplitude vibration of a beam restrained by a nonlinear sleeve joint.  
*Journal of Sound and Vibration*, 1(184):19–34, 1995.
- [10] R.E.D. Bishop and D.C Johnson.  
*The Mechanics of Vibration*.  
Cambridge University Press, 1960.
- [11] N.N. Bogoliubov and J.A. Mitropolsky.  
*Asymptotic Methods in the Theory of Non-Linear Oscillations*.  
Hindustan Publishing Company, 1963.
- [12] S. Bohlen and L. Gaul.  
Vibration of structures coupled by nonlinear transfer behaviour of joints: A combined  
computacional and experimental approach.  
In *5th IMAC*, pages 86–91, 1987.
- [13] N. Boivin and C. Pierre.  
Nonlinear modal analysis of structural systems featuring internal resonances.  
*Journal of Sound and Vibration*, 782(2):336–341, 1995.
- [14] G. Booch.  
*Object-Oriented Analysis and Design with Applications*.  
The Benjamin/Cummings Publishing Company, Inc., 1994.
- [15] D.R. Brillhart, D.L. Hunt, and M.St. Pierre.  
Advantages of excitation using plastic stinger rods.  
In *11th IMAC*, pages 1217–1220, 1993.
- [16] M. Burdekin, N. Back, and A. Cowley.  
Experimental study of normal and shear characteristics of machined surfaces in con-  
tact.  
*Journal of Mechanical Engineering Science*, 20(20):129–132, 1978.
- [17] M. Burdekin, A. Cowley, and N. Back.  
An elastic mechanism for the microsliding characteristics between contacting ma-  
chined surfaces.  
*Journal of Mechanical Engineering Science*, 20(3):121–127, 1978.

- 
- [18] H.R. Busby, C. Nopporn, and R. Singh.  
Experimental modal analysis of non-linear systems: A feasibility study.  
*Journal of Sound and Vibration*, 180(3):415–427, 1986.
- [19] T.M. Cameron and Griffin J.H.  
An alternating frequency/time domain method for calculating the steady-state response of non-linear dynamic system.  
*Journal of Applied Mechanics*, 56:149–154, 1989.
- [20] D.W. Childs.  
The space shuttle main engine high-pressure fuel turbopump rotordynamic instability problem.  
*ASME Journal of Engineering for Power*, 100:48–57, 1978.
- [21] T. Chouychai and T. Vinh.  
Analysis of non linear structure by programmed impact testing and higher order transfer function.  
In *4th IMAC*, pages 743–747, 1986.  
London.
- [22] T. Chouychai and T. Vinh.  
Impact testing of non-linear structures.  
In *5th IMAC*, pages 1384–1399, 1987.  
London.
- [23] M.D. Comert and H.N. Ozguven.  
A method for forced harmonic response of substructures coupled by non-linear elements.  
In *13th IMAC*, pages 139–145, 1995.
- [24] R.R. Craig and M.C.C. Bamptom.  
Coupling of substructures for dynamic analysis.  
*AIAA*, 6(7):1313–1319, July 1968.
- [25] J.P. Den Hartog.  
Forced vibrations with combined coulomb and viscous friction.  
*Transactions of ASME*, 53:105–107, 1931.
- [26] M.A. Dokainish and K. Subbaraj.

- A survey of direct time-integration methods in computational structural dynamics:  
I, explicit methods.  
*International Journal of Computers and Structures*, 32:1371–1386, 1989.
- [27] M.A. Dokainish and K. Subbaraj.  
A survey of direct time-integration methods in computational structural dynamics:  
Ii, implicit methods.  
*International Journal of Computers and Structures*, 32:1387–1401, 1989.
- [28] M.L. Duarte.  
*Experimentally-derived structural models for use in further dynamic analysis*.  
PhD thesis, Imperial College of Science, Technology and Medicine, 1996.
- [29] F. Ehrich.  
Nonlinear phenomena in dynamic response of rotors in anisotropic mounting systems.  
*ASME Journal of Vibration, Acoustics, Stress and Reliability in Design*, 117:154–161,  
1995.
- [30] D.J. Ewins.  
The effects of slight non-linearities on modal testing of helicopter-like structure.  
*Vertica*, 7:1–8, 1983.
- [31] D.J. Ewins.  
*Modal Testing: Theory and Practice*.  
Research Studies Press, 1984.
- [32] D.J. Ewins.  
Analysis of modified or coupled structures using frf properties.  
Internal Report 86002, Dynamics Section, Department of Mechanical Engineering,  
Imperial College, London SW7 2BX, March 1986.
- [33] D.J. Ewins, J. HE, and R.M. Lin.  
Modal analysis of the non-linear dynamic characteristics of the eth box.  
Internal Report 88012, Dynamics Section, Department of Mechanical Engineering,  
Imperial College, London SW7 2BX, July 1988.
- [34] D.J. Ewins and M. Imregun.  
State-of-the-art assessment of structural dynamic response analysis methods (dynas).  
*Shock and Vibration Bulletin*, 56:59–90, August 1986.
- [35] D.J. Ewins and J. Sidhu.

- Modal testing and the linearity of structures.  
*Mechanique Materiaux Electricite*, (389-390-391):297–302, 1982.
- [36] J.V. Ferreira and D.J. Ewins.  
Nonlinear receptance coupling approach based on describing functions.  
In *14th IMAC*, pages 1034–1040, 1996.
- [37] J.V. Ferreira and D.J. Ewins.  
Algebraic nonlinear impedance equation using multi-harmonic describing function.  
In *15th IMAC*, pages 1595–1601, 1997.
- [38] J.V. Ferreira and D.J. Ewins.  
Multi-harmonic nonlinear receptance coupling approach.  
In *15th IMAC*, pages 27–33, 1997.
- [39] A.A. Ferri and A.C. Bindemann.  
Damping and vibration of beams with various types of frictional support conditions.  
*ASME Journal of Vibrations and Acoustics*, 114:289–296, 1992.
- [40] B.W.R. Forde.  
*An application of selected artificial techniques to engineering analysis*.  
PhD thesis, The University of British Columbia, 1989.
- [41] B.W.R. Forde, R.O. Foshi, and S.F. Stiemer.  
Object-oriented finite element analysis.  
*Computers and Structures*, 34(3):355–374, 1990.
- [42] A. Frachebourg.  
Using volterra model with impact excitation: a simple solution to identify nonlinearities.  
In *7th IMAC*, pages 1372–1378, 1989.
- [43] A. Frachebourg.  
Identification of nonlinearities: application of the volterra-model to discrete mdof systems; possibilities and limits.  
In *9th IMAC*, pages 1029–1035, 1991.
- [44] R. Gasch.  
Vibration of large turbo-rotors in fluid-film bearing on an elastic foundation.  
*Journal of Sound and Vibration*, 47(1):53–73, 1976.

- 
- [45] L. Gaul, U. Nckenhorst, K. Willner, and J. Lenz.  
Nonlinear vibration damping of structures with bolted joint.  
In *12th IMAC*, pages 875–881, 1994.
- [46] A. Gelb and W. E. Vander Velde.  
*Multiple-Input Describing Functions and Non-Linear System Design*.  
Mc Graw-Hill, 1968.
- [47] J.E. Gibson.  
*Nonlinear Automatic Control*.  
MacGraw-Hill, 1963.
- [48] S.J. Gifford and G.R. Tomlinson.  
Recent advances in the application of functional series to nonlinear structures.  
*Journal of Sound and Vibration*, 135(2):289–317, 1989.
- [49] S.J. Gifford and G.R. Tomlinson.  
Understanding multi degree of freedom nonlinear systems via higher order frequency response functions.  
In *7th IMAC*, pages 1356–1364, 1989.
- [50] D.A. Glasgow and H.D. Nelson.  
Stability analysis of rotor-bearing systems using component mode synthesis.  
*ASME Journal of Mechanical Design*, 102:352–359, 1980.
- [51] D.E. Glisinn.  
A high order generalised method of averaging.  
*SIAM*, 42(1):113–114, April 1982.
- [52] L.E. Goodman and C.B. Brown.  
Energy dissipation in contact friction: constant normal and cyclic tangential loading.  
*ASME Journal of Applied Mechanics*, pages 17–22, 1962.
- [53] E.J. Gunter, L.E. Barret, and P.E. Allaire.  
Design of nonlinear squeeze-film dampers for aircraft engines.  
*Journal of Lubrication Technology*, pages 57–64, 1977.
- [54] S. Han.  
Analysis on natural frequency distortion due to the attachment of shaker.  
In *13th IMAC*, pages 1715–1721, 1995.

- 
- [55] C.M. Harris and C.E. Crede.  
chapter 4, pages 1–28.  
McGraw-Hill, 1976.
- [56] K.H. Haslinger.  
Experimental characterization of sliding and impact friction coefficients between steam generator tubes and avb supports.  
*Journal of Sound and Vibration*, 181(5):851–871, 1995.
- [57] C. Hayashi.  
*Non-Linear Oscillations in Physical Systems*.  
Mc Graw-Hill, 1964.
- [58] J. He and D.J. Ewins.  
A simple method of interpretation for the modal analysis of non-linear structures.  
In *5th IMAC*, pages 626–634, 1987.  
London.
- [59] J. He, R.M. Lin, and D.J. Ewins.  
Evaluation of some non-linear modal analysis methods.  
In *13th International Modal Analysis Seminar*, 1988.  
Leuven.
- [60] G.M. Hieber.  
Non-toxic stingers.  
In *6th IMAC*, pages 1371–1379, 1988.
- [61] W.C. Hurty.  
Dynamic analysis of structural systems using component modes.  
*AIAA*, 3(4):678–685, April 1965.
- [62] W.D. Iwan.  
On a class of models for the yielding behaviour of continuous and composite systems.  
*ASME Journal of Applied Mechanics*, 89:612–617, 1967.
- [63] B. Jetmundsen, R.L. Bielawa, and W.G. Flannelly.  
Generalized frequency domain substructure synthesis.  
*Journal of the American Helicopter Society*, pages 55–64, January 1988.
- [64] L. Jezequel, H.D. Setio, and S. Setio.  
Non-linear modal synthesis in frequency domain.

- In *8th IMAC*, pages 1278–1283, 1990.
- [65] D.W. Jordan and P. Smith.  
*Non-Linear Ordinary Differential Equations*.  
Oxford University Press, 1987.
- [66] J. Kirshenboim and D.J. Ewins.  
A method for recognising structural non-linearities in steady state harmonic testing.  
*ASME Journal of Vibration, Acoustics, Stress and Reliability in Design*, 106:49–52,  
1984.
- [67] A.L. Klosterman and J.R. Lemon.  
Building block approach to structural dynamic.  
In *America Society of Mechanical Enginnering Annual Vibrations Conference*, 1969.  
Publication VIBR-30.
- [68] E. Kramer.  
*Dynamics of Rotors and Foundations*.  
Springer-Verlag, 1993.
- [69] B. Kuran.  
Dynamic analysis of harmonically excited non-linear structures by using iteratively  
modal method.  
Master's thesis, Middle East Technical University, Ankara, Turkey, 1992.
- [70] B. Kuran and H.N. Ozguven.  
A modal superposition method for non-linear structures.  
*Journal of Sound and vibration*, 3(189):315–319, 1996.
- [71] J. Lee and Y. Chou.  
The effects of stingers on modal testing.  
In *11th IMAC*, pages 293–299, 1993.
- [72] R. Lin.  
*Identification of the dynamic characteristics of nonlinear structures*.  
PhD thesis, Imperial College of Science, Technology and Medicine, 1991.
- [73] R.M. Lin.  
Non-linear coupling analysis based on a describing function.  
Master's thesis, Department of Mechanical Engineering, Imperial College, London  
SW7 2BX, 1988.

- 
- [74] R.M. Lin.  
Nonlinear coupling analysis based on describing functions.  
Internal Report 88030, Dynamics Section, Department of Mechanical Engineering,  
Imperial College, London SW7 2BX, November 1988.
- [75] J.W. Lund.  
Modal response of flexible rotor in fluid-film bearings.  
*ASME Journal of Engineering for Industry*, pages 525–533, 1974.
- [76] J.W. Lund.  
Stability and damped critical speeds of a flexible rotor in fluid-film bearings.  
*ASME Journal of Engineering for Industry*, pages 509–517, 1974.
- [77] J.W. Lund and F.K. Orcutt.  
Calculations and experiments on the unbalance response of a flexible rotor.  
*ASME Journal of Engineering for Industry*, pages 785–795, 1974.
- [78] M. Masuko, Y. Ito, and T. Koizumi.  
Horizontal stiffness and micro-slip on bolted joint subjected to repeated tangential  
static loads.  
*Bulletin of the Journal of Mechanical Engineering and Science*, 17(113):1494–1501,  
1974.
- [79] K.G. McConnell and P.S. Varoto.  
An experimental study of the exciter-structure interaction in vibrating testing.  
In *12th IMAC*, pages 1720–1727, 1994.
- [80] P. Menetrey and T. Zimmermann.  
Object-oriented nonlinear finite element analysis: Application to 2D plasticity.  
*Computers and Structures*, 49(5):767–777, 1993.
- [81] C-H. Menq and J.H. Griffin.  
A comparison of transient and steady state finite element analysis on the forced  
response of a frictionally damped beam.  
*ASME Journal of Vibration, Acoustics, Stress and Reliability in Design*, 107:19–25,  
1985.
- [82] C-H. Menq, J.H. Griffin, and J. Bilelak.  
The forced vibration of shrouded fan stages.

- ASME Journal of Vibration, Acoustics, Stress and Reliability in Design*, 108:50–55, 1986.
- [83] C.H. Menq, J. Bielak, and J.H. Griffin.  
The influence of microslip on vibratory response. part i: A new microslip model.  
*Journal of Sound and Vibration*, 107(2):279–293, 1986.
- [84] T.J. Mentel.  
Joints interface layer damping.  
*ASME Journal of Engineering for Industry*, pages 797–805, 1967.
- [85] M. Miki and Yoshisada Murotsu.  
Object-oriented approach to modeling and analysis of truss structures.  
*AIAA*, 33(2):348–354, February 1995.
- [86] R.D. Mindlin, W.P. Mason, T.F. Osmer, and H. Deresiewicz.  
Effects of an oscillating tangential force on the contact surfaces of elastic spheres.  
In *First US national congress on applied mechanics*, pages 203–209, 1961.
- [87] N.F. Morris.  
The use of mode superposition in non-linear dynamics.  
*International Journal of Computers and Structures*, 7:65–72, 1977.
- [88] K. Murakami and H. Sato.  
Vibration characteristics of a beam with support accompanying clearance.  
*ASME Journal of Vibrations and Acoustics*, 112:508–514, 1990.
- [89] S.W. Nam, S.B. Kim, and E.J. Powers.  
Nonlinear system identification with random excitation using discrete third-order  
volterra series.  
In *8th IMAC*, pages 334–340, 1990.
- [90] H.D. Nelson and J.M. McVaugh.  
The dynamics of rotor-bearing systems using finite elements.  
*ASME Journal of Engineering for Industry*, pages 593–600, 1976.
- [91] H.D. Nelson, W.L. Meachan, D.P. Fleming, and A.F. Kascak.  
Nonlinear analysis of rotor-bearing systems using component mode synthesis.  
*ASME Journal of Engineering for Power*, 105:606–614, 1983.
- [92] R.E. Nickel.

Non-linear dynamics by mode superposition.

*Computational Methods in Applied Mechanical Engineering*, 7:107–129, 1976.

[93] N.L. Olsen.

Using and understanding electrodynamic shakers in modal applications.

In *4th IMAC*, pages 1160–1167, 1986.

[94] D. Otte, J. Leuridan, H. Grangier, and R. Aquilina.

Prediction of the dynamics of structural assemblies using measured frf-data: some improved data enhancement techniques.

In *9th IMAC*, pages 909–918, 1991.

[95] R. Penrose.

A generalised inverse for matrices.

In *Cambridge Philos. Soc.*, pages 406–413, 1955.

[96] R.M. Pidaparti and A.V. Hudli.

Dynamic analysis of structures using object-oriented techniques.

*Computers and Structures*, 49(1):149–156, 1993.

[97] W.H. Press, S.A. Teukolsky, W.T. Vetterling, and B.P. Flannery.

*Numerical Recipes in C*.

Cambridge University Press, 1992.

[98] S.Z. Rad.

*Methods for updating numerical models in structural dynamics*.

PhD thesis, Imperial College of Science, Technology and Medicine, 1997.

[99] D.K. Rao.

Electrodynamic interaction between a resonating structure and an exciter.

In *5th IMAC*, pages 1142–1150, 1987.

[100] Y. Ren and C.F. Beards.

A generalised receptance coupling technique.

In *11th IMAC*, pages 868–871, 1993.

[101] Y. Ren and C.F. Beards.

On the nature of frf joint identification technique.

In *11th IMAC*, pages 473–478, 1993.

[102] Y.S. Ren, J.M. Yang, Z.L. Zhao, and Y.H. Wang.

- Nonlinear vibration analysis of beams with dry friction joint.  
In *12th IMAC*, pages 1720–1727, 1994.
- [103] H.J. Rice and K.Q. Xu.  
Linear path identification of general nonlinear systems.  
*Mechanical Systems and Signal Processing*, 10(1):55–63, 1996.
- [104] P.F. Rogers and G. Boothroyd.  
Damping at metallic interfaces subject to oscillating tangential loads.  
*ASME Journal of Engineering for Industry*, pages 1087–1093, 1975.
- [105] R.M. Rosenberg.  
The normal modes of nonlinear n-degree-of-freedom systems.  
*ASME Journal of Applied Mechanics*, pages 7–14, 1962.
- [106] K.E. Rouch.  
Dynamic reduction in rotor dynamics by the finite element method.  
*ASME Journal of Mechanical Design*, 102:360–368, 1980.
- [107] K.Y. Sanliturk and D.J. Ewins.  
Modelling two-dimensional friction contact and its application using harmonic balance method.  
*Journal of Sound and Vibration*, 193(2):511–523, 1996.
- [108] K.Y. Sanliturk, M. Imregum, and D.J. Ewins.  
Harmonic balance vibration analysis of turbine blades with friction dampers.  
*ASME Journal of Vibrations and Acoustics*, 119:96–103, 1997.
- [109] K.Y. Sanliturk, A.B. Stambbridge, and Ewins D.J.  
Friction damper optimization for turbine blades: experimental and theoretical predictions.  
In *IMechE- Sixth International Conference in Vibrations in Rotating Machinery*, number C500/019/96, pages 171–186, 1996.
- [110] R. Schmidt.  
Updating nonlinear components.  
*Mechanical Systems and Signal Processing*, 8(6):679–690, 1994.
- [111] S.P. Scholz.  
Elements of an object-oriented fem++ program in c++.  
*Computers and Structures*, 43(3):517–529, 1992.

- 
- [112] S.N. Shoukry.  
A mathematical model for the stiffness of fixed joints between machine parts.  
In *NUMETA 85 Conference*, pages 851–858, 1985.  
Swansea, U.K.
- [113] D.D. Sijak.  
*Nonlinear Systems: A Parametr Analysis and Design*.  
John Wiley and Sons, 1969.
- [114] M. Simon and G.R. Tomlinson.  
Use of the hilbert transform in the modal analysis of linear and non-linear structures.  
*Journal of Sound and Vibration*, 96(4):421–436, 1984.
- [115] G.W. Skingle.  
*Structural dynamic modification using experimental data*.  
PhD thesis, Imperial College of Science, Technology and Medicine, 1989.
- [116] D.M. Storer and G.R. Tomlinson.  
Recent developments in the measurement and interpretation of higher order transfer  
functions from nonlinear structures.  
*Mechanical Systems and Signal Processing*, 7(2):173–189, 1993.
- [117] B. Stroustrup.  
*The C++ Programming Language*.  
Addison-Wesley Publishing Company, 1994.
- [118] M. Stylianou and B. Tabarrok.  
Finite element analysis of an axially moving beam, part i: time integration.  
*Journal of Sound and Vibration*, 4(178):443–453, 1994.
- [119] W. Szemplinska.  
A study of main and secondary resonances in non-linear multi-degree-of-freedom vi-  
brating systems.  
*International Journal Non-Linear Mechanics*, 10:289–304, 1975.
- [120] W. Szemplinska.  
Non-linear normal modes and the generalized ritz method in the problems of vibrations  
of non-linear elastic continuous systems.  
*International Journal Non-Linear Mechanics*, 18(2):149–165, 1983.
- [121] O. Tanrikulu.

- Forced periodic response analysis of non-linear structures for harmonic excitation.  
Master's thesis, Department of Mechanical Engineering, Imperial College, London  
SW7 2BX, 1991.
- [122] O. Tanrikulu, B. Kuran, H.N. Ozguven, and M. Imregun.  
Forced harmonic response analysis of non-linear structures.  
*AIAA*, 31(7):1313–1320, July 1993.
- [123] F. Thouverez and L. , Jezequel.  
Identification of nonlinearity joints from dynamical tests.  
In *9th IMAC*, pages 1583–1588, 1991.
- [124] G. R. Tomlinson.  
Force distortion in resonance testing of structures with electro-dynamic vibration  
exciters.  
*Journal of Sound and Vibration*, 63(3):337–350, 1979.
- [125] G. R. Tomlinson and J. H. Hibbert.  
Identification of the dynamic characteristics of a structure with coulomb friction.  
*Journal of Sound and Vibration*, 64(2):233–242, 1979.
- [126] G. R. Tomlinson and J. Lam.  
Frequency response characteristics of structures with single and multiple clearance-  
type non-linearity.  
*Journal of Sound and Vibration*, 96(1):111–125, 1984.
- [127] G.R. Tomlinson.  
An analysis of the distortion effects of coulomb damping on the vector plots of lightly  
damped systems.  
*Journal of Sound and Vibration*, 71(3):443–451, 1980.
- [128] G.R. Tomlinson.  
Developments in the use of hilbert transform for detecting and quantifying non-  
linearity in frequency response functions.  
*Mechanical Systems and Signal Processing*, 1(2):151–173, 1987.
- [129] G.R. Tomlinson.  
A simple theoretical and experimental study of the force characteristics from eletro-  
dynamic exciters on linear and nonlinear systems.  
In *5th IMAC*, pages 1479–1486, 1987.

- [130] J.S. Tsai and Y.F. Chou.  
The identification of dynamic characteristics of a single bolt joint.  
*Journal of Sound and Vibration*, 3(125):487–502, 1988.
- [131] A.P.V. Urgueira.  
*Dynamic Analysis of Coupled Structures Using Experimental Data*.  
PhD thesis, Imperial College of Science, Technology and Medicine, 1989.
- [132] B. Van der Pol.  
Forced oscillation in a circuit with non-linear resistance.  
*The London, Edinburgh, and Dublin Philosophical Magazine and Journal of Science*,  
3:65–80, 1927.
- [133] T. Vinh and H. Liu.  
Extension of modal analysis to nonlinear systems (possibility, mathematical models,  
limitation).  
In *7th IMAC*, pages 1379–1385, 1989.
- [134] O. Vinogradov and I. Pivovarov.  
Vibration of a system with non-linear hysteresis.  
*Journal of Sound and Vibration*, 111(1):145–152, 1986.
- [135] J.H. Wang and W.K. Chen.  
Investigation of the vibration of a blade with friction damper by hbm.  
In *The American Society of Mechanical Engineers*, 1992.  
92-GT-8, accepted at ASME September/92.
- [136] K. Watanabe and H. Sato.  
Development of non-linear building block approach.  
*ASME Journal of Vibrations, Stress, and Reliability in Design*, 110:36–41, January  
1988.
- [137] K. Watanabe and H. Sato.  
A modal analysis approach to nonlinear multi-degrees-of-freedom system.  
*ASME Journal of Vibrations, Stress, and Reliability in Design*, 110:410–411, July  
1988.
- [138] I. White.  
*Rational Rose Essentials using the Booch Method*.  
The Benjamin/Cummings Publishing Company, Inc., 1994.

- 
- [139] K. Wyckaert, P. Vanherck, H.V. Brussel, and P. Sas.  
Predictive response calculation of linear structures coupled with local non-linear elements.  
In *9th IMAC*, pages 1215–1222, 1991.
- [140] Ren Y.  
*The analysis and identification of friction joint parameters in the dynamic response of structures.*  
PhD thesis, Department of Mechanical Engineering, Imperial College, Exhibition Road, London, SW7 3DU, 1992.
- [141] M.S. Yao.  
Nonlinear structural dynamic finite element analysis using ritz vector reduced basis method.  
*Shock and Vibration*, 3(4):259–268, May 1996.
- [142] N. Ymaki.  
Non-linear vibration of a clamped beam with initial deflection and initial axial displacement-part i.  
*Journal of Sound and Vibration*, 71(3):333–346, 1980.
- [143] R. Youngsheng and Z. Demao.  
The steady state response calculation and damping vibration analysis of shrouded blades.  
In *12th IMAC*, pages 1713–1719, 1994.
- [144] Z. Yu, Y.L. Xu, and J.M. Ko.  
Nonlinear behaviour of cables with moved end-supports.  
In *14th IMAC*, pages 1041–1047, 1996.
- [145] L.D. Zavodney.  
Can the modal analyst afford to be ignorant of nonlinear vibration phenomena?  
In *5th IMAC*, pages 154–159, 1987.
- [146] T. Zimmermann, Y. Dubois-Pelerin, and P. Bomme.  
Object-oriented finite element programming: I.governing principles.  
*Computers Methods in Applied Mechanics and Engineering*, 98:291–303, 1992.

# Appendix A

## Refined Formulation of FRF Coupling

Let us assume two structures A and B where some coordinates will be connected by rigid links. The equation of the coupled system, relating displacement vectors and force vector is shown in matrix form as:

$$\begin{Bmatrix} X_{i_a} \\ X_{c_a} \\ X_{c_b} \\ X_{i_b} \end{Bmatrix} = \begin{bmatrix} H_{i_a i_a} & H_{i_a c_a} & H_{i_a c_b} & H_{i_a i_b} \\ H_{c_a i_a} & H_{c_a c_a} & H_{c_a c_b} & H_{c_a i_b} \\ H_{c_b i_a} & H_{c_b c_a} & H_{c_b c_b} & H_{c_b i_b} \\ H_{i_b i_a} & H_{i_b c_a} & H_{i_b c_b} & H_{i_b i_b} \end{bmatrix} \begin{Bmatrix} F_{i_a} \\ F_{c_a} \\ F_{c_b} \\ F_{i_b} \end{Bmatrix} \quad (\text{A.1})$$

Looking at the substructures, the displacement in each point can be written as:

$$\begin{Bmatrix} x_{i_a} \\ x_{c_a} \end{Bmatrix} = \begin{bmatrix} h_{i_a i_a} & h_{i_a c_a} \\ h_{c_a i_a} & h_{c_a c_a} \end{bmatrix} \begin{Bmatrix} f_{i_a} \\ f_{c_a} \end{Bmatrix} \quad (\text{A.2})$$

$$\begin{Bmatrix} x_{i_b} \\ x_{c_b} \end{Bmatrix} = \begin{bmatrix} h_{i_b i_b} & h_{i_b c_b} \\ h_{c_b i_b} & h_{c_b c_b} \end{bmatrix} \begin{Bmatrix} f_{i_b} \\ f_{c_b} \end{Bmatrix} \quad (\text{A.3})$$

The equilibrium conditions can be written as:

$$\begin{aligned} F_{c_a} &= F_{c_b} = f_{c_a} + f_{c_b} \\ F_{i_a} &= f_{i_a} \\ F_{i_b} &= f_{i_b} \end{aligned} \quad (\text{A.4})$$

In the case where the joints are assumed to have linear properties such as infinite or constant stiffness, the compatibility conditions can be written as:

$$\begin{aligned} X_{i_a} &= x_{i_a} \\ X_{i_b} &= x_{i_b} \\ x_{c_a} - x_{c_b} &= 0 \end{aligned} \quad (\text{A.5})$$

Substituting equations (A.2),(A.3) into (A.5) yields:

$$h_{c_a i_a} f_{i_a} + h_{c_a c_a} f_{c_a} - h_{c_b i_b} f_{i_b} - h_{c_b c_b} f_{c_b} = 0 \quad (\text{A.6})$$

Substituting the equilibrium equations (A.4) into (A.6) yields:

$$h_{c_a i_a} F_a + h_{c_a c_a} f_{c_a} - h_{c_b i_b} F_b - h_{c_b c_b} (F_{c_b} - f_{c_a}) = 0 \quad (\text{A.7})$$

Isolating the internal force as a function of the external force yields:

$$f_{c_a} = (B)^{-1} (h_{c_b i_b} F_b - h_{c_a i_a} F_a + h_{c_b c_b} F_{c_b}) \quad (\text{A.8})$$

$$f_{c_b} = F_{c_b} - (B)^{-1} (h_{c_b i_b} F_b - h_{c_a i_a} F_a + h_{c_b c_b} F_{c_b}) \quad (\text{A.9})$$

where:

$$B = h_{c_a c_a} + h_{c_b c_b}$$

Equations (A.2),(A.3) can be written as:

$$\{x_{i_a}\} = [h_{i_a i_a}] \{f_{i_a}\} + [h_{i_a c_a}] \{f_{c_a}\} \quad (\text{A.10})$$

$$\{x_{c_a}\} = [h_{c_a i_a}] \{f_{i_a}\} + [h_{c_a c_a}] \{f_{c_a}\} \quad (\text{A.11})$$

$$\{x_{i_b}\} = [h_{i_b i_b}] \{f_{i_b}\} + [h_{i_b c_b}] \{f_{c_b}\} \quad (\text{A.12})$$

$$\{x_{c_b}\} = [h_{c_b i_b}] \{f_{i_b}\} + [h_{c_b c_b}] \{f_{c_b}\} \quad (\text{A.13})$$

Substituting equations (A.3),(A.2) into (A.5) yields:

$$h_{c_b i_b} f_{i_b} + h_{c_b c_b} f_{c_b} - h_{c_a i_a} f_{i_a} - h_{c_a c_a} f_{c_a} = 0 \quad (\text{A.14})$$

Substituting the equilibrium equations (A.4) into (A.14) yields:

$$h_{c_b i_b} F_b + h_{c_b c_b} f_{c_b} - h_{c_a i_a} F_a - h_{c_a c_a} (F_{c_a} - f_{c_b}) = 0 \quad (\text{A.15})$$

Isolating the internal force in function of the external force yields:

$$f_{c_b} = (B)^{-1} (h_{c_a i_a} F_a - h_{c_b i_b} F_b + h_{c_a c_a} F_{c_a}) \quad (\text{A.16})$$

$$f_{c_a} = F_{c_a} - (B)^{-1} (h_{c_a i_a} F_a - h_{c_b i_b} F_b + h_{c_a c_a} F_{c_a}) \quad (\text{A.17})$$

where:

$$B = h_{c_a c_a} + h_{c_b c_b}$$

Equations (A.2),(A.3) can be written as:

$$\{x_{i_a}\} = [h_{i_a i_a}]\{f_{i_a}\} + [h_{i_a c_a}]\{f_{c_a}\} \quad (\text{A.18})$$

$$\{x_{c_a}\} = [h_{c_a i_a}]\{f_{i_a}\} + [h_{c_a c_a}]\{f_{c_a}\} \quad (\text{A.19})$$

$$\{x_{i_b}\} = [h_{i_b i_b}]\{f_{i_b}\} + [h_{i_b c_b}]\{f_{c_b}\} \quad (\text{A.20})$$

$$\{x_{c_b}\} = [h_{c_b i_b}]\{f_{i_b}\} + [h_{c_b c_b}]\{f_{c_b}\} \quad (\text{A.21})$$

Substituting equations (A.17), (A.4) into (A.18) yields:

$$\begin{aligned} \{X_a\} &= [h_{i_a i_a}]\{F_a\} + [h_{i_a c_a}]\{F_{c_a}\} - \\ & [h_{i_a c_a}][B]^{-1} ([h_{c_a i_a}]\{F_a\} - [h_{c_b i_b}]\{F_b\} + [h_{c_a c_a}]\{F_{c_a}\}) \end{aligned} \quad (\text{A.22})$$

Comparing equation (A.22) with equation (A.1) yields:

$$[H_{i_a i_a}] = [h_{i_a i_a}] - [h_{i_a c_a}][B]^{-1}[h_{c_a i_a}] \quad (\text{A.23})$$

$$[H_{i_a c_a}] = [h_{i_a c_a}] - [h_{i_a c_a}][B]^{-1}[h_{c_a c_a}]rf \quad (\text{A.24})$$

$$[H_{i_a c_b}] = [0] \quad (\text{A.25})$$

$$[H_{i_a i_b}] = [h_{i_a c_a}][B]^{-1}[h_{c_b i_b}] \quad (\text{A.26})$$

Substituting equations (A.17), (A.4) into (A.19) yields:

$$\begin{aligned} \{X_{c_a}\} &= [h_{c_a i_a}]\{F_a\} + [h_{c_a c_a}]\{F_{c_a}\} - \\ & [h_{c_a c_a}][B]^{-1}([h_{c_a i_a}]\{F_a\} - [h_{c_b i_b}]\{F_b\} + [h_{c_a c_a}]\{F_{c_a}\}) \end{aligned} \quad (\text{A.27})$$

Comparing equation (A.27) with equation (A.1) yields:

$$[H_{c_a i_a}] = [h_{c_a i_a}] - [h_{c_a c_a}][B]^{-1}[h_{c_a i_a}] \quad (\text{A.28})$$

$$[H_{c_a c_a}] = [h_{c_a c_a}] - [h_{c_a c_a}][B]^{-1}[h_{c_a c_a}] \quad (\text{A.29})$$

$$[H_{c_a c_b}] = [0] \quad (\text{A.30})$$

$$[H_{c_a i_b}] = [h_{c_a c_a}][B]^{-1}[h_{c_b i_b}] \quad (\text{A.31})$$

Substituting equations (A.9), (A.4) into (A.20) yields:

$$\begin{aligned} \{X_b\} &= [h_{i_b i_b}]\{F_b\} + [h_{i_b c_b}]\{F_{c_b}\} - \\ & [h_{i_b c_b}][B]^{-1}([h_{c_b i_b}]\{F_b\} - [h_{c_a i_a}]\{F_a\} + [h_{c_b c_b}]\{F_{c_b}\}) \end{aligned} \quad (\text{A.32})$$

Comparing equation (A.32) with equation (A.1) yields:

$$[H_{i_b i_a}] = [h_{i_b c_b}][B]^{-1}[h_{c_a i_a}] \quad (\text{A.33})$$

$$[H_{i_b c_b}] = [h_{i_b c_b}] - [h_{i_b c_b}][B]^{-1}[h_{c_b c_b}] \quad (\text{A.34})$$

$$[H_{b c_a}] = [0] \quad (\text{A.35})$$

$$[H_{i_b i_b}] = [h_{i_b i_b}] - [h_{i_b c_b}][B]^{-1}[h_{c_b i_b}] \quad (\text{A.36})$$

Substituting equations (A.9), (A.4) into (A.21) yields:

$$\begin{aligned} \{X_{c_b}\} &= [h_{c_b i_b}]\{F_b\} + [h_{c_b c_b}]\{F_{c_b}\} - \\ & [h_{c_b c_b}][B]^{-1}([h_{c_b i_b}]\{F_b\} - [h_{c_a i_a}]\{F_a\} + [h_{c_b c_b}]\{F_{c_b}\}) \end{aligned} \quad (\text{A.37})$$

Comparing equation (A.37) with equation (A.1) yields:

$$[H_{c_b i_a}] = [h_{c_b c_b}][B]^{-1}[h_{c_a i_a}] \quad (\text{A.38})$$

$$[H_{c_b c_a}] = [h_{c_b c_b}] - [h_{c_b c_b}][B]^{-1}[h_{c_b c_b}] \quad (\text{A.39})$$

$$[H_{c_b c_b}] = [0] \quad (\text{A.40})$$

$$[H_{c_b i_b}] = [h_{c_b i_b}] - [h_{c_b c_b}][B]^{-1}[h_{c_b i_b}] \quad (\text{A.41})$$

Substituting Equations (A.23) to (A.26), (A.28) to (A.31), (A.33) to (A.36), (A.38) to (A.41) into (A.1) yields the refined formulation of FRF Coupling as follows:

$$\begin{Bmatrix} X_{i_a} \\ X_{c_a} \\ X_{c_b} \\ X_{i_b} \end{Bmatrix} = \begin{bmatrix} h_{i_a i_a} & h_{i_a c_a} & 0 & 0 \\ h_{c_a i_a} & h_{c_a c_a} & 0 & 0 \\ 0 & 0 & h_{c_b c_b} & h_{c_b i_b} \\ 0 & 0 & h_{i_b c_b} & h_{i_b i_b} \end{bmatrix} - \begin{Bmatrix} h_{i_a c_a} \\ h_{c_a c_a} \\ h_{c_b c_b} \\ h_{i_b c_a} \end{Bmatrix} [h_{c_a c_a} + h_{c_b c_b}]^{-1} \begin{Bmatrix} h_{i_a c_a} \\ h_{c_a c_a} \\ h_{c_b c_b} \\ h_{i_b c_a} \end{Bmatrix}^T \begin{Bmatrix} F_{i_a} \\ F_{c_a} \\ F_{c_b} \\ F_{i_b} \end{Bmatrix} \quad (\text{A.42})$$

where:

**subscript  $a$**  = substructure a

**subscript  $b$**  = substructure b

**subscript  $i$**  = internal connections

**subscript  $c$**  = coupling connections

# Appendix B

## Local iterations

Consider the equation for this Collected Substructure, relating the displacement vectors and the force vector shown in matrix form as follows:

$$\begin{Bmatrix} x_i \\ x_{\bar{c}} \\ x_{\tilde{c}} \end{Bmatrix} = \begin{bmatrix} H_{ii} & H_{i\bar{c}} & H_{i\tilde{c}} \\ H_{\bar{c}i} & H_{\bar{c}\bar{c}} & H_{\bar{c}\tilde{c}} \\ H_{\tilde{c}i} & H_{\tilde{c}\bar{c}} & H_{\tilde{c}\tilde{c}} \end{bmatrix} \begin{Bmatrix} f_i \\ f_{\bar{c}} \\ f_{\tilde{c}} \end{Bmatrix} \quad (\text{B.1})$$

Looking at the Assembled System, the displacement in each point can be written as:

$$\begin{Bmatrix} X_I \\ X_{\bar{C}} \\ X_{\tilde{C}} \end{Bmatrix} = \begin{bmatrix} H_{II} & H_{I\bar{C}} & H_{I\tilde{C}} \\ H_{\bar{C}I} & H_{\bar{C}\bar{C}} & H_{\bar{C}\tilde{C}} \\ H_{\tilde{C}I} & H_{\tilde{C}\bar{C}} & H_{\tilde{C}\tilde{C}} \end{bmatrix} \begin{Bmatrix} F_I \\ F_{\bar{C}} \\ F_{\tilde{C}} \end{Bmatrix} \quad (\text{B.2})$$

The displacements  $x_i$ ,  $x_{\bar{c}}$ ,  $x_{\tilde{c}}$  can be written as:

$$\{x_i\} = \begin{Bmatrix} x_{i_d} \\ x_{i_u} \end{Bmatrix} \quad \{x_{\bar{c}}\} = \begin{Bmatrix} x_{\bar{c}_d} \\ x_{\bar{c}_u} \end{Bmatrix} \quad \{x_{\tilde{c}}\} = \begin{Bmatrix} x_{\tilde{c}_d} \\ x_{\tilde{c}_u} \end{Bmatrix} \quad (\text{B.3})$$

where:

$i$  = all internal DOFs

$i_d$  = internal DOFs where the response is required

$i_u$  = internal DOFs where the response is not required

$\bar{c}$ ,  $\tilde{c}$  = all connection DOFs

$\bar{c}_d, \tilde{c}_d$  = connection DOFs where the response is required

$\bar{c}_u, \tilde{c}_u$  = connection DOFs where the response is not required

The equation for this Collected Substructure, relating displacement vectors where the response is required and the force vector is shown in matrix form as:

$$\begin{Bmatrix} x_{i_d} \\ x_{\bar{c}_d} \\ x_{\tilde{c}_d} \end{Bmatrix} = \begin{bmatrix} H_{i_d i} & H_{i_d \bar{c}} & H_{i_d \tilde{c}} \\ H_{\bar{c}_d i} & H_{\bar{c}_d \bar{c}} & H_{\bar{c}_d \tilde{c}} \\ H_{\tilde{c}_d i} & H_{\tilde{c}_d \bar{c}} & H_{\tilde{c}_d \tilde{c}} \end{bmatrix} \begin{Bmatrix} f_i \\ f_{\bar{c}} \\ f_{\tilde{c}} \end{Bmatrix} \quad (\text{B.4})$$

Looking at the Assembled System, the displacements where the response is required can be written as:

$$\begin{Bmatrix} X_{I_d} \\ X_{\bar{C}_d} \\ X_{\tilde{C}_d} \end{Bmatrix} = \begin{bmatrix} H_{I_d I} & H_{I_d \bar{C}} & H_{I_d \tilde{C}} \\ H_{\bar{C}_d I} & H_{\bar{C}_d \bar{C}} & H_{\bar{C}_d \tilde{C}} \\ H_{\tilde{C}_d I} & H_{\tilde{C}_d \bar{C}} & H_{\tilde{C}_d \tilde{C}} \end{bmatrix} \begin{Bmatrix} F_I \\ F_{\bar{C}} \\ F_{\tilde{C}} \end{Bmatrix} \quad (\text{B.5})$$

where:

$I_d$  = internal DOFs where the response is desired

$\bar{C}_d, \tilde{C}_d$  = connection DOFs where the response is desired

The equilibrium conditions can be written as:

$$\begin{aligned} \{F_{\bar{C}}\} &= \{F_{\tilde{C}}\} = \{f_{\bar{c}}\} + \{f_{\tilde{c}}\} \\ \{f_i\} &= \{F_I\} \end{aligned} \quad (\text{B.6})$$

The compatibility conditions can be written in two forms:

$$\begin{aligned} \{x_{i_d}\} &= \{X_{I_d}\} \\ \{x_{\bar{c}_d}\} &= \{X_{\bar{C}_d}\} \\ \{x_{\tilde{c}_d}\} &= \{X_{\tilde{C}_d}\} \\ \{x_{\bar{c}}\} - \{x_{\tilde{c}}\} &= -[\mathbf{G}_{\bar{c}\tilde{c}}]^{-1} \{f_{\bar{c}}\} \end{aligned} \quad (\text{B.7})$$

or

$$\begin{aligned} \{x_{i_d}\} &= \{X_{I_d}\} \\ \{x_{\bar{c}_d}\} &= \{X_{\bar{C}_d}\} \\ \{x_{\tilde{c}_d}\} &= \{X_{\tilde{C}_d}\} \\ \{x_{\bar{c}} - x_{\tilde{c}}\} &= -[\mathbf{G}_{\bar{c}\tilde{c}}]^{-1} \{f_{\bar{c}}\} \end{aligned} \quad (\text{B.8})$$

Substituting equations (B.1) into (B.7) yields:

$$H_{\bar{c}i}f_i + H_{\bar{c}\bar{c}}f_{\bar{c}} + H_{\bar{c}\bar{c}}f_{\bar{c}} - H_{\bar{c}i}f_i - H_{\bar{c}\bar{c}}f_{\bar{c}} - H_{\bar{c}\bar{c}}f_{\bar{c}} + f_{\bar{c}}/\mathbf{G}_{\bar{c}\bar{c}} = 0 \quad (\text{B.9})$$

Substituting the equilibrium equations (B.6) into (B.9) yields:

$$H_{\bar{c}i}F_I + H_{\bar{c}\bar{c}}f_{\bar{c}} + H_{\bar{c}\bar{c}}(F_{\bar{C}} - f_{\bar{c}}) - H_{\bar{c}i}F_I - H_{\bar{c}\bar{c}}f_{\bar{c}} - H_{\bar{c}\bar{c}}(F_{\bar{C}} - f_{\bar{c}}) + f_{\bar{c}}/\mathbf{G}_{\bar{c}\bar{c}} = 0 \quad (\text{B.10})$$

Isolating the force of the collected substructure in terms of the force of the assembled system yields:

$$f_{\bar{c}} = (B)^{-1}\{(H_{\bar{c}i} - H_{\bar{c}i})F_I + (H_{\bar{c}\bar{c}} - H_{\bar{c}\bar{c}})F_{\bar{C}}\} \quad (\text{B.11})$$

$$f_{\bar{c}} = (1 - (B)^{-1})(H_{\bar{c}\bar{c}} - H_{\bar{c}\bar{c}})F_{\bar{C}} - (B)^{-1}(H_{\bar{c}i} - H_{\bar{c}i})F_I \quad (\text{B.12})$$

where:

$$B = H_{\bar{c}\bar{c}} + H_{\bar{c}\bar{c}} + 1/\mathbf{G}_{\bar{c}\bar{c}} - H_{\bar{c}\bar{c}} - H_{\bar{c}\bar{c}} \quad (\text{B.13})$$

Substituting equations (B.1) into (B.8) yields:

$$H_{\bar{c}i}f_i + H_{\bar{c}\bar{c}}f_{\bar{c}} + H_{\bar{c}\bar{c}}f_{\bar{c}} - H_{\bar{c}i}f_i - H_{\bar{c}\bar{c}}f_{\bar{c}} - H_{\bar{c}\bar{c}}f_{\bar{c}} + f_{\bar{c}}/\mathbf{G}_{\bar{c}\bar{c}} = 0 \quad (\text{B.14})$$

Substituting the equilibrium equations (B.6) into (B.14) yields:

$$H_{\bar{c}i}F_I + H_{\bar{c}\bar{c}}(F_{\bar{C}} - f_{\bar{c}}) + H_{\bar{c}\bar{c}}f_{\bar{c}} - H_{\bar{c}i}F_I - H_{\bar{c}\bar{c}}(F_{\bar{C}} - f_{\bar{c}}) - H_{\bar{c}\bar{c}}f_{\bar{c}} + f_{\bar{c}}/\mathbf{G}_{\bar{c}\bar{c}} = 0 \quad (\text{B.15})$$

Isolating the force of the collected substructure in terms of the force of the assembled system yields

$$f_{\bar{c}} = (B)^{-1}\{(H_{\bar{c}i} - H_{\bar{c}i})F_I + (H_{\bar{c}\bar{c}} - H_{\bar{c}\bar{c}})F_{\bar{C}}\} \quad (\text{B.16})$$

$$f_{\bar{c}} = (1 - (B)^{-1})(H_{\bar{c}\bar{c}} - H_{\bar{c}\bar{c}})F_{\bar{C}} - (B)^{-1}(H_{\bar{c}i} - H_{\bar{c}i})F_I \quad (\text{B.17})$$

Equation (B.4), can be written as:

$$\{x_{i_d}\} = [H_{i_d i}]\{f_i\} + [H_{i_d \bar{c}}]\{f_{\bar{c}}\} + [H_{i_d \bar{c}}]\{f_{\bar{c}}\} \quad (\text{B.18})$$

$$\{x_{\bar{c}_d}\} = [H_{\bar{c}_d i}]\{f_i\} + [H_{\bar{c}_d \bar{c}}]\{f_{\bar{c}}\} + [H_{\bar{c}_d \bar{c}}]\{f_{\bar{c}}\} \quad (\text{B.19})$$

$$\{x_{\bar{c}_d}\} = [H_{\bar{c}_d i}]\{f_i\} + [H_{\bar{c}_d \bar{c}}]\{f_{\bar{c}}\} + [H_{\bar{c}_d \bar{c}}]\{f_{\bar{c}}\} \quad (\text{B.20})$$

Substituting equations (B.6), (B.11), (B.12) into (B.18) yields:

$$\begin{aligned} \{X_{I_d}\} &= [H_{i_d i}]\{F_I\} + [H_{i_d \bar{c}}]\{F_{\bar{C}}\} + \\ & \quad ([H_{i_d \bar{c}}] - [H_{i_d \bar{c}}])[B]^{-1}([H_{\bar{c}i}] - [H_{\bar{c}i}])\{F_I\} + \\ & \quad ([H_{i_d \bar{c}}] - [H_{i_d \bar{c}}])[B]^{-1}([H_{\bar{c}\bar{c}}] - [H_{\bar{c}\bar{c}}])\{F_{\bar{C}}\} \end{aligned} \quad (\text{B.21})$$

Comparing equation (B.5) with equation (B.21) yields:

$$[H_{I_d I}] = [H_{i_d i}] - ([H_{i_d \bar{c}}] - [H_{i_d \bar{c}}])[B]^{-1}([H_{\bar{c}i}] - [H_{\bar{c}i}]) \quad (\text{B.22})$$

$$[H_{I_d \bar{C}}] = [H_{i_d \bar{c}}] - ([H_{i_d \bar{c}}] - [H_{i_d \bar{c}}])[B]^{-1}([H_{\bar{c}\bar{c}}] - [H_{\bar{c}\bar{c}}]) \quad (\text{B.23})$$

Substituting equations (B.6), (B.16), (B.17) into (B.18) yields:

$$\begin{aligned} \{X_{I_d}\} &= [H_{i_d i}]\{F_I\} + [H_{i_d \bar{c}}]\{F_{\bar{C}}\} + \\ & \quad ([H_{i_d \bar{c}}] - [H_{i_d \bar{c}}])[B]^{-1}([H_{\bar{c}i}] - [H_{\bar{c}i}])\{F_I\} + \\ & \quad ([H_{i_d \bar{c}}] - [H_{i_d \bar{c}}])[B]^{-1}([H_{\bar{c}\bar{c}}] - [H_{\bar{c}\bar{c}}])\{F_{\bar{C}}\} \end{aligned} \quad (\text{B.24})$$

Comparing equation (B.2) with equation (B.24) yields:

$$[H_{I_d I}] = [H_{i_d i}] - ([H_{i_d \bar{c}}] - [H_{i_d \bar{c}}])[B]^{-1}([H_{\bar{c}i}] - [H_{\bar{c}i}]) \quad (\text{B.25})$$

$$[H_{I_d \bar{C}}] = [H_{i_d \bar{c}}] - ([H_{i_d \bar{c}}] - [H_{i_d \bar{c}}])[B]^{-1}([H_{\bar{c}\bar{c}}] - [H_{\bar{c}\bar{c}}]) \quad (\text{B.26})$$

Substituting equations (B.6), (B.11), (B.12), into (B.19) yields:

$$\begin{aligned} \{X_{\bar{C}_d}\} &= [H_{\bar{c}_d i}]\{F_I\} + [H_{\bar{c}_d \bar{c}}]\{F_{\bar{C}}\} + \\ & \quad ([H_{\bar{c}_d \bar{c}}] - [H_{\bar{c}_d \bar{c}}])[B]^{-1}([H_{\bar{c}i}] - [H_{\bar{c}i}])\{F_I\} + \\ & \quad ([H_{\bar{c}_d \bar{c}}] - [H_{\bar{c}_d \bar{c}}])[B]^{-1}([H_{\bar{c}\bar{c}}] - [H_{\bar{c}\bar{c}}])\{F_{\bar{C}}\} \end{aligned} \quad (\text{B.27})$$

Comparing equation (B.27) with equation (B.5) yields:

$$[H_{\bar{C}_d I}] = [H_{\bar{c}_d i}] - ([H_{\bar{c}_d \bar{c}}] - [H_{\bar{c}_d \bar{c}}])[B]^{-1}([H_{\bar{c}i}] - [H_{\bar{c}i}]) \quad (\text{B.28})$$

$$[H_{\bar{C}_d \bar{C}}] = [H_{\bar{c}_d \bar{c}}] - ([H_{\bar{c}_d \bar{c}}] - [H_{\bar{c}_d \bar{c}}])[B]^{-1}([H_{\bar{c}\bar{c}}] - [H_{\bar{c}\bar{c}}]) \quad (\text{B.29})$$

Substituting equations (B.6), (B.16), (B.17) into (B.19) yields:

$$\begin{aligned} \{X_{\bar{C}_d}\} &= [H_{\bar{c}_d i}]\{F_I\} + [H_{\bar{c}_d \bar{c}}]\{F_{\bar{C}}\} + \\ & \quad ([H_{\bar{c}_d \bar{c}}] - [H_{\bar{c}_d \bar{c}}])[B]^{-1}([H_{\bar{c}i}] - [H_{\bar{c}i}])\{F_I\} + \\ & \quad ([H_{\bar{c}_d \bar{c}}] - [H_{\bar{c}_d \bar{c}}])[B]^{-1}([H_{\bar{c}\bar{c}}] - [H_{\bar{c}\bar{c}}])\{F_{\bar{C}}\} \end{aligned} \quad (\text{B.30})$$

Comparing equation (B.5) with equation (B.30) yields:

$$[H_{\bar{C}_d I}] = [H_{\bar{c}_d i}] - ([H_{\bar{c}_d \bar{c}}] - [H_{\bar{c}_d \bar{c}}])[B]^{-1}([H_{\bar{c}i}] - [H_{\bar{c}i}]) \quad (\text{B.31})$$

$$[H_{\bar{C}_d \bar{C}}] = [H_{\bar{c}_d \bar{c}}] - ([H_{\bar{c}_d \bar{c}}] - [H_{\bar{c}_d \bar{c}}])[B]^{-1}([H_{\bar{c}\bar{c}}] - [H_{\bar{c}\bar{c}}]) \quad (\text{B.32})$$

Substituting equations (B.6), (B.11), (B.12) into (B.20) yields:

$$\begin{aligned} \{X_{\tilde{C}_d}\} &= [H_{\tilde{c}_d i}]\{F_I\} + [H_{\tilde{c}_d \bar{c}}]\{F_{\tilde{C}}\} + \\ & \quad ([H_{\tilde{c}_d \bar{c}}] - [H_{\tilde{c}_d \bar{c}}])[B]^{-1}([H_{\tilde{c}i}] - [H_{\tilde{c}i}])\{F_I\} + \\ & \quad ([H_{\tilde{c}_d \bar{c}}] - [H_{\tilde{c}_d \bar{c}}])[B]^{-1}([H_{\tilde{c}\bar{c}}] - [H_{\tilde{c}\bar{c}}])\{F_{\tilde{C}}\} \end{aligned} \quad (\text{B.33})$$

Comparing equation (B.5) with equation (B.33) yields:

$$[H_{\tilde{C}_d I}] = [H_{\tilde{c}_d i}] - ([H_{\tilde{c}_d \bar{c}}] - [H_{\tilde{c}_d \bar{c}}])[B]^{-1}([H_{\tilde{c}i}] - [H_{\tilde{c}i}]) \quad (\text{B.34})$$

$$[H_{\tilde{C}_d \tilde{C}}] = [H_{\tilde{c}_d \bar{c}}] - ([H_{\tilde{c}_d \bar{c}}] - [H_{\tilde{c}_d \bar{c}}])[B]^{-1}([H_{\tilde{c}\bar{c}}] - [H_{\tilde{c}\bar{c}}]) \quad (\text{B.35})$$

Substituting equations (B.6), (B.16), (B.17) into (B.20) yields:

$$\begin{aligned} \{X_{\tilde{C}_d}\} &= [H_{i_d i}]\{F_I\} + [H_{\tilde{c}_d \bar{c}}]\{F_{\tilde{C}}\} + \\ & \quad ([H_{\tilde{c}_d \bar{c}}] - [H_{\tilde{c}_d \bar{c}}])[B]^{-1}([H_{\tilde{c}i}] - [H_{\tilde{c}i}])\{F_I\} + \\ & \quad ([H_{\tilde{c}_d \bar{c}}] - [H_{\tilde{c}_d \bar{c}}])[B]^{-1}([H_{\tilde{c}\bar{c}}] - [H_{\tilde{c}\bar{c}}])\{F_{\tilde{C}}\} \end{aligned} \quad (\text{B.36})$$

Comparing equation (B.5) with equation (B.36) yields:

$$[H_{\tilde{C}_d I}] = [H_{i_d i}] - ([H_{\tilde{c}_d \bar{c}}] - [H_{\tilde{c}_d \bar{c}}])[B]^{-1}([H_{\tilde{c}i}] - [H_{\tilde{c}i}]) \quad (\text{B.37})$$

$$[H_{\tilde{C}_d \tilde{C}}] = [H_{\tilde{c}_d \bar{c}}] - ([H_{\tilde{c}_d \bar{c}}] - [H_{\tilde{c}_d \bar{c}}])[B]^{-1}([H_{\tilde{c}\bar{c}}] - [H_{\tilde{c}\bar{c}}]) \quad (\text{B.38})$$

Equations (B.22), (B.23), (B.25), (B.26), (B.28), (B.29), (B.31), (B.32), (B.34), (B.35), (B.37), (B.38), can be arranged as:

$$\begin{aligned} \begin{Bmatrix} X_{I_d} \\ X_{\bar{C}_d} \\ X_{\tilde{C}_d} \end{Bmatrix} &= \begin{pmatrix} \begin{bmatrix} H_{i_d i} & H_{i_d \bar{c}} & H_{i_d \tilde{c}} \\ H_{\bar{c}_d i} & H_{\bar{c}_d \bar{c}} & H_{\bar{c}_d \tilde{c}} \\ H_{\tilde{c}_d i} & H_{\tilde{c}_d \bar{c}} & H_{\tilde{c}_d \tilde{c}} \end{bmatrix} \\ \begin{Bmatrix} (H_{i_d \bar{c}} - H_{i_d \tilde{c}}) \\ (H_{\bar{c}_d \bar{c}} - H_{\bar{c}_d \tilde{c}}) \\ (H_{\tilde{c}_d \bar{c}} - H_{\tilde{c}_d \tilde{c}}) \end{Bmatrix} \end{pmatrix} [H_{\bar{c}\bar{c}} + H_{\tilde{c}\tilde{c}} - H_{\bar{c}\tilde{c}} - H_{\tilde{c}\bar{c}} + 1/\mathbf{g}_{\bar{c}\tilde{c}}]^{-1} \begin{pmatrix} \begin{Bmatrix} (H_{i\bar{c}} - H_{i\tilde{c}}) \\ (H_{\bar{c}\bar{c}} - H_{\bar{c}\tilde{c}}) \\ (H_{\tilde{c}\bar{c}} - H_{\tilde{c}\tilde{c}}) \end{Bmatrix}^T \\ \begin{Bmatrix} F_I \\ F_{\bar{C}} \\ F_{\tilde{C}} \end{Bmatrix} \end{pmatrix} \end{aligned} \quad (\text{B.39})$$

Equation (B.39) can be arranged in a more concise form as:

$$\begin{aligned} \begin{Bmatrix} X_{I_d} \\ X_{C_d} \end{Bmatrix} &= \begin{pmatrix} \begin{bmatrix} H_{i_d i} & H_{i_d c} \\ H_{c_d i} & H_{c_d c} \end{bmatrix} \\ \begin{Bmatrix} (H_{i_d \bar{c}} - H_{i_d \tilde{c}}) \\ (H_{c_d \bar{c}} - H_{c_d \tilde{c}}) \end{Bmatrix} \end{pmatrix} [H_{\bar{c}\bar{c}} + H_{\tilde{c}\tilde{c}} - H_{\bar{c}\tilde{c}} - H_{\tilde{c}\bar{c}} + 1/\mathbf{g}_{\bar{c}\tilde{c}}]^{-1} \begin{pmatrix} \begin{Bmatrix} (H_{i\bar{c}} - H_{i\tilde{c}}) \\ (H_{\bar{c}\bar{c}} - H_{\bar{c}\tilde{c}}) \end{Bmatrix}^T \\ \begin{Bmatrix} F_I \\ F_C \end{Bmatrix} \end{pmatrix} \end{aligned} \quad (\text{B.40})$$

# Appendix C

## Floating-Point Operations in *HANORCA*

### C.1 Basic Concepts

Considering real variables, each multiplication, division, subtraction, addition counts as one flop.

### C.2 Matrix Algebra

#### C.2.1 Matrix Addition and Subtraction

For matrix addition and subtraction the number of operations can be counted using the following expressions:

$$\begin{aligned} A_{xy} + B_{xy} & \text{ counts } x * y \text{ flops} \\ A_{xy} - B_{xy} & \text{ counts } x * y \text{ flops} \end{aligned} \tag{C.1}$$

#### C.2.2 Matrix Multiplication

For matrix multiplication, the number of operations can be counted using the following expression:

$$A_{xy} * B_{yz} \text{ counts } 2 * x * y * z \text{ flops} \tag{C.2}$$

### C.2.3 Matrix Inverse

In order to obtain an approximate expression that gives the number of operations required to find a matrix inverse of order  $n$ , two functions available in MATLAB were used: the inverse matrix function that inverts a matrix of order  $m$  and the flops function that gives the number of floating-point operations (KFLOPS). Varying the order of the matrix from 0 to 500, for each matrix order the MATLAB inverse function algorithm was used and the number of operations required in this process was evaluated using the MATLAB flops function. Then the following expression was fitted to these points:

$$\text{invf}(m) = 2.69066 * m + 5.07287 * m^2 + 1.99589 * m^3 \quad (\text{C.3})$$

where:

$m$  = order of the matrix

The evaluated points and the expression fitted can be seen in figure (C.1).

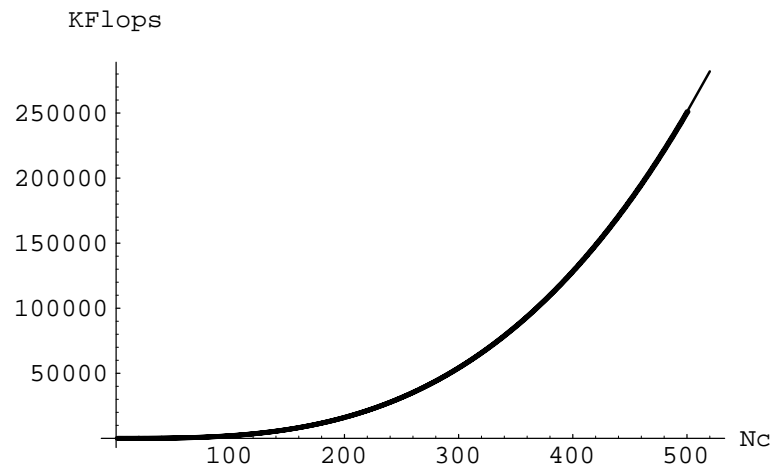


Figure C.1: Fitted curve in INV

### C.2.4 Matrix Inverse using Singular Value Decomposition

In order to obtain an approximate expression that gives the number of operations required to find the singular values with the respective singular vectors of a matrix order  $m$ , two

functions available in MATLAB program were used, the Singular Value decomposition function that gives the singular values with respective eigenvector of a matrix order  $m$  and the flops function that gives the number of floating-point operations (KFLOPS). Varying the order of the matrix from 0 to 500, for each matrix order the MATLAB Singular Value Decomposition function algorithm was used and the number of operations required in this process was evaluated using the MATLAB flops function. Then the following expression was fitted to these points:

$$svdf(m) = -39.2029 * m + 23.739 * m^2 + 16.5502 * m^3 \quad (C.4)$$

where:

$m$  = order of the matrix

The evaluated points and the expression fitted can be seen in figure (C.2).

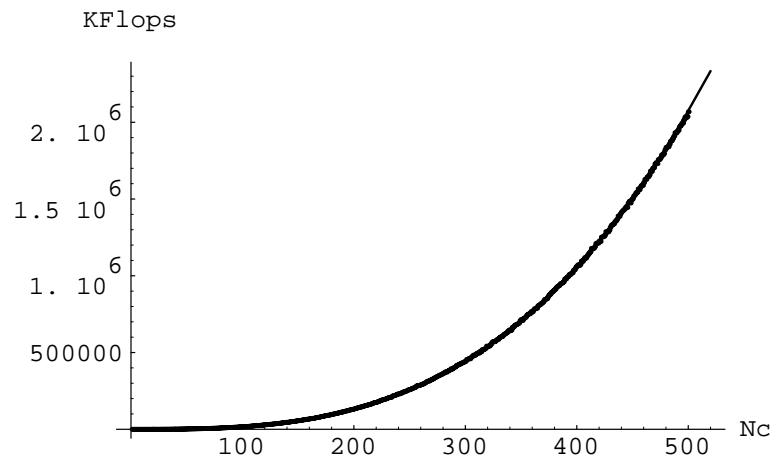


Figure C.2: Fitted curve in SVD

The evaluated points using the expression (C.3), (C.4) can be seen in figure (C.3).

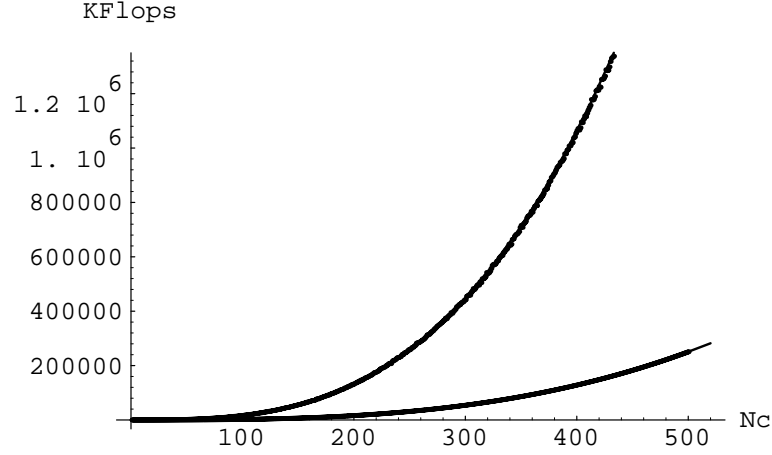


Figure C.3: SVD and INV

### C.2.5 Partitioned Matrix Inverse

The expression that gives the number of operations required for equation (4.107) to find a matrix inverse of order  $m$ , with partition of size  $n$ , is given by the follow expression:

$$invfp(m, n) = xnn + xln + xll \quad (C.5)$$

where:

$xnn = invf(l) + (2 * n * l * l) + (2 * n * l * n) + (n * n) + invf(n)$ , flops related with equation (4.101)

$xll = (2 * l * n * n) + (2 * l * l * n)$ , flops related with equation (4.98)

$xln = (2 * l * n * l) + (l * l)$ , flops related with equation (4.102)

$m$  = order of the matrix  $B$  in equation (4.107)

$n$  = order of the partition  $B_{nn}$  in equation (4.107)

$l = m - n$ , order of the partition  $B_{ll}$  in equation (4.107)

$invf$  = function that gives the number of operation for inverse a matrix, equation (C.3)

The evaluated points using the expression (C.3) and (C.5) can be seen in figure (C.4).

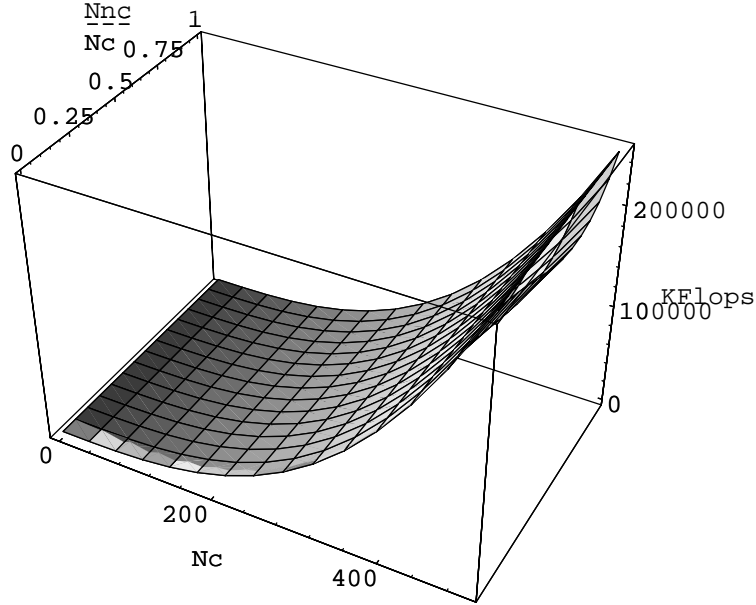


Figure C.4: INV partitioned

## C.2.6 Partitioned Matrix Inverse using Singular Value Decomposition

The expression that gives the number of operations required for equation (4.107) to find a matrix inverse of order  $m$ , with partition of size  $n$  using the singular value decomposition algorithm to invert the matrices, is given by the follow expression:

$$svdfp(m, n) = xnn + xln + xll \quad (C.6)$$

where:

$$xnn = invf(l) + (2 * n * l * l) + (2 * n * l * n) + (n * n) + svdf(n), \text{ flops related with equation (4.101)}$$

$$xll = (2 * l * n * n) + (2 * l * l * n), \text{ flops related with equation (4.98)}$$

$$xln = (2 * l * n * l) + (l * l), \text{ flops related with equation (4.102)}$$

$$m = \text{order of the matrix } B \text{ in equation (4.107)}$$

$n$  = order of the partition  $B_{nn}$  in equation (4.107)

$l = m - n$ , order of the partition  $B_{ll}$  in equation (4.107)

$svdf$  = function that gives the number of operation for inverse a matrix, equation (C.4)

The evaluated points using the expression (C.3), (C.5), (C.4), (C.6), can be seen in figure (C.5).

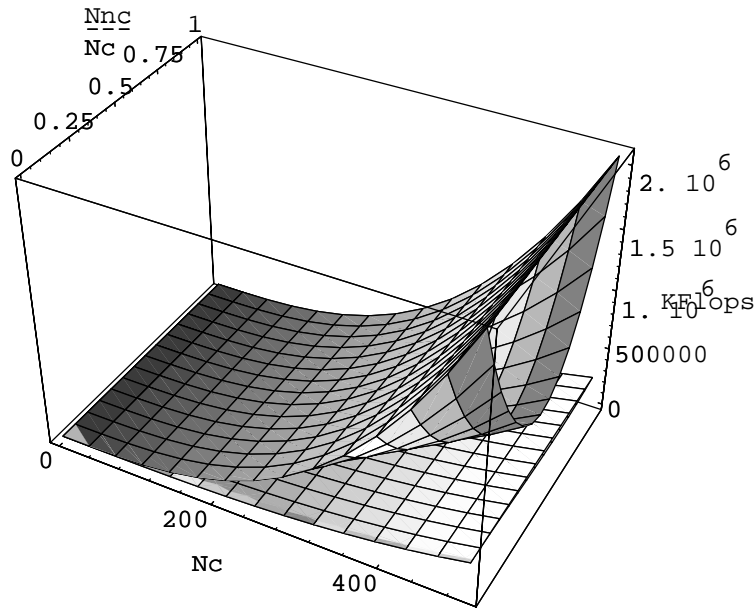


Figure C.5: SVD and INV partitioned

### C.2.7 Partitioned Matrix Inverse using Singular Value Decomposition for HANORCA

The expression that gives the number of operations required for equation (4.107) to find a matrix inverse of order  $m$ , with partition of size  $n$ , with  $n_i$  iteration knowing that just the  $B_{nn}$  submatrix varies during the process and using the singular value decomposition algorithm to invert the matrices is given by the follow expression:

$$svdfpr(m, n, n_i) = svdf(l) + n_i * (xnni + xln + xll) \quad (C.7)$$

where:

$svdf(l)$  = flops related with expression  $[B_{ll}]^{-1}$  in equation (4.101)

$xnni = (2 * n * l * l) + (2 * n * l * n) + (n * n) + invf(n)$ , flops related with expression  $[B_{ll}]^{-1}[B_{ln}][\mathcal{X}_{nn}][B_{nl}][B_{ll}]^{-1}$  in equation (4.101)

$xln = (2 * l * n * n) + (2 * l * l * n)$ , flops related with equation (4.98)

$xll = (2 * l * n * l) + (l * l)$ , flops related with equation (4.102)

$m$  = order of the matrix  $B$  in equation (4.107)

$n$  = order of the partition  $B_{nn}$  in equation (4.107)

$l = m - n$ , order of the partition  $B_{ll}$  in equation (4.107)

$svdf$  = function that gives the number of operation for inverse a matrix, equation (C.4)

$n_i$  = number of iterations

It is possible to see from equation (C.7) that the inverse of matrix  $B_{ll}$  is going to be calculated just once because this partitioned matrix does not change during the iteration process.

### C.3 KFLOPS in Traditional Impedance Method

The Traditional Impedance Method (TIM) [131] in its general equation to be solved is known as:

$$X = ([HA]^{-1} + [HB]^{-1} + [G_{nj}])^{-1} * F \quad (C.8)$$

The expression that gives the number of operations is dependent on the order of the system  $m$ , the number of connections  $\bar{c}$  that is the same order of  $\bar{c}$ , the number of nonlinear connections  $n$ , and the number of iterations  $n_i$ , and is given by the follow expression:

$$\begin{aligned} TIM(m, \bar{c}, n, n_i) = n_i * (2 * svdf(mab) + \\ 2 * (mab * mab) + svdf(ms) + (2 * ms * ms * 1) + n * 1 + 4 * n) \end{aligned} \quad (C.9)$$

where:

$(\bar{c})$  = number of connections

$(n)$  = number of nonlinear connections

$(l)$  =  $\bar{c} - n$ , number of linear connections

$(iab)$  =  $(m - 2 * l - 2 * n)/2$ , order of the non-connection coordinates of system  $A$  and  $B$

$(mab)$  =  $l + n + iab$ , order of the system  $A$  and  $B$

$(ms)$  =  $2 * n + 2 * iab + l$ , order of the system  $A$  and  $B$

$(2 * svdf(mab))$  = related with the two inverse  $(HA)^{-1}$  and  $(HB)^{-1}$

$(2 * mab * mab)$  = related with the addition of  $(HA)^{-1}$  and  $(HB)^{-1}$

$(svdf(ms))$  = related with the calculation of  $((HA)^{-1} + (HB)^{-1})^{-1}$  by equation (C.4)

$(2 * ms * ms * 1)$  = related with the multiplication between

$$((HA)^{-1} + (HB)^{-1})^{-1} \text{ and } F$$

$(n * 1)$  = related with the subtraction between  $x_{\bar{c}_n}$  and  $x_{\bar{c}_n}$  to use in describing function

$(4 * n)$  = related with the addition of the nonlinear part from describing function  $G_{nj}$  in  $(HA)^{-1} + (HB)^{-1}$

## C.4 KFLOPS in HANORCA in General Equation

The HANORCA in general equation (4.81) to be solved can be written in a more concise form as:

$$X = (A - B * [C + 1/G_{nj}]^{-1} * B^T) * F \quad (\text{C.10})$$

The expression that gives the number of operations is dependent on the order of the system  $m$ , the number of connections  $\bar{c}$  that is the same order of  $\bar{c}$ , the number of nonlinear connections  $n$  and the number of iterations  $n_i$ , and is given by the follow expression:

$$\begin{aligned} HANORCA(m, \bar{c}, n, n_i) = n_i * ((m * m) + (2 * m * \bar{c} * \bar{c}) + \\ (2 * m * \bar{c} * m) + (2 * m * m * 1) + (n * 1) + (svdf(\bar{c})) + (n * 1)) \end{aligned} \quad (\text{C.11})$$

where:

$(m * m)$  = related with the difference between  $A$  and  $(B * C^{-1} * B^T)$

$(2 * m * \bar{c} * \bar{c})$  = related with the multiplication between  $B$  and  $C^{-1}$

$(2 * m * \bar{c} * m)$  = related with the multiplication between  $(B * C^{-1})$  and  $B^T$

$(2 * m * m * 1)$  = related with the multiplication between  
 $(A - (B * C^{-1} * B^T))$  and  $F$

$(n * 1)$  = related with the subtraction between  $x_{\bar{c}_n}$  and  $x_{\tilde{c}_n}$  to use in describing function

$(svdf(\bar{c}))$  = related with the calculation of  $C^{-1}$  by equation (C.4)

$(n * 1)$  = related with the addition of the nonlinear part from describing function  $G_{nj}$  in  $C$

## C.5 KFLOPS in HANORCA considering local iterations refinements in response desired coordinate

The local iteration algorithm included the improvements developed to reduce the number of operations during the iteration process relative to the nonlinear coordinates  $X_{c_n}$ . The HANORCA local iterations equation (4.118) to be solved can be written in a more concise form as:

$$X_{c_n} = (A_{r_n} - B_{r_n} * [C + 1/G_{nj}]^{-1} * B^T) * F \quad (\text{C.12})$$

where:

$X_{c_n}$  = response only in nonlinear connection coordinates

$r_n$  = refined considering the nonlinear coordinates involved in the process

After it converges, it is possible to calculate the desired response in all coordinates as follows:

$$X = (A - B * [C + 1/G_{nj}]^{-1} * B^T) * F \quad (\text{C.13})$$

where:

$X$  = response in all coordinates

The expression that gives the number of operations is dependent on the order of the system  $m$ , the number of connections  $\bar{c}$  that is the same order of  $\tilde{c}$ , the number of nonlinear

connections  $n$ , and the number of iterations  $n_i$ , and is given by the follow expression:

$$\begin{aligned} HANORCA(m, c, n, n_i) = & n_i * ((c_n * m) + (2 * c_n * \bar{c} * \bar{c}) + \\ & (2 * c_n * \bar{c} * m) + (2 * c_n * m * 1) + (n * 1) + \\ & (svdf(\bar{c})) + (n * 1)) + x_t \end{aligned} \quad (C.14)$$

where:

$(c_n * m)$  = related with the difference between  $A_{r_n}$  and  $(B_{r_n} * C^{-1} * B^T)$

$(2 * c_n * \bar{c} * \bar{c})$  = related with the multiplication between  $B_{r_n}$  and  $C^{-1}$

$(2 * c_n * \bar{c} * m)$  = related with the multiplication between  $(B_{r_n} * C^{-1})$  and  $B^T$

$(2 * c_n * m * 1)$  = related with the multiplication between

$(A_{r_n} - (B_{r_n} * C^{-1} * B^T))$  and  $F$

$(n * 1)$  = related with the subtraction between  $x_{\bar{c}_n}$  and  $x_{\bar{c}_n}$  to use in describing function

$(svdf(\bar{c}))$  = related with the calculation of  $C^{-1}$  by equation (C.4)

$(n * 1)$  = related with the addition of the nonlinear part from describing function  $G_{nj}$  in  $C$

$x_t = (m * m) + (2 * m * \bar{c} * \bar{c}) + (2 * m * \bar{c} * m) + (2 * m * m * 1)$ , flops related with equation C.13

$n$  = number of nonlinear connection

$c_n = 2 * n$ , number of nonlinear connection coordinates

## C.6 KFLOPS in HANORCA considering local iterations refinements in response desired and excitation force coordinates

The local iteration algorithm included both improvements developed to reduce the number of operations during the iterations process, one related to the nonlinear coordinates,  $X_{c_n}$ , and the other relative with the excitation coordinates,  $F_{r_f}$ . The HANORCA equation

(4.118) to be solved using the local iteration refinements can be written in a more concise form as:

$$X_{c_n} = (A_{r_n} - B_{r_n} * [C + 1/G_{nj}]^{-1} * B_{r_f}^T) * F_{r_f} \quad (\text{C.15})$$

where:

$X_{c_n}$  = response only in nonlinear connection coordinates

$r_n$  = refined considering the nonlinear coordinates involved in the process

$r_f$  = refined considering the excitation coordinates involved in the process

After it converges, it is possible to calculate the desired response in all coordinates:

$$X = (A - B * [C + 1/G_{nj}]^{-1} * B_{r_f}^T) * F_{r_f} \quad (\text{C.16})$$

where:

$X$  = response in all coordinates

$r_f$  = refined considering the excitation coordinates involved in the process

The expression that gives the number of operations is dependent on the order of the system,  $m$ , the number of connections  $\bar{c}$  that is the same order of  $\tilde{c}$ , the number of nonlinear connections,  $n$ , the number of excitation points,  $c_f$  and the number of iterations,  $n_i$ , and is given by the follow expression:

$$\begin{aligned} \text{HANORCA}(m, c, n, n_i) = & n_i * ((c_n * c_f) + (2 * c_n * \bar{c} * \bar{c}) + \\ & (2 * c_n * \bar{c} * c_f) + (2 * c_n * c_f * 1) + (n * 1) + \\ & (\text{svdf}(\bar{c})) + (n * 1)) + x_t \end{aligned} \quad (\text{C.17})$$

where:

$(c_n * c_f)$  = related with the difference between  $A_{r_n}$  and  $(B_{r_n} * C^{-1} * B_{r_f}^T)$

$(2 * c_n * \bar{c} * \bar{c})$  = related with the multiplication between  $B$  and  $C^{-1}$

$(2 * c_n * \bar{c} * c_f)$  = related with the multiplication between  $(B * C^{-1})$  and  $B^T$

$(2 * c_n * c_f * 1)$  = related with the multiplication between

$(A_{r_n} - (B_{r_n} * C^{-1} * B_{r_f}^T))$  and  $F_{r_f}$

- $(\bar{c} * 1)$  = related with the subtraction between  $x_{\bar{c}_n}$  and  $x_{\bar{c}_n}$  to use in describing function
- $(svdf(\bar{c}))$  = related with the calculation of  $C^{-1}$  by equation (C.4)
- $(n * 1)$  = related with the addition of the nonlinear part from describing function  $G_{nj}$  in  $C$
- $x_t = (m * c_f) + (2 * m * \bar{c} * \bar{c}) + (2 * m * \bar{c} * c_f) + (2 * m * c_f * 1)$ , flops related with equation C.16
- $n$  = number of nonlinear connection
- $c_n = 2 * n$ , number of nonlinear connection coordinates

## C.7 KFLOPS in refined HANORCA equation

The refined HANORCA equation included all the improvements developed to reduce the number of operations during the whole process, one relative to the nonlinear coordinates  $X_{c_n}$ , another relative to the excitation coordinates,  $F_{r_f}$ , and another relative with the partition of the matrix to be inverted,  $C$ . The refined HANORCA in equation (4.118) using partitioned inverse matrix equation (4.107) can be written in a more concise form as:

$$X_{c_n} = (A_{r_n} - B_{r_n} * [C + 1/G_{nj}]^{-1} * B_{r_f}^T) * F_{r_f} \quad (\text{C.18})$$

where:

$X_{c_n}$  = response only in nonlinear connection coordinates

$r_n$  = refined considering the nonlinear coordinates involved in the process

$r_f$  = refined considering the excitation coordinates involved in the process

After it converges, it is possible to calculate the desired response in all coordinates as follows:

$$X = (A - B * [C + 1/G_{nj}]^{-1} * B_{r_f}^T) * F_{r_f} \quad (\text{C.19})$$

where:

$X$  = response in all coordinates

$r_f$  = refined considering the excitation coordinates involved in the process

The expression that gives the number of operations is dependent on the order of the system  $m$ , the number of connections  $\bar{c}$  that is the same order of  $\bar{c}$ , the number of nonlinear connections  $n$ , the number of excitation points  $c_f$  and the number of iterations  $n_i$ , and is given by the follow expression:

$$\begin{aligned} HANORCA_r(m, c, n, n_i) = & n_i * ((c_n * c_f) + (2 * c_n * \bar{c} * \bar{c}) + \\ & (2 * c_n * \bar{c} * c_f) + (2 * c_n * c_f * 1) + (n * 1) + \\ & (svdfp(\bar{c}, c_n, n_i)) + (n * 1)) + x_t \end{aligned} \quad (C.20)$$

where:

$(c_n * c_f)$  = related with the difference between  $A$  and  $(B * C^{-1} * B^T)$

$(2 * c_n * \bar{c} * \bar{c})$  = related with the multiplication between  $B$  and  $C^{-1}$

$(2 * c_n * \bar{c} * c_f)$  = related with the multiplication between  $(B * C^{-1})$  and  $B^T$

$(2 * c_n * c_f * 1)$  = related with the multiplication between  
 $(A - (B * C^{-1} * B^T))$  and  $F$

$(\bar{c} * 1)$  = related with the subtraction between  $x_{\bar{c}_n}$  and  $x_{\bar{c}_n}$  to use in describing function

$(svdfp(\bar{c}, c_n, n_i))$  = related with the calculation of  $C^{-1}$  by equation (C.6)

$(n * 1)$  = related with the addition of the nonlinear part from describing function  $G_{nj}$  in  $C$

$x_t = (m * c_f) + (2 * m * \bar{c} * \bar{c}) + (2 * m * \bar{c} * c_f) + (2 * m * c_f * 1)$ , flops related with equation  
C.19

$(n * 1)$  = number of nonlinear connection coordinates

$(n * 1) = 2 * n$ , number of nonlinear coordinates

# Appendix D

## Multi-Harmonic Nonlinear Receptance Coupling using Multi-Harmonic Describing Function

Assuming that all the substructures to be connected and the assembled system are as presented in section 4.2 . The equation of the Collected Substructure, relating the displacement vector and the force vector for  $n$  harmonics for the displacement and  $m$  harmonics for the force is shown in matrix form as:

$$\begin{pmatrix} x_i^1 \\ x_c^1 \\ x_c^1 \\ x_i^2 \\ x_c^2 \\ x_c^2 \\ \vdots \\ x_i^n \\ x_c^n \\ x_c^n \end{pmatrix} = \begin{bmatrix} H_{ii}^{11} & H_{ic}^{11} & H_{ic}^{11} & \cdots & H_{ii}^{1m} & H_{ic}^{1m} & H_{ic}^{1m} \\ & \vdots & & \ddots & & \vdots & \\ H_{ii}^{n1} & H_{ic}^{n1} & H_{ic}^{n1} & \cdots & H_{ii}^{nm} & H_{ic}^{nm} & H_{ic}^{nm} \\ H_{ci}^{11} & H_{cc}^{11} & H_{cc}^{11} & \cdots & H_{ci}^{1m} & H_{cc}^{1m} & H_{cc}^{1m} \\ & \vdots & & \ddots & & \vdots & \\ H_{ci}^{n1} & H_{cc}^{n1} & H_{cc}^{n1} & \cdots & H_{ci}^{nm} & H_{cc}^{nm} & H_{cc}^{nm} \\ H_{ci}^{11} & H_{cc}^{11} & H_{cc}^{11} & \cdots & H_{ci}^{1m} & H_{cc}^{1m} & H_{cc}^{1m} \\ & \vdots & & \ddots & & \vdots & \\ H_{ci}^{n1} & H_{cc}^{n1} & H_{cc}^{n1} & \cdots & H_{ci}^{nm} & H_{cc}^{nm} & H_{cc}^{nm} \end{bmatrix} \begin{pmatrix} f_i^1 \\ f_c^1 \\ f_c^1 \\ f_i^2 \\ f_c^2 \\ f_c^2 \\ \vdots \\ f_i^n \\ f_c^n \\ f_c^n \end{pmatrix} \quad (D.1)$$

For the Assembled System, the displacement in each point can be written as:

$$\begin{pmatrix} X_I^1 \\ X_{\bar{C}}^1 \\ X_{\bar{C}}^1 \\ X_I^2 \\ X_{\bar{C}}^2 \\ X_{\bar{C}}^2 \\ X_{\bar{C}}^2 \\ \vdots \\ X_I^n \\ X_{\bar{C}}^n \\ X_{\bar{C}}^n \end{pmatrix} = \begin{bmatrix} H_{II}^{11} & H_{I\bar{C}}^{11} & H_{\bar{C}\bar{C}}^{11} & \cdots & H_{II}^{1m} & H_{I\bar{C}}^{nm} & H_{\bar{C}\bar{C}}^{1m} \\ & \vdots & & \ddots & & \vdots & \\ H_{II}^{n1} & H_{I\bar{C}}^{n1} & H_{\bar{C}\bar{C}}^{n1} & \cdots & H_{II}^{nm} & H_{I\bar{C}}^{nm} & H_{\bar{C}\bar{C}}^{nm} \\ H_{\bar{C}I}^{11} & H_{\bar{C}\bar{C}}^{11} & H_{\bar{C}\bar{C}}^{11} & \cdots & H_{\bar{C}I}^{1m} & H_{\bar{C}\bar{C}}^{1m} & H_{\bar{C}\bar{C}}^{1m} \\ & \vdots & & \ddots & & \vdots & \\ H_{\bar{C}I}^{n1} & H_{\bar{C}\bar{C}}^{n1} & H_{\bar{C}\bar{C}}^{n1} & \cdots & H_{\bar{C}I}^{nm} & H_{\bar{C}\bar{C}}^{nm} & H_{\bar{C}\bar{C}}^{nm} \\ H_{\bar{C}I}^{11} & H_{\bar{C}\bar{C}}^{11} & H_{\bar{C}\bar{C}}^{11} & \cdots & H_{\bar{C}I}^{1m} & H_{\bar{C}\bar{C}}^{1m} & H_{\bar{C}\bar{C}}^{1m} \\ & \vdots & & \ddots & & \vdots & \\ H_{\bar{C}I}^{n1} & H_{\bar{C}\bar{C}}^{n1} & H_{\bar{C}\bar{C}}^{n1} & \cdots & H_{\bar{C}I}^{nm} & H_{\bar{C}\bar{C}}^{nm} & H_{\bar{C}\bar{C}}^{nm} \end{bmatrix} \begin{pmatrix} F_i^1 \\ F_{\bar{C}}^1 \\ F_{\bar{C}}^1 \\ F_I^2 \\ F_{\bar{C}}^2 \\ F_{\bar{C}}^2 \\ F_{\bar{C}}^2 \\ \vdots \\ F_I^n \\ F_{\bar{C}}^n \\ F_{\bar{C}}^n \end{pmatrix} \quad (D.2)$$

Assuming that all the harmonics order of the displacement can be arranged in a the set called  $Q_r$  and that all the harmonics order of the force can be arranged in a the set called  $Q_s$ . For the displacement harmonic  $n = q_r$  and for the force harmonic  $m = q_s$ , the Collected Substructure equation can be written in a more concise form as:

$$\begin{pmatrix} x_i^{q_r} \\ x_{\bar{c}}^{q_r} \\ x_{\bar{c}}^{q_r} \end{pmatrix} = \begin{bmatrix} H_{ii}^{q_r q_s} & H_{i\bar{c}}^{q_r q_s} & H_{\bar{c}\bar{c}}^{q_r q_s} \\ H_{\bar{c}i}^{q_r q_s} & H_{\bar{c}\bar{c}}^{q_r q_s} & H_{\bar{c}\bar{c}}^{q_r q_s} \\ H_{\bar{c}i}^{q_r q_s} & H_{\bar{c}\bar{c}}^{q_r q_s} & H_{\bar{c}\bar{c}}^{q_r q_s} \end{bmatrix} \begin{pmatrix} f_i^{q_s} \\ f_{\bar{c}}^{q_s} \\ f_{\bar{c}}^{q_s} \end{pmatrix} \quad (D.3)$$

and the Assembled System equation can also be written in a more concise form as:

$$\begin{pmatrix} X_I^{q_r} \\ X_{\bar{C}}^{q_r} \\ X_{\bar{C}}^{q_r} \end{pmatrix} = \begin{bmatrix} H_{II}^{q_r q_s} & H_{I\bar{C}}^{q_r q_s} & H_{\bar{C}\bar{C}}^{q_r q_s} \\ H_{\bar{C}I}^{q_r q_s} & H_{\bar{C}\bar{C}}^{q_r q_s} & H_{\bar{C}\bar{C}}^{q_r q_s} \\ H_{\bar{C}I}^{q_r q_s} & H_{\bar{C}\bar{C}}^{q_r q_s} & H_{\bar{C}\bar{C}}^{q_r q_s} \end{bmatrix} \begin{pmatrix} F_I^{q_s} \\ F_{\bar{C}}^{q_s} \\ F_{\bar{C}}^{q_s} \end{pmatrix} \quad (D.4)$$

The equilibrium conditions can be written as:

$$\begin{aligned} \{F_{\bar{C}}^{q_s}\} &= \{F_{\bar{C}}^{q_s}\} = \{f_{\bar{c}}^{q_s}\} + \{f_{\bar{c}}^{q_s}\} \\ \{f_i^{q_s}\} &= \{F_I^{q_s}\} \end{aligned} \quad (D.5)$$

The compatibility conditions can be written in two forms:

$$\begin{aligned}
\{y_{\tilde{c}\tilde{c}}^{qr}\} &= \{x_{\tilde{c}}^{qr}\} - \{x_{\tilde{c}}^{qr}\} \\
\{x_i^{qr}\} &= \{X_I^{qr}\} \\
\{x_{\tilde{c}}^{qr}\} &= \{X_{\tilde{C}}^{qr}\} \\
\{x_{\tilde{c}}^{qr}\} &= \{X_{\tilde{C}}^{qr}\} \\
\{y_{\tilde{c}\tilde{c}}^{qr}\} &= -[\mathcal{G}_{\tilde{c}\tilde{c}}^{qsqr}]^{-1}\{f_{\tilde{c}}^{qs}\}
\end{aligned} \tag{D.6}$$

or:

$$\begin{aligned}
\{y_{\tilde{c}\tilde{c}}^{qr}\} &= \{x_{\tilde{c}}^{qr}\} - \{x_{\tilde{c}}^{qr}\} \\
\{x_i^{qr}\} &= \{X_I^{qr}\} \\
\{x_{\tilde{c}}^{qr}\} &= \{X_{\tilde{C}}^{qr}\} \\
\{x_{\tilde{c}}^{qr}\} &= \{X_{\tilde{C}}^{qr}\} \\
\{x_{\tilde{c}}^{qr}\} - \{x_{\tilde{c}}^{qr}\} &= -[\mathcal{G}_{\tilde{c}\tilde{c}}^{qsqr}]^{-1}\{f_{\tilde{c}}^{qs}\}
\end{aligned} \tag{D.7}$$

Substituting equations (D.3) into (D.6), yields:

$$[H_{\tilde{c}i}^{qrqs}]\{f_i^{qs}\} + [H_{\tilde{c}\tilde{c}}^{qrqs}]\{f_{\tilde{c}}^{qs}\} + [H_{\tilde{c}\tilde{c}}^{qrqs}]\{f_{\tilde{c}}^{qs}\} - [H_{\tilde{c}i}^{qrqs}]\{f_i^{qs}\} - [H_{\tilde{c}\tilde{c}}^{qrqs}]\{f_{\tilde{c}}^{qs}\} - [H_{\tilde{c}\tilde{c}}^{qrqs}]\{f_{\tilde{c}}^{qs}\} + [\mathcal{G}_{\tilde{c}\tilde{c}}^{qsqr}]^{-1}\{f_{\tilde{c}}^{qs}\} = 0 \tag{D.8}$$

Substituting the equilibrium equations (D.5) into (D.8), yields:

$$\begin{aligned}
&[H_{\tilde{c}i}^{qrqs}]\{F_I^{qs}\} + [H_{\tilde{c}\tilde{c}}^{qrqs}]\{f_{\tilde{c}}^{qs}\} + [H_{\tilde{c}\tilde{c}}^{qrqs}](\{F_{\tilde{C}}^{qs}\} - \{f_{\tilde{c}}^{qs}\}) - [H_{\tilde{c}i}^{qrqs}]\{F_I^{qs}\} - \\
&- [H_{\tilde{c}\tilde{c}}^{qrqs}]\{f_{\tilde{c}}^{qs}\} - [H_{\tilde{c}\tilde{c}}^{qrqs}](\{F_{\tilde{C}}^{qs}\} - \{f_{\tilde{c}}^{qs}\}) + [\mathcal{G}_{\tilde{c}\tilde{c}}^{qsqr}]^{-1}\{f_{\tilde{c}}^{qs}\} = 0
\end{aligned} \tag{D.9}$$

Isolating the Collected Substructure force  $\{f\}$  in terms of the Assembled System force  $\{F\}$ , yields:

$$\{f_{\tilde{c}}^{qs}\} = [B]^{-1}\{([H_{\tilde{c}i}^{qrqs}] - [H_{\tilde{c}i}^{qrqs}])\{F_I^{qs}\} + ([H_{\tilde{c}\tilde{c}}^{qrqs}] - [H_{\tilde{c}\tilde{c}}^{qrqs}])\{F_{\tilde{C}}^{qs}\}\} \tag{D.10}$$

$$\{f_{\tilde{c}}^{qs}\} = ([I] - [B]^{-1}([H_{\tilde{c}\tilde{c}}^{qrqs}] - [H_{\tilde{c}\tilde{c}}^{qrqs}]))\{F_{\tilde{C}}^{qs}\} - [B]^{-1}([H_{\tilde{c}i}^{qrqs}] - [H_{\tilde{c}i}^{qrqs}])\{F_I^{qs}\} \tag{D.11}$$

where matrix  $B$  is given by:

$$[B] = [H_{\tilde{c}\tilde{c}}^{qrqs}] + [H_{\tilde{c}\tilde{c}}^{qrqs}] - [H_{\tilde{c}\tilde{c}}^{qrqs}] - [H_{\tilde{c}\tilde{c}}^{qrqs}] + [\mathcal{G}_{\tilde{c}\tilde{c}}^{qsqr}]^{-1} \tag{D.12}$$

Substituting equations (D.3) into (D.7), yields:

$$[H_{\tilde{c}i}^{qrqs}] \{f_i^{qs}\} + [H_{\tilde{c}\tilde{c}}^{qrqs}] \{f_{\tilde{c}}^{qs}\} + [H_{\tilde{c}\tilde{c}}^{qrqs}] \{f_{\tilde{c}}^{qs}\} - [H_{\tilde{c}i}^{qrqs}] \{f_i^{qs}\} - [H_{\tilde{c}\tilde{c}}^{qrqs}] \{f_{\tilde{c}}^{qs}\} - [H_{\tilde{c}\tilde{c}}^{qrqs}] \{f_{\tilde{c}}^{qs}\} + [\mathcal{G}_{\tilde{c}\tilde{c}}^{qsqr}]^{-1} \{f_{\tilde{c}}^{qs}\} = 0 \quad (D.13)$$

Substituting the equilibrium equations (D.5) into (D.13), yields:

$$[H_{\tilde{c}i}^{qrqs}] \{F_I^{qs}\} + [H_{\tilde{c}\tilde{c}}^{qrqs}] (\{F_{\tilde{C}}^{qs}\} - \{f_{\tilde{c}}^{qs}\}) + [H_{\tilde{c}\tilde{c}}^{qrqs}] \{f_{\tilde{c}}^{qs}\} - [H_{\tilde{c}i}^{qrqs}] \{F_I^{qs}\} - [H_{\tilde{c}\tilde{c}}^{qrqs}] (\{F_{\tilde{C}}^{qs}\} - \{f_{\tilde{c}}^{qs}\}) - [H_{\tilde{c}\tilde{c}}^{qrqs}] \{f_{\tilde{c}}^{qs}\} + [\mathcal{G}_{\tilde{c}\tilde{c}}^{qsqr}]^{-1} \{f_{\tilde{c}}^{qs}\} = 0 \quad (D.14)$$

Isolating the internal force in terms of the external force yields:

$$\{f_{\tilde{c}}^{qs}\} = [B]^{-1} \{([H_{\tilde{c}i}^{qrqs}] - [H_{\tilde{c}i}^{qrqs}]) \{F_I^{qs}\} + ([H_{\tilde{c}\tilde{c}}^{qrqs}] - [H_{\tilde{c}\tilde{c}}^{qrqs}]) \{F_{\tilde{C}}^{qs}\}\} \quad (D.15)$$

$$\{f_{\tilde{c}}^{qs}\} = ([I] - [B]^{-1} ([H_{\tilde{c}\tilde{c}}^{qrqs}] - [H_{\tilde{c}\tilde{c}}^{qrqs}]) \{F_{\tilde{C}}^{qs}\} - [B]^{-1} ([H_{\tilde{c}i}^{qrqs}] - [H_{\tilde{c}i}^{qrqs}]) \{F_I^{qs}\} \quad (D.16)$$

Equation (D.3), can be written as:

$$\{x_i^{qr}\} = [H_{ii}^{qrqs}] \{f_i^{qs}\} + [H_{i\tilde{c}}^{qrqs}] \{f_{\tilde{c}}^{qs}\} + [H_{i\tilde{c}}^{qrqs}] \{f_{\tilde{c}}^{qs}\} \quad (D.17)$$

$$\{x_{\tilde{c}}^{qr}\} = [H_{\tilde{c}i}^{qrqs}] \{f_i^{qs}\} + [H_{\tilde{c}\tilde{c}}^{qrqs}] \{f_{\tilde{c}}^{qs}\} + [H_{\tilde{c}\tilde{c}}^{qrqs}] \{f_{\tilde{c}}^{qs}\} \quad (D.18)$$

$$\{x_{\tilde{c}}^{qr}\} = [H_{\tilde{c}i}^{qrqs}] \{f_i^{qs}\} + [H_{\tilde{c}\tilde{c}}^{qrqs}] \{f_{\tilde{c}}^{qs}\} + [H_{\tilde{c}\tilde{c}}^{qrqs}] \{f_{\tilde{c}}^{qs}\} \quad (D.19)$$

Substituting equations (D.5), (D.10), (D.11) into (D.17) yields:

$$\begin{aligned} \{X_I^{qr}\} &= [H_{ii}^{qrqs}] \{F_I^{qs}\} + [H_{i\tilde{c}}^{qrqs}] \{F_{\tilde{C}}^{qs}\} + \\ &([H_{i\tilde{c}}^{qrqs}] - [H_{i\tilde{c}}^{qrqs}]) [B]^{-1} ([H_{\tilde{c}i}^{qrqs}] - [H_{\tilde{c}i}^{qrqs}]) \{F_I^{qs}\} + \\ &([H_{i\tilde{c}}^{qrqs}] - [H_{i\tilde{c}}^{qrqs}]) [B]^{-1} ([H_{\tilde{c}\tilde{c}}^{qrqs}] - [H_{\tilde{c}\tilde{c}}^{qrqs}]) \{F_{\tilde{C}}^{qs}\} \end{aligned} \quad (D.20)$$

Comparing equation (D.4) with equation (D.20) yields:

$$[H_{II}^{qrqs}] = [H_{ii}^{qrqs}] - ([H_{i\tilde{c}}^{qrqs}] - [H_{i\tilde{c}}^{qrqs}]) [B]^{-1} ([H_{\tilde{c}i}^{qrqs}] - [H_{\tilde{c}i}^{qrqs}]) \quad (D.21)$$

$$[H_{I\tilde{C}}^{qrqs}] = [H_{i\tilde{c}}^{qrqs}] - ([H_{i\tilde{c}}^{qrqs}] - [H_{i\tilde{c}}^{qrqs}]) [B]^{-1} ([H_{\tilde{c}\tilde{c}}^{qrqs}] - [H_{\tilde{c}\tilde{c}}^{qrqs}]) \quad (D.22)$$

Substituting equations (D.5), (D.15), (D.16) into (D.17) yields:

$$\begin{aligned} \{X_I^{qr}\} &= [H_{ii}^{qrqs}] \{F_I^{qs}\} + [H_{i\bar{c}}^{qrqs}] \{F_{\bar{C}}^{qs}\} + \\ &([H_{i\bar{c}}^{qrqs}] - [H_{i\bar{c}}^{qrqs}])[B]^{-1}([H_{\bar{c}i}^{qrqs}] - [H_{\bar{c}i}^{qrqs}]) \{F_I^{qs}\} + \\ &([H_{i\bar{c}}^{qrqs}] - [H_{i\bar{c}}^{qrqs}])[B]^{-1}([H_{\bar{c}\bar{c}}^{qrqs}] - [H_{\bar{c}\bar{c}}^{qrqs}]) \{F_{\bar{C}}^{qs}\} \end{aligned} \quad (D.23)$$

Comparing equation (D.4) with equation (D.23) yields:

$$[H_{II}^{qrqs}] = [H_{ii}^{qrqs}] - ([H_{i\bar{c}}^{qrqs}] - [H_{i\bar{c}}^{qrqs}])[B]^{-1}([H_{\bar{c}i}^{qrqs}] - [H_{\bar{c}i}^{qrqs}]) \quad (D.24)$$

$$[H_{I\bar{C}}^{qrqs}] = [H_{i\bar{c}}^{qrqs}] - ([H_{i\bar{c}}^{qrqs}] - [H_{i\bar{c}}^{qrqs}])[B]^{-1}([H_{\bar{c}\bar{c}}^{qrqs}] - [H_{\bar{c}\bar{c}}^{qrqs}]) \quad (D.25)$$

Substituting equations (D.5), (D.10), (D.11) into (D.18) yields:

$$\begin{aligned} \{X_{\bar{C}}^{qr}\} &= [H_{\bar{c}i}^{qrqs}] \{F_I^{qs}\} + [H_{\bar{c}\bar{c}}^{qrqs}] \{F_{\bar{C}}^{qs}\} + \\ &([H_{\bar{c}\bar{c}}^{qrqs}] - [H_{\bar{c}\bar{c}}^{qrqs}])[B]^{-1}([H_{\bar{c}i}^{qrqs}] - [H_{\bar{c}i}^{qrqs}]) \{F_I^{qs}\} + \\ &([H_{\bar{c}\bar{c}}^{qrqs}] - [H_{\bar{c}\bar{c}}^{qrqs}])[B]^{-1}([H_{\bar{c}\bar{c}}^{qrqs}] - [H_{\bar{c}\bar{c}}^{qrqs}]) \{F_{\bar{C}}^{qs}\} \end{aligned} \quad (D.26)$$

Comparing equation (D.4) with equation (D.26) yields:

$$[H_{\bar{C}I}^{qrqs}] = [H_{\bar{c}i}^{qrqs}] - ([H_{\bar{c}\bar{c}}^{qrqs}] - [H_{\bar{c}\bar{c}}^{qrqs}])[B]^{-1}([H_{\bar{c}i}^{qrqs}] - [H_{\bar{c}i}^{qrqs}]) \quad (D.27)$$

$$[H_{\bar{C}\bar{C}}^{qrqs}] = [H_{\bar{c}\bar{c}}^{qrqs}] - ([H_{\bar{c}\bar{c}}^{qrqs}] - [H_{\bar{c}\bar{c}}^{qrqs}])[B]^{-1}([H_{\bar{c}\bar{c}}^{qrqs}] - [H_{\bar{c}\bar{c}}^{qrqs}]) \quad (D.28)$$

Substituting equations (D.5), (D.15), (D.16) into (D.18) yields:

$$\begin{aligned} \{X_{\bar{C}}^{qr}\} &= [H_{\bar{c}i}^{qrqs}] \{F_I^{qs}\} + [H_{\bar{c}\bar{c}}^{qrqs}] \{F_{\bar{C}}^{qs}\} + \\ &([H_{\bar{c}\bar{c}}^{qrqs}] - [H_{\bar{c}\bar{c}}^{qrqs}])[B]^{-1}([H_{\bar{c}i}^{qrqs}] - [H_{\bar{c}i}^{qrqs}]) \{F_I^{qs}\} + \\ &([H_{\bar{c}\bar{c}}^{qrqs}] - [H_{\bar{c}\bar{c}}^{qrqs}])[B]^{-1}([H_{\bar{c}\bar{c}}^{qrqs}] - [H_{\bar{c}\bar{c}}^{qrqs}]) \{F_{\bar{C}}^{qs}\} \end{aligned} \quad (D.29)$$

Comparing equation (D.4) with equation (D.29) yields:

$$[H_{\bar{C}I}^{qrqs}] = [H_{\bar{c}i}^{qrqs}] - ([H_{\bar{c}\bar{c}}^{qrqs}] - [H_{\bar{c}\bar{c}}^{qrqs}])[B]^{-1}([H_{\bar{c}i}^{qrqs}] - [H_{\bar{c}i}^{qrqs}]) \quad (D.30)$$

$$[H_{\bar{C}\bar{C}}^{qrqs}] = [H_{\bar{c}\bar{c}}^{qrqs}] - ([H_{\bar{c}\bar{c}}^{qrqs}] - [H_{\bar{c}\bar{c}}^{qrqs}])[B]^{-1}([H_{\bar{c}\bar{c}}^{qrqs}] - [H_{\bar{c}\bar{c}}^{qrqs}]) \quad (D.31)$$

Substituting equations (D.5), (D.10), (D.11) into (D.19) yields:

$$\begin{aligned} \{X_{\tilde{C}}^{qr}\} &= [H_{\tilde{c}i}^{qrqs}] \{F_I^{qs}\} + [H_{\tilde{c}\tilde{c}}^{qrqs}] \{F_{\tilde{C}}^{qs}\} + \\ & \quad ([H_{\tilde{c}\tilde{c}}^{qrqs}] - [H_{\tilde{c}\tilde{c}}^{qrqs}]) [B]^{-1} ([H_{\tilde{c}i}^{qrqs}] - [H_{\tilde{c}i}^{qrqs}]) \{F_I^{qs}\} + \\ & \quad ([H_{\tilde{c}\tilde{c}}^{qrqs}] - [H_{\tilde{c}\tilde{c}}^{qrqs}]) [B]^{-1} ([H_{\tilde{c}\tilde{c}}^{qrqs}] - [H_{\tilde{c}\tilde{c}}^{qrqs}]) \{F_{\tilde{C}}^{qs}\} \end{aligned} \quad (D.32)$$

Comparing equation (D.4) with equation (D.32) yields:

$$[H_{\tilde{C}I}^{qrqs}] = [H_{\tilde{c}i}^{qrqs}] - ([H_{\tilde{c}\tilde{c}}^{qrqs}] - [H_{\tilde{c}\tilde{c}}^{qrqs}]) [B]^{-1} ([H_{\tilde{c}i}^{qrqs}] - [H_{\tilde{c}i}^{qrqs}]) \quad (D.33)$$

$$[H_{\tilde{C}\tilde{C}}^{qrqs}] = [H_{\tilde{c}\tilde{c}}^{qrqs}] - ([H_{\tilde{c}\tilde{c}}^{qrqs}] - [H_{\tilde{c}\tilde{c}}^{qrqs}]) [B]^{-1} ([H_{\tilde{c}\tilde{c}}^{qrqs}] - [H_{\tilde{c}\tilde{c}}^{qrqs}]) \quad (D.34)$$

Substituting equations (D.5), (D.15), (D.16) into (D.19) yields:

$$\begin{aligned} \{X_{\tilde{C}}^{qr}\} &= [H_{\tilde{i}i}^{qrqs}] \{F_I^{qs}\} + [H_{\tilde{c}\tilde{c}}^{qrqs}] \{F_{\tilde{C}}^{qs}\} + \\ & \quad ([H_{\tilde{c}\tilde{c}}^{qrqs}] - [H_{\tilde{c}\tilde{c}}^{qrqs}]) [B]^{-1} ([H_{\tilde{c}i}^{qrqs}] - [H_{\tilde{c}i}^{qrqs}]) \{F_I^{qs}\} + \\ & \quad ([H_{\tilde{c}\tilde{c}}^{qrqs}] - [H_{\tilde{c}\tilde{c}}^{qrqs}]) [B]^{-1} ([H_{\tilde{c}\tilde{c}}^{qrqs}] - [H_{\tilde{c}\tilde{c}}^{qrqs}]) \{F_{\tilde{C}}^{qs}\} \end{aligned} \quad (D.35)$$

Comparing equation (D.4) with equation (D.35) yields:

$$[H_{\tilde{C}I}^{qrqs}] = [H_{\tilde{c}i}^{qrqs}] - ([H_{\tilde{c}\tilde{c}}^{qrqs}] - [H_{\tilde{c}\tilde{c}}^{qrqs}]) [B]^{-1} ([H_{\tilde{c}i}^{qrqs}] - [H_{\tilde{c}i}^{qrqs}]) \quad (D.36)$$

$$[H_{\tilde{C}\tilde{C}}^{qrqs}] = [H_{\tilde{c}\tilde{c}}^{qrqs}] - ([H_{\tilde{c}\tilde{c}}^{qrqs}] - [H_{\tilde{c}\tilde{c}}^{qrqs}]) [B]^{-1} ([H_{\tilde{c}\tilde{c}}^{qrqs}] - [H_{\tilde{c}\tilde{c}}^{qrqs}]) \quad (D.37)$$

Equations (D.21), (D.22), (D.24), (D.25), (D.27), (D.28), (D.30), (D.31), (D.33), (D.34), (D.36), (D.37), can be arranged as:

$$\begin{aligned} \begin{Bmatrix} \{X_I^{qr}\} \\ \{X_{\tilde{C}}^{qr}\} \\ \{X_{\tilde{C}}^{qr}\} \end{Bmatrix} &= \left( \begin{bmatrix} [H_{\tilde{i}i}^{qrqs}] & [H_{\tilde{i}\tilde{c}}^{qrqs}] & [H_{\tilde{i}\tilde{c}}^{qrqs}] \\ [H_{\tilde{c}i}^{qrqs}] & [H_{\tilde{c}\tilde{c}}^{qrqs}] & [H_{\tilde{c}\tilde{c}}^{qrqs}] \\ [H_{\tilde{c}i}^{qrqs}] & [H_{\tilde{c}\tilde{c}}^{qrqs}] & [H_{\tilde{c}\tilde{c}}^{qrqs}] \end{bmatrix} \right) - \\ & \quad \left( \begin{bmatrix} ([H_{\tilde{i}\tilde{c}}^{qrqs}] - [H_{\tilde{i}\tilde{c}}^{qrqs}]) \\ ([H_{\tilde{c}\tilde{c}}^{qrqs}] - [H_{\tilde{c}\tilde{c}}^{qrqs}]) \\ ([H_{\tilde{c}\tilde{c}}^{qrqs}] - [H_{\tilde{c}\tilde{c}}^{qrqs}]) \end{bmatrix} \right) \left( [H_{\tilde{c}\tilde{c}}^{qrqs}] + [H_{\tilde{c}\tilde{c}}^{qrqs}] - [H_{\tilde{c}\tilde{c}}^{qrqs}] - [H_{\tilde{c}\tilde{c}}^{qrqs}] + [\mathcal{G}_{\tilde{c}\tilde{c}}^{qsqr}]^{-1} \right)^{-1} \left( \begin{bmatrix} ([H_{\tilde{i}\tilde{c}}^{qrqs}] - [H_{\tilde{i}\tilde{c}}^{qrqs}]) \\ ([H_{\tilde{c}\tilde{c}}^{qrqs}] - [H_{\tilde{c}\tilde{c}}^{qrqs}]) \\ ([H_{\tilde{c}\tilde{c}}^{qrqs}] - [H_{\tilde{c}\tilde{c}}^{qrqs}]) \end{bmatrix} \right)^T \begin{Bmatrix} \{F_I^{qs}\} \\ \{F_{\tilde{C}}^{qs}\} \\ \{F_{\tilde{C}}^{qs}\} \end{Bmatrix} \end{aligned} \quad (D.38)$$

Equation (D.38) can be arranged in a more concise form as:

$$\begin{aligned} \begin{Bmatrix} \{X_I^{qr}\} \\ \{X_C^{qr}\} \end{Bmatrix} &= \left( \begin{bmatrix} [H_{ii}^{qrqs}] & [H_{ic}^{qrqs}] \\ [H_{ci}^{qrqs}] & [H_{cc}^{qrqs}] \end{bmatrix} \right)^{-1} \\ &\quad \begin{Bmatrix} ([H_{ic}^{qrqs}] - [H_{ic}^{qrqs}]) \\ ([H_{cc}^{qrqs}] - [H_{cc}^{qrqs}]) \end{Bmatrix} \left\{ [H_{cc}^{qrqs}] + [H_{cc}^{qrqs}] - [H_{cc}^{qrqs}] - [H_{cc}^{qrqs}] + [\mathcal{G}_{cc}^{qsqr}]^{-1} \right\}^{-1} \begin{Bmatrix} ([H_{ic}^{qrqs}] - [H_{ic}^{qrqs}]) \\ ([H_{cc}^{qrqs}] - [H_{cc}^{qrqs}]) \end{Bmatrix}^T \begin{Bmatrix} \{F_I^{qs}\} \\ \{F_C^{qs}\} \end{Bmatrix} \end{aligned} \quad (\text{D.39})$$

where matrix  $[\mathcal{G}_{cc}^{qsqr}]$  is given by

$$[\mathcal{G}_{cc}^{qsqr}] = \begin{bmatrix} \mathcal{G}_{cc}^{11} & \mathcal{G}_{cc}^{12} & \dots & \mathcal{G}_{cc}^{1q_r} \\ \vdots & & \ddots & \vdots \\ \mathcal{G}_{cc}^{q_s 1} & \mathcal{G}_{cc}^{q_s 2} & \dots & \mathcal{G}_{cc}^{q_s q_r} \end{bmatrix}$$

# Appendix E

## Illustration of the *HANORCA*

### E.1 Basic Impedance Coupling Process

Let us assume two structures to be connected with one local nonlinear element, as shown by figure (E.1):

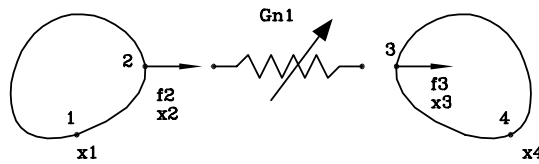


Figure E.1: Two structures connected with one local nonlinear element

The equation of the coupled system, relating displacement vectors and force vectors is shown in matrix form as:

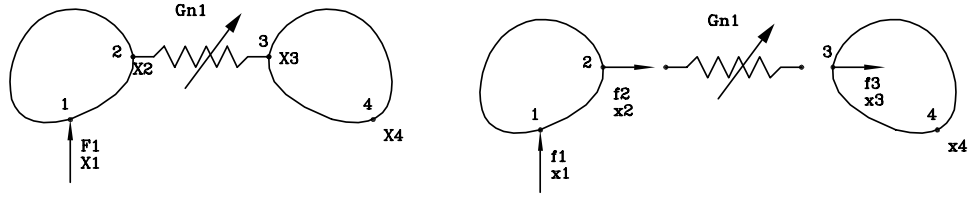
$$\begin{Bmatrix} X_1 \\ X_2 \\ X_3 \\ X_4 \end{Bmatrix} = \begin{bmatrix} \gamma_{11} & \gamma_{12} & \gamma_{13} & \gamma_{14} \\ \gamma_{21} & \gamma_{22} & \gamma_{23} & \gamma_{24} \\ \gamma_{31} & \gamma_{32} & \gamma_{33} & \gamma_{34} \\ \gamma_{41} & \gamma_{42} & \gamma_{43} & \gamma_{44} \end{bmatrix} \begin{Bmatrix} F_1 \\ F_2 \\ F_3 \\ F_4 \end{Bmatrix} \quad (\text{E.1})$$

Consider a force  $F_1$  applied in coordinate 1 as shown in figure (E.2):

Looking at the substructures, the displacement in each point can be written as:

$$x_1 = H_{11}f_1 + H_{12}f_2 \quad (\text{E.2})$$

$$x_2 = H_{21}f_1 + H_{22}f_2 \quad (\text{E.3})$$

Figure E.2: Force applied in  $x_1$ 

$$x_3 = H_{33}f_3 \quad (\text{E.4})$$

$$x_4 = H_{43}f_3 \quad (\text{E.5})$$

The equilibrium conditions can be written as:

$$\begin{aligned} f_2 + f_3 &= 0 \implies f_2 = -f_3 \\ F_1 &= f_1 \end{aligned} \quad (\text{E.6})$$

The compatibility conditions can be written as:

$$\begin{aligned} X_1 &= x_1 \\ X_2 &= x_2 \\ X_3 &= x_3 \\ X_4 &= x_4 \\ x_3 - x_2 &= -f_3/G_{n1} \end{aligned} \quad (\text{E.7})$$

Substituting equations (E.4),(E.3) into (E.7) yields:

$$H_{33}f_3 - H_{21}f_1 - H_{22}f_2 + f_3/G_{n1} = 0 \quad (\text{E.8})$$

Substituting equation (E.6) into (E.8) yields:

$$(H_{33} + H_{22} + 1/G_{n1})f_3 = H_{21}F_1 \quad (\text{E.9})$$

$$f_3 = (H_{33} + H_{22} + 1/G_{n1})^{-1}H_{21}F_1 \quad (\text{E.10})$$

As the external force is applied in coordinate  $X_1$  and now it is known that the internal forces as function of this external force, it is possible to calculate all the elements of the

first column of equation (E.1) as follows:

$$\begin{cases} \gamma_{11} = X_1/F_1 \\ X_1 = H_{11}F_1 - H_{12}(H_{33} + H_{22} + 1/G_{n1})^{-1}H_{21}F_1 \end{cases} \quad (\text{E.11})$$

$$\gamma_{11} = H_{11} - H_{12}(H_{33} + H_{22} + 1/G_{n1})^{-1}H_{21} \quad (\text{E.12})$$

$$\begin{cases} \gamma_{21} = X_2/F_1 \\ X_2 = H_{21}F_1 - H_{22}(H_{33} + H_{22} + 1/G_{n1})^{-1}H_{21}F_1 \end{cases} \quad (\text{E.13})$$

$$\gamma_{21} = H_{21} - H_{22}(H_{33} + H_{22} + 1/G_{n1})^{-1}H_{21} \quad (\text{E.14})$$

$$\begin{cases} \gamma_{31} = X_3/F_1 \\ X_3 = H_{33}(H_{33} + H_{22} + 1/G_{n1})^{-1}H_{21}F_1 \end{cases} \quad (\text{E.15})$$

$$\gamma_{31} = H_{33}(H_{33} + H_{22} + 1/G_{n1})^{-1}H_{21} \quad (\text{E.16})$$

$$\begin{cases} \gamma_{41} = X_4/F_1 \\ X_4 = H_{43}(H_{33} + H_{22} + 1/G_{n1})^{-1}H_{21}F_1 \end{cases} \quad (\text{E.17})$$

$$\gamma_{41} = H_{43}(H_{33} + H_{22} + 1/G_{n1})^{-1}H_{21} \quad (\text{E.18})$$

Consider a force  $F_2$  applied in coordinate 2 as shown in figure (E.3):

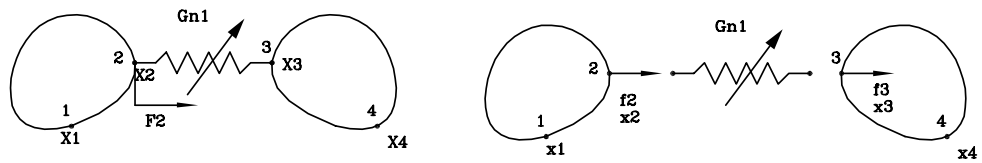


Figure E.3: Force applied in  $x_2$

Looking at the substructures, the displacement in each point can be written as:

$$x_1 = H_{12}f_2 \quad (\text{E.19})$$

$$x_2 = H_{22}f_2 \quad (\text{E.20})$$

$$x_3 = H_{33}f_3 \quad (\text{E.21})$$

$$x_4 = H_{43}f_3 \quad (\text{E.22})$$

The equilibrium conditions can be written as:

$$f_2 + f_3 = F_2 \implies f_2 = F_2 - f_3 \quad (\text{E.23})$$

The compatibility conditions can be written as:

$$\begin{aligned} X_1 &= x_1 \\ X_2 &= x_2 \\ X_3 &= x_3 \\ X_4 &= x_4 \\ x_3 - x_2 &= -f_3/G_{n1} \end{aligned} \quad (\text{E.24})$$

Substituting equations (E.21),(E.20) into (E.24) yields:

$$H_{33}f_3 - H_{22}f_2 + f_3/G_{n1} = 0 \quad (\text{E.25})$$

$$(H_{33} + 1/G_{n1})f_3 = H_{22}f_2 \quad (\text{E.26})$$

Substituting equation (E.23) into (E.26) yields:

$$f_3 = (H_{33} + H_{22} + 1/G_{n1})^{-1}H_{22}F_2 \quad (\text{E.27})$$

$$f_2 = (1 - (H_{33} + H_{22} + 1/G_{n1})^{-1}H_{22})F_2 \quad (\text{E.28})$$

As the external force is applied in coordinate  $X_2$  and now it is known that the internal forces as function of this external force, it is possible to calculate all the elements of the second column of equation (E.1) as follows:

$$\begin{cases} \gamma_{12} = X_1/F_2 \\ X_1 = H_{12}F_2 - H_{12}(H_{33} + H_{22} + 1/G_{n1})^{-1}H_{22}F_2 \end{cases} \quad (\text{E.29})$$

$$\gamma_{12} = H_{12} - H_{12}(H_{33} + H_{22} + 1/G_{n1})^{-1}H_{22} \quad (\text{E.30})$$

$$\begin{cases} \gamma_{22} = X_2/F_2 \\ X_2 = H_{22}F_2 - H_{22}(H_{33} + H_{22} + 1/G_{n1})^{-1}H_{22}F_2 \end{cases} \quad (\text{E.31})$$

$$\gamma_{22} = H_{22} - H_{22}(H_{33} + H_{22} + 1/G_{n1})^{-1}H_{22} \quad (\text{E.32})$$

$$\begin{cases} \gamma_{32} = X_3/F_2 \\ X_3 = H_{33}(H_{33} + H_{22} + 1/G_{n1})^{-1}H_{22}F_2 \end{cases} \quad (\text{E.33})$$

$$\gamma_{32} = H_{33}(H_{33} + H_{22} + 1/G_{n1})^{-1}H_{22} \quad (\text{E.34})$$

$$\begin{cases} \gamma_{42} = X_4/F_2 \\ X_4 = H_{43}(H_{33} + H_{22} + 1/G_{n1})^{-1}H_{22}F_2 \end{cases} \quad (\text{E.35})$$

$$\gamma_{42} = H_{43}(H_{33} + H_{22} + 1/G_{n1})^{-1}H_{22} \quad (\text{E.36})$$

Consider a force  $F_3$  applied in coordinate 3 as shown in figure (E.4):

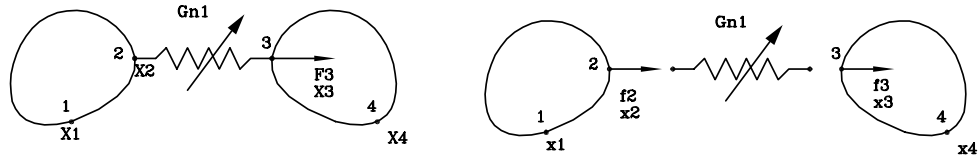


Figure E.4: Force applied in  $x_3$

Looking at the substructures, the displacement in each point can be written as:

$$x_1 = H_{12}f_2 \quad (\text{E.37})$$

$$x_2 = H_{22}f_2 \quad (\text{E.38})$$

$$x_3 = H_{33}f_3 \quad (\text{E.39})$$

$$x_4 = H_{43}f_3 \quad (\text{E.40})$$

The equilibrium conditions can be written as:

$$f_2 + f_3 = F_3 \implies f_3 = F_3 - f_2 \quad (\text{E.41})$$

The compatibility conditions can be written as:

$$\begin{aligned} X_1 &= x_1 \\ X_2 &= x_2 \\ X_3 &= x_3 \\ X_4 &= x_4 \\ x_2 - x_3 &= -f_2/G_{n1} \end{aligned} \quad (\text{E.42})$$

Substituting equations (E.38),(E.39) into (E.42) yields:

$$H_{22}f_2 - H_{33}f_3 + f_2/G_{n1} = 0 \quad (\text{E.43})$$

$$(H_{22} + 1/G_{n1})f_2 = H_{33}f_3 \quad (\text{E.44})$$

Substituting equation (E.41) into (E.44) yields:

$$f_2 = (H_{33} + H_{22} + 1/G_{n1})^{-1}H_{33}F_3 \quad (\text{E.45})$$

$$f_3 = (1 - (H_{33} + H_{22} + 1/G_{n1})^{-1}H_{33})F_3 \quad (\text{E.46})$$

As the external force is applied in coordinate  $X_3$  and now it is known that the internal forces as function of this external force, it is possible to calculate all the elements of the third column of equation (E.1) as follows:

$$\begin{cases} \gamma_{13} = X_1/F_3 \\ X_1 = H_{12}(H_{33} + H_{22} + 1/G_{n1})^{-1}H_{33}F_3 \end{cases} \quad (\text{E.47})$$

$$\gamma_{13} = H_{12}(H_{33} + H_{22} + 1/G_{n1})^{-1}H_{33} \quad (\text{E.48})$$

$$\begin{cases} \gamma_{23} = X_2/F_3 \\ X_2 = H_{22}(H_{33} + H_{22} + 1/G_{n1})^{-1}H_{33}F_3 \end{cases} \quad (\text{E.49})$$

$$\gamma_{23} = H_{22}(H_{33} + H_{22} + 1/G_{n1})^{-1}H_{33} \quad (\text{E.50})$$

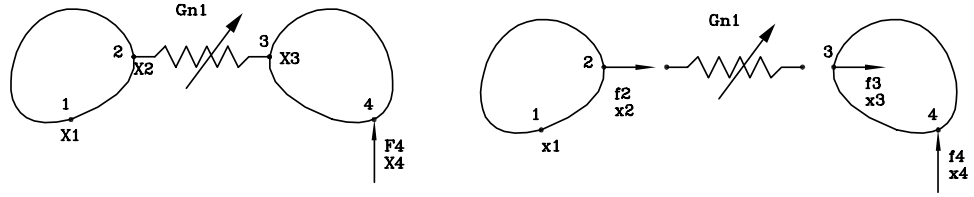
$$\begin{cases} \gamma_{33} = X_3/F_3 \\ X_3 = H_{33}F_3 - H_{33}(H_{33} + H_{22} + 1/G_{n1})^{-1}H_{33}F_3 \end{cases} \quad (\text{E.51})$$

$$\gamma_{33} = H_{33} - H_{33}(H_{33} + H_{22} + 1/G_{n1})^{-1}H_{33} \quad (\text{E.52})$$

$$\begin{cases} \gamma_{43} = X_4/F_3 \\ X_4 = H_{43}F_3 - H_{43}(H_{33} + H_{22} + 1/G_{n1})^{-1}H_{33}F_3 \end{cases} \quad (\text{E.53})$$

$$\gamma_{43} = H_{43} - H_{43}(H_{33} + H_{22} + 1/G_{n1})^{-1}H_{33} \quad (\text{E.54})$$

Consider a force  $F_4$  applied in coordinate 4 as shown in figure (E.5):

Figure E.5: Force applied in  $x_4$ 

Looking at the substructures, the displacement in each point can be written as:

$$x_1 = H_{12}f_2 \quad (\text{E.55})$$

$$x_2 = H_{22}f_2 \quad (\text{E.56})$$

$$x_3 = H_{33}f_3 + H_{34}f_4 \quad (\text{E.57})$$

$$x_4 = H_{43}f_3 + H_{44}f_4 \quad (\text{E.58})$$

The equilibrium conditions can be written as:

$$\begin{aligned} F_4 &= f_4 \\ f_2 + f_3 &= 0 \implies f_2 = -f_3 \end{aligned} \quad (\text{E.59})$$

The compatibility conditions can be written as:

$$\begin{aligned} X_1 &= x_1 \\ X_2 &= x_2 \\ X_3 &= x_3 \\ X_4 &= x_4 \\ x_2 - x_3 &= -f_2/G_{n1} \end{aligned} \quad (\text{E.60})$$

Substituting equations (E.56),(E.57) into (E.60) yields:

$$H_{22}f_2 - H_{33}f_3 - H_{34}f_4 + f_2/G_{n1} = 0 \quad (\text{E.61})$$

Substituting equation (E.59) into (E.61) yields:

$$(H_{33} + H_{22} + 1/G_{n1})f_3 = -H_{34}F_4 \quad (\text{E.62})$$

$$f_3 = -(H_{33} + H_{22} + 1/G_{n1})^{-1} H_{34} F_4 \quad (\text{E.63})$$

As the external force is applied in coordinate  $X_4$  and now it is known that the internal forces as function of this external force, it is possible to calculate all the elements of the fourth column of equation (E.1) as follows:

$$\begin{cases} \gamma_{14} = X_1/F_4 \\ X_1 = H_{12}(H_{33} + H_{22} + 1/G_{n1})^{-1} H_{34} F_4 \end{cases} \quad (\text{E.64})$$

$$\gamma_{14} = H_{12}(H_{33} + H_{22} + 1/G_{n1})^{-1} H_{34} \quad (\text{E.65})$$

$$\begin{cases} \gamma_{24} = X_2/F_4 \\ X_2 = H_{22}(H_{33} + H_{22} + 1/G_{n1})^{-1} H_{34} F_4 \end{cases} \quad (\text{E.66})$$

$$\gamma_{24} = H_{22}(H_{33} + H_{22} + 1/G_{n1})^{-1} H_{34} \quad (\text{E.67})$$

$$\begin{cases} \gamma_{34} = X_3/F_4 \\ X_3 = H_{34} F_4 - H_{33}(H_{33} + H_{22} + 1/G_{n1})^{-1} H_{34} F_4 \end{cases} \quad (\text{E.68})$$

$$\gamma_{34} = H_{34} - H_{33}(H_{33} + H_{22} + 1/G_{n1})^{-1} H_{34} \quad (\text{E.69})$$

$$\begin{cases} \gamma_{44} = X_4/F_4 \\ X_4 = H_{44} F_4 - H_{43}(H_{33} + H_{22} + 1/G_{n1})^{-1} H_{34} F_4 \end{cases} \quad (\text{E.70})$$

$$\gamma_{44} = H_{44} - H_{43}(H_{33} + H_{22} + 1/G_{n1})^{-1} H_{34} \quad (\text{E.71})$$

The equation of the coupled system, relating displacement vectors and force vector can be written in matrix form using the properties of each component as:

$$\begin{Bmatrix} X_1 \\ X_4 \\ X_2 \\ X_3 \end{Bmatrix} = \begin{bmatrix} H_{11} - H_{12}(B)^{-1} H_{21} & H_{12}(B)^{-1} H_{34} & H_{12} - H_{12}(B)^{-1} H_{22} & H_{12}(B)^{-1} H_{33} \\ H_{43}(B)^{-1} H_{21} & H_{44} - H_{43}(B)^{-1} H_{34} & H_{43}(B)^{-1} H_{22} & H_{43} - H_{43}(B)^{-1} H_{33} \\ H_{21} - H_{22}(B)^{-1} H_{21} & H_{22}(B)^{-1} H_{34} & H_{22} - H_{22}(B)^{-1} H_{22} & H_{22}(B)^{-1} H_{33} \\ H_{33}(B)^{-1} H_{21} & H_{34} - H_{33}(B)^{-1} H_{34} & H_{33}(B)^{-1} H_{22} & H_{33} - H_{33}(B)^{-1} H_{33} \end{bmatrix} \begin{Bmatrix} F_1 \\ F_4 \\ f_2 \\ f_3 \end{Bmatrix} \quad (\text{E.72})$$

where:

$$B = H_{33} + H_{22} + 1/G_{n1}$$

Equation (E.72) can be arranged in a more concise form as:

$$\begin{Bmatrix} X_1 \\ X_4 \\ X_2 \\ X_3 \end{Bmatrix} = \left( \begin{bmatrix} H_{11} & 0 & H_{12} & 0 \\ 0 & H_{44} & 0 & H_{43} \\ H_{21} & 0 & H_{22} & 0 \\ 0 & H_{34} & 0 & H_{33} \end{bmatrix} - \begin{Bmatrix} -H_{12} \\ H_{43} \\ -H_{22} \\ H_{33} \end{Bmatrix} [H_{33} + H_{22} + 1/G_{n1}]^{-1} \begin{Bmatrix} -H_{12} \\ H_{43} \\ -H_{22} \\ H_{33} \end{Bmatrix}^T \right) \begin{Bmatrix} F_1 \\ F_4 \\ f_2 \\ f_3 \end{Bmatrix} \quad (\text{E.73})$$

## E.2 HANORCA of two linear structures with a local nonlinear element

This approach was applied to obtain the equation of the Assembled System composed of two substructures and one nonlinear element, as shown in figure (E.6): The analytical

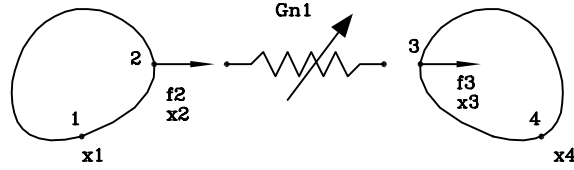


Figure E.6: Two linear structures with local nonlinear element

expression for this system can be obtained using the equilibrium condition, as derived in section E.1, leading to the following equation:

$$\begin{Bmatrix} X_1 \\ X_4 \\ X_2 \\ X_3 \end{Bmatrix} = \left( \begin{bmatrix} H_{11} & 0 & H_{12} & 0 \\ 0 & H_{44} & 0 & H_{43} \\ H_{21} & 0 & H_{22} & 0 \\ 0 & H_{34} & 0 & H_{33} \end{bmatrix} - \begin{Bmatrix} H_{12} \\ -H_{43} \\ H_{22} \\ -H_{33} \end{Bmatrix} [H_{33} + H_{22} + 1/G_{n1}]^{-1} \begin{Bmatrix} H_{12} \\ -H_{43} \\ H_{22} \\ -H_{33} \end{Bmatrix}^T \right) \begin{Bmatrix} F_1 \\ F_4 \\ F_2 \\ F_3 \end{Bmatrix} \quad (\text{E.74})$$

The same result can be obtained from the approach of Nonlinear Receptance Coupling approach. This example has only one pair of connection coordinate  $(x_2, x_3)$  and two external coordinates as shown in the following groups:

$$\begin{aligned} i &= \{1, 4\} \\ \bar{c} &= \{2\} \\ \tilde{c} &= \{3\} \\ c &= \{2, 3\} \end{aligned} \quad (\text{E.75})$$

Using the groups in equation(E.75), it is possible to set the following submatrices:

$$\begin{aligned}
 H_{ii} &= \begin{bmatrix} H_{11} & 0 \\ 0 & H_{44} \end{bmatrix} \\
 H_{i\bar{c}} &= \begin{bmatrix} H_{12} \\ 0 \end{bmatrix} \\
 H_{\bar{c}i} &= \begin{bmatrix} H_{21} & 0 \end{bmatrix} \\
 H_{\bar{c}\bar{c}} &= \begin{bmatrix} H_{22} \end{bmatrix} \\
 H_{i\tilde{c}} &= \begin{bmatrix} 0 \\ H_{43} \end{bmatrix} \\
 H_{\tilde{c}i} &= \begin{bmatrix} 0 & H_{34} \end{bmatrix} \\
 H_{\tilde{c}\bar{c}} &= \begin{bmatrix} H_{33} \end{bmatrix} \\
 H_{\bar{c}\tilde{c}} &= \begin{bmatrix} 0 \end{bmatrix} \\
 H_{\tilde{c}\tilde{c}} &= \begin{bmatrix} 0 \end{bmatrix}
 \end{aligned} \tag{E.76}$$

The equation of the Assembled System can be determined substituting equations (E.76) in equation(4.81) leading to the following equation:

$$\begin{Bmatrix} X_1 \\ X_4 \\ X_2 \\ X_3 \end{Bmatrix} = \left( \begin{bmatrix} H_{11} & 0 & H_{12} & 0 \\ 0 & H_{44} & 0 & H_{43} \\ H_{21} & 0 & H_{22} & 0 \\ 0 & H_{34} & 0 & H_{33} \end{bmatrix} - \begin{Bmatrix} H_{12} \\ -H_{43} \\ H_{22} \\ -H_{33} \end{Bmatrix} [H_{22} + H_{33} + 1/G_{n1}]^{-1} \begin{Bmatrix} H_{12} \\ -H_{43} \\ H_{22} \\ -H_{33} \end{Bmatrix}^T \right) \begin{Bmatrix} F_1 \\ F_4 \\ F_2 \\ F_3 \end{Bmatrix} \tag{E.77}$$

### E.3 HANORCA of three linear structures with a local nonlinear element and rigid connections

This approach was applied to obtain the equation of the Assembled System composed of three substructures, one nonlinear element, one point rigid connected with two other points as shown in figure (E.7):

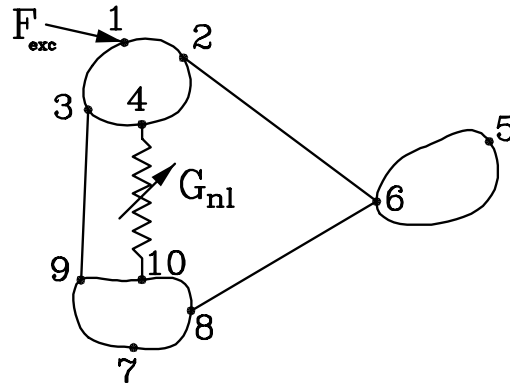


Figure E.7: Three linear structures with local nonlinear element and rigid connections

This example has four pair of connection coordinate  $(x_2, x_6)$ ,  $(x_6, x_8)$ ,  $(x_3, x_9)$ ,  $(x_4, x_{10})$  and three external coordinates as shown in the following groups:

$$\begin{aligned}
 i &= \{1, 5, 7\} \\
 \bar{c} &= \{2, 6, 3, 4\} \\
 \tilde{c} &= \{6, 8, 9, 10\} \\
 c &= \{2, 3, 4, 10\} \\
 c_d &= \{4, 10\} \\
 i_d &= \{\} \\
 c_f &= \{\} \\
 i_f &= \{1\}
 \end{aligned} \tag{E.78}$$

Using the groups in equation(E.79), it is possible to set the following submatrices:

$$H_{ii} = \begin{bmatrix} H_{11} & 0 & 0 \\ 0 & H_{55} & 0 \\ 0 & 0 & H_{77} \end{bmatrix}$$

$$\begin{aligned}
H_{i\bar{c}} &= \begin{bmatrix} H_{12} & 0 & H_{13} & H_{14} \\ 0 & H_{56} & 0 & 0 \\ 0 & 0 & 0 & 0 \end{bmatrix} \\
H_{\bar{c}\bar{c}} &= \begin{bmatrix} H_{22} & 0 & H_{23} & H_{24} \\ 0 & H_{66} & 0 & 0 \\ H_{32} & 0 & H_{33} & H_{34} \\ H_{42} & 0 & H_{43} & H_{44} \end{bmatrix} \\
H_{i\bar{c}} &= \begin{bmatrix} 0 & 0 & 0 & 0 \\ H_{56} & 0 & 0 & 0 \\ 0 & H_{78} & H_{79} & H_{710} \end{bmatrix} \\
H_{\bar{c}\bar{c}} &= \begin{bmatrix} H_{66} & 0 & 0 & 0 \\ 0 & H_{88} & H_{89} & H_{810} \\ 0 & H_{98} & H_{99} & H_{910} \\ 0 & H_{108} & H_{109} & H_{1010} \end{bmatrix} \\
H_{\bar{c}\bar{c}} &= \begin{bmatrix} 0 & 0 & 0 & 0 \\ H_{66} & 0 & 0 & 0 \\ 0 & 0 & 0 & 0 \\ 0 & 0 & 0 & 0 \end{bmatrix} \\
H_{i\bar{c}} &= \begin{bmatrix} H_{12} & H_{13} & H_{14} & 0 \\ 0 & 0 & 0 & 0 \\ 0 & 0 & 0 & H_{710} \end{bmatrix} \\
H_{cc} &= \begin{bmatrix} H_{22} & H_{23} & H_{24} & 0 \\ H_{32} & H_{33} & H_{34} & 0 \\ H_{42} & H_{43} & H_{44} & 0 \\ 0 & 0 & 0 & H_{1010} \end{bmatrix}
\end{aligned} \tag{E.79}$$

$$H_{c\bar{c}} = \begin{bmatrix} H_{22} & 0 & H_{23} & H_{24} \\ H_{32} & 0 & H_{33} & H_{34} \\ H_{42} & 0 & H_{43} & H_{44} \\ 0 & 0 & 0 & 0 \end{bmatrix}$$

$$H_{c\tilde{c}} = \begin{bmatrix} 0 & 0 & 0 & 0 \\ 0 & 0 & 0 & 0 \\ 0 & 0 & 0 & 0 \\ 0 & 0 & 0 & H_{1010} \end{bmatrix}$$

$$H_{c_d i} = \begin{bmatrix} H_{41} & 0 & 0 \\ 0 & 0 & H_{107} \end{bmatrix}$$

$$H_{c_d c} = \begin{bmatrix} H_{42} & H_{43} & H_{44} & 0 \\ 0 & 0 & 0 & H_{1010} \end{bmatrix}$$

$$H_{c_d \bar{c}} = \begin{bmatrix} H_{42} & 0 & H_{43} & H_{44} \\ 0 & 0 & 0 & 0 \end{bmatrix}$$

$$H_{c_d \tilde{c}} = \begin{bmatrix} 0 & 0 & 0 & 0 \\ 0 & H_{108} & H_{109} & H_{1010} \end{bmatrix}$$

$$H_{i_f \bar{c}} = \begin{bmatrix} H_{12} & 0 & H_{13} & H_{14} \end{bmatrix}$$

$$H_{i_f \tilde{c}} = \begin{bmatrix} 0 & 0 & 0 & 0 \end{bmatrix}$$

The equation of the Assembled System relating all non repetitive coordinates can be determined substituting equations (E.79) in equation(4.81) leading to the following equa-

tion:

$$\left\{ \begin{array}{c} X_1 \\ X_5 \\ X_7 \\ X_2 \\ X_3 \\ X_4 \\ X_{10} \end{array} \right\} = \left( \left[ \begin{array}{cccccc} H_{11} & 0 & 0 & H_{12} & H_{13} & H_{14} & 0 \\ 0 & H_{55} & 0 & 0 & 0 & 0 & 0 \\ 0 & 0 & H_{77} & 0 & 0 & 0 & H_{710} \\ H_{12} & 0 & 0 & H_{22} & H_{23} & H_{24} & 0 \\ H_{13} & 0 & 0 & H_{32} & H_{33} & H_{34} & 0 \\ H_{14} & 0 & 0 & H_{42} & H_{43} & H_{44} & 0 \\ 0 & 0 & H_{710} & 0 & 0 & 0 & H_{1010} \end{array} \right] - \right. \quad (\text{E.80})$$

$$\left. \left\{ \begin{array}{c} H_{12} & 0 & H_{13} & H_{14} \\ -H_{56} & H_{56} & 0 & 0 \\ 0 & -H_{78} & -H_{79} & -H_{710} \\ H_{22} & 0 & H_{23} & H_{24} \\ H_{32} & 0 & H_{33} & H_{34} \\ H_{42} & 0 & H_{43} & H_{44} \\ 0 & -H_{108} & -H_{109} & -H_{1010} \end{array} \right\} [B]^{-1} \left\{ \begin{array}{c} H_{12} & 0 & H_{13} & H_{14} \\ -H_{56} & H_{56} & 0 & 0 \\ 0 & -H_{78} & -H_{79} & -H_{710} \\ H_{22} & 0 & H_{23} & H_{24} \\ H_{32} & 0 & H_{33} & H_{34} \\ H_{42} & 0 & H_{43} & H_{44} \\ 0 & -H_{108} & -H_{109} & -H_{1010} \end{array} \right\}^T \left\{ \begin{array}{c} F_1 \\ F_5 \\ F_7 \\ F_2 \\ F_3 \\ F_4 \\ F_{10} \end{array} \right\}$$

where

$$[B] = \left[ \begin{array}{cccc} H_{22} + H_{66} & -H_{66} & H_{23} & H_{24} \\ -H_{66} & H_{66} + H_{88} & H_{89} & H_{810} \\ H_{32} & H_{98} & H_{33} + H_{99} & H_{34} + H_{910} \\ H_{42} & H_{108} & H_{43} + H_{109} & H_{44} + H_{1010} + 1/G_{nl} \end{array} \right] \quad (\text{E.81})$$

The equation of the Assembled System relating only the desired connection coordinates can be determined substituting equations (E.79) in equation(4.118) leading to the following equation:

$$\left\{ \begin{array}{c} X_4 \\ X_{10} \end{array} \right\} = \left( \left[ \begin{array}{cccccc} H_{14} & 0 & 0 & H_{42} & H_{43} & H_{44} & 0 \\ 0 & 0 & H_{710} & 0 & 0 & 0 & H_{1010} \end{array} \right] - \right. \quad (\text{E.82})$$

$$\left. \left\{ \begin{array}{c} H_{42} & 0 & H_{43} & H_{44} \\ 0 & -H_{108} & -H_{109} & -H_{1010} \end{array} \right\} [B]^{-1} \left\{ \begin{array}{c} H_{12} & 0 & H_{13} & H_{14} \\ -H_{56} & H_{56} & 0 & 0 \\ 0 & -H_{78} & -H_{79} & -H_{710} \\ H_{22} & 0 & H_{23} & H_{24} \\ H_{32} & 0 & H_{33} & H_{34} \\ H_{42} & 0 & H_{43} & H_{44} \\ 0 & -H_{108} & -H_{109} & -H_{1010} \end{array} \right\}^T \left\{ \begin{array}{c} F_1 \\ F_5 \\ F_7 \\ F_2 \\ F_3 \\ F_4 \\ F_{10} \end{array} \right\}$$

The equation of the Assembled System relating both the desired connection and excitation points can be determined substituting equations (E.79) in equation(4.118) leading to the following equation:

$$\begin{aligned} \begin{Bmatrix} X_4 \\ X_{10} \end{Bmatrix} &= \left( \begin{bmatrix} H_{14} \\ 0 \end{bmatrix} \right) - \\ &\begin{Bmatrix} H_{42} & 0 & H_{43} & H_{44} \\ 0 & -H_{108} & -H_{109} & -H_{1010} \end{Bmatrix} [B]^{-1} \begin{Bmatrix} H_{12} & 0 & H_{13} & H_{14} \end{Bmatrix}^T \begin{Bmatrix} F_1 \end{Bmatrix} \end{aligned} \quad (\text{E.83})$$

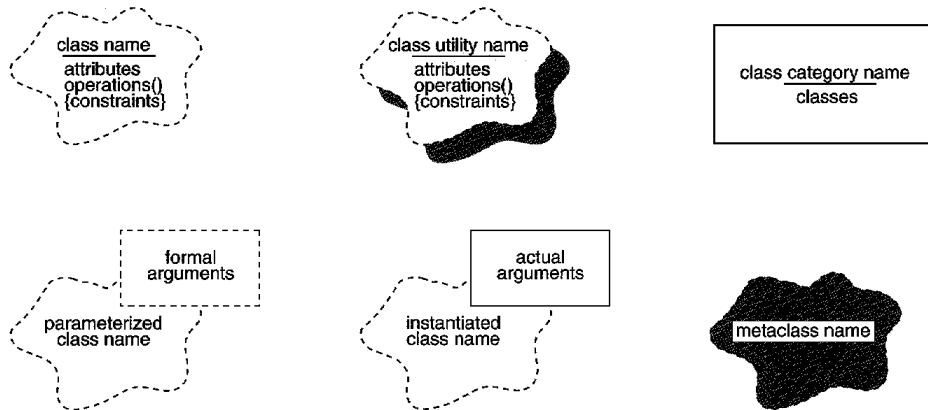
# Appendix F

## Booch Notation

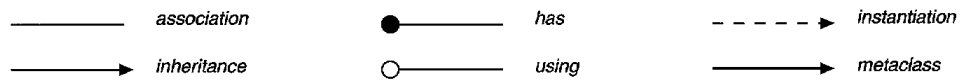
### Class Diagram

Shows the existence of classes and their relationships in the logical view of a system.

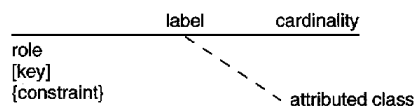
#### Class icons



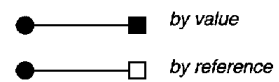
#### Class relationships



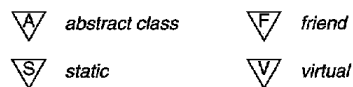
#### Relationship adornments



#### Containment adornments



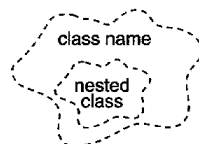
#### Properties



#### Export control



#### Nesting



#### Notes

